La duda es uno de los nombres de la inteligencia

Jorge Luis Borges

Universitat Politècnica de Catalunya
Escola Tècnica Superior d'Enginyers de Camins, Canals i Ports de Barcelona
Departament d'Enginyeria del Terreny, Cartogràfica i Geofísica

Proposal of energy spectra for earthquake resistant design based on Turkish registers

Ahmet Utku Yazgan

Annem ve Babam için

Curs acadèmic: 2012 / 2013

Acta de qualificació de tesi doctoral

Nom i cognoms
Ahmet Utku Yazgan

DNI / NIE / Passaport
X5552696-J

Programa de doctorat
Enginyeria sísmica i dinàmica estructural

Unitat estructural responsable del programa
Departament d'enginyeria del terreny, cartogràfica i geodèsica

Resolució del Tribunal

Reunit el Tribunal designat a l'efecte, el doctorand / la doctoranda exposa el tema de la seva tesi doctoral titulada
Proposal of energy spectra for earthquake resistant design based on Turkish registers

Acabada la lectura i després de donar resposta a les qüestions formulades pels membres titulars del tribunal, aquest atorga la qualificació:

☐ APTA/E ☐ NO APTA/E

(Nom, cognoms i signatura)		(Nom, cognoms i signatura)
President/a		Secretari/ària
(Nom, cognoms i signatura)	(Nom, cognoms i signatura)	(Nom, cognoms i signatura)
Vocal	Vocal	Vocal

_____, _____ d'/de _____ de _____

El resultat de l'escrutini dels vots emesos pels membres titulars del tribunal, efectuat per l'Escola de Doctorat, a instància de la Comissió de Doctorat de la UPC, atorga la MENCIÓ CUM LAUDE:

☐ SI ☐ NO

(Nom, cognoms i signatura)	(Nom, cognoms i signatura)
Presidenta de la Comissió de Doctorat	Secretària de la Comissió de Doctorat

Barcelona, _____ d'/de _____ de _____

Acknowledgements

First of all, the author wants to express special thanks to his thesis supervisors, Dr. Francesc López Almansa and Dr. Amadeu Benavet Climent for the opportunity, confidence and support. As well, the strong help from his tutor, Dr. Lluís G. Pujades, is gratefully acknowledged.

Professors Polat Gülkan and Erol Kalkan have provided useful guidance in the earlier stages of research. This author also wishes to express his gratitude to the Earthquake Department of the Disaster and Emergency Management Presidency of the Republic of Turkey Prime Ministry.

The author would like express his deepest gratitude for the funding of this study during his stay in Spain by the Spanish Government (Ministry of Foreign Affairs, "Becas MAEC-AECID"), Grant No. 447958.

Thank to the people who accompanied me and offered their help in different ways on the road and offered their hands when mine were not enough. My gratitude to all my friends, Ilker Demiroğlu, Ilker Demirkol, Boğaçhan Tahirbegi, Billur Cakirer, Jordi Blanco, David Domínguez, Helbert Gonzales, Juan Carlos Castro, Miguel Ángel Montaña, Edgar Segués, Nayive Jaramillo, Celia Costa and Andrea Verónica Amestoy.

Last but foremost the author wholeheartedly wishes to thank his parents, Kazim Yazgan & Hatice Yazgan and his sister Açalya Akdogan for their years of help and support.

Resumen

Este trabajo propone espectros de proyecto de energía en términos de velocidad equivalente, destinados a regiones con aceleración sísmica de proyecto 0.3 g o superior. Estos espectros se han obtenido a través de análisis dinámicos lineales y no lineales en una serie de registros sísmicos fuertes de Turquía. En los tramos de períodos largos y medianos los análisis son lineales, aprovechando la insensibilidad de los espectros con respecto a los parámetros estructurales, excepto el período fundamental y la masa; por el contrario, en el tramo de períodos cortos, los espectros son más sensibles a los parámetros estructurales y, por lo tanto, es necesario es necesario efectuar análisis no lineales. Los registros seleccionados se clasifican en ocho grupos con respecto al tipo de suelo (suelo duro y suelo blando), a la gravedad del terremoto en términos de magnitud superficial ($M_s \leq 5{,}5$ y $M_s > 5{,}5$) y la relevancia de efectos de proximidad de falla (registros impulsivos y vibratorios). Para cada uno de estos grupos, se proponen espectros medianos y característicos; dichos niveles corresponden a los percentiles de 50% y 95%, respectivamente. Estos espectros tienen una rama inicial lineal creciente en el intervalo de períodos cortos, una rama horizontal en el intervalo de períodos medios y una rama descendente en el intervalo de períodos largos. Se proponen criterios empíricos para estimar la energía histéretica a partir de la energía de entrada. Los espectros de proyecto propuestos se comparan con los obtenidos a partir de otros estudios.

Summary

This work proposes design energy spectra in terms of an equivalent velocity, intended for regions with design peak acceleration 0.3 g or higher. These spectra have been derived through linear and nonlinear dynamic analyses on a number of Turkish selected strong ground motion records. In the long and mid period ranges the analyses are linear, taking profit of the rather insensitivity of the spectra to the structural parameters other than the fundamental period; conversely, in the short period range, the spectra are more sensitive to the structural parameters and, hence, nonlinear analyses are required. The selected records are classified in eight groups with respect to the soil type (stiff soil and soft soil), the severity of the earthquake in terms of surface magnitude M_s ($M_s \leq 5.5$ and $M_s > 5.5$) and the relevance of the near-source effects (impulsive and vibratory). For each of these groups, median and characteristic spectra are proposed; such levels are intended to correspond to 50% and to 95% percentiles, respectively. These spectra have an initial linear growing branch in the short period range, a horizontal branch in the mid period range and a descending branch in the long period range. Empirical criteria for estimating the hysteretic energy from the input energy are suggested. The proposed design spectra are compared with those obtained from other studies.

List of Figures

List of Tables

List of symbols

a: Exponent of the descending branch of the proposed spectra
a, b, c, d: Parameters used in the expressions of the best fit of the V_D / V_E ratio
a, a', e, f, p: Parameters used at the reference [Decanini, Mollaioli 2001]
a_{max}: Maximum ground acceleration
c: Damping. Dimensionless coefficient used at the proposed expression for V_D/V_E
d: Displacement
d_{max}: Maximum displacement
d_y: Yielding displacement
f_1, f_2: Lower and upper cut frequencies in the numerical filtering of the signals
f_{bw}: Amplitude of the frequency band
f_i: Frequency of Fourier spectra (corresponding to point i)
k: Stiffness. Dimensionless coefficient used at the proposed expression for V_D/V_E
m: Mass
m_μ: Slope of the regression line for the ductility μ
m_1: Slope of the regression line for the ductility equal to 1
n: Number of years. Index of damage concentration
n, k, c: Dimensionless coefficients in the fit of the V_D / V_E ratio
p, r: Dimensionless coefficients used at the proposed design energy spectra
p_n: Probability of exceedance of the determined seismic action in n years
q: Ductility factor (EC-8)
t: Time, duration
t_{br}: Bracket duration of a register
t_{tf}: Triffunac duration of a register
v_s, $v_{s,30}$: Shear-wave velocity, shear-wave velocity averaged along to top 30 m of soil
x: Absolute displacement
$\ddot{x}$: Absolute acceleration
y: Relative displacement between the structure and the ground
y_{max}: Maximum displacement (relative to the structure and the ground)
y_y: Yield displacement (relative to the structure and the ground)
z_g: Ground displacement
$\ddot{z}_g$: Ground acceleration

AE_I: Factor for the seismic action used at the reference [Decanini, Mollaioli 1998]
C_i: Amplitude (of point i) of the Fourier spectra
C_0, C_1, C_2, C_3: Coefficeints for obtaining the target displacement
D: Displacement of the upper floor of the building relative to the ground. Park & Ang Damage index
D_f: Epicentral distance
D_i: Damage index for the structural component i
E: Energy
E_a: Cumulative inelastic strain energy
E_D: Energy that contributes to damage
E_e: Elastic vibrational energy
E_H: Hysteretic energy
E_I: Energy introduced to the structure by a given register (input energy)
$E_{I,abs}$: Absolute energy contributed by earthquake
E^{max}_I: Maximum value (respect to the period) of E_I
E_k: Kinetic energy (relative)
$E_{k,abs}$: Kinetic Energy (absolute)
E_s: Elastic strain energy (relative).
E_ζ: Energy absorption due to the damping

F: Force (Equivalent force)
F_e, F_u, F_y: Design elastic, ultimate and yielding forces
I_A: Arias intensity
I_D: Dimensionless seismic index
K_e: Effective stiffness
K_i: Stiffness of the i-th mode
M: Magnitude
M_L: Local magnitude
M_s: Surface magnitude
M_w: Moment magnitude
N: Number of points
PGA: Peak Ground Acceleration
PGA_d: Maximum design acceleration according to Turkish Seismic Code (TSC-98)
PGV: Peak Ground Velocity
Q: Restoring force
Q_y: Yielding value of the restoring force
R: Response reduction factor (American and Turkish code). Minimum distance to the rupture of the fault plane
R_d: Ratio among the elastic design (F_e) and ultimate forces (F_u)
R_{jb}: Joyner-Boore distance of a register to a rupture plane
R_{rup}: Rupture distance of a register (closest distance to a rupture plane)
R_{epi}: Epicentral distance of a register
S: Soil coefficient
S_a: Acceleration response spectrum (absolute)
S_d: Displacement response spectrum (relative)
S_{pv}: Pseudo-velocity response spectrum (relative)
S_v: Velocity response spectrum (relative)
T: Natural vibration period of the structure. Return period of the earthquake.
T_0: Natural elastic vibration period of the structure
T_A, T_B: Periods used at the design spectrum of the Spanish code
T_A, T_B, T_C, T_D: Periods used at the design spectrum of eurocode and in the proposed spectra
T_e: Effective fundamental period
T_i: Period of the mode i. Corresponding period (at the spectra) of a discrete point i.
T_1: Natural period (fundamental) of the first mode of vibration of the structure
T_1, T_2, T_3 and T_4: Periods used at the reference [Decanini, Mollaioli 2001]
V: Earthquake force (base shear).
V_D: Energy that contributes to the damage expressed as equivalent velocity
V_E: Input energy expressed as equivalent velocity
$\|V_E\|_T$: Integral under the V_E spectra in the range $0 - T$
V_{Ei}: Input energy expressed as equivalent velocity corresponding to the discrete point i
$V_{E,NS}$: Input energy expressed as equivalent velocity for the north-south component
$V_{E,EW}$: Input energy expressed as equivalent velocity for the east-west component
W: Weight of the building
W_u: Energy absorption capacity

β: Empirical coefficient at the Park & Ang index
δ: Displacement
δ_{max}: Maximum displacement
δ_M: Maximum displacement
δ_t: Target displacement
δ_u: Ultimate displacement
δ_y: Yielding displacement
η: Cumulated ductility. Correction coefficient of the spectra according to the damping (eurocode).

λ_i: Weighting coefficient of the Park & Ang damage indices
μ: Ductility. Displacement ductility
μ_c: Cyclic ductility.
ν: Correction coefficient of the spectra according to the damping (Spanish code)
ρ: Importance factor of the building
τ: Time (auxiliary variable)
ω: Frequency
ω_d: Natural frequency of the system with damping
ω_0: Natural frequency of the system without damping
ζ: Damping factor
ζ_{eq}: Equivalent damping factor
Δ: Increment
Ω: Damping factor (Spanish code). Ovserstrength factor (ratio among the ultimate F_u and yielding forces F_y)

1 Introduction

1.1 Background and Motivation

Turkey is located on the relatively small Anatolian plate, which is squeezed between three other major tectonic plates. The north-moving African and Arabian plates are located to the south, and the south-moving Eurasian plate is located to the north. The combination of these plate movements is forcing the Anatolian plate to move west into the Aegean Sea. Sandwiched in between the Eurasian, Arabian and African plates, the Anatolian plate is being slowly spun in a counter-clockwise direction to accommodate the more prodigious northward progress and slight westward penchant of the Arabian plate relative to the African plate. This movement produces fault structures at the boundary between the plates. It is largely accommodated by left-lateral slip on the East Anatolian Fault and right-lateral slip along the North Anatolian Fault (McKenzie, 1972). The movement is slow, but persistent with occasionally spectacular results. [Ambraseys, Finkel 1995; Barka, Kadinsky-Cade 1998].

Fifty-seven destructive earthquakes have struck Turkey in the twentieth century, most occurring along the 1,500 km long North Anatolian Fault. The M 7.9 Erzincan earthquake of December 27 1939, was the largest of these earthquakes [Sezen et al. 2000]. Since the scientific studies indicate that the probability of occurrence of severe and destructive earthquakes in Turkey is very high, this situation presents a serious threat to the large building stock and their occupants and lifelines in the country [Aschheim, Gulkan et al. 2000].

In Turkey there are thousands of apartment buildings that are prone to severe damage in a moderate or larger earthquake. These buildings are typically three-to-seven storeys and consist of relatively poorly detailed and constructed reinforced concrete frame members infilled to various extents by unreinforced masonry walls [Aschheim, Gulkan et al. 2000]. The main characteristics of these buildings are described in the Appendix A to better understand their behaviors during the earthquakes.

One of the principal current challenges in structural engineering concerns the development of innovative design concepts to better protect structures from the destructive damaging effects of the earthquakes. It is possible to reduce structural vibrations for improved safety and/or serviceability under wind and earthquake loadings by structural control [Büyüköztürk 2000]. The main research needed with conventional design and strengthening methods is the optimization of design to achieve a satisfactory structural performance level based on seismic demand and structural capacity.

In conventional earthquake-resistant design of buildings (and other constructions) the dynamic effect of the input is represented by static equivalent forces, which are obtained from normalized acceleration response spectra defined as the ratio between the peak ground acceleration (PGA) and the maximum absolute acceleration in an equivalent Single-Degree-of-Freedom (SDOF) system. This approach presents several drawbacks: (i) these equivalent forces are strongly coupled to the elastic and hysteretic characteristics of the structure, thus making the seismic design cumbersome, (ii) after the onset of yielding, the correlation between the design

forces and the structural damage is not feasible, and (iii) the damage caused by the cumulative inelastic excursions [Fajfar, Vidic 1994] is not accounted for. More recently, the displacement-based design procedures have been proposed [Priestley, Calvi, Kowalsky 2007]; in these strategies, the dynamic effect of the input is represented by imposed displacements, that are obtained from displacement response spectra relating the PGA to the maximum relative displacement in the top of the building. This formulation uncouples partially the input effect, in terms of displacement, from the characteristics of the structure and allows a satisfactory correlation between the imposed displacement and the component of the structural damage that is related to the maximum displacement. Conversely, the component of damage that is related to the cumulative plastic strain energy cannot be appropriately considered. A more rational seismic design approach, which overcomes also this difficulty, is to express the dynamic input effect through energy response spectra. Interpreting the effect of earthquakes in terms of energy is gaining extensive attention [Housner 1956; Berg, Tomaides 1960; Kato, Akiyama 1975; Housner, Jennings 1977; Hall et al. 1984; Zahrah, Hall 1984; Akiyama 1985; Uang, Bertero 1988 and 1990; Kuwamura et al. 1994; Bruneau, Wang 1996; Bertero et al. 1996; Yei, Otani 1999; Chou et al. 2000; Chou, Uang 2003; Adang 2007; Leelataviwat et al. 2009; Jiao et al. 2011]. This approach has three major advantages: (i) the input effect in terms of energy and the structural resistance in terms of energy dissipation capacity are basically uncoupled, (ii) except in the short period range, the input energy, E_I, introduced by a given ground motion in a structure is a stable quantity, governed primarily by the natural period T and the mass m, and scarcely by other structural properties such as resistance, damping and hysteretic behavior, and (iii) the consideration of the cumulative damage fits well with this formulation and can be directly addressed. In the energy-based methods the design criterion is constituted by the comparison between the energy absorption capacity of the structure (i.e. its seismic resistance) and the input energy (i.e. the effect of the ground motion). It is then necessary to establish the input energy spectrum corresponding to the expected earthquake, i.e. design input energy spectrum.

This work consists of proposing energy spectra for earthquake-resistant design based on accelerograms registered in high seismicity regions of Turkey. The spectra have been derived through linear and nonlinear dynamic analyses on the selected Turkish accelerograms. In the long and mid period ranges the analyses are linear, taking profit of the rather low sensitivity of the spectra to the structural parameters other than the mass and the fundamental period. Conversely, in the short period range, the spectra are more sensitive to the degree of plastification of the structure and, hence, the analyses have to be nonlinear; about them, elastic-perfectly plastic systems with constant-ductility are considered.

The considered registers are selected among those available in Turkey. The chosen records are treated (base-line correction and filtering) and classified according to the design input acceleration (e.g. the seismic zone), the soil type of the seismic station (following the classification of the Eurocode 8), the magnitude of the earthquake and the relevance of the near-source effects, namely the velocity pulses. The design energy spectra are envelopes of the actual spectra, in terms of equivalent velocity, corresponding to each input (pair of horizontal components); the influence of the vertical components has been disregarded. These derived spectra have an initial growing branch (starting from zero) in the short period range, a horizontal branch in the mid period range and a descending branch in the long period range. Median and characteristic spectra are proposed; regardless of the statistical distribution of the spectral ordinates, such levels are intended to correspond to 50% and to 95% percentiles, respectively.

Empirical criteria for estimating the energy input contributable to damage (hysteretic energy) from the total input energy are also suggested. These criteria take mainly into account the damping level, the degree of plastification, and the period.

The proposed design energy input spectra are compared with those obtained from other studies.

1.2 Objectives

1.2.1 Main Objective

The main goals of this study are:

- Proposal of energy spectra for earthquake resistant design in high seismicity regions based on Turkish registers.

- Proposal of empirical criteria for estimating the ratio between the hysteretic energy in terms of velocity (V_D) from the input energy in terms of velocity (V_E).

This study can be applied not only to Turkey but also to regions with similar seismicity.

1.2.2 Specific Objectives

To reach the aforementioned main objectives, these specific objectives are pursued:

- To obtain the registers with the good quality data form and the ones that are in the range of selection criteria, which is set to be PGA > 0.01 g primarily.
- To treat the registers to eliminate the noise and other errors that can contain.
- Grouping the selected registers, according to their soil type, their seismic zone, their magnitude, and their impulsivity.
- Carrying out linear dynamic analyses for each selected register to obtain energy spectra. Two types of spectra are obtained, such as the one without any scaling and the one that is scaled according to the norm that is described within the text.
- Carrying out dynamic non-linear analyses under constant ductility for each selected registers to obtain energy spectra that are valid for the short period.
- Determining envelopes for each spectrum.
- Proposing design spectra based on these envelopes.
- Comparing the design energy input spectra proposed in that study with those proposed by other researchers.
- Developing an empirical formulation for calculating the hysteretic energy (i.e. contributing to the structural damage) as a function of the input energy.

1.3 Methodology

This section describes in more detail the investigation carried out to achieve each of the above specific objectives.

Obtaining strong-motion registers in Turkey. Registers of the national strong ground-motion network, which is operated by the Earthquake Research Department, are used in this study. The database is recently updated and provides the detailed information for the processing of the selected registers; thanks to the project carried out recently named as “Compilation of National Strong Ground-Motion Database in Accordance with International Standards”. As result, 169 registers corresponding to 82 seismic events and being recorded in 90 stations are considered in this study. Every register contains horizontal (NS and EW) and vertical accelerograms; vertical components are disregarded

Analyzing and processing the registers. The registers are treated with baseline correction and with bi-directional, zero-shift (“acausal”), 4^{th}-order Butterworth filtering. The low and high-cut frequencies are taken as defined in the work of Erdogan [Erdogan 2008; Akkar et al. 2010]. The low-cut frequency ranges generally in between 0.05 and 0.5 Hz (2 and 20 s) and the high-cut

frequency ranges in between 15 and 40 Hz (0.067 and 0.025 s). Later case by case the uncorrected and corrected PGV, PGA and PGD values are checked. Also the obtained Fourier spectra, resulting velocity and displacement traces are examined visually.

Linear dynamic analyses are carried out to determine the shape of the input energy spectra in the range of periods above the natural (characteristic) period of the soil. The horizontal components of selected records were used for linear dynamic analysis. In the mid and long period ranges the input energy is a rather stable quantity that is primarily governed by the total mass and fundamental period T of the structure, being scarcely affected by its strength or hysteretic properties: therefore, in these ranges the linear input energy spectrum obtained by linear dynamic analyses can be considered valid also for nonlinear systems.

Non-linear dynamic analyses are carried out to determine the shape of the input energy spectra in the short period range, where the energy spectral ordinates are not as clearly independent on the resistance and the hysteretic behavior. Analyses are carried out for viscous damping of 2%, 5% and 10%. Respect to the ductility, it is considered elasto-plastic (without hardening) and analyses are performed at constant ductility of 2, 3, 5, 10, 15 and 20. These spectra are also used for estimating the V_D / V_E ratio.

Proposal of design input energy spectra. By using the results of linear and nonlinear analyses, design input energy spectra for earthquake-resistant design of structures in regions of moderate to high seismicity, is proposed. For the proposal of design energy spectra, the registers are classified into 12 groups according to soil type, magnitude of the earthquake, and the presence of near-fault effects. The proposed spectra have three branches, corresponding roughly to short, medium and long period ranges, respectively; the first branch is linear starting from zero, the second branch is constant, and the third branch is decreasing.

Comparison with other studies. The obtained spectra are compared with those proposed by Decanini and Mollaioli [1998, 2001] and with those proposed from registers from Colombia [Benavent et al. 2010], Iran [Amiri el al. 2008] and Greece [Tselentis et al. 2010]. As well, the proposed spectra are compared with those proposed for Japan by the current Japanese seismic code [BSL 2009] and by Akiyama [Akiyama 1985].

Empirical formulation for hysteretic energy. Hysteretic energy is the portion of the input energy contributing to structural damage; it is important to know the relation between these two values for desing purposes. Comparing the analysis proposed by other researchers, an empirical equation is formulated for soft soil and stiff soil, which assesses this relationship as a ratio depending on the cumulative ductility. This process is performed for different values of damping.

1.4 Organization of this document

This document is organized into seven chapters, where the first chapter is this introduction. The second chapter is the state of art, which is a review of seismic design methodologies, along with a summary of Housner-Akiyama formulation and recent contributions. The third chapter describes the seismicity of Turkey, the current seismic standards, the available registers and the processing of the selected registers. The fourth chapter presents the proposal of design input energy spectra in terms of velocity, V_E. In the fifth chapter the obtained hysteretic energy spectra and the proposal of new empirical expressions to calculate the V_D / V_E ratio is defined. In chapter 6, the proposed design input energy spectra are compared with other similar studies. Chapter seven presents the overall conclusions of the research and the future investigations. Appendix A describes briefly the most common construction technologies in Turkey, Appendix B describes the calculation of the slope of the initial branch of input energy and Appendix C lists the publications generated during this research.

2 State of Art

2.1 Earthquake Resistant design Methods

This section presents a brief introduction and a concise historical review of earthquake-resistant design strategies of structures. Although this study has a general context, it is especially applicable for the buildings subjected to horizontal seismic inputs. Formulations for other situations (e.g. vertical inputs or structures other than buildings) are basically similar.

The first seismic analysis methods appear on the year 1923 in Japan (after the earthquake in Kanto [Ohashi 1993]) and can be included within the package of so-called *Earthquake Analysis Methods Based on Resistance.* Basically these procedures were intended to provide buildings with lateral (horizontal) resistance; it was believed that if the structure of the building had enough lateral resistance it should be capable to survive the design earthquake. This resistance is guaranteed by designing the structure to be able to withstand horizontal forces applied at each floor level and in each direction of the building (usually two orthogonal directions). Figure 2-1 illustrates this concept.

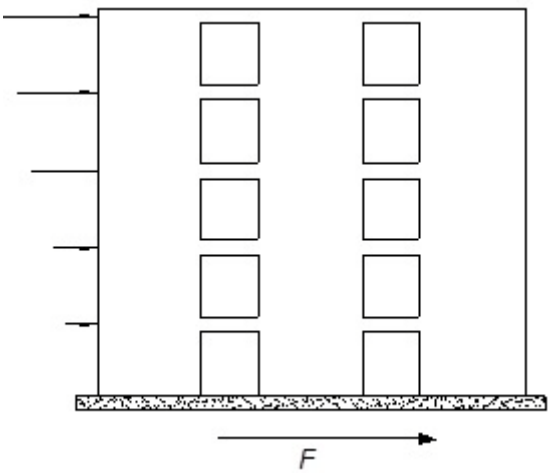

Figure 2-1 Lateral forces that are equivalent to a seismic input

In Figure 2-1, *F* is the sum of the forces acting at each floor level; in other words, the horizontal interaction force between the ground and the building. *F* is also known as base shear. Obviously, the value of *F* quantifies the severity of the earthquake effect on the building.

In the firstly developed earthquake-resistant design methods, horizontal forces represented in Figure 2-1 were obtained by multiplying the weight of each floor by a constant coefficient. This ratio between the horizontal and vertical forces was called seismic coefficient and in the first 1923 Japanese Seismic Code [Ohashi 1993] it was estimated as 0.1. This value gradually increased as it was experienced that structures designed with this resistance value failed when

an earthquake stronger than expected occurred. This ratio took to the values of 0.10, 0.15 and 0.20 until, thanks to the development of computers and by having more and more seismic experiences, it was concluded that structures that had been designed with a certain lateral resistance, did not reach collapse but could suffer damage in the case of a larger earthquake. After that, resistance was not the primary goal and everybody started paying more attention to the ductility; it can be roughly defined as the ability of a given structure to resist after the onset of damage. The ductility of a given building can be estimated from observed damages or by numerical simulation. The regulations began to introduce the concept of ductility by quantifying it with a *response reduction factor*, which reduces the equivalent lateral forces (Figure 2-1); it was mentioned in the 1957 American design code [Housner 1990]. Thus, this approach has been incorporated to the current worldwide regulations. In summary, most of the earthquake-resistant regulations require to provide buildings with a certain level of lateral resistance. This resistance is obtained by dividing the resistance that a given building should have to remain in the elastic range under the design input by the aforementioned response reduction factor. This factor should obviously be equal to or greater than the unity. This coefficient is represented by different symbols in each standard; in the case of Spain [NCSE-02 2002] it is termed μ, in the European standard [EN-1998 2004] it is named q, in the United States [IBC 2000] and in Turkey it is known as R. It is remarkable that, in fact, this ratio does not take into account only the ductile behaviour of the structure but also includes the over-resistance of the building due to the conservative considerations that are regularly considered (safety factors, among others) and the increase of the material resistance under dynamic inputs ("strain rate effect").

In any case, it should be kept in mind that in these methods the effect of the earthquake on the structure is characterized by means of equivalent static forces (Figure 2-1); they are determined as those that generate a lateral displacement equal to the maximum one that would occur along the duration of the earthquake. However, another possible strategy is to represent the seismic action by a much more direct way: as input accelerograms. In this case, dynamic analysis must be performed to determine the time-history responses; then, the maximum values will be selected, they would represent the design demands. This formulation is often referred to as *earthquake resistant design based on dynamic calculations*. This strategy seems appropriate and has apparently shown to be quite capable of simulating the actual seismic behaviour of structures with great accuracy and reliability; however, there are some drawbacks that hinder the use of such formulations: (1) the information about the earthquakes that may occur for a particular structure during its lifetime is limited, which severely impairs the accuracy of the study, (2) for economic reasons, structures are designed to behave non-linearly during the design earthquake (the most severe earthquake expected with a reasonable probability) and, hence, nonlinear dynamic analyses are a must. Dynamic analyses in the nonlinear regime are much more complex than the, already complex, dynamic linear calculations. Currently the most common way of characterizing the dynamic effect of earthquakes is by equivalent static forces (or other non-dynamic quantities, e.g. not forming part of a dynamic calculation) obtained from elastic response spectra. Next section explains how to determine these values using response spectra.

2.1.1 Earthquake resistant design based on spectra

2.1.1.1 Response spectra

In general terms, these methods are based on estimating the equivalent static forces (which characterize the effect of the seismic action) in terms of the fundamental period of the structure. This is done by using response spectra; they are plots whose ordinates are certain response magnitudes and whose abscissas are the natural periods of SDOF systems that represent the structure. Up to date, three types of spectra have been basically proposed: absolute acceleration, relative displacement, and energy spectra. In the absolute acceleration spectra the ordinates are the ratio between the maximum absolute acceleration in the top of the building and the maximum input acceleration in the base of the building. In the relative displacement spectra the ordinates are the ratio between the maximum relative displacement between the top and the base

of the building and the maximum input relative displacement. In the energy spectra the ordinates are the input energy introduced by the seismic input in the building. These three types of spectra are described next in this subsection; applications to earthquake resistant design are described in the three following subsections, respectively. It is noteworthy that each of these three spectra considers a meaningful response magnitude: the relative displacement is an indicator of the apparent structural damage level (i.e. not cumulative), the absolute acceleration is related the human perception of the motion and the damage to the facilities (and, more generally, to all the non-structural elements) and the energy reports on the accumulated structural damage.

The energy spectra are usually expressed in terms of equivalent velocity which is the square root of the ratio between the double of the input energy and the mass.

Linear spectra plot the ratio between the maximum values of the response of an elastic single-degree-of-freedom system and of the input acceleration. Figure 2-2 shows an elastic model of a single-degree-of freedom system undergoing a horizontal ground motion z_g.

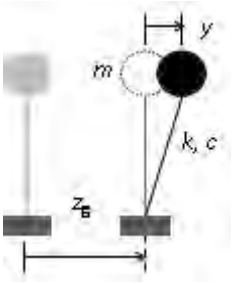

Figure 2-2 Elastic single degree of freedom systems

In Figure 2-2, *m*, *c* and *k* are the mass, damping and stiffness coefficients, respectively, *y* is the relative displacement between the mass and the base (degree-of-freedom) and z_g is the displacement of the ground. Yet this formulation is commonly applied to horizontal motion, can be also considered for vertical vibrations.

The equation of motion of the system described in Figure 2-2 is given by

$$m\ddot{y} + c\dot{y} + ky = -m\ddot{z}_g \tag{2-1}$$

By dividing both sides by *m*, relation (2-1) becomes

$$\ddot{y} + 2\zeta\omega_0\dot{y} + \omega_0^2 y = -\ddot{z}_g \tag{2-2}$$

In this relationship, ω_0 is the undamped natural frequency of the system and ζ is the critical damping factor. These coefficients are given by

$$\omega_0 = \sqrt{\frac{k}{m}} \qquad \zeta = \frac{c}{2m\omega_0} \tag{2-3}$$

The damped natural frequency ω_d is related to ω_0 and to ζ by

$$\omega_d = \omega_0\sqrt{1-\zeta^2} \tag{2-4}$$

It is remarkable that, unless the damping ζ takes extremely high values, ω_0 and ω_d are nearly coincident.

The acceleration, velocity and displacement spectra are obtained, for each input $z_g(t)$, as the maximum values of the absolute acceleration $\ddot{x}$ (where $\ddot{x} = \ddot{y} + \ddot{z}_g$), relative velocity $\dot{y}$ and relative displacement y. They depend on the natural period T ($T = 2\,\pi/\,\omega_0$) and on the damping factor ζ. These quantities are obtained by the following linear relationships [Clough, Penzien 1993; Chopra 2001; García Reyes 1998]:

$$y(t) = -\frac{1}{m\omega_d}\int_0^t m\,\ddot{z}_g(\tau)\sin\omega_d(t-\tau)e^{-\zeta\omega_0(t-\tau)}d\tau \tag{2-5}$$

$$\dot{y}(t) = \int_0^t \ddot{z}_g(\tau)\cos\omega_d(t-\tau)e^{-\zeta\omega_0(t-\tau)}d\tau - \frac{\zeta\omega_0}{\omega_d}\int_0^t \ddot{z}_g(\tau)\sin\omega_d(t-\tau)e^{-\zeta\omega_0(t-\tau)}d\tau \tag{2-6}$$

$$\ddot{x}(t) = \left(\frac{2\zeta^2\omega_0^2}{\omega_d} - \frac{\omega_0^2}{\omega_d}\right)\int_0^t \ddot{z}_g\cos\omega_d(t-\tau)e^{-\zeta\omega_0(t-\tau)}d\tau - -2\zeta\omega_0\int_0^t \ddot{z}_g(\tau)\cos\omega_d(t-\tau)e^{-\zeta\omega_0(t-\tau)}d\tau \tag{2-7}$$

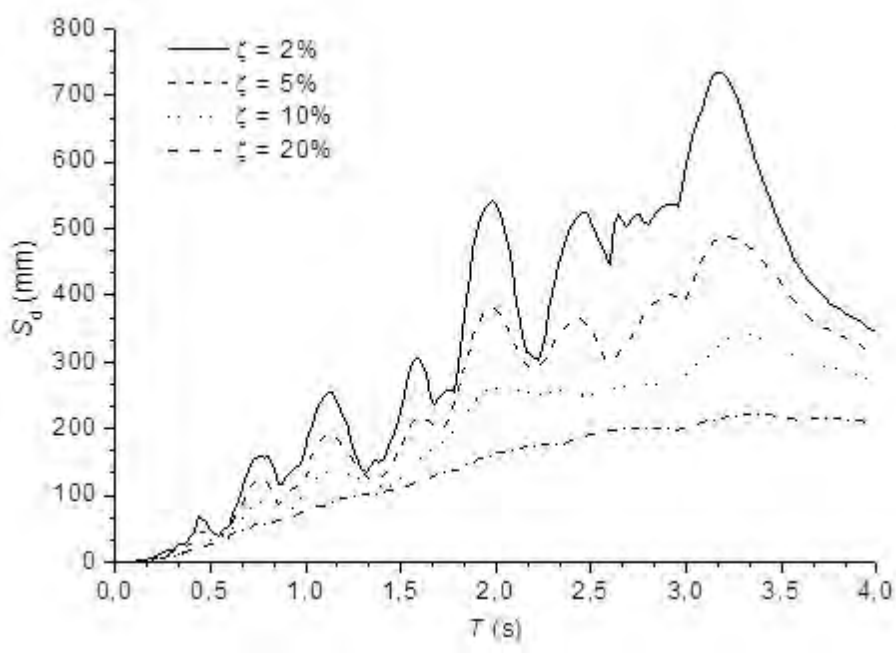

Figure 2-3 Relative Displacement Spectra

Figure 2-3, Figure 2-4 and Figure 2-5 show, relative displacement, relative velocity and absolute acceleration spectra, respectively. Such spectra correspond to the accelerogram registered in the ICA2 station (E-W component) during the Pisco earthquake, 15 august 2007.

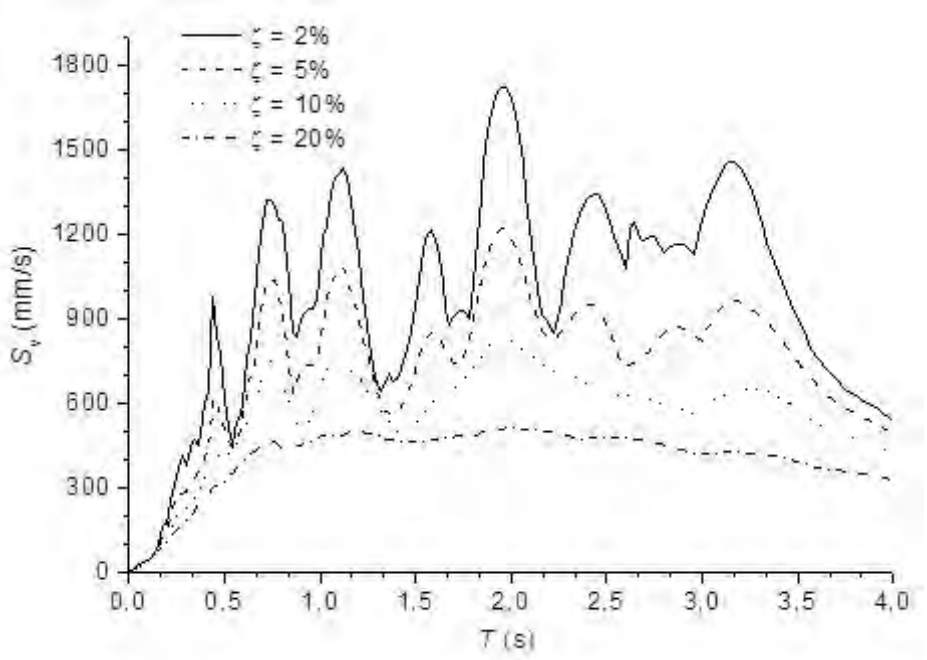

Figure 2-4 Relative Velocity Spectra

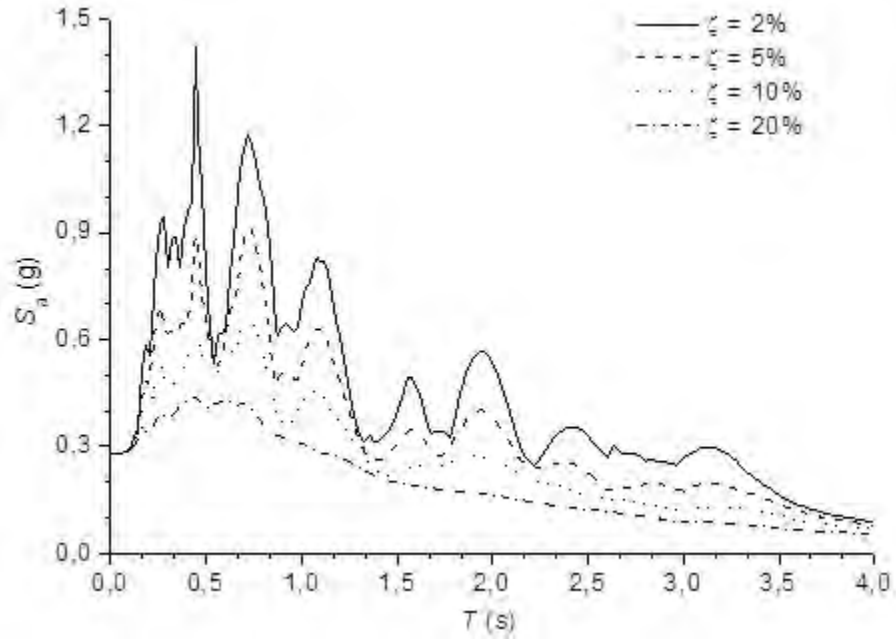

Figure 2-5 Absolute Acceleration Spectra

Figure 2-3, Figure 2-4 and Figure 2-5 show that the spectral ordinates decrease with the increasing damping ratio; this shows that damping has a beneficial effect, since it contributes to reduce relevant response magnitudes (relative displacement, relative velocity and absolute acceleration). Moreover, the spectrum corresponding to zero damping exhibits sharper peaks

than the spectra for non-zero damping; it means damping contributes to smoothen the spectra, e.g. making it less sensitive to small period changes.

It has been demonstrated [Chopra 2001] that for small values of damping and not too long periods (under 10 seconds), the velocity spectra are obtained by multiplying the acceleration spectra by $T / 2\pi$ and that the displacement spectra are obtained in the same way from the velocity ones:

$$S_v = S_a \ (T / 2\,\pi) \qquad S_d = S_v \ (T / 2\,\pi) = S_a \,(T / 2\,\pi) \tag{2-8}$$

These relationshipe among the three types of spectra allows an easy shifting among them. At this point it should be clarified that, in fact, in order to satisfy these relationships it is necessary to modify slightly the spectra of velocity and acceleration; hence, they should be termed in a more correct way pseudo-velocity and pseudo-acceleration spectra [Clough, Penzien 1993; Chopra 2001; García Reyes 1998]. In this thesis, we will usually replace these names by velocity and acceleration spectra.

Figure 2-3, Figure 2-4 and Figure 2-5 correspond to the spectrum of a single input, and consequently are not applicable for the earthquake resistant design of a particular structure as it would not be reasonable to design it only to support that single input. In fact, different accelerograms should be considered and then the spectrum envelope should be taken. The earthquake-resistant design standards propose different spectra whose shape is similar to those of Figure 2-3, Figure 2-4 and Figure 2-5, although they are significantly smoother. As an example, the spectrum of the Spanish code [NCSE-02 2002] is shown in Figure 2-6.

2.1.1.2 Absolute acceleration response spectrum

As discussed in the previous subsection, the absolute acceleration response spectra are curves that represent, in ordinates, the ratio between the maximum values of the absolute acceleration of the SDOF system that represents the dynamic behaviour of the structure in a given vibration mode and the ground acceleration. The design spectra are smoothed envelopes obtained from a number of individual records.

Figure 2-6 shows, the design spectrum of the Spanish regulation [NCSE-02 2002].

Figure 2-6 Design acceleration spectra [NCSE-02 2002]

The spectrum shown in Figure 2-6 consists of three branches: a linearly increasing one (e.g. with exponent 1), a constant one (e.g. with exponent 0) and a hyperbolically decreasing one (e.g. with exponent −1). Periods T_A and T_B depend on the characteristics of the soil, being higher as it has less stiffness; in some codes, the spectral ordinate (e.g. the height of spectrum) also grows as the flexibility of the soil does. The interpretation of each of these branches in terms of

the effect of the earthquake on the structure is quite clear: (1) short-period structures are very rigid (usually they are low-rise) and tend to behave as the surrounding soil, but its motion is amplified as its rigidity decreases, (2) in the medium period range, the ground motion reaches its highest amplification inside the building and, (3) in the long periods range, structures are flexible enough so that its stiffness is not capable of overcoming the high inertia forces. This interpretation helps us to understand the influence of the soil stiffness in T_A and T_B: for stiff soil the range of building periods whose motion is highly amplified (in between T_A and T_B) is narrow, while this range widens and encompasses higher rise buildings as the soil becomes less stiff.

This spectrum is commonly presented in dimensionless form (the ordinates S_a are dimensionless); in this way the base shear is determined as the product of the weight of the building (W), the soil coefficient (S), the importance factor (ρ) and the peak ground acceleration (a_{max}), divided by the ductility factor R:

$$F = S_a(T_1)\, W\, S\, \rho\, a_{max} / R \tag{2-9}$$

In this relation W is the weight of the building; obviously it depends on the percentage of live load that is simultaneous with the design earthquake, each code specifies this percentage in terms of the use of the building. S is the soil coefficient; for hard soil (rock and stiff soil) its value is usually 1 and it takes higher values for softer soils (S rarely reaches values greater than 1.50, except on very soft soils). The importance factor ρ is a coefficient that quantifies the severity of the consequences of the collapse of the building; in buildings of normal importance (such as residential constructions) is $\rho = 1$ and for more important buildings is $\rho > 1$. a_{max} is the design peak ground acceleration expressed in "g". The values of a_{max} are specified by the seismic design codes; usually each country is divided into distinct zones, each of them with its own value of a_{max}. In the Spanish seismic regulations, the values of a_{max} range from 0.04 g (minimum considered value) and 0.25 g (for some municipalities in the province of Granada). The Spanish regulations quantify a_{max} as the expected seismic acceleration on stiff soil (not rock) for an earthquake with 500 years return period. It is remarkable that this criterion does not coincide with those considered in most countries; normally it is considered as the expected seismic acceleration in rock for a return period of 475 years. Finally, the response reduction factor R (*ductility* behavior factor) represents the ability of of the structure of undergoing plastic deformation until failure; in other words it represents the safety margin of the structure after the onset of plastification. The current design standards estimate the values of R in a rather empirical way; these values basically depend on the type of structure and of the structural detailing, especially the connections among members. In the Spanish code [NCSE-02 2002] this coefficient is denoted by μ and four situations are considered: $\mu = 1$ (no ductility), $\mu = 2$ (low ductility), $\mu = 3$ (high ductility) and $\mu = 4$ (very high ductility); other codes often consider higher values for this coefficient. Figure 2-6 shows that $S_a(0) = 1$; replacing this result in equation (2-9) we conclude that for structures of high horizontal stiffness when $S = \rho = 1$, the equivalent static force is equal to $a_{max}\, W / R$. Consequently, since the acceleration in the base and the top of this type of structures should be virtually alike regardless of ductility, it follows that R should tend to 1 when T approaches zero.

In multi-storey buildings, F represents the sum of the forces acting on each floor; in other words, it is the horizontal interaction force between the ground and the building (Figure 2-1). This force has to be distributed among the floors proportion to their masses and modal amplitudes (for the considered vibration mode of the building). The forces acting at the each level represent the equivalent seismic effect; hence, they can be used to obtain the lateral resistance to be provided to the building.

In single-degree-of-freedom systems (typically, used to describe single-story buildings), the interpretation of the abscissa of the spectrum is very clear, as it represents the natural period of

the system. In actual structures (typically multi-storey buildings), multi-degree-of-freedom models should be considered. In this case, the application of this method is carried out usually in modal coordinates; in each *i-th* mode, its natural period T_i is considered. The structure should be decomposed in different vibration modes, the maximum response for each mode is calculated and then such responses are combined by using empirical rules (SRSS "Square Root of the Sum of the Squares", CQC "Complete Quadratic Combination" [NCSE-02 2002], among others). Typically, the combinations are set in terms of the shear forces at each floor, in other words, the sum of shear forces on the columns and walls of each floor. For each mode the situation is similar to that described in Figure 2-1; the main difference is that the interaction force *F* has to be distributed among the different floors in proportion to their masses and modal amplitudes corresponding to the considered mode. The regulations usually specify the number *r* of modes to be included in the calculation, two types of criteria are generally provided: empirical ones and more complex criteria based on the distribution of equivalent modal masses [Clough, Penzien 1993; Chopra 2001; García Reyes 1998]. The empirical criteria often link the value of *r* with the fundamental period of the building and its plan symmetry; *r* generally ranges from 1 (for symmetrical buildings of small to medium height) and 4 (for high-rise buildings asymmetric). The criteria based on the equivalent mass of each mode often recommends a value of *r* such that the sum of the equivalent masses of the modes included in the combinations reach at least 90% of the total mass of the building, in some cases [EN-1998 2004] also reports that should include all modes whose equivalent modal mass exceed 5% of the total mass of the building.

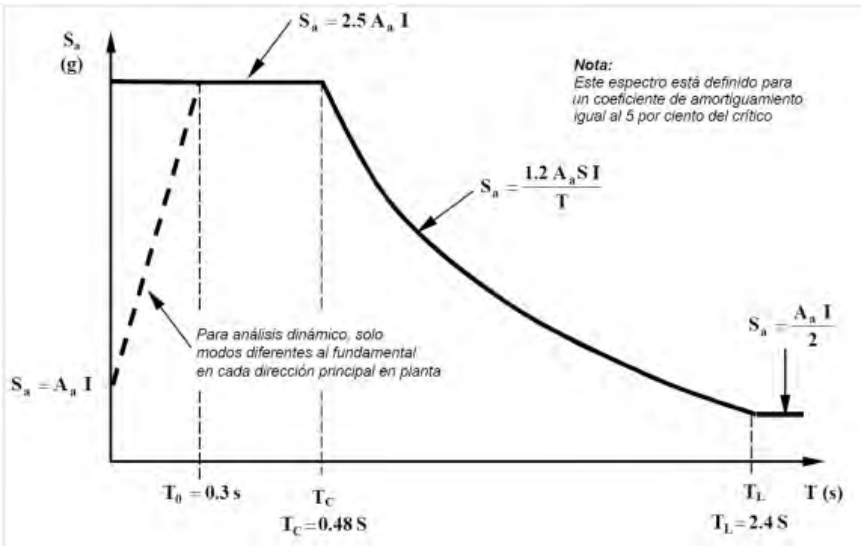

Figure 2-7 Design acceleration response spectra [NSR-98 1998]

It should be emphasized that equation (2-9) represents, with minor modifications, the approach suggested by almost all the current earthquake-resistant regulations.

Figure 2-7 shows another example of design acceleration spectrum, obtained from the Colombian standard [NSR-98 1998]. Figure 2-7 shows, similarly to Figure 2-6, a typical absolute acceleration spectrum, which is divided into four segments: (1) short periods ($T < T_0$), the spectrum presents a linearly increasing branch, (2) medium periods ($T_0 < T < T_C$), the spectrum shows a horizontal branch (commonly known as plateau), (3) long periods ($T_C < T < T_L$), the spectrum usually decreases hyperbolically (with exponent -1) and (4) very long periods ($T_L < T$), the spectrum is again horizontal but with lower height than the medium periods plateau. Similarly to what happens in Figure 2-6 with periods T_A and T_B, the values of the periods T_0, T_C and T_L depend on the characteristics of the soil, being higher as the soil is more flexible. In the very long periods, the reduction of the spectral ordinate is interrupted not to minimize in excess the effect on tall buildings.

It is remarkable that in some cases [EN-1998 2004] in the very long periods, instead of levelling the height of the spectrum, there is a sharper decrease of spectral ordinate. This fact is shown in Figure 2-8. In the two decreasing branches in Figure 2-8 (between T_C and T_D periods and beyond period T_D) the exponents usually take values close to – 1 and – 2, respectively (hence, the branch between T_C and T_D periods is hyperbolic).

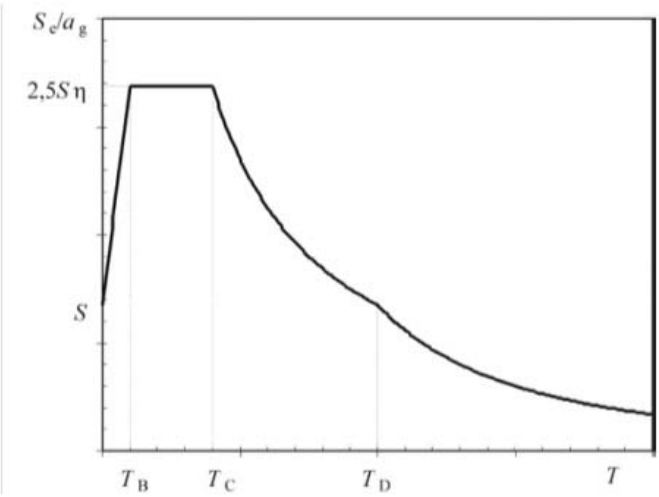

Figure 2-8 Design acceleration response spectra [EN-1998 2004]

The spectral ordinates grow as the damping of the structure decreases; this is consistent with Figure 2-3, Figure 2-4 and Figure 2-5 with the interpretation that damping reduces the response of the structure. The spectra proposed by the codes correspond generally to damping 5% since most of buildings correspond to this level of damping. The regulations generally incorporate correction coefficients for other levels of damping; for example, the Spanish standard includes a coefficient given by $\nu = (5/\Omega)^{0.4}$ where Ω is the damping factor expressed in percentage and the European standard [EN-1998 2004] includes a similar expression given by $\eta = [7/(2+\zeta)]^{0.5}$ where ζ is the damping factor expressed in percentage. For example, for a damping factor 4%, the Spanish legislation proposes a coefficient $\nu = (5/4)^{0.4} = 1.09$ and European standard proposes a coefficient $\eta = [7/(2+4)]^{0.5} = 1.08$; for a damping factor of 6%, $\nu = (5/6)^{0.4} = 0.93$ y $\eta = [7/(2+6)]^{0.5} = 0.935$. It is remarkable that, since the damping exerts a beneficial effect of reducing the structural response, the adoption of damping factors greater than 0.05 needs adequate justification.

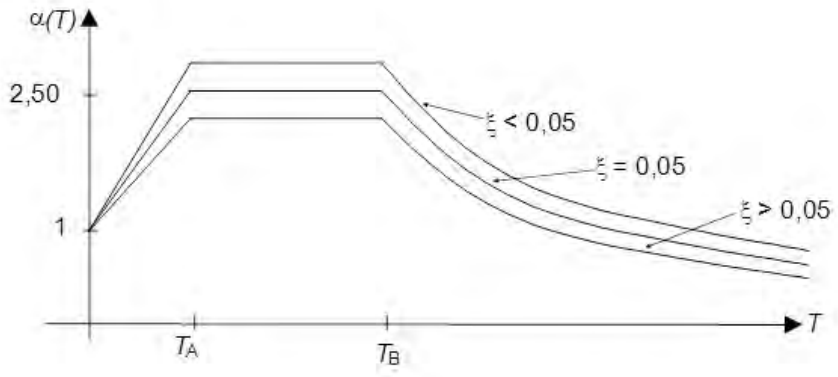

Figure 2-9 Design acceleration spectra for different values of damping

The damping correction of the design spectra is usually done by multiplying it by the corresponding coefficient (ν or η in the above examples) but keeping the initial value $S_a = 1$ for

$T = 0$ (what is consistent with Figure 2-5). Figure 2-9 shows the spectrum of Figure 2-6 with the adjusted values of damping above and below 5%.

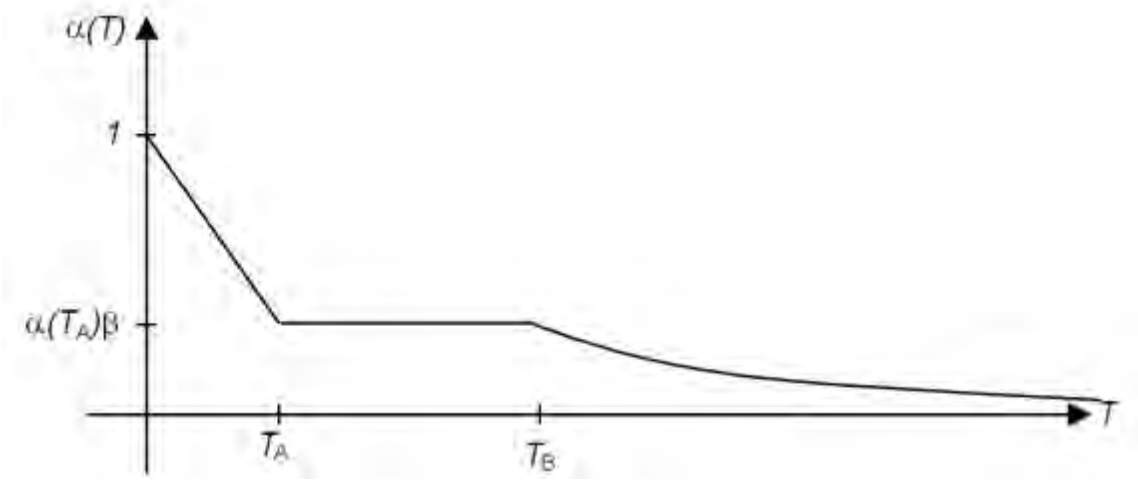

Figure 2-10 Non-Linear Design Acceleration Spectrum

The codes consider the ductility by reducing the force *F*, it is divided by the ductility coefficient (response reduction factor). In some cases, this operation is carried out of the spectrum, as shown in equation (2-9), but often it is incorporated into the spectrum by dividing their ordinates by that coefficient. In that way there are two types of spectra, those in which the ordinates are not divided by any factor and those in which they have been divided by it. The first spectra are termed linear (or elastic) spectra and the second spectra are termed nonlinear. Obviously, the spectra shown in Figure 2-3 to Figure 2-9 are linear; Figure 2-10 shows a nonlinear spectrum obtained essentially dividing the spectrum of Eurocode 8 in Figure 2-8 by the ductility coefficient (*q*).

Remarkably, since the normalized spectral ordinate of the plateau is usually equal to 2.5, if the ductility factor is higher than that value, the initial branch is decreasing instead of increasing; this fact is reflected in the spectrum of Figure 2-10.

It should be noted that the absolute response acceleration spectra characterize the dynamic effect of a group of earthquakes in terms of forces (as represented in Figure 2-6 to Figure 2-10). This involves several drawbacks, first of all (and possibly one of the most important) the quantification of the severity of an earthquake in terms of the force *F* is only meaningful when the structure is maintained in elastic regime, since the more severe the earthquake, the greater the response acceleration and the internal forces; therefore, this is directly related to the resistance that must be provided to the structure. However, when the structure yields, the lateral force *F* is maintained essentially constant, hence, the internal forces are kept constant; therefore, the force ceases to be a valid parameter to characterize the dynamic effect of the earthquake. For example, even if the peak ground acceleration and/or the duration of a given input accelerogram is several times larger and/or longer than another one, if both earthquakes are severe enough to induce an inelastic response of the structure, both will produce approximately the same lateral force on the structure, while the response in terms of maximun displacements and damage can be completelly different. The more severe the earthquake, the higher the structural damage and the maximum displacements; therefore, the damage cannot be characterized in terms of forces. In other words, there is a more direct correlation between damage and displacement comparing to the existing correlation between damage and force. The following subsection describes the relative displacement spectra discussing how avoiding this drawback.

2.1.1.3 Relative Displacement Response Spectra

The dynamic effect of the seismic action is characterized through relative displacement spectra. As discussed previously, they consist of representations of maximum relative displacement of a SDOF system that represents the response of the structure in a given vibration mode (in ordinates) as a function of its period (in abscissas). Equation (2-8) indicates that these diagrams can be obtained from the absolute acceleration spectra by multiplying them by $(T / 2\ \pi)^2$. Figure 2-11 shows an example of design displacement spectra obtained from the reference [Priestley, Calvi, Kowalski 2007] and corresponding to the acceleration spectrum of the European code [EN-1998 2004]. The horizontal axis contains the natural period of the mode under consideration and the vertical axis contains the relative displacement between the mass of the equivalent SDOF system and its base. These spectra correspond to the envelope of the maximum values of equation (2-5) for the expected accelerograms. In other words, they are the envelopes of individual spectra as those represented in Figure 2-3. The comparison with Figure 2-8 confirms that these spectra can be obtained by multiplying the acceleration spectra by $(T / 2\ \pi)^2$. Equation (2-5) shows that the displacement spectra are dependent on damping, as the acceleration spectra (as described in the preceding paragraph).

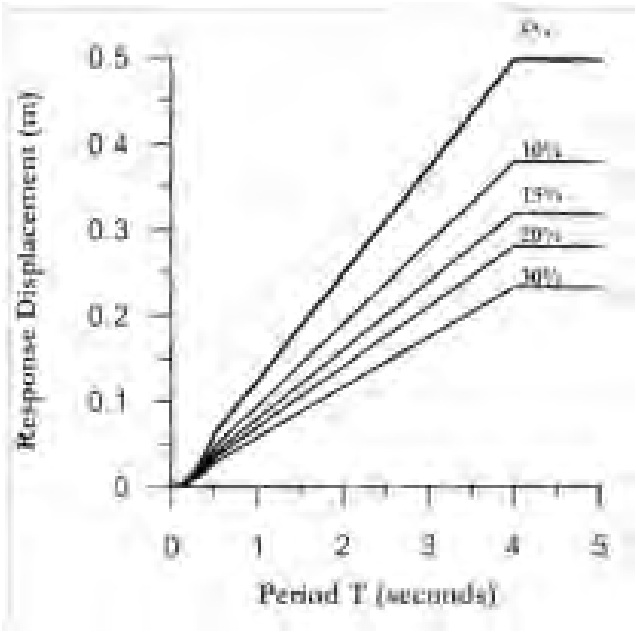

Figure 2-11 Design Displacement Spectra [Priestley, Calvi, Kowalski 2007]

This strategy (based on displacements) constitutes an advance compared to the methods based on forces since beyond the linear range, it is more reasonable to quantify the input as an imposed motion than as an equivalent force. To characterize the effect of the seismic action through forces is appropriate as long as the structure remains elastic, but is no longer valid as the structure yields.

While the behaviour of the structure is linear (in other words, there is no any damage) the force is a fairly reliable index of the damage. But once the structure yields, it rapidly loses its rigidity and the displacement increase significantly faster than the forces (assuming a possitive post-yield stiffness), so that a small variation of forces can generate a significant change in displacement and therefore in structural damage. Since there is a strong correlation between the displacement and the damage, "Displacement Based Design" is usually identified with "Performance Based Design" (described in subsection 2.1.2) [Priestley, Calvi, Kowalski 2007].

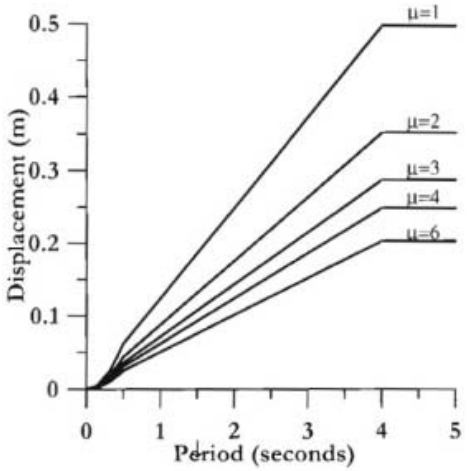

Figure 2-12 Design Displacement Spectra for Different levels of Ductility [Priestley, Calvi, Kowalski 2007]

The nonlinear behaviour of structures can be represented in terms of an equivalent viscous damping coefficient. Alternatively, similarly to the seismic design methods based on forces, a ductility coefficient can be considered. Figure 2-12 represents displacement spectra for different values of the displacement ductility factor μ (ratio between the maximum displacement d_{max} and the yielding displacement d_y: $\mu = d_{max} / d_y$). It is remarkable that the influence of μ is not linear; the reference [Priestley, Calvi, Kowalski 2007] provides procedures to quantify it.

2.1.1.4 Input Energy Response Spectra

This formulation consists basically of characterizing the dynamic effect of the seismic action by energy spectra; they are representations of the energy introduced into the structure by the earthquake (E_I) (in ordinates) in function of the period of an SDOF system that represents the structure in a given vibration mode (in abscissas). Typically, the energy is expressed in terms of equivalent velocity (V_E) by the relation

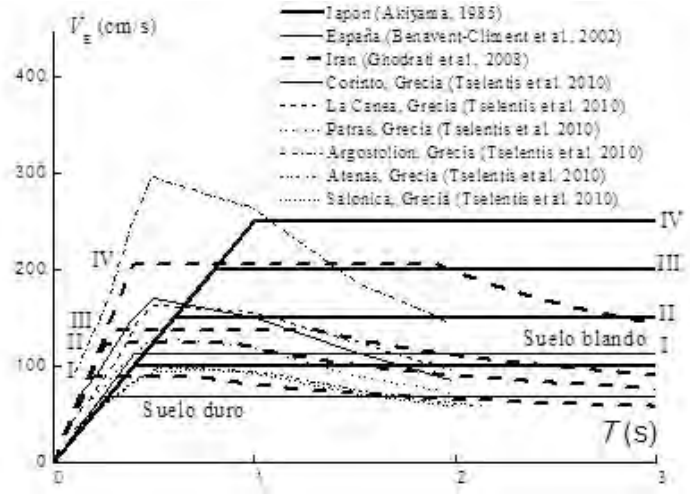

Figure 2-13 Examples of design energy spectrum (in terms of velocity) proposals for Japan, Greece, Spain and Iran

$$V_E = \sqrt{2E_I / m} \tag{2-10}$$

In this expression m is the mass of the structure. Figure 2-13 shows an example of energy spectra in terms of equivalent velocity.

Most of the spectra that are represented in Figure 2-13 are bilinear with an initial branch starting from the origin and a horizontal branch; as well, in some spectra decreasing branches are observed for long periods. Comparing the bilinear spectra represented in Figure 2-13 with the acceleration spectrum in Figure 2-6 confirms that, except in the short period range, these spectra (velocity) may be obtained approximately by multiplying the acceleration by $T / 2\pi$, as indicated by equations (2-8). In this case the period T_B in Figure 2-6 corresponds to the intersection between both branches. In fact, the increasing branch between $T = 0$ and $T = T_A$ in the velocity spectrum corresponds to a parabolic segment, but in practice it resembles a straight line, whereby the energy spectra in terms of velocity generally have a linearly increasing branch in the range of periods between 0 and T_B. Moreover, comparing the spectra with decreasing branches represented in Figure 2-13 with the acceleration spectrum in Figure 2-8 shows that these branches correspond to the periods higher than T_D in Figure 2-8. Figure 2-13 illustrates the energy levels in terms of equivalent velocity (equation (2-10)) for different soil types: type I corresponds to hard rock or very hard conglomerates where the shear velocity v_s is higher than 750 m/s, type II corresponds to hard packed sand and gravel with $375 \leq v_s < 750$ m/s, type III corresponds to intermediate soils like sands and gravels semi-compact with $175 \leq v_s < 375$ m/s, and type IV is soft soil with $v_s < 175$ m/s. The characterization of very soft ground (with $v_s <$ 175 m/s) requires special studies as there are important differences among the existing types.

The methods that are based on energy spectra are the basis for this study. The seismic input is not characterized in terms of forces (as in the methods based on acceleration spectra) nor in terms of displacement (as in the methods based on displacement spectra) but in terms of the product of both quantities (force per displacement), in other words, in terms of energy.

The main advantages of the methods based on energy spectra are:

- The ability to quantify the amount of energy that the design earthquake introduces in a given structure provides conceptual clarity and allows representing the effect of the seismic input by a simple scalar quantity.

- We can define from the design stage how do we want the structure dissipates the energy: deforming plastically, storing it temporarily (along the input duration) as elastic vibration energy and allowing then it to dissipate by the natural damping of the structure or by a combination of both.

- Damage can be quantified in the structure after an earthquake, by means of cumulated plastic deformation energy.

The methods based on energy balance (also known as methods based on the energy balance-Housner-Akiyama) have their origins in the work of George Housner [Housner 1956], Tanahashi [Tanahashi 1956], Berg and Thomaides [Berg, Thomaides 1960], Kato and Akiyama [Kato, Akiyama 1975], Housner and Jennings [Housner, Jennings 1977], [Housner 1956], Uang and Bertero [Uang, Bertero 1988; Uang, Bertero 1990], McCabe and Hall [McCabe , Hall 1989], Fajfar et al. [Fajfar et al. 1992], Zhu and Tsu [Zhu, Tsu 1992], Wang and Bruneau [Bruneau, Wang 1996], Chapman [Chapman 1999] and Chou and Uang [Chou, Uang 2000], among others. Housner died in 2008, having been one of the most productive and successful researchers in earthquake engineering, especially in energy methods. The wrong idea that Housner's concept of energy was inherited by Veletsos and Newmark [Veletsos, Newmark 1960] has hindered the development of energy-based methods. During many years, it was

wrongly understood that the concept of energy proposed by Housner had been continued in the work of Veletsos and Newmark. However, Veletsos and Newmark were not interested in calculating the energy that an earthquake introduced into the structure, they used the energy stored/dissipated by elastic/elastoplastic SDOF systems under monotonic loading up to the maximum displacement (not the total energy input during the cyclic loading reversals), to relate the maximum displacements in a given range of periods.

One of the greatest contributions to this methodology is due to Professor Hiroshi Akiyama, whose investigations are an important part of its current theoretical framework. Akiyama [Akiyama 1985] showed that the amount of energy introduced by an earthquake in a given structure is a highly stable quantity with respect to the structural resistance, the distribution of its rigidity and mass, the damping level and the hysteretic behavior of the structural elements; it depends basically on the fundamental period of vibration of the structure and its mass. This conclusion has also been verified experimentally by dynamic tests on earthquake simulators [Uang, Bertero 1990]. Moreover, the dependence of the energy on the mass is proportional; in consequence, the energy expressed in equivalent velocity (V_E) is independent of the mass, as expressed by the relationship (2-10). These circumstances provide a significant advantage when interpreting the effect of the earthquake on the structure in terms of energy instead of forces; the advantage is that the problem of assessing the seismic force induced by the earthquake and the problem of estimating the resistance of the structure (the term resistance is understood in a broad sense) can be uncoupled, in other words, can be treated separately.

However, it should be noted that the independence between the energy E_I and the properties of strength, stiffness, damping and hysteretic behavior of the structure has some exceptions, among these are the quasi-harmonic motion, in other words, a narrow frequency content. For example, the energy introduced by a harmonic motion in an undamped system can reach infinite values if the frequency of excitation corresponds to the natural frequency of the structure (in this case, resonance occurs if the duration of excitation is sufficient); consequently it is strongly dependent on the damping of the structure. In summary, in narrow-band inputs (typical of soft soil) the energy introduced by the earthquake E_I depends heavily on the properties of the structure. This is a limitation of the seismic design methods based on energy

In the seismic design methodology based on energy balance, the effect of the earthquake on the structure is expressed in terms of the energy introduced by the earthquake and the strength of the structure is measured by its limit capacity for energy absorption W_u. The condition for the structure to survive the earthquake can be written as follows:

$$W_u > E_I \tag{2-11}$$

This relationship is the basic criterion of energy balance for checking the suitability of the structure to withstand the design earthquake by accepting a certain level of damage. However, it should be noted that in fact it is not true that a certain structure has a single value of energy dissipation capacity; in fact, it depends on the type of excitation and, specially, on the history of loading [Benavent 2007; Chai 1995; Chai 2004; Erberik, Sucuoğlu 2004; Sucuoğlu, Erberik 2004]. This makes the evaluation of the ultimate energy dissipation capacity of structures a cumbersome issue that, for design purposed, can be addresed by using lower bound values. On the other hand, obviously, the energy absorption capacity of a structure depends on its general characteristics, and consequently analyses for different types of most common structural systems (concrete frames, concrete walls, steel frames, steel braced frames, masonry buildings, wooden buildings, buildings with base isolation, energy dissipation buildings, etc.) must be carried out. The usual strategy [Akiyama 1999] is first, to define the regions of the structure where plastic strain energy is expected to be released (plastic hinges), second, to determine the capacity of each floor and, third, to analyze the distribution of damage among the different floors. The third part is the most important and cumbersone one, and at the same time one of the

main advantages of energy-based seismic methods, because the proness of a structure to damage concentration in given stories can be addressed, controlled and forseen. For this purpose a damage concentration coefficient *n* is defined, in the reference [Akiyama 2003] it is described the calculation of this coefficient from dynamic analyses. The applicability of this study is limited because it is based on an excessively low number of earthquakes. For the purpose of further studies, the hysteretic models described in references [Erberik, Sucuoğlu 2004; Sucuoğlu, Erberik 2004] can be useful as they relate the degradation of stiffness and strength to the energy consumption.

The capacity of each floor (or the whole structure) can be estimated mainly in two ways: from its hysteretic behavior (subsection 2.1.3.4), or from the results of nonlinear dynamic analyses of the structure under seismic actions. The first procedure is described in [Akiyama 1985] and basically consists of identifying the damage with the cumulated ductility η. The second procedure is based on determining the values of damage indices that quantify the damage to the structure; the values of these indices are obtained from the dynamic analyses. Different indices to assess structural damage have been proposed in the literature [Lybas, Sozen 1977; Banon, Veneciano 1982; Park; Ang 1985; Soo et al. 1989]. Among them, the Park & Ang index [Park, Ang 1985] is one of the most used for reinforced concrete structures and has the advantage of being calibrated experimentally, so that the values adopted may be related to damage levels observed in real structures. The index of Park & Ang damage referred to a particular structural component is defined by the following expression:

$$D = \frac{\delta_M}{\delta_u} + \frac{\beta}{Q_y \delta_u} \int dE_H \tag{2-12}$$

δ_M is the maximum strain response (in absolute value) and δ_u is the ultimate deformation capacity under monotonic forces. Q_y is the yield strength and β is an empirical calibration factor ranging between 0.03 and 1.2, with an average value of 0.15. In the reference [Cosenza et al. 1990] it is shown that β = 0.15 provides a good correlation with other indices of damage. Importantly, the term δ_M of the above formula includes the elastic deformation. Accordingly, in cases where the structural element is kept within the elastic domain (i.e. without structural damage) the index value of Park & Ang can be different from zero. The index of Park & Ang of a part or of all the structure can be estimated by the weighting average of the damage indices of the components:

$$D = \sum \lambda_i D_i \tag{2-13}$$

The summation extends along all the involved structural components. D_i is the damage index of the structural component *i* and λ_i is a weighting factor defined as the ratio of the plastic energy in the structural component *i* and the plastic energy in all the structural components of the storey or in the whole structure. The index of Park & Ang damage has been calibrated by many researchers from the observation of damage to actual structures under past earthquakes [Park et al. 1987; Gunturi 1992; Leon, Ang 1985; Stone, Taylor 1994] and its correlation with these are indicated in Table 2-1.

Table 2-1 Correlation between the Park & Ang index and the observed damage

Observed damage	**Damage index Park & Ang**
Small damage	0.1 – 0.2
Medium damage	0.2 – 0.5
Severe damage	0.5 – 1
Collapse	> 1

In general, the collapse of the structure is defined as the state in which one of the structural elements (mainly beam or column) loses its restoring force. One of the main shortcomings of

the Park and Ang indexes of damage is that they do not consider the influence of the loading path (i.e. history of loading) followed by the structure. An alternative index that takes into account the loading path was proposed by Benavent-Climent [16] in the context of steel structures.

2.1.2 Displacement based earthquake-resistant design

The objective of the current seismic design codes is to prepare the structure to resist the design seismic input only under ultimate limit state; in other words, the structure is intended to resist the design earthquake with an acceptable level of serious damage but without collapse (in other words, avoiding at all costs the loss of human lives). Remarkably, that approach does not include any requirement about the behavior under seismic actions with lower or higher level of severity; this contrasts with the usual strategy against other type of actions (gravity, for example) where two types of limit states (ultimate and service) are considered. This approach is broadly valid and has been used for decades but was in shortage especially after the Northridge earthquake in 1994 and Kobe in 1995; after these highly severe earthquakes it was found that some structures, even those relatively new and that had been designed with the latest seismic standards, did not collapse (and in them there were no human casualties), but the damage to buildings (both structural and non-structural) was very serious. In the Kobe earthquake, some hospitals had been so intensely reinforced that effectively its structure did not collapse but absolute accelerations in the building were so high that it damaged the installations and were unusable at the time of greatest need (a few hours after the earthquake). After these events, the earthquake engineering was directed not only to prevent loss of human lives but also to quantify, reduce and prevent the damage. Depending on the damage we are able to accept when an earthquake occurs, different solutions can be proposed. This strategy is commonly known as "Performance Based Design"; it is mainly described in the references [Bertero et al. 1996], [Hamburger 1998], [SEAOC 1995], [FEMA 350 2000], [FEMA 356 2000], [FEMA 349 2000], [EERC 1995] and [ATC-58 2002]. These documents present different seismic design methodologies oriented to control and to quantify the level of structural damage due to seismic action and to design structures that do not exceed the corresponding level.

Based on structural and non-structural damage the following four levels of performance ("Performance States") [SEAOC 1995] are defined:

Based on structural and non-structural damage defines the following four levels of performance ("Performance States") [SEAOC 1995]:

- **Fully Operational**. Uninterrupted service. Negligible structural and non-structural damage.

- **Operational**. Most of the activities can be resumed immediately. The structure is safe and can be inhabited. The essential activities are maintained while the non-essential ones are interrupted. Repairs are necessary to resume the non-essential activities. Slight damage.

- **Life Safe**. Moderate damage, the structure remains safe. Some elements or components of the building may be protected to avoid damage. The risk of loss of life is low. The building may need to be evacuated after the earthquake. The repair is possible, but can be economically unfeasible.

- **Near Collapse**. Severe damage, but without risk of collapse. Possible fall of non-structural elements.

More recently, another similar classification is considered [ATC-40 1996; FEMA 350 2000; FEMA 356 2000; FEMA 349 2000]:

- **Immediate Occupancy**. Occupants' safety. Important services are not uninterrupted. Negligible structural damage. The global damage is minor. The period of lack of functionality ("down time") is about 14 hours.

- **Damage Control**. Slight structural damage. Achievable occupants' safety. The essential activities are repairable. Moderate overall damage. The period of lack of functionality ("down time") is about 2 or 3 weeks.

- **Life Safety**. Probable structural damage but no collapse. No risk from falling non-structural elements. The evacuation of the occupants can be done without risk. Possibility of irreparable building.

- **Collapse Prevention**. Severe structural damage, with risk of collapse. Likely fall of non-structural elements. The evacuation of the occupants may involve risk. Building likely irreparable.

These four levels are often represented by their initials: IO, DC, LS and CP. The three levels IO, LS and CP are the most commonly used for seismic design; Figure 2-14 presents a graphical and easily understandable way, the practical significance of these levels and their relationship with the percentage of damage. The case "operational" in this case refers to a building without any damage

For each structural type, more precise definitions of these levels have been developed depending on the type of experienced structural damage..

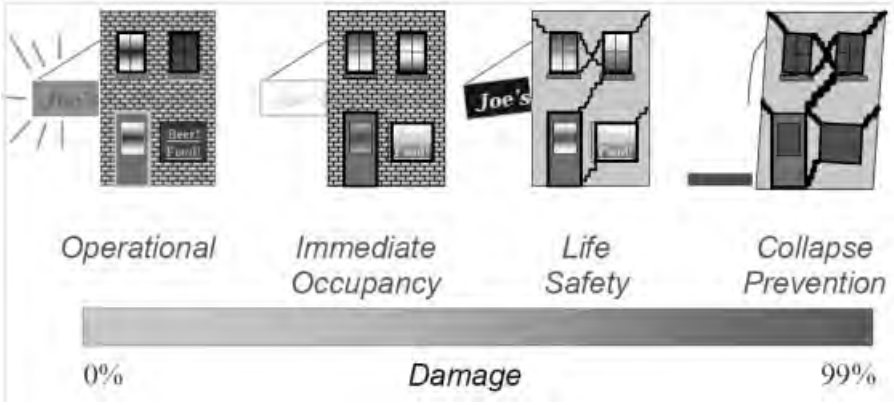

Figure 2-14 Damage Levels [Hamburger 1998]

Regarding the seismic action, four levels of severity as defined as specified in Table 2-2.

Table 2-2 Severity levels of the seismic inputs

Design Earthquake	Return Periods (years)	Probability of Occurrence
Frequent	43	50% in 30 years
Occasional	72	50% in 50 years
Rare	475	10% in 50 years
Very rare	970	10% in 100 years

Table 2-2 shows that the severity of the earthquakes is quantified in terms of their return period; it is understood as the average of the elapsed time among earthquakes with the same magnitude or, almost equivalently, as the inverse of the probability of occurrence in one year. In some cases seismic actions more severe than those contained in Table 2-2 are considered; the so-called MCE ("Maximum Considered Earthquake") [Malhotra 2006] corresponds to a return period of about 2475 years. The relationship between the return period T and the probability p_n of being exceeded n years is given by the expression$T = -n/ln(1 - p_n)$; it is often used to indicate the severity of an earthquake by the probability p_{50} to be exceeded in 50 years, for example, in the case of MCE is $p_{50} = 1 - e^{-\frac{50}{2475}} = 0.02$ and in the case of an earthquake "Rare" is $p_{50} = 1 - e^{-\frac{50}{475}} = 0.10$.

Table 2-3 shows the demand levels of for each of the four performance levels previously described [SEAOC 1995], when the earthquakes that have the probability of occurrence specified in Table 2-2 occur.

Table 2-3 shows three levels of protection (expressed by the three represented diagonals): less intense for systems of moderate importance ("Basic Facilities"), more intense for major facilities ("Essential / Hazardous Facilities") and even more intense for crucial facilities ("Safety critical Facilities"). For example, in "Essential / Hazardous Facilities" (diagonal terms) it is required that for an earthquake of return period of 75 years the building remains fully operational, for an earthquake of return period of 475 years the building keeps operating in its major functions and for a return period of 970 years the building is able to preserve the lives of its occupants.

Table 2-3 Required levels of protection for each severity level of the seismic action [SEAOC 1995]

Levels of the expected earthquake	**Level of required behaviour**			
	Full Functionality	Functionality	Life Safety	Near Collapse
Frequent (43 years)			Unacceptable Behaviour	
Occasional (72 years)				
Rare (475 years)				
Very Rare (970 years)				

2.1.3 Non Linear Static Analyses ("push-over")

2.1.3.1 Capacity Curves

The method of earthquake-resistant design based on displacements consists basically of comparing the capacity of the structure, characterized by a curve representing its behavior under incremental forces, with the effect of the design earthquake, characterized by a demand curve. The intersection between both curves is termed as "target drift" (or displacement) or "performance point", in other words, that point indicates the effect produced by the earthquake on the structure [ATC-40 1996]. The capacity curve is usually expressed by representing on the ordinates the interaction force F between the building and the base (Figure 2-1) and on the abscissas the displacement of the top floor [Krawinkler 1998; Kircher et al. 1997]. The analysis that generates this curve is static and obviously non-linear, being commonly known as push-over. Figure 2-15 shows an example of a capacity curve obtained from a push-over analysis.

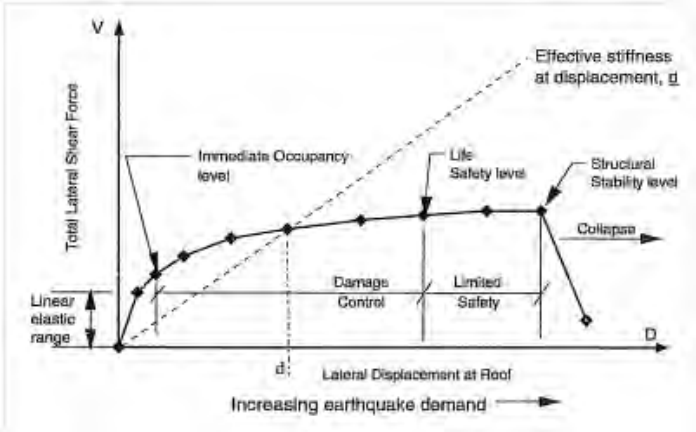

Figure 2-15 Capacity curve obtained from "push-over" analyses [ATC-40 1996]

In Figure 2-15 *V* represents the interaction force between the building and the ground (base shear force) and *D* is the displacement of the upper floor. The correspondence between the values of *D* and the aforementioned performance levels is also indicated.

In the push-over analyses the base shear force is distributed along the floors according to certain patterns; the most commonly used are the first modal shape or linear ("triangular") distributions. The push-over analyses are made incrementally, in other words, the lateral forces are increased progressively. For small values of *F*, the behavior of the structure is linear and as *F* increases the structure is becoming gradually more damaged; the stiffness of the structure decreases and its capacity curve becomes more flat. The smallest slope of the capacity curve with the increasing displacement illustrates clearly the elongation of the natural period of the structure.

Some researchers [Fajfar, Fischinger 1988; Bracci et al. 1997; Gupta, Kunnath 2000] have proposed techniques to modify the distribution of the lateral forces among the floors to take into account the variation of the modal properties (mainly the first mode modal vector) by the increasing degradation of the structure. Other studies have proposed techniques to take into account the contribution of the higher modes [Gupta, Kunnath 2000; Paret et al. 1996; Sasaki, Freeman, Parent 1998; Kunnath, Gupta 2000; Matsumori et al. 2000], also [Chopra 2001; Goel, Chopra 2002; Chintanapakdee, Chopra 2002] have proposed a new formulation known as Modal Push-Over Analysis.

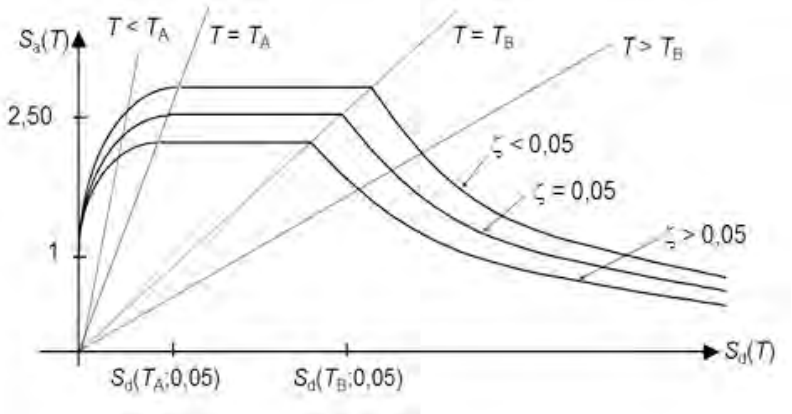

Figure 2-16 Acceleration spectra vs. Displacement spectra

2.1.3.2 Target Displacement

The demand is characterized by the design spectrum for the considered level of seismic action (Table 2-2); to be able to intersect it with the capacity curve, it is represented as the absolute

acceleration spectrum S_a (vertical axis) vs. the relative displacement spectrum S_d (horizontal axis). This type of representation is commonly known as "Acceleration-Displacement Response Spectra" (SARD). Figure 2-16 shows a spectrum from Figure 2-9 plotted using these coordinates.

The methods mostly used to obtain the target displacements are:

- Capacity Spectrum Method [ATC-40 1996]
- Displacement Coefficient Method [FEMA 356 2000]
- Equivalent linearization method [FEMA 440 2005]
- Modified displacement coefficient method [FEMA 440 2005]
- Modified Capacity Spectrum [ATC-40 1996]

Capacity Spectrum Method

In order to intersect the curves as shown in Figure 2-14 and Figure 2-15, they must be represented in the same coordinates. In this strategy [ATC-40 1996], the capacity curve is modified as (Figure 2-14): the ordinate is divided by the part of the building mass that corresponds to its first mode (in other words, the equivalent modal mass divided by the total mass) [Clough & Penzien 1993; Chopra 2001; García Reyes 1998] and the abscissa is multiplied by the modal participation factor of the first mode [Clough & Penzien 1993; Chopra 2001; Garcia Reyes 1998]. The capacity curve expressed in these coordinates is usually termed as capacity spectrum. Obtaining a target displacement for each level of damage (characterized by design displacement, horizontal axis of the spectrum of Figure 2-16) is performed in an iterative way according to the following process:

- To select the desired value for the design displacement and to find the corresponding acceleration determined by the spectrum in Figure 2-16.
- To determine, from the capacity curve, the horizontal force (on the vertical axis) that corresponds to the selected displacement. The curve between the origin and this point will be replaced by an equivalent bilinear plot. The first branch of this plot coincides with the linear part of the capacity curve (from the origin) but extends beyond it. The second branch of this plot is similar to the actual capacity curve; it is selected with the provision that the areas bounded by the bilinear plot and the actual capacity curve (until the design displacement) are equal. Figure 2-17 shows an example of this process. Once the bilinear plot is generated, the equivalent damping viscous damping ζ_{eq} is determined; ζ_{eq} is selected (as usual, [Clough & Penzien 1993; Chopra 2001; García Reyes 1998]) by equalling the areas of the hysteresis loops for the bilinear plot and with viscous damping. This damping is added to the inherent damping in the structure, whose value is usually 5%.
- The acceleration-displacement spectrum is corrected to fit the value of ζ_{eq} obtained in the previous stage. The intersection between the corrected spectrum and the capacity curve (in the coordinates according to the formulation given in [ATC-40 1996]) is determined. If the abscissa of this intersection is close to the selected displacement (with a predetermined tolerance), the point corresponds to the target displacement. Otherwise, the process has to be repeated iteratively until a sufficient approximation is reached.

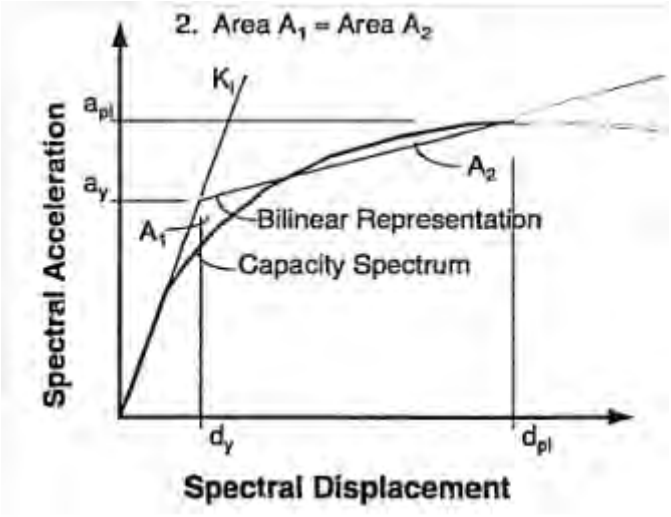

Figure 2-17 Bilinear approximation of the capacity curve [ATC-40 1996]

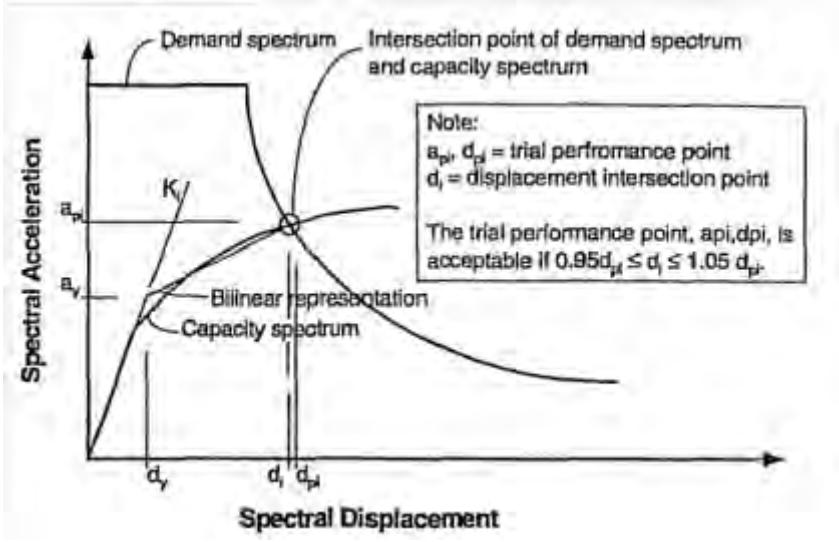

Figure 2-18 Obtaining the target displacement [ATC-40 1996]

Figure 2-18 describes the iterative process for obtaining the target displacement.

Displacement Coefficient Method

This method uses the following empirical formula for calculating the target displacement:

$$\delta_t = C_0 C_1 C_2 C_3 S_a \frac{T_e^2}{4\pi^2} g \tag{2-14}$$

T_e is the effective fundamental period of the equivalent SDOF system, calculated using the bilinear approximation of the capacity curve (Figure 2-19):

$$T_e = T_i \sqrt{\frac{K_i}{K_e}} \tag{2-15}$$

T_i is the fundamental period calculated by an elastic dynamic analysis and K_i is the lateral stiffness. K_e is the effective lateral stiffness that is taken as the secant stiffness corresponding to a base shear force equal to 60% of the effective yield strength of the structure.

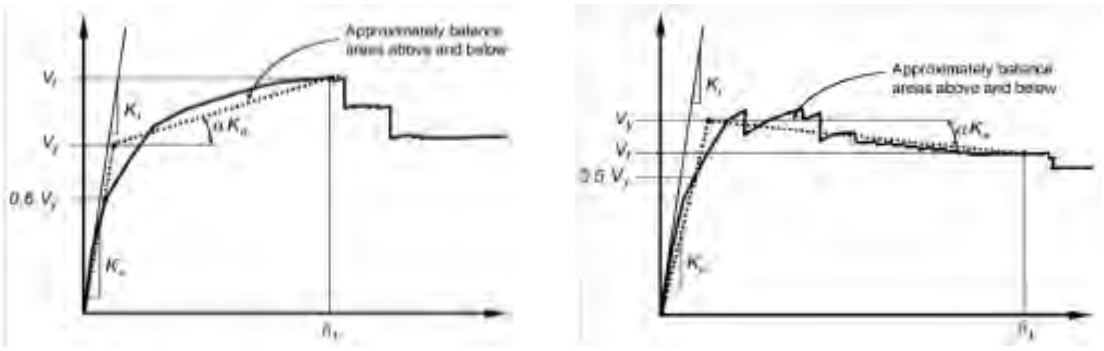

(a) Positive post-yielding slope (b) Negative post-yielding slope

Figure 2-19 Idealized Force – Displacement curves [FEMA 356 2000]

C_0 is a coefficient that relates the displacement of an equivalent single-degree-of-freedom system with the displacement on the roof of the building. Table 2-4 presents a way to obtain the values of C_0 [FEMA 356 2000] as a function of the number of stories of the structure, the building type and variation of the forces through the height obtained from the push-over analysis.

Table 2-4 Values for modification factor C_0 [FEMA 356 2000]

Table 3-2 Values for Modification Factor C_0[1]

	Shear Buildings[2]		Other Buildings
Number of Stories	Triangular Load Pattern (1.1, 1.2, 1.3)	Uniform Load Pattern (2.1)	Any Load Pattern
1	1.0	1.0	1.0
2	1.2	1.15	1.2
3	1.2	1.2	1.3
5	1.3	1.2	1.4
10+	1.3	1.2	1.5

1. Linear interpolation shall be used to calculate intermediate values.
2. Buildings in which, for all stories, interstory drift decreases with increasing height.

In equation (2-14) C_1 is a modification factor that relates the expected inelastic displacements with those calculated for the linear elastic response: for $T_e \geq T_s$ is $C_1 = 1$ and for $T_e \geq T_s$ is $C_1 = [1 + (R - 1)T_S / T_e] / R$. T_s is the characteristic period of the response spectrum (transition between the branches of constant acceleration and constant velocity) and R is the ratio between the elastic and inelastic demands calculated by $R = [S_a / (V_y / W) / C_m]$ where V_y is the yield strength obtained from the idealized capacity curve, W is the weight of the building and C_m is the equivalent modal mass participation factor of the first mode; alternately [FEMA 356 2000] proposes a table ("Table 3.1") with approximate values

In equation (2-14) C_2 is a modification factor representing the effect of the shape of the hysteresis loops. Table 2-5 presents the values of C_2 [FEMA 356 2000] depending on the level of damage, the type of frame and the fundamental period of the building.

Table 2-5 Values for modification factor C_2 [FEMA 356 2000]

Table 3-3 Values for Modification Factor C_2

Structural Performance Level	$T \le 0.1$ second[3]		$T \ge T_S$ second[3]	
	Framing Type 1[1]	Framing Type 2[2]	Framing Type 1[1]	Framing Type 2[2]
Immediate Occupancy	1.0	1.0	1.0	1.0
Life Safety	1.3	1.0	1.1	1.0
Collapse Prevention	1.5	1.0	1.2	1.0

1. Structures in which more than 30% of the story shear at any level is resisted by any combination of the following components, elements, or frames: ordinary moment-resisting frames, concentrically-braced frames, frames with partially-restrained connections, tension-only braces, unreinforced masonry walls, shear-critical, piers, and spandrels of reinforced concrete or masonry.
2. All frames not assigned to Framing Type 1.
3. Linear interpolation shall be used for intermediate values of T.

In equation (2-14) C_3 is a modification factor that represents the increment of displacement due to the second order effects. For buildings with positive post-yield stiffness Figure 2-19(b)), C_3 is equal to 1 and for buildings with negative post-yield stiffness (Figure 2-19 (a)) C_3 is calculated as $C_3 = 1 + [|\alpha| (R - 1)^{3/2}] / T_e$. α is the ratio of post-yield stiffness to the effective elastic rigidity, with the relation of force-displacement (capacity curve) represented by a bilinear approximation (Figure 2-19).

These operations must be carried out iteratively:

- Estimate a (Δ) value for the displacement. Make a bilinear approximation. Get K_e, T_e and the ductility factor μ.
- Check the response spectra S_a (for a damping factor 5%) with the period T_e.
- From S_a obtain H (m S_a) and the displacement Δ.
- Get factors C_1, C_2 and C_3 and the scaled displacement Δ C_1 C_2 C_3.
- Compare the scaled displacement Δ with its initial value, the iteration should continue until both are equal (with a prescribed tolerance).

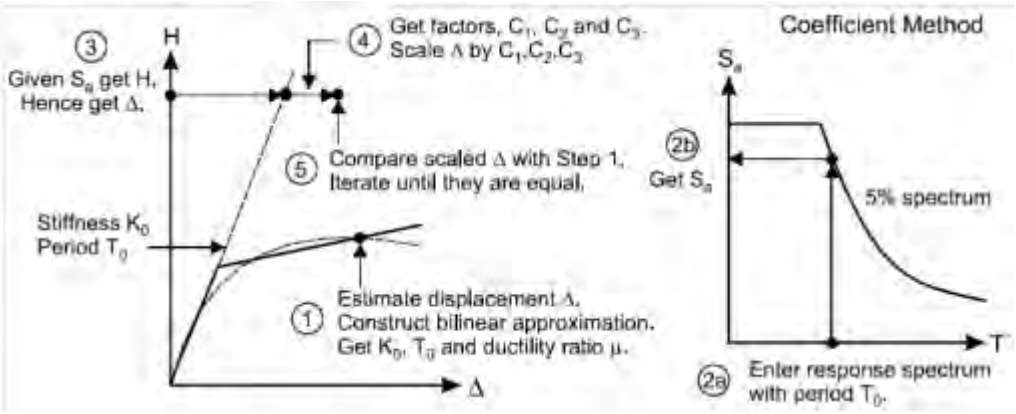

Figure 2-20 Iterative operations in the displacement coefficient method

Linearization method

The following operations should be performed iteratively (Figure 2-21):

- Estimate an initial value (Δ) for the displacement. Make a bilinear approximation. Get K_e, K_h, T_e and the ductility factor μ.
- From K_e, K_h, T_e and μ obtain the effective stiffness K_{eff}, the effective period T_{eff} and the damping factor B_{eff}.

- Obtain the S_a ordinate of the response spectrum with the period T_e and the damping B_{eff}.
- From S_a obtain H (m S_a) and displacement Δ.
- Compare the scaled displacement Δ to the initial value; the iteration should continue until both are equal (with a prescribed tolerance).

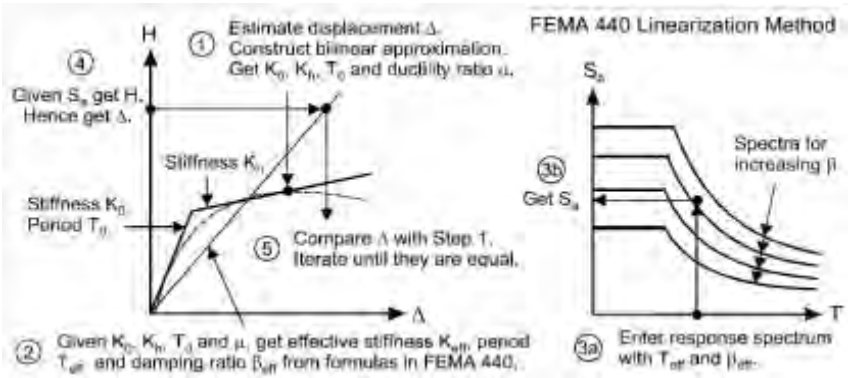

Figure 2-21 Iterative operations in the method of linearization

Modified Displacement Coefficient Method

In [FEMA 440 2005] modification of the displacement coefficient method, it is to propose new expressions for the coefficients C_1 and C_2 and eliminate the coefficient C_3 and replace it with a limitation of the maximum value of the resistance to avoid dynamic instability.

Modified Capacity Spectrum

The improved capacity spectrum method [ATC-40 1996] determines the equivalent linear parameters, effective period T_{eff} and effective damping B_{eff}, by a statistical analysis that minimizes the extreme differences among the maximum response of an actual single-degree-of-freedom inelastic system and their equivalent linear counterpart [Guyader & Iwan 2006].

2.1.3.3 Obtaining the Response Reduction Factor

In the earthquake-resistant design method based on forces (through absolute acceleration response spectra) the values of the design equivalent horizontal forces (Figure 2-1) are obtained by dividing the elastic forces F_e by a reduction coefficient provided by the linear design response spectra, usually represented by R (Figure 2-10). This subsection describes the determination of this coefficient from capacity curves.

Early studies [Veletsos and Newmark 1960] proposed to determine the value of R from the displacement ductility μ (obtained from the capacity curves). Their proposal consists of three expressions: $R = 1$ for $T = 0$; $R = \sqrt{2\mu - 1}$ for $0 \le T < 0.5$ s and $R = \mu$ for $T \ge 0.5$ s. The first expression arises from the obvious consideration that the static response should not be affected by the ductility, the second expression comes from finding that energies in this range of periods corresponding to elastic and inelastic behavior are basically the same and the third expression is obtained assuming that the maximum displacements of elastic and inelastic systems are basically the same ("Equal displacement approach"). The dependence of the coefficient of reduction of the overall ductility and the structural period has prevailed in the design codes; although recent research has shown that applying these factors is unsafe for low periods and excessively conservative for intermediate and long periods, [Ordaz and Pérez-Rocha 1998].

The capacity curves usually show an ultimate strength greater than the yield value F_y (Figure 2-15). This on-resistance is usually quantified by a dimensionless coefficient Ω, ratio of ultimate strength to yield strength ($\Omega = F_u / F_y$); in actual structures, the values of this

coefficient usually range between 2 and 3. By using this ratio, the response reduction factor is usually expressed as

$$R = R_d \, \Omega = (F_e / F_u) \, (F_u / F_y) = F_e / F_y \tag{2-16}$$

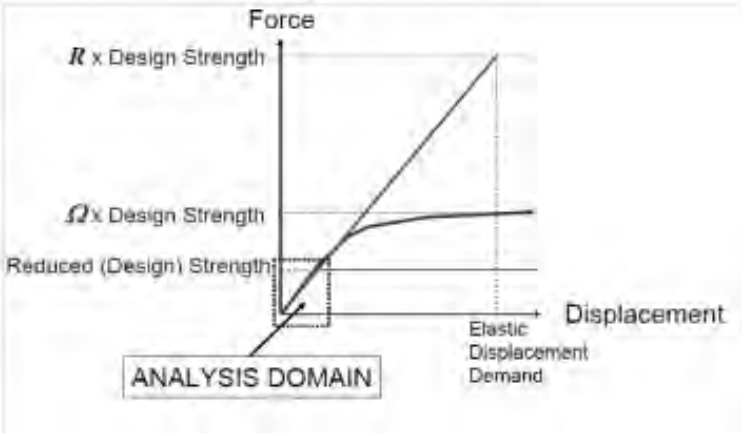

Figure 2-22 Factors contained in the response reduction factor [FEMA 450 2006]

Figure 2-22 illustrates the meaning of this expression. Some relevant studies related to the response reduction factor are [Newmark, Hall 1973; Miranda, Bertero 1994], among others.

2.1.3.4 Limitations of the push-over analyses

The main limitations of earthquake design methods based on displacement are described next. The analysis push-over characterizes the nonlinear dynamic behavior of the structure by means of increasing static forces. The main drawback of this strategy is that the response of the structure to a given input is not incremental but cyclical and the push-over analyses cannot take into account the accumulated plastic strain, in other words, the cumulated damage. Therefore, we cannot establish a clear relationship between the maximum displacement of the structure and the energy stored during plastic deformation cycles. When the structure enters the inelastic range, deterioration occurs by the accumulation of plastic incursions; that can produce the complete breakdown of structural elements for deformations smaller than those that could be resisted under monotonic forces. This type of failure is called low cycle fatigue or plastic fatigue [Teran-Gilmore, Jirsa 2007] (as opposed to the fatigue caused by a high number of cycles, which does not involve plastic deformations). Fajfar [Fajfar 1992] proposed a method to take into account the effect of cumulated damage in which the ductility of the structure is reduced by a dimensionless parameter which represents a normalization of the energy. Recently, Teran-Gilmore and Jirsa [Teran-Gilmore, Jirsa 2005] have used the correlation between energy and the response reduction factor, *R*, to propose two simple calculation procedures for low cycle fatigue; the energy demand is indirectly controlled through the concept of ductility. However, the disadvantages of the calculation procedures based on forces already have been previously pointed out; those disadvantages are closely related to the fact that equivalent forces representing the effect of the input depend on the elastic and plastic characteristics of the structure, which in its own turn regulate the structural strength. This coupling between the effect of the earthquake and strength of the structure makes the seismic calculation more complex and cumbersome. Furthermore, the concept of ductility allows determining only indirectly the cumulative fatigue damage for low number of cycles, and requires the use of large numbers of empirical parameters. The main reason to address indirectly the accumulated damage through the concept of equivalent ductility factor is that it provides a calculation process that can adapt easily to the current codes and practices. Since designers are reluctant to change radically their state of practice, new procedures are more likely to be accepted if they represent only a small change in a concept, such as ductility factor, which is well understood and has been widely used

in practice. The calculation procedures based on displacements solve several of the drawbacks of the procedures based on forces, but are also incapable of dealing with the effects of cumulated damage in a simple and satisfactory manner.

Another drawback of the earthquake design strategy based on displacements is that the hysteretic behavior is interpreted as an equivalent viscous damping (ζ_{eq}); this introduces a relevant error, especially for significant levels of damping. Moreover, such identification is not based on any physical principle that justifies, in inelastic systems, the existence of a direct relationship between the energy corresponding to the maximum displacement and the equivalent viscous damping.

Another strategy to bypass that the push-over analysis cannot take into account the cumulated deformations is to use energy spectra. The main motivation that has inspired its development is that the plastic deformation energy is fairly accurate to quantify the damage in the structure. These procedures exploit the difference between ductility μ, which expresses essentially the relationship between maximum deformation δ_{max} and the yield deformation δ_y, and the accumulated η ductility. The meaning of μ and η is described in Figure 2-23 [Benavent-Climent et al. 2001].

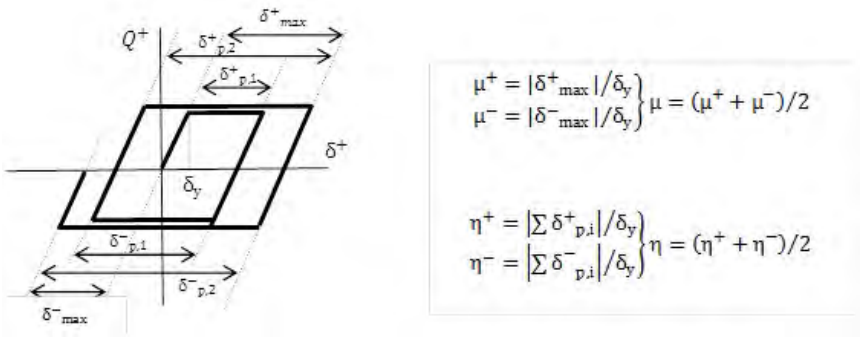

Figure 2-23 Meaning of the coefficients of ductility μ and η [Benavent-Climent et al. 2001]

Figure 2-23 shows that the ductility μ is defined as the average of the positive and negative values of displacement δ; each of them is calculated as the ratio between the maximum displacement (in other words, measured from the beginning of the yield) and the yielding displacement δ_y. The cumulative ductility η is also defined as the average of the values corresponding to positive and negative displacements; each of them is calculated by dividing the sum of the displacements of each plastic branch (horizontal in Figure 2-23) and the yielding displacement δ_y.

The limitations and disadvantages of earthquake-resistant design methods based on displacements are avoided in energy-based methods, which are described in the following subsection. Moreover, these procedures are quite appropriate in buildings with energy dissipation devices.

2.1.4 Dynamic Analysis

This procedure evaluates the effect of earthquakes on buildings based on determining the dynamic response (commonly known as “time history”) to the expected accelerograms. The most relevant response quantities are the maximum relative displacements (along the duration of the earthquake) in between consecutive floors (inter-story drifts) and the maximum absolute accelerations thereof; the maximum relative displacements report about the experienced level of structural damage and the maximum absolute accelerations are directly correlated with the non-structural damage (for facilities and non-structural elements) and the human comfort conditions.

Since the dynamic calculations take into account the performance of buildings under seismic inputs in a more direct way than in the methodologies based on response spectra, in general the dynamic analyses are able to provide more accurate results. In particular, the comparison between the nonlinear static methods (push-over) and the nonlinear dynamic methods is clearly favorable to them because, besides being more accurate in general, they have two important advantages: (i) by considering the cyclical behavior they are able to reproduce the accumulated plastic damage and (ii) the consideration of the effect of damping (both the present in the undamaged structure and the generated for increasing damage) is more direct.

The considered inputs are selected from the available information on the seismicity in the intended location and may consist either in records of historical earthquakes or in accelerograms generated artificially. Given the considerable uncertainty about the characteristics of the expected input, one must consider several accelerograms and then determine the average of the responses of the structure to each of them; in fact, in the earthquake-resistant design methodologies based on spectra equivalent operations have been done since the design spectra are smoothed, in other words, have been obtained as averaged envelopes of a group of spectra corresponding to individual accelerograms, as shown in Figure 2-3, Figure 2-4 and Figure 2-5. These figures show that the maximum response to each record is highly sensitive to the fundamental period of the building, particularly for low values of damping; therefore, considering an excessively low number of accelerograms generate a false information since the fit (or proximity) between the fundamental period of the building and any spectral peak will predict a structural response that is abnormally large. To avoid such problems the seismic design codes generally require considering at least five [NCSE-02 2002] or seven [ASCE 7-05 2005; NSR-10 2010; NBCC 2005] accelerograms; the response that is used for the earthquake-resistant design of the structure is determined as an average of the corresponding responses to each of such accelerograms. Some codes [ASCE 7-05 2005; NSR-10 2010] allow using only three accelerograms, but in that case the maximum response to them has to be considered.

The registers from historic events should be scaled to adjust its characteristics to the seismicity of the zone; since only the ordinates (acceleration) but not the abscissa (time) are changed, the frequency content is not modified. Usually this operation is done by comparing the design spectrum (specified in the regulations of the zone) with the response spectrum of the considered register, in the codes [ASCE 7-05 2005; EN-1998 2004] the comparison criteria is often described. These criteria usually indicate sets of minimum values for the spectral ordinates at periods near to the fundamental period of the structure. Furthermore, the synthetic accelerograms are generated so that its frequency content corresponds to the design spectrum and that its duration and other temporal characteristics match those of the expected records.

In zones of medium or high seismicity, buildings are often designed by accepting a given level of structural damage under the design earthquake (see Table 2-2). Accordingly, in these cases the dynamic analyses should be nonlinear, in other words, must be able to reproduce the behavior of the structure when it been damaged and therefore has experienced significant reductions in its strength and rigidity. Moreover, second-order analyses may be necessary because of the significant relative horizontal displacements, this being another source of complexity and increased computational cost. Although the nonlinear dynamic analyses are increasingly used in the earthquake-resistant design of important structures, this procedure is rarely used in the design of ordinary structures, this is due to the high computational cost involved and to the effort required to properly interpret the large amount of generated information.

The results of dynamic and push-over analyses can be compared. If the dynamic analyses are performed with accelerograms, either actual or synthetic, whose response spectra fits the one considered in the push-over analysis, the conclusions of both formulations should be similar. In [Powell 2007] the similarities and differences to be expected are discussed.

2.1.5 Incremental Dynamic Analyses

With the main purpose of alleviating the problem derived from the fact that the push-over analysis cannot take into account the accumulated plastic strain, the so-called incremental dynamic analysis (IDA, Incremental Dynamic Analysis) has been proposed [Vamvatsikos, Cornell 2001; Vamvatsikos, Cornell 2002; Vamvatsikos 2002]. The reference [Vega del Rey, Alarcón 2009] proposes a method to investigate the impact of bridge decks against the abutments. This strategy consists of determining the dynamic response of the structure to one or more inputs scaled with increasing factors; in this way capacity curves are obtained similarly to the push-over analyses. If the incremental dynamic analysis is performed for a single record, such analysis is usually called *dynamic push-over analyses* (DPO, Dynamic Push-Over). It is remarkable that the incremental dynamic analyses require making several nonlinear dynamical calculations, which are expensive in computational time; on the other hand, it may be necessary to perform second-order analyses. However, the incremental dynamic analyses, especially when applied to several earthquakes, constitute powerful formulations, which may provide greater and more useful information than the rest of approaches that have been described in this section.

The results of these procedures are usually represented by the so-called IDA curves. These representations consist of capacity curves similar to the result of the push-over analyses; on the horizontal axis an index related to the magnitude of the response is usually represented and the vertical axis usually contains an index related to the severity of excitation. Figure 2-24 shows the results of this kind; Figure 2-24 (a) corresponds to a single record and Figure 2-24 (b) corresponds to multiple (30) records. In both representations the severity of the seismic action is quantified by the ordinate of acceleration response spectrum for the first mode $S_a(T_1,0.05)$ and the magnitude of the response is quantified by the maximum value (along the duration of the earthquake) of the relative displacement between floors (inter-story drift). Figure 2-24 (a) shows both increases and decreases of the damage on the upper floors with increasing severity of excitation, this effect is obviously due to the "protection" provided by the lower floors. None of the other methods described in this section are able to predict this phenomenon so clearly. Figure 2-24 (b) shows the remarkable variability in the response of a determined structure to records that have, in first approximation, a comparable level of severity

Usually the damage thresholds IO, LS and CP are related with certain values of the index that quantify the magnitude of the excitation (ordinate in Figure 2-24); in this way performance-based analyses can be made from incremental dynamic calculations.

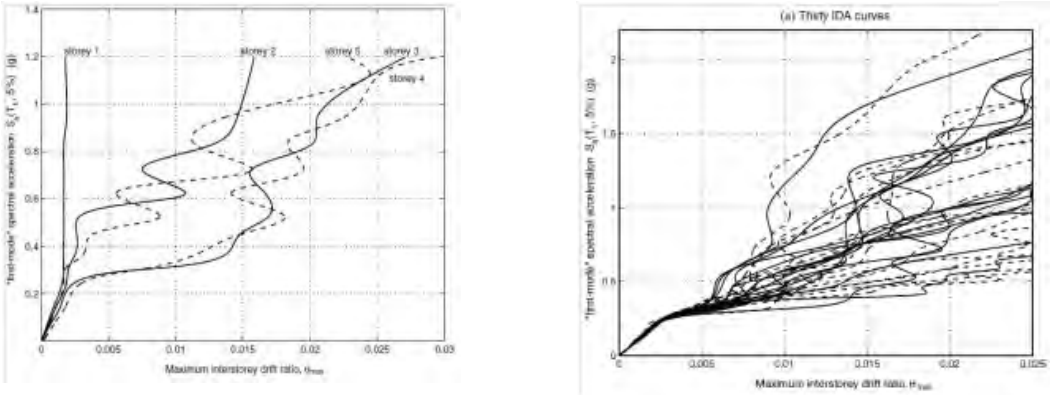

(a) Single Register

(b) Thirty Registers

Figure 2-24 Examples of IDA curves [Vamvatsikos, Cornell 2002]

It is remarkable that FEMA [FEMA 350 2000] has recently adopted these strategies as the reference method for assessing the earthquake resistant capacity of structures.

2.2 Housner-Akiyama Formulation

2.2.1 Energy Balance Expressions

The equation of motion of a SDOF system subjected to a horizontal ground motion is given by the following ordinary differential equation:

$$m\ddot{y} + c\dot{y} + Q(y) = -m\ddot{z}_{\mathrm{g}} \tag{2-17}$$

Where *m* is the mass, *c* is the viscous damping coefficient, *Q*(y) is the restoring force, *y* is the displacement relative to the ground and $\ddot{z}_g$ is the ground acceleration.

This relationship differs from (2-1) (corresponding to the same system but with a linear behavior) only in the term *Q*(*y*) that corresponds to the restoring force and which, moreover, replaces the elastic term *k y*.

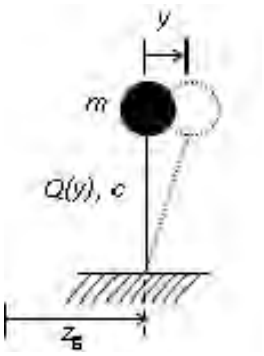

Figure 2-25 Non-linear SDOF system

The balance of the energy introduced into the system at a specific instant *t*, is obtained by multiplying equation (2-17) by *dy* and integrating in between the initial time *t* = 0 and the current time *t*:

$$m\int_0^t \ddot{y}\dot{y}dt + c\int_0^t \dot{y}^2 dt + \int_0^t Q(y)\dot{y}dt = -\int_0^t m\ddot{z}_{\mathrm{g}}\dot{y}dt \tag{2-18}$$

Each term in equation (2-18) can be interpreted in terms of energy:

$$E_{\mathrm{k}}(t) = m\int_0^t \ddot{y}\dot{y}dt = \frac{m\dot{y}^2(t)}{2} \tag{2-19}$$

$$E_{\mathrm{a}}(t) = \int_0^t Q(y)\dot{y}dt \tag{2-20}$$

$$E_{\xi}(t) = c\int_0^t \dot{y}^2 dt \tag{2-21}$$

$$E_{\mathrm{I}}(t) = -\int_0^t m\ddot{z}_{\mathrm{g}}\dot{y}dt \tag{2-22}$$

The meanings of these terms are:

$E_{\mathrm{k}}(t)$: Kinetic energy (relative).
$E_{\mathrm{a}}(t)$: Energy absorbed by the spring (both elastic and plastic).
$E_{\zeta}(t)$: Energy dissipated by the inherent damping.
$E_{\mathrm{I}}(t)$: The energy introduced into the system by the accelerogram.

In the expression (2-19) it has been assumed that at the instant $t = 0$ the relative velocity is zero ($\dot{y}(0) = 0$). By substituting expressions (2-19) to (2-22) in (2-18) we have the following energy balance relationship:

$$E_k + E_\zeta + E_a = E_I \tag{2-23}$$

In its turn, the strain energy E_a can be decomposed into Es, the elastic term (energy that can be recovered once the earthquake ends) and the term representing E_H, the irrecoverable hysteretic energy (e.g. contributing to the structural damage):

$$E_a = E_s + E_H \tag{2-24}$$

The elastic energy E_s is given by

$$E_s(t) = k\int_0^t y\dot{y}dt = \frac{ky^2(t)}{2} \tag{2-25}$$

In this relation k is the initial rigidity of the system. It is assumed that at the initial time $t = 0$ and the relative displacement is zero: $y(0) = 0$.

The sum of E_k, kinetic energy and E_s, elastic strain energy is termed as E_e, elastic vibrational energy, e.g. the energy generated by the vibration of the structure that can be recovered upon termination of the earthquake:

$$E_e(t) = E_k(t) + E_s(t) = \frac{m\dot{y}^2(t)}{2} + \frac{ky^2(t)}{2} \tag{2-26}$$

It is remarkable that E_e, the vibrational energy vanishes once the structure stop moving after the seismic action, unless it has some permanent deformation. Substituting (2-24) and (2-26) in (2-23), the energy balance relation becomes:

$$E_e + E_\zeta + E_H = E_I \tag{2-27}$$

This equation states that the energy from the earthquake (E_I), is transformed into (E_ζ) vibrational elastic energy, (E_ζ) energy dissipated by the inherent damping and (E_H) hysteretic energy.

The difference between energy introduced by the input (E_I) and the energy dissipated by the damping of the structure (E_ζ) was named by Housner [Housner 1956] as energy that contributes to the damage (E_D):

$$E_D = E_I - E_\zeta \tag{2-28}$$

The relation (2-26) shows that the energy E_e practically vanishes when the structure stops vibrating; shortly after the end of the ground motion, therefore, the expression (2-27) shows that in practice hysteretic energy can be identified as the energy that contribute to damage:

$$E_D \approx E_H \tag{2-29}$$

In summary, the two most important energy quantities are (E_I) the energy introduced by earthquake and (E_D) energy that contributes to the damage. Typically, both energies are expressed in terms of equivalent velocity (similar to (2-10)) and are normalized with respect to m, the mass of the structure:

$$V_E = \sqrt{2E_I / m} \qquad V_D = \sqrt{2E_D / m} \tag{2-30}$$

Since at the formulation the relative displacement is considered (Figure 2-19), the energies E_I and E_K also defined as "relative". In the reference [Uang, Bertero 1990] a different formulation is considered, which leads to absolute magnitudes, the corresponding energies in that studies are called $E_{I,abs}$ (absolute input energy) and $E_{k,abs}$ (absolute kinetic energy). The difference between E_I and $E_{I,abs}$ is the effect of rigid body translational (rigid body) of the structure. If these energies are evaluated at the end of the ground motion, their values coincide. In the case that E_I and $E_{I,abs}$ are taken as the maximum values evaluated through the whole ground motion duration, it is found [Uang, Bertero 1990] that these peaks are quite similar in the range of periods of interest in earthquake engineering (from about 0.3 to 5 seconds). Further, in nonlinear damped systems with period T within this range subjected to ground motions distinct from near-fault earthquakes, the maximum value of E_I takes place at the end of the ground motion duration. Moreover, it should be emphasized that the energies E_ξ and E_H are defined in the same way in the "relative" and "absolute" formulations, i.e. their values match in both cases.

2.2.2 Envelope Spectra for Earthquake-Resistant Design

Each earthquake has its own energy spectrum in terms of velocity V_E (equation (2-30)). For a certain location, we define the design spectrum as the envelope of the spectra corresponding to different seismic records available or expected. The reference [Akiyama 1985] proposes a strategy for generating the envelope. This strategy consists of the three following consecutive steps:

Step 1. Calculate the V_E spectrum for each strong ground motion available. These spectra should correspond to a damping ratio ζ = 0.10 (10% damping) and be calculated for linear single-degree-of-freedom systems. Spectra were obtained from the relations (2-22) and (2-30); in the integral involved in (2-22) the velocity is determined by the expression (2-6). Usually each strong ground motion register has three components, two horizontal and one vertical; we neglect the contribution of the vertical component. With respect to the horizontal components, in general they correspond to the north-south and east-west; both spectra should be obtained, being represented by $V_{E,NS}$ and $V_{E,EW}$, respectively. Subsequently, these spectra must be combined according to the following quadratic criterion:

$$V_E = \sqrt{V_{E,NS}^2 + V_{E,EW}^2} \tag{2-31}$$

Step 2. Draw a piece-wise bilinear envelope of the V_E vs. T. curves. The first line goes through the origin and envelopes the energy input spectra in the short period. The second line is horizontal and represents the energy input in the medium and high period ranges.

Step 3. Multiply the slope of the first line by 1.20 to take into account the fact that in the short period range, the lengthening of the vibration period associated with the plastification of the structure tends to increase the input energy E_I.

As discussed previously, in the reference [Akiyama 1985] it is shown that the input energy E_I introduced by an earthquake in a given structure is a relatively stable magnitude with respect to the distribution of rigidity and mass, to the damping, to the level of plastification (except in the short period range) and to the hysteretic behavior of the structure, depending basically on its fundamental vibration period T and its mass m. As also discussed by Akiyama [Akiyama, 1985] and mentioned above, in the short period range the input energy E_I tends to increase with the level of plastificacion of the structure, but this increment is relativelly small. Akiyama estimated this increment in at most 20% as indicated in step 3 above. Moreover, the energy dependence on the mass is proportional; in consequence, the energy expressed in equivalent velocity (V_E) is independent of the mass, as expressed by the relationship (2-10). Based on these considerations and for the sake of simplicity, Akiyama proposed for design purposes to use the spectra

obtained according to this strategy (for linear elastic behavior) for both elastic and inelastic (non-linear) systems.

3 Seismic Information of Turkey

3.1 Seismicity of Turkey

Turkey is located on the relatively small Anatolian plate, which is squeezed between three other major tectonic plates. The north-moving African and Arabian plates located to the south, and the south-moving Eurasian plate located to the north. The combination of these plate movements is forcing the Anatolian plate to move west into the Aegean Sea as shown in Figure 3-1.

The plate interactions of this region are dominated by convergent boundaries involving both subduction and collision. The Arabian and African plates are pushing northward into the Eurasian plate. According to recent plate tectonic models, the African plate is moving northward relative to the Eurasian plate at approximately 10 mm/yr and is being subducted along the Hellenic Arc. The Arabian plate is moving north-northwest relative to Eurasia at 18-25 mm/yr. The result is a continental collision along the Bitlis-Zagros fold and thrust belt. The smaller Anatolian plate is caught in the middle of all of this movement. This movement produces fault structures at the boundary between the plates. It is largely accommodated by left-lateral slip on the East Anatolian Fault and right-lateral slip along the North Anatolian Fault [McKenzie 1972].

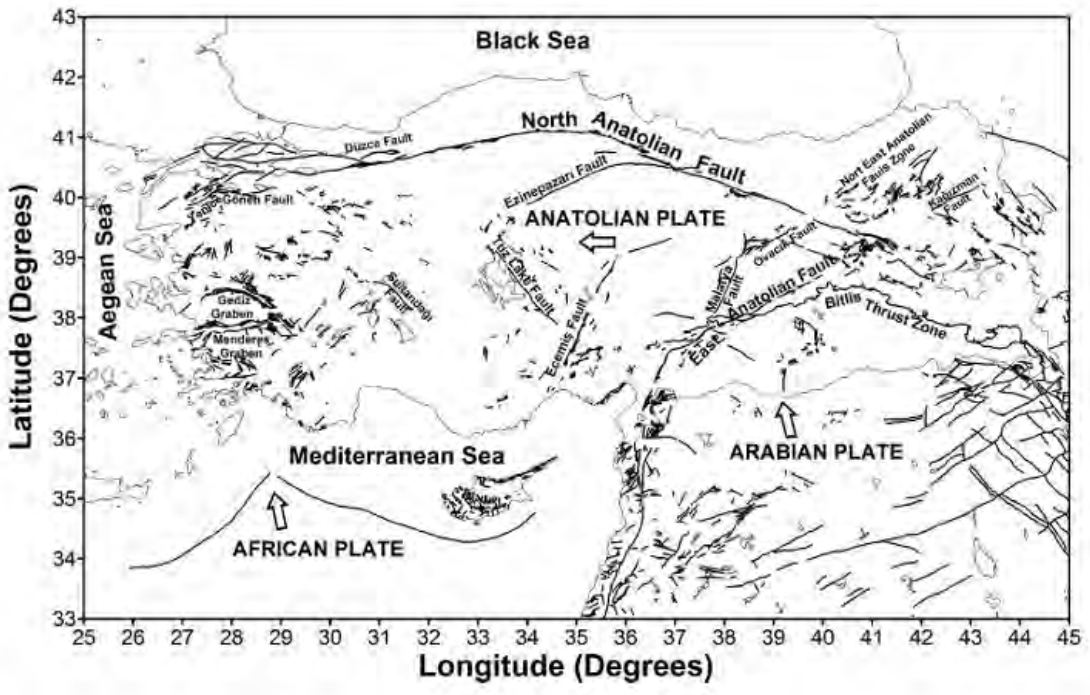

Figure 3-1. The major tectonic structures in Turkey [Şaroğu et al. 1992]

The major tectonic structures of Turkey can be summarized as:

The African Plate is descending beneath the Anatolian Plate in the N-NE direction and forms Anatolian Graben Complexes (WAGC). Extensive investigations have showed that, numerous graben systems have been forming in the E-W and WNW-ESE directions due to the N-S substantial extension in the Western Anatolia [Ketin 1968; Dewey et al. 1973; Şengör 1979; Jackson and Mc Kenzie 1972].

Convergence between the African and Anatolian plates in the Eastern Mediterranean takes place by subduction along the Aegean and Cyprus arcs [McKenzie 1978; Papazachos and Comninakis 1971].

NAFZ is one of the best known strike-slip faults in the world because of its remarkable seismic activity. It is a right lateral strike-slip type fault that bounds the Anatolian plate from the Aegean Sea in the west to the Karliova Triple Junction in the east; that fault stretches 1,500 km across Turkey [Şengör et al. 1985]. Throughout the history NAFZ was the source of many major earthquakes (magnitude 6.7 or greater) starting with the 1939 Erzincan Earthquake (M_w = 7.9).

EAFZ was first described by [Allen 1969] and this fault zone is a transform fault forming parts of boundaries between the Anatolian and the Eurasian plates, as well as between the Arabian and African plates. It is considered as a conjugate structure to the NAFZ. The East Anatolian Fault (EAFZ) is an active left-lateral strike slip fault forming the boundary between the Anatolian Block to the northwest and the Arabian - African plates to the southeast. The EAFZ runs in the NE-SW direction and is approximately 650 km long and 1-30 km wide. It connects the NAFZ to the Dead Sea - Read Sea Fault System and extends its south-western terminus to the immediate east of Cyprus.

The Bitlis Thrust Zone is a complex continent-continent and continent-ocean collisional boundary that lies north of the fold-and-thrust belt of the Arabian platform and extends from southeastern Turkey to the Zagros Mountains in Iran [Şengör 1979; Hempton 1985]. It has also produced lots of destructive earthquakes. Historical data suggest that this area was very active during the past 2000 years.

At the eastern end of the Turkish plate, the motion is taken up by thrust faults associated with the Caucasus. The result of this geometry is a thickening of the continent throughout the active region, which continues to elevate the Caucasus. Thrusting in eastern Turkey and the Caucasus transforms to strike-slip motion between the Turkish and Eurasian plates at the eastern outset of the NAF [Erdik et al. 1999].

3.2 Turkish Earthquake-Resistant Design Regulations

Two codes rule the design and construction of reinforced concrete buildings in Turkey: TS-500, *Building Code Requirements for Reinforced Concrete* [TS-500 1985], commonly termed the "building code" in this work, and *Specification for Structures To Be Built in Disaster Areas* Ministry of Public Works and Settlement [TSC 1975, 1997, 2007], termed the "seismic code".

The requirements for the designing and detailing of reinforced concrete components is presented at the building code, and is similar to ACI-318 [ACI 2008] except for the coverage of earthquake effects, which is not considered by the building code. Since the building code did not contain any special seismic detailing requirements, the designer was sent to the seismic code for such information. The first seismic design code for buildings was published in 1940; The Turkish Ministry of Public Works and Settlement formed a committee to prepare a seismic zone map. The formation of this committee was the first step toward developing regulations for the seismic design of buildings in Turkey. The Evaluation of the Seismic codes in Turkey is summarized at Figure 3-2 [Bayülke 1992; Duyguluer 1997]

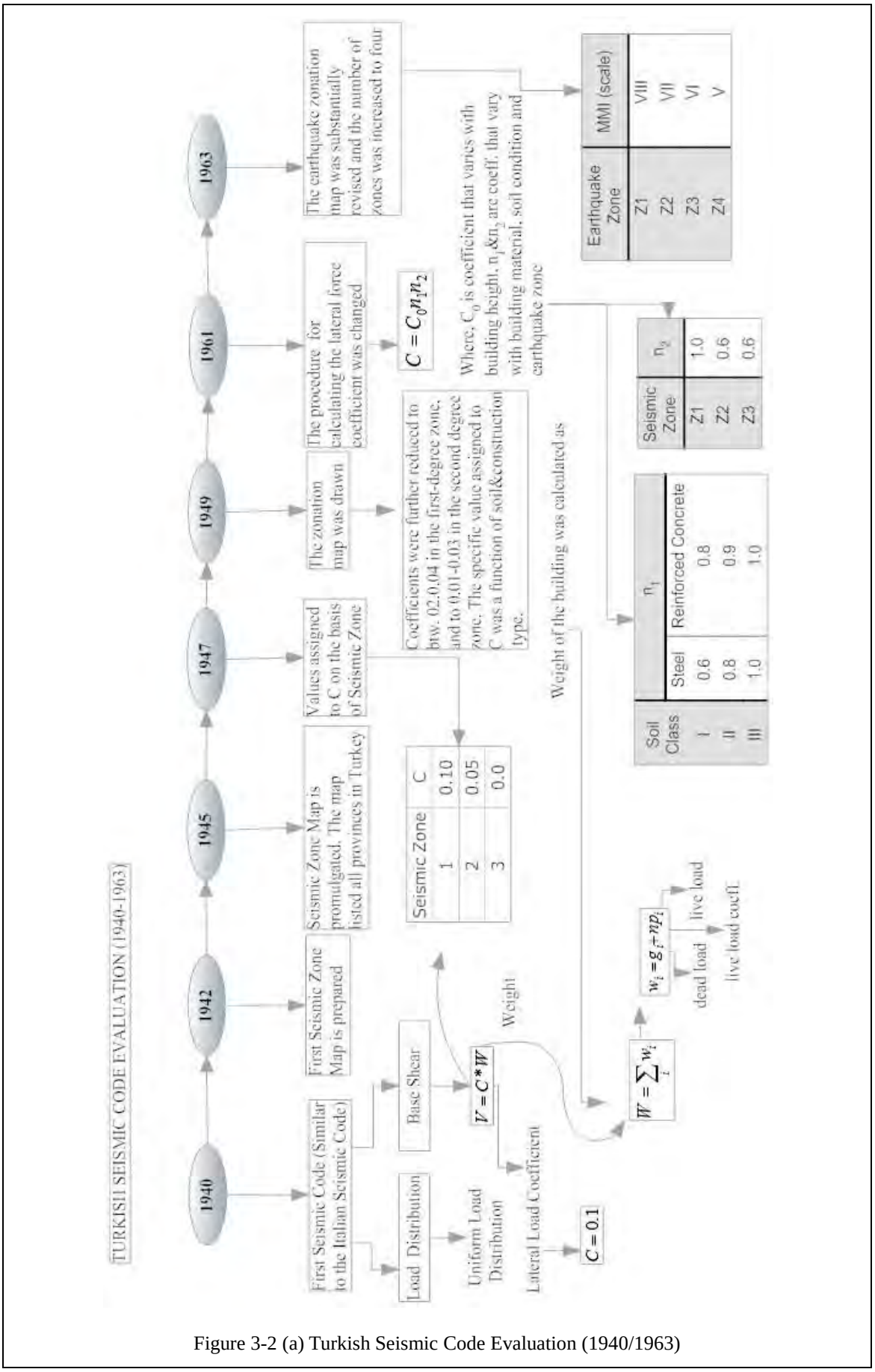

Figure 3-2 (a) Turkish Seismic Code Evaluation (1940/1963)

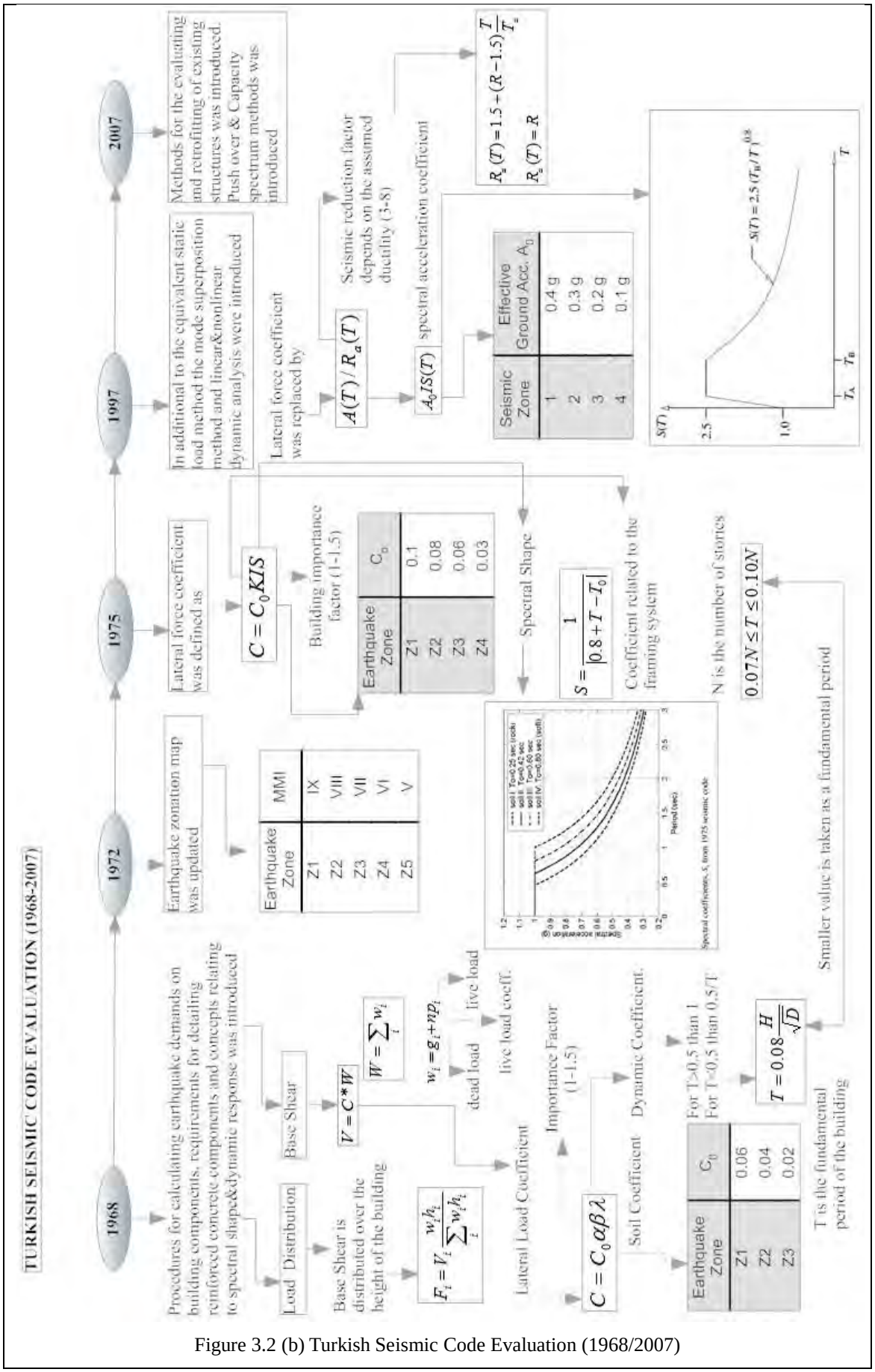

Figure 3.2 (b) Turkish Seismic Code Evaluation (1968/2007)

3.3 Turkish Registers

A dataset from 1976 to 2006 [Erdogan 2008; Akkar et al. 2010] constitutes the main base for this work. It covers 4203 registers from 2818 seismic events; such accelerograms have been recorded in 327 stations. Within the aforementioned 4203 registers, 1320 ones corresponding to earthquakes with $M_w > 4$ are selected; among them, 540 high quality waveform registers from 131 earthquakes are kept. Among them, 149 registers with PGA ≥ 0.01 g corresponding to 80 earthquakes have been finally kept for this study. The highest moment magnitude is 7.6, Kocaeli earthquake (17/08/1999). The latest earthquakes of Kütahya-Simav (19/05/2011) and Van-Muradiye-Merkez (23/10/2011) have been also incorporated; from the Kütahya-Simav 17 registers have PGA ≥ 0.01 g are kept while from the Van-Muradiye-Merkez 4 registers with PGA ≥ 0.01 g have been also added. Finally, 169 registers corresponding to 82 seismic events and being recorded in 90 stations are considered in this study. Every register contains horizontal (NS and EW) and vertical accelerograms; vertical components are disregarded.

Table 3-1 displays the most relevant information about the considered registers. The severity of the earthquakes is characterized by the local, moment and surface magnitudes, denoted by M_L, M_W, and M_S, respectively. The soil is classified in: soft soil, stiff soil and rock. When the shear wave velocity averaged in the top 30 m ($v_{s,30}$) is available (in 175 stations), the classification is based on that parameter; soft soil, stiff soil, and rock sites correspond to 180 m/s < $v_{s,30}$ < 360 m/s, 360 m/s < $v_{s,30}$ < 800 m/s and $v_{s,30}$ > 800 m/s, respectively. In the EC-8 [EN-1998 2004], these three categories correspond to ground types C, B and A, respectively; no stations with $v_{s,30}$ < 180 m/s exist, hence, this study does not cover soil types D and E. In 5 stations the soil classification is not based on $v_{s,30}$ and in 13 stations (corresponding to 13 registers) the soil type is not known; such 13 registers are disregarded. The seismic zone corresponds to the Turkish design code [TSC 2007]; for seismic zones 1, 2 and 3 the design seismic acceleration is 0.4 g, 0.3 g and 0.2 g, respectively. R_{jb}, R_{rup} and R_{epi} correspond to Joyner-Boore, rupture and epicentral distances, respectively [Erdogan 2008]. Bracket duration (t_{br}) [Kempton, Stewart 2006] is comprised in between the instants when the 5% of the maximum acceleration is exceeded for the first and last time, respectively. Triffunac duration [Triffunac, Brady 1975] (t_{tf}) corresponds to the time interval in between the 5% and the 95% of integral $\int \ddot{z}_g^2 dt$. Arias intensity I_A [Arias 1970] constitutes a measure of the destructive capacity of an accelerogram and is defined as

$$I_A = \frac{\pi}{2g}\int \ddot{z}_g^2 dt \tag{3-1}$$

Dimensionless index I_D [Manfredi 2001] is an indicator of the impulsive characteristics of the ground motions and is defined by

$$I_D = \frac{\int \ddot{z}_g^2 dt}{\ddot{z}_g^{max}\dot{z}_g^{max}} \tag{3-2}$$

The integral extends to the ground motion bracket duration. Impulsive ground motions show typically low values of I_D (say, less than 10) whereas non-impulsive ground motions exhibit large I_D (say, greater than 10).

In Table 3-1 most of the information has been obtained from the work [Erdogan 2008]; however, the values of the bracket and Triffunac durations and of the Arias and dimensionless indexes are determined in this study.

Table 3-2 displays the PGA (Peak Ground Acceleration), PGV (Peak Ground Velocity) and PGD (Peak Ground Displacement) of the registers listed in Table 3-1. The treatment of the registers is described in the next section.

Figure 3-3 displays the location and the soil type of the 90 registering stations that correspond to registers in Table 3-1; 3 of them correspond to rock, 35 to stiff soil and 42 to soft soil and in 10 the soil type is not known. Such information is superposed with the design peak ground acceleration established by the Turkish seismic design code [TSC 2007].

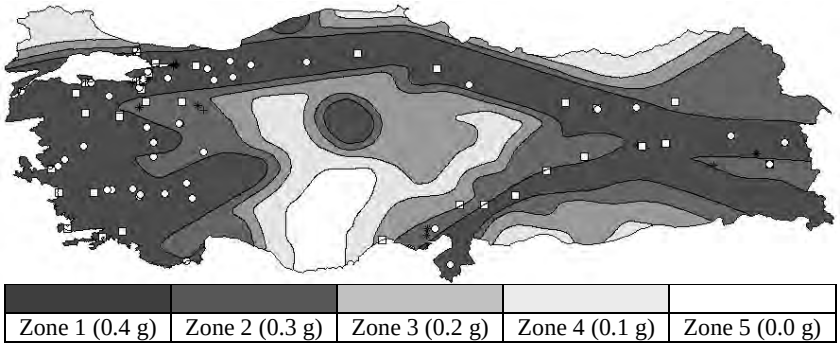

Figure 3-3. Location and soil type of the registering stations. Rock: "✚". Stiff soil: "□". Soft soil: "○". Unknown: "✳".

Figure 3-3 shows that most of the registering stations lay inside zone 1, i.e. the highest seismicity region of Turkey.

Figure 3-4 displays the location of the epicenters of the 82 earthquakes together with their magnitude.

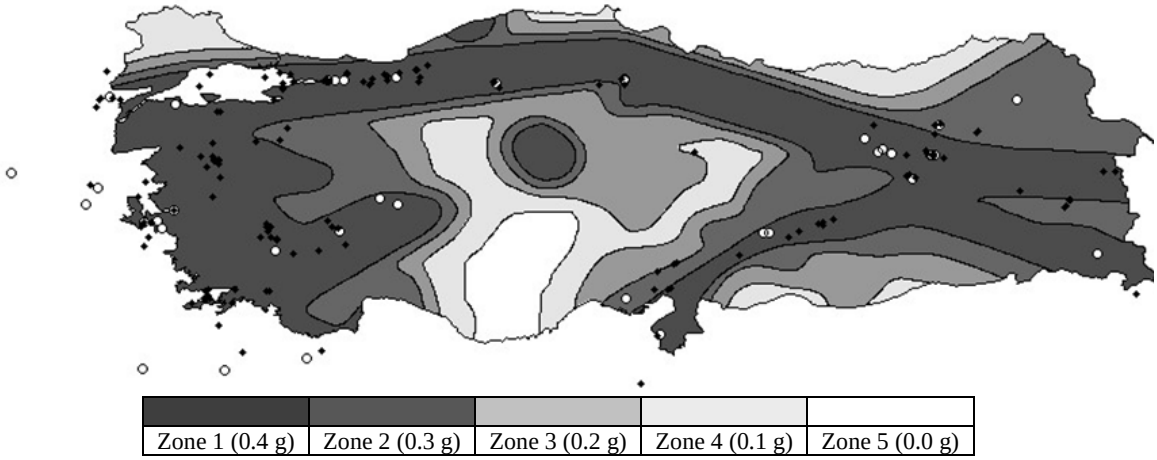

Figure 3-4**.** Locations of the epicentres and magnitudes of the earthquakes. $M_s \leq 5.5$: "◆". $M_s > 5.5$: "○".

Figure 3-4 shows that a relevant part of the epicenters are located in land; it indicates that important near-source effects are expectable; this is confirmed by the important number of impulsive registers in Table 3-1.

3.4 Processing of the Registers

The waveform quality of records may contain non standard and digitization problems and should not be used directly in strong-motion studies. Some of these problems can be corrected by special techniques. The most common problems are categorized as specified in the literature and shown in Figure 3-5 [Douglas 2003].

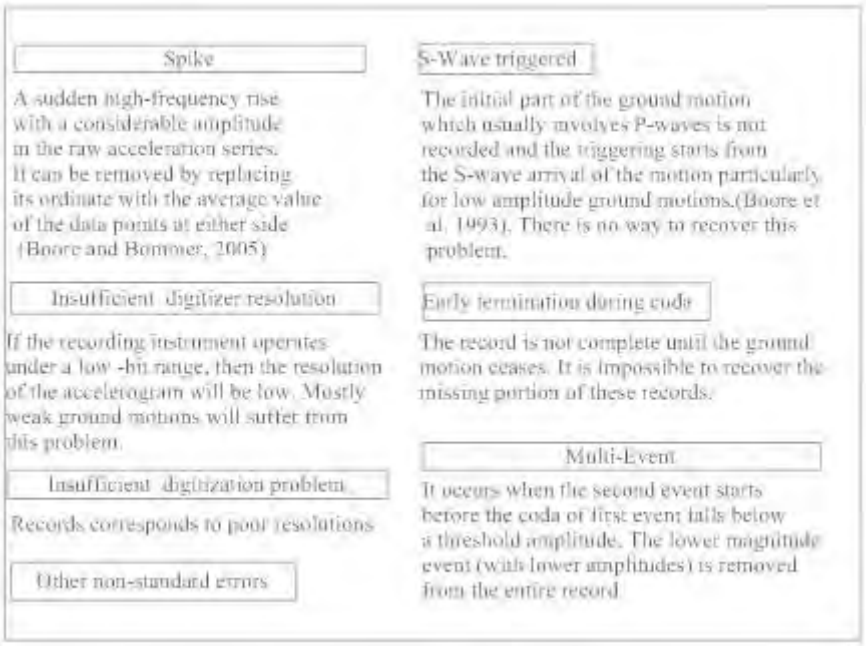

Figure 3-5 Non-standard and digitization problems of strong-motion registers

The registers are treated with baseline correction and with bi-directional, zero-shift ("acausal"), 4th-order Butterworth filtering [Boore 2005]. The purpose of the band-pass filtering is to remove long-period and short-period noise. The low and high-cut frequencies are taken as defined in the work of Erdogan [Erdogan 2008; Akkar et al. 2010]. The low-cut frequency ranges generally in between 0.05 and 0.5 Hz (2 and 20 s) and the high-cut frequency ranges in between 15 and 40 Hz (0.067 and 0.025 s). This information is indicated in last two columns of Table 3-1. Later case by case the uncorrected and corrected PGV, PGA and PGD values are checked. Also the obtained Fourier spectra, resulting velocity and displacement traces are examined visually.

3.5 Classification of the Selected Registers

For the proposal of design energy spectra, the registers in Table 3-1 are classified in 12 groups according to the following issues:

- **Soil type**. The three aforementioned soil types (rock / stiff soil / soft soil) are considered.
- **Magnitude of the earthquake**. The Eurocode 8 [EN-1998 2004] proposes two different design spectra, termed as Type 1 and Type 2; since they correspond to registers from earthquakes with surface magnitude higher and smaller than 5.5, respectively, the registers in Table 3-1 are classified in those arising from earthquakes with $M_s > 5.5$ and $M_s \leq 5.5$.
- **Near-fault effects**. Impulsive and vibratory registers are separately considered; as discussed after equation (3-2), such categories correspond to $I_D \leq 10$ and to $I_D > 10$, respectively.

Given the scarcity of results corresponding to rock, only stiff soil and soft soil are considered; therefore, 8 groups of registers are finally analyzed: stiff soil / soft soil, $M_s > 5.5$ / $M_s \leq 5.5$ and impulsive / vibratory. However, for rock, some incomplete results about design spectra are also proposed; the lack of seismic information for Turkey is partially compensated by the one provided by other sources.

Table 3-1 Considered Turkish registers

Register Index	EARTHQUAKE INFORMATION						STATION INFORMATION							REGISTER INFORMATION									
	Date	Earthquake	Hypo central depth (km)	Magnitude			Station Code	$V_{s,30}$ (m/s)	Soil Type	Seismic Zone	Distance			Duration (NS)		Duration (EW)		Arias Intensity		ID		Filtering range f_1 / f_2 (Hz)	
				M_L	M_w	M_s					R_{jb} (km)	R_{rup} (km)	R_{epi} (km)	t_{br} (s)	t_{tf} (s)	t_{br} (s)	t_{tf} (s)	NS	EW	I_{D-NS}	I_{D-EW}	NS	EW
1	19/08/1976	Denizli	19.8	6.1	6.1	6.03	2001	346	Soft	1	6.4	17.9	9.9	13.6	5.2	14.6	5.9	72.3	52.4	5.1	7.2	0.5/40	0.7/35
2	16/12/1977	Izmir-Guzelyali	24.2	5.6	5.6	5.41	3506	771	Stiff	1	9.5	-	9.5	2.2	0.8	9.0	2.1	36.9	6.6	4.5	6.6	0.4/25	0.5/25
3	18/07/1979	Balikesir	7.0	5.3	5.3	4.93	1010	496	Stiff	1	5.1	7.1	6.5	11.8	3.3	9.7	2.5	20.2	21.0	6.0	5.7	0.3/30	0.35/30
4	05/07/1983	Balikesir	6.9	6.1	6.1	6	1012	520	Stiff	1	47.6	47.8	55.4	17.2	8.1	17.3	10.5	3.9	2.3	9.0	13.4	0.25/25	0.4/25
5							1014	397	Stiff	1	37.8	38	44.1	14.6	11.4	14.7	9.0	2.3	2.9	7.7	17.1	0.2/30	0.3/22
6	05/05/1986	Adiyaman	4.4	6.0	6.0	5.90	203	-	Stiff	1	23.9	24	29.2	19.5	10.5	19.6	10.8	15.7	4.7	5.8	6.8	0.15/20	0.2/20
7	06/06/1986	Adiyaman	10.6	5.8	5.8	5.66	203	-	Stiff	1	30.3	31.1	34.4	14.8	7.7	14.9	8.5	5.1	1.5	5.5	6.6	0.3/20	0.4/20
8	13/03/1992	Erzincan	22.6	6.6	6.6	6.6	2402	-	Soft	1	3.3	16.8	12.8	25.1	9.1	23.5	9.8	163.7	177.6	2.3	3.0	0.1/30	0.1/35
9							2403	433	Stiff	1	63	65.5	76.4	16.8	12.0	16.9	10.3	5.2	5.8	11.5	12.3	0.3/25	0.2/20
10	15/03/1992	Erzincan	28.5	5.9	5.9	5.78	2402	-	Stiff	1	41.7	48.6	45.4	31.3	16.9	31.6	19.3	1.7	2.1	10.0	7.3	0.15/20	0.1/22
11	06/11/1992	Aydin	17.2	6.0	6.0	5.90	905	369	Stiff	1	38.1	40.3	38.7	22.5	9.5	22.7	10.6	6.4	9.4	11.1	24.6	0.35/35	0.35/35
12	13/11/1994	Mugla	10.0	5.3	5.3	4.93	4804	372	Stiff	1	30.1	32.2	33.2	9.6	4.3	9.5	4.7	3.9	4.9	9.1	8.8	0.35/30	0.4/20
13	29/01/1995	Erzincan	28.2	5.2	5.2	4.76	2405	320	Soft	1	19.6	33.3	21.7	16.4	10.2	16.6	10.1	3.0	3.3	17.8	11.6	0.35/25	0.2/20
14	01/10/1995	Afyon-Dinar	5.0	6.4	6.4	6.4	1501	335	Soft	1	29	29	39.1	25.1	17.3	25.2	17.8	3.9	4.2	15.5	15.7	0.3/15	0.3/15
15							2006	-	Soft	1	43.9	43.9	49.6	27.7	13.6	27.7	13.9	7.7	7.2	24.7	19.1	0.3/15	0.3/15
16							302	198	Soft	1	0	2.9	0.5	27.1	16.9	26.9	15.6	165.5	203.3	12.7	9.0	0.2/30	0.15/30
17							2002	356	Soft	1	86.9	86.9	95.4	131.4	61.4	123.6	62.8	1.6	1.4	20.0	16.3	0.07/20	0.1/20
18	05/12/1995	Erzincan	25.5	5.8	5.8	5.66	2401	314	Soft	1	58.9	65	61.6	65.0	21.5	65.8	30.5	1.9	1.5	19.9	32.4	0.1/25	0.1/25
19	14/08/1996	Amasya	11.9	5.7	5.7	5.54	502	443	Stiff	1	43.5	44.4	47.8	36.9	10.0	20.5	5.8	1.0	2.8	18.4	14.3	0.1/30	0.2/20
20	14/08/1996	Amasya	11.9	5.7	5.7	5.54	6002	-	Soft	1	115	115	119	48.2	13.2	47.3	23.4	0.3	0.2	16.2	20.4	0.25/15	0.25/15
21	14/08/1996	Amasya	2.7	5.6	5.6	5.4	502	443	Stiff	1	44.3	44.3	47.9	39.7	11.4	26.6	8.1	0.5	0.8	14.4	10.8	0.25/20	0.2/20
22							6002	-	Soft	1	116	116	120	46.7	13.3	47.3	22.9	0.5	0.3	14.7	15.0	0.3/15	0.2/15
23	22/01/1997	Hatay	45.4	5.7	5.7	5.54	3102	-	Soft	1	19.2	46.8	19.8	31.9	13.4	26.9	15.1	18.7	16.2	15.8	11.1	0.1/35	0.1/30
24	28/02/1997	Amasya	4.9	5.2	5.2	4.76	502	443	Stiff	1	39.8	39.9	42.1	30.3	9.2	30.8	9.2	0.4	0.4	9.7	16.9	0.2/20	0.2/25
25	14/11/1997	Canakkale	2.3	5.8	5.8	5.66	1701	192	Soft	1	150	150	154	34.8	23.1	34.6	24.1	0.4	0.4	17.0	17.8	0.15/20	0.2/25
26	04/04/1998	Afyon-Dinar	19.3	5.2	5.2	4.8	2006	-	Soft	1	50	54.2	51.8	14.2	7.0	14.1	7.3	0.7	0.7	25.6	27.0	0.4/30	0.5/25
27							302	198	Soft	1	2	18	4.4	20.5	9.8	22.2	9.1	10.9	14.2	8.1	5.6	0.25/20	0.2/25
28	13/04/1998	Bingol	15.3	5.2	5.2	4.76	1208	485	Stiff	1	36.9	39.2	37.6	35.9	13.4	30.5	9.9	0.1	0.2	9.8	6.0	0.15/20	0.15/20
29	09/05/1998	Elazig	26.5	5.1	5.1	4.58	2301	407	Stiff	2	47.7	53.9	49.2	26.1	12.3	39.1	16.1	0.5	0.4	6.0	15.5	0.15/25	0.15/20
30	27/06/1998	Adana-Ceyhan	46.6	6.2	6.2	6.1	105	264	Soft	2	40	58.2	48.2	27.4	13.0	27.1	13.2	94.2	105.8	8.8	10.6	0.1/22	0.1/30
31							3301	366	Stiff	3	57.5	71.2	64.9	20.8	11.3	20.9	10.3	8.2	8.9	3.2	5.4	0.2/15	0.3/15
32							3102	-	Soft	1	101	111	103	31.9	15.7	31.9	16.2	1.6	1.6	14.8	9.4	0.1/35	0.2/30
33	04/07/1998	Adana	54.6	5.4	5.4	5.1	107	-	-	2	39.2	65.5	42.2	50.5	25.0	59.9	27.2	0.9	0.7	11.1	20.2	0.05/40	0.05/30

Register Index	EARTHQUAKE INFORMATION						STATION INFORMATION							REGISTER INFORMATION									
	Date	Earthquake	Hypo central depth (km)	Magnitude			Station Code	$V_{s,30}$ (m/s)	Soil Type	Seismic Zone	Distance			Duration (NS)		Duration (EW)		Arias Intensity		ID		Filtering range f_1 / f_2 (Hz)	
				M_L	M_w	M_s					R_{jb} (km)	R_{rup} (km)	R_{epi} (km)	t_{br} (s)	t_{tf} (s)	t_{br} (s)	t_{tf} (s)	NS	EW	I_{D-NS}	I_{D-EW}	NS	EW
34							108	-	-	2	30.9	61.1	33.8	33.9	13.7	40.8	13.8	0.8	0.6	20.8	19.2	0.1/35	0.1/40
35	24/07/1999	Balikesir	10.0	5.0	5.0	4.41	1001	662	Stiff	1	37.9	39.5	39.8	68.9	52.5	66.3	52.8	0.1	0.1	8.1	7.7	0.15/30	0.07/35
36	25/07/1999	Balikesir	15.2	5.2	5.2	4.76	1001	662	Stiff	1	35.1	37.4	37.3	36.8	16.5	37.3	10.9	0.2	0.2	9.4	10.1	0.15/30	0.07/35
37	17/08/1999	Kocaeli	17.0	7.6	7.6	7.9	1604	-	-	1	61.8	63.2	94.7	80.4	79.1	98.2	79.0	7.9	7.3	9.9	12.7	0.05/25	0.05/25
38							8101	282	Soft	1	46	46.2	101	22.5	11.9	24.8	11.9	139.9	113.2	4.1	3.8	0.05/22	0.05/25
39							4106	701	Stiff	1	4.9	6.2	42.8	35.4	29.6	44.2	28.9	56.7	33.5	6.3	12.3	0.2/30	0.2/30
40							1404	348	Soft	1	44.2	45.7	80.7	25.5	11.5	25.4	11.6	20.4	26.3	7.9	10.5	0.05/25	0.07/25
41							3401	595	Stiff	1	43.4	43.5	86.5	71.1	38.1	78.7	37.4	4.1	4.8	4.7	9.5	0.05/40	0.05/40
42							1612	197	Soft	1	33.2	34.8	40.3	52.2	33.3	52.1	32.5	30.9	53.6	10.6	10.2	0.05/20	0.05/25
43							4101	826	Rock	1	0.6	3.9	3.4	50.7	34.1	49.1	34.4	74.1	98.2	12.5	7.1	0.1/35	0.1/30
44	17/08/1999	Kocaeli	17.0	7.6	7.6	7.9	4501	340	Soft	1	286	287	325	140.9	61.4	144.3	62.6	0.6	0.4	10.0	16.8	0.05/15	0.05/15
45							301	226	Soft	2	221	222	225	156.5	62.9	146.9	55.5	1.2	1.6	16.2	13.0	0.05/15	0.05/15
46							1001	662	Stiff	1	171	172	217	93.4	52.4	93.3	37.9	1.1	1.0	8.5	7.0	0.07/25	0.07/25
47							1701	192	Soft	1	255	255	309	129.7	53.7	131.2	61.1	4.1	3.9	12.4	14.5	0.07/20	0.07.20
48							4302	243	Soft	2	148	149	148	155.2	104.0	154.8	106.4	0.0	0.0	25.6	14.4	0.03/20	0.03/25
49							3701	362	Stiff	1	290	290	345	102.6	85.0	104.1	79.0	0.7	0.6	7.1	10.1	0.05/15	0.05/15
50							6401	285	Soft	2	228	229	236	101.9	54.7	99.7	44.7	0.7	0.7	21.7	7.2	0.07/20	0.07/20
51	31/08/1999	Sakarya	4.0	5.1	5.1	4.58	5401	412	Stiff	1	35.8	36.1	37.7	23.9	9.5	31.2	11.4	0.2	0.3	3.4	12.9	0.1/25	0.1/25
52	13/09/1999	Sakarya	10.4	5.8	5.8	5.7	3401	595	Stiff	2	91.3	92.3	96.4	49.5	15.8	53.5	13.5	0.2	0.2	9.9	10.3	0.07/40	0.07/30
53							1612	197	Soft	1	41.2	41.9	46	27.7	13.5	27.8	9.9	2.8	3.8	6.3	3.4	0.2/25	0.2/23
54							4302	243	Soft	2	146	146	148	88.0	34.7	89.2	33.2	0.5	0.7	15.5	12.0	0.05/20	0.05/20
55							5401	412	Stiff	1	20.5	21.8	25.5	30.1	10.1	29.8	10.4	1.2	2.4	7.4	14.8	0.05/35	0.05/30
56	29/09/1999	Sakarya	12.2	5.2	5.2	4.76	5401	412	Stiff	1	86	87.2	88.6	46.3	10.4	38.4	8.7	0.1	0.2	8.2	16.3	0.15/25	0.15/25
57	11/11/1999	Sakarya	7.5	5.6	5.6	5.4	4302	243	Soft	2	145	145	149	63.7	27.3	64.0	29.3	0.2	0.2	11.6	21.0	0.1/20	0.1/20
58							5401	412	Stiff	1	10.4	11.3	11.2	13.4	3.4	10.8	2.3	19.8	44.6	4.3	8.2	0.25/22	0.2/25
59	12/11/1999	Duzce	10.4	7.1	7.1	7.3	1401	294	Soft	1	8	8.6	36.1	17.2	8.6	24.0	9.0	386.3	252.6	5.8	2.9	0.05/25	0.05/40
60							8101	282	Soft	1	0	9.7	5.3	23.7	10.9	25.2	11.2	304.8	282.4	4.5	6.4	0.05/40	0.07/35
61							4302	243	Soft	2	164	164	184	116.6	57.8	116.6	44.0	1.9	4.6	13.6	13.9	0.05/15	0.07/15
62							1406	355	Soft	1	32.1	32.3	37.5	28.8	16.8	28.5	15.5	9.5	21.2	6.0	10.6	0.07/20	0.07/25
63							5401	412	Stiff	1	40.5	40.8	68.6	82.0	30.0	74.4	24.8	0.9	1.7	7.4	8.6	0.07/30	0.07/30
64	13/11/1999	Bolu	5.2	5.0	5.0	4.41	1401	294	Soft	1	47.6	47.8	49.7	23.1	4.7	23.0	8.3	0.2	0.1	10.6	11.5	0.25/22	0.25/23
65	14/02/2000	Duzce	10.0	5.3	5.3	4.93	8101	282	Soft	1	51.7	52.4	54	43.4	10.9	40.6	10.8	0.8	1.0	9.4	10.6	0.25/25	0.25/25
66	02/04/2000	Sakarya	8.8	4.5	4.5	3.53	5401	412	Stiff	1	15.3	17.3	15.6	7.2	2.1	6.6	1.2	0.6	1.9	6.4	5.3	0.20/25	0.07/30
67	21/04/2000	Sakarya	19.9	5.4	5.4	5.11	2002	356	Soft	1	22.6	28.5	23.4	68.0	42.6	81.3	43.5	1.4	1.3	12.4	20.5	0.1/35	0.1/35
68	06/06/2000	Cankiri-Cerkes	10.0	6.0	6.0	5.9	1801	348	Soft	1	8.2	11.1	15.2	63.5	33.6	65.8	39.7	11.4	9.3	14.2	14.7	0.07/25	0.07/40
69							3701	362	Stiff	1	90.9	91.8	95.5	60.6	29.3	61.2	31.0	0.3	0.2	18.6	14.7	0.15/25	0.15/25
70	08/06/2000	Cankiri-Cerkes	32.6	4.9	4.9	4.23	1801	348	Soft	1	9.5	32.9	11.2	43.5	20.4	42.1	17.7	0.5	0.4	15.8	15.8	0.07/40	0.07/40

Register Index	EARTHQUAKE INFORMATION						STATION INFORMATION							REGISTER INFORMATION									
	Date	Earthquake	Hypo central depth (km)	Magnitude			Station Code	$V_{s,30}$ (m/s)	Soil Type	Seismic Zone	Distance			Duration (NS)		Duration (EW)		Arias Intensity		ID		Filtering range f_1 / f_2 (Hz)	
				M_L	M_w	M_s					R_{jb} (km)	R_{rup} (km)	R_{epi} (km)	t_{br} (s)	t_{tf} (s)	t_{br} (s)	t_{tf} (s)	NS	EW	I_{D-NS}	I_{D-EW}	NS	EW
71	09/06/2000	Cankiri-Cerkes	3.9	5.0	5.0	4.41	1801	348	Soft	1	9	9.3	10.7	44.8	24.5	43.6	21.8	0.5	0.6	19.8	13.7	0.1/40	0.07/40
72	23/08/2000	Sakarya	10.5	5.3	5.3	4.9	5402	272	Soft	1	14.2	16.6	17	31.5	11.1	23.5	13.9	6.9	10.0	3.3	3.4	0.07/25	0.1/25
73							8101	282	Soft	1	30.9	32.1	33.5	25.2	13.3	25.1	13.8	0.4	0.4	8.9	14.0	0.1/30	0.07/40
74							1612	197	Soft	1	93.6	93.9	96	39.8	14.7	44.2	20.0	1.1	0.7	11.3	12.8	0.07/25	0.1/25
75							5401	412	Stiff	1	29.8	31.6	32.5	28.4	11.9	26.6	10.0	0.3	0.6	11.4	17.4	0.1/15	0.2/15
76	04/10/2000	Denizli	2.8	5.0	5.0	4.41	2002	356	Soft	1	9.9	10.1	11.9	23.2	18.1	22.5	16.2	3.3	4.2	31.2	33.1	0.35/30	0.25/30
77	15/11/2000	Van	48.4	5.5	5.5	5.28	6501	363	Stiff	2	36.8	59.4	40.6	66.2	33.1	66.2	33.4	0.3	0.4	18.5	27.1	0.15/25	0.2/30
78	16/01/2001	Istanbul	13.8	4.0	4.0	2.65	3401	595	Stiff	2	17.6	21.8	18	18.4	6.9	9.8	4.5	0.0	0.0	6.3	4.8	0.4/15	0.4/15
79	22/03/2001	Cankiri	10.8	4.7	4.7	3.88	1801	348	Soft	1	22.6	24.6	24	41.5	12.7	41.6	12.5	0.3	0.3	9.4	19.8	0.6/30	0.6/35
80	29/05/2001	Erzurum	20.3	4.9	4.9	4.23	2501	375	Stiff	2	33.9	38.6	35.3	31.1	11.5	36.3	13.6	0.5	0.4	8.8	11.7	0.1/30	0.1/30
81	22/06/2001	Balikesir	7.0	5.2	5.2	4.76	1001	662	Soft	1	33.8	34.2	34.8	26.5	8.9	27.1	9.7	0.1	0.1	9.1	11.9	0.07/25	0.1/25
82	25/06/2001	Kahramanmaras	10.0	5.4	5.4	5.11	4603	466	Rock	2	73.7	74.7	75.8	74.0	24.6	73.1	23.9	0.3	0.4	21.3	20.8	0.1/25	0.1/20
83	10/07/2001	Erzurum	22.5	5.4	5.4	5.11	2501	375	Stiff	2	31.2	37.1	34.1	36.2	11.2	34.9	11.4	0.7	0.9	8.9	12.8	0.07/30	0.07/25
84	26/08/2001	Bolu	8.8	5.2	5.2	4.76	1401	294	Soft	1	22.8	23.8	24.2	4.5	1.6	5.6	2.3	6.5	3.0	6.5	7.8	0.6/35	0.6/35
85	02/12/2001	Van	19.6	4.8	4.8	4.06	6501	363	Stiff	2	12.8	22.7	14.2	26.1	10.9	27.9	13.9	0.7	0.5	7.8	12.8	0.1/30	0.2/35
86	03/02/2002	Afyon	22.1	6.5	6.5	6.5	301	226	Soft	2	51.7	57.7	64.7	30.3	14.2	31.9	16.7	13.7	17.1	5.8	13.5	0.07/17	0.1/17
87							4302	243	Soft	2	133	135	144	42.1	25.9	41.9	24.8	1.7	1.7	13.7	13.7	0.1/22	0.07/15
88	03/02/2002	Afyon	24.9	5.8	5.8	5.66	301	226	Soft	2	30.8	37.9	34	55.6	28.6	45.8	20.1	3.5	5.4	17.2	12.4	0.1/20	0.1/20
89	30/07/2002	Denizli	6.0	4.7	4.7	3.88	2002	356	Soft	1	24	25.1	25.4	39.5	21.3	38.8	17.1	0.3	0.4	23.1	18.8	0.1/45	0.2/35
90	19/11/2002	Malatya	10.0	4.8	4.8	4.06	4401	481	Stiff	1	35.2	37.1	35.9	20.6	6.7	17.0	4.9	0.1	0.2	11.2	6.0	0.2/30	0.15/35
91	14/12/2002	Kahramanmaras	29.2	4.8	4.8	4.06	4604	611	Stiff	2	17.3	32.9	19.1	8.1	3.1	9.7	3.8	1.3	0.9	6.0	8.4	0.2/25	0.2/30
92	10/04/2003	Izmir	11.3	5.7	5.7	5.5	3502	270	Soft	1	33.2	34.6	37.5	25.2	11.0	37.4	13.3	4.2	2.5	5.4	10.8	0.07/35	0.05/27
93							908	269	Soft	1	129	129	133	50.0	31.5	50.0	33.6	0.3	0.2	17.0	21.6	0.2/30	0.15/25
94	01/05/2003	Bingol	10.0	6.3	6.3	6.27	1201	529	Stiff	1	2.2	5.8	11.8	23.9	4.6	23.9	6.8	200.3	82.7	7.4	8.0	0.2/25	0.1/25
95	08/05/2003	Bingol	8.6	4.9	4.9	4.2	1202	-	-	1	13.3	15	14	36.0	15.9	29.2	15.7	0.8	0.4	14.4	12.7	0.05/30	0.1/30
96							1201	529	Stiff	1	11.6	13.4	12.9	25.2	11.1	23.7	11.2	0.2	0.3	12.3	4.9	0.15/20	0.1/20
97							1205	529	Stiff	1	11.6	13.4	12.9	33.3	16.7	28.4	14.7	0.6	0.9	17.7	8.0	0.1/45	0.07/45
98							1203	-	-	1	16.4	17.8	18	28.7	14.9	25.9	13.3	0.5	0.6	8.9	7.5	0.1/17	0.1/25
99							1204	-	-	1	12.9	14.6	14.3	27.9	13.6	31.3	13.3	0.1	0.0	10.4	8.4	0.1/40	0.1/22
100	10/05/2003	Bingol	10.0	4.8	4.8	4.06	1205	529	Stiff	1	19.5	21.2	20.8	30.2	14.1	32.8	17.4	0.5	0.2	10.7	14.4	0.15/22	0.1/22
101	21/05/2003	Duzce	5.0	4.4	4.4	3.36	8101	282	Soft	1	15.7	16.1	16.4	31.7	13.6	21.8	12.7	0.3	0.4	13.4	8.8	0.1/30	0.3/30
102	09/06/2003	Bandirma	9.1	4.8	4.8	4.06	1007	417	Stiff	1	17	19.9	18.2	16.3	4.0	17.0	5.2	0.7	0.4	5.6	7.1	03/35	0.2/35
103	06/07/2003	Canakkale	17.1	5.7	5.7	5.54	1701	192	Soft	1	44.1	46.8	45.9	58.2	31.9	58.7	28.1	1.3	1.1	13.2	22.2	0.1/30	0.07/25
104	13/07/2003	Malatya	12.9	5.5	5.5	5.28	4401	481	Stiff	1	55	55.9	56.3	39.6	15.3	38.9	17.9	0.2	0.2	8.1	11.4	0.07/30	0.1/30
105	23/07/2003	Denizli	28.3	5.3	5.3	4.9	2007	232	Soft	1	10.9	28.3	13.3	90.0	12.0	21.3	11.3	5.6	7.3	7.7	7.8	0.07/30	0.07/30
106							907	301	Soft	1	37.4	45.7	39.9	26.5	10.7	35.3	10.5	0.5	0.5	9.5	13.7	0.05/40	0.05/30
107							908	269	Soft	1	47.4	54.1	49.9	49.3	23.9	51.1	18.6	0.8	1.0	15.3	16.4	0.07/30	0.1/35

Register Index	EARTHQUAKE INFORMATION						STATION INFORMATION							REGISTER INFORMATION									
	Date	Earthquake	Hypo central depth (km)	Magnitude			Station Code	$V_{s,30}$ (m/s)	Soil Type	Seismic Zone	Distance			Duration (NS)		Duration (EW)		Arias Intensity		ID		Filtering range f_1 / f_2 (Hz)	
				M_L	M_w	M_s					R_{jb} (km)	R_{rup} (km)	R_{epi} (km)	t_{br} (s)	t_{tf} (s)	t_{br} (s)	t_{tf} (s)	NS	EW	I_{D-NS}	I_{D-EW}	NS	EW
108							2002	356	Soft	1	30.2	39.9	32.9	42.0	23.4	33.0	16.7	0.6	1.1	19.4	12.3	0.15/35	0.1/40
109							2007	232	Soft	1	18.8	19.1	20	22.7	11.3	38.6	15.1	1.2	0.9	12.9	12.8	0.07/30	0.1/30
110	26/07/2003	Denizli	5.0	4.9	4.9	4.2	907	301	Soft	1	42.8	43	43.2	35.6	11.3	30.1	10.5	0.1	0.1	8.6	11.6	0.07/40	0.1/30
111							908	269	Soft	1	52.1	52.2	52.6	48.6	20.6	41.6	18.4	0.2	0.3	24.3	18.1	0.15/40	0.2/40
112							2007	232	Soft	1	11.2	22	13.8	37.4	15.5	36.8	18.3	10.8	10.4	11.6	12.9	0.05/30	0.05/30
113							2002	356	Soft	1	29.2	34.8	32.2	50.9	32.9	50.4	32.2	0.9	1.3	15.8	20.1	0.1/15	0.1/15
114	26/07/2003	Denizli	21.3	5.4	5.4	5.1	907	301	Soft	1	40	44.3	42.5	36.1	11.6	36.2	10.7	0.8	0.7	8.9	18.6	0.05/30	0.1/30
115							908	269	Soft	1	49.9	53.4	52.5	62.4	20.8	59.9	19.6	1.1	1.4	16.8	19.7	0.1/30	0.1/35
116							904	371	Stiff	1	76.3	78.7	79	37.3	11.4	53.5	12.6	0.1	0.1	11.2	11.5	0.1/30	0.1/30
117	26/07/2003	Denizli	7.3	4.9	4.9	4.2	2007	232	Soft	1	16.8	17.8	18.5	65.0	32.0	51.7	27.8	0.3	0.3	16.6	12.0	0.15/35	0.1/35
118							908	269	Soft	1	48.2	48.5	49.9	49.5	20.5	47.6	23.2	0.3	0.3	12.4	9.8	0.1/40	0.2/40
119	26/02/2004	Malatya	5.0	4.9	4.9	4.23	4401	481	Stiff	1	44.1	44.6	45.6	17.7	9.9	29.8	11.8	0.1	0.1	7.2	18.5	0.3/40	0.3/40
120	03/03/2004	Malatya	7.2	4.6	4.6	3.71	1201	529	Stiff	1	17.8	18.8	18.7	17.5	8.8	28.5	12.6	0.1	0.1	4.0	11.6	0.2/40	0.25/30
121	13/04/2004	Bolu	5.0	4.4	4.4	3.36	1401	294	Soft	1	7.3	8.3	7.4	34.8	5.6	28.7	5.3	1.7	1.9	4.8	14.4	0.2/25	0.35/22
122	04/08/2004	Mugla	10.0	5.5	5.5	5.3	4802	747	Stiff	1	33.1	35.2	36.5	32.2	6.2	31.2	6.5	0.3	0.4	6.1	4.9	0.15/30	0.2/35
123							4802	747	Stiff	1	34.2	36.2	37	14.2	3.7	15.9	4.0	0.3	0.3	3.6	8.4	0.07/30	0.1/30
124	11/08/2004	Elazig	7.4	5.6	5.6	5.41	2301	407	Stiff	2	33.4	33.8	37	44.9	15.2	43.5	15.7	0.6	1.0	8.1	8.2	0.1/20	0.1/15
125	20/12/2004	Mugla	12.5	5.3	5.3	4.9	4804	372	Stiff	1	33.8	35.5	36.7	21.8	9.0	33.5	13.2	0.4	0.2	10.3	15.9	0.07/30	0.2/30
126							4805	393	Stiff	1	16.2	19.4	18.7	50.4	14.3	35.6	12.7	1.7	2.8	19.4	26.4	0.07/12	0.15/12
127	10/01/2005	Mugla	15.8	5.4	5.4	5.11	4805	393	Stiff	1	40.2	42.5	43.3	54.2	16.1	42.0	16.8	0.5	0.5	13.1	19.7	0.07/12	0.1/12
128	11/01/2005	Mugla	14.9	5.0	5.0	4.41	4802	747	Stiff	1	25.5	29.7	27.4	27.5	8.7	26.9	8.2	0.0	0.1	15.6	16.3	0.1/30	0.1/12
129	23/01/2005	Antalya	12.1	5.8	5.8	5.66	703	299	Soft	1	75.2	75.9	80	58.8	19.9	65.2	28.3	1.5	1.2	11.0	9.6	0.07/20	0.1/22
130	06/06/2005	Bingol	10.5	5.6	5.6	5.41	1208	485	Stiff	1	45.4	46	48.5	39.9	12.4	33.3	9.8	0.3	0.3	15.4	15.9	0.15/25	0.1/25
131	17/10/2005	Izmir	20.5	5.5	5.5	5.28	3502	270	Soft	1	53	56	56.2	37.6	14.0	36.6	13.6	0.4	0.3	14.6	10.0	0.3/30	0.3/30
132	17/10/2005	Izmir	18.6	5.8	5.8	5.66	3502	270	Soft	1	51.3	53.5	56.1	37.1	12.9	35.4	14.7	0.6	0.6	10.3	14.0	0.15/25	0.07/25
133	17/10/2005	Izmir	11.0	5.2	5.2	4.76	3502	270	Soft	1	56.1	57.1	58.3	37.1	14.3	37.0	15.6	0.2	0.2	9.8	15.1	0.1/30	0.1/30
134	20/10/2005	Izmir	15.4	5.8	5.8	5.7	3502	270	Soft	1	54.1	55.4	59	45.7	15.1	42.4	15.7	1.3	1.2	16.1	8.7	0.0730	0.07/35
135							4501	340	Soft	1	75.4	76.4	80.3	61.4	17.0	38.9	15.1	0.3	0.4	18.2	7.3	0.1/25	0.1/25
136	26/11/2005	Malatya	19.1	5.1	5.1	4.58	4401	481	Stiff	1	47.6	50.6	49.2	28.2	12.6	33.7	15.6	0.1	0.1	8.8	13.6	0.1/35	0.1/35
137							2007	232	Soft	1	14.2	18.3	15.8	34.8	10.2	35.6	13.6	0.6	0.4	8.2	14.3	0.1/25	0.1/40
138	05/06/2006	Denizli	11.1	4.8	4.8	4.1	907	301	Soft	1	22.8	25	24.5	12.7	5.6	10.4	4.2	0.9	1.1	12.3	6.1	0.2/25	0.2/25
139							908	269	Soft	1	33.5	35	35.2	40.9	16.9	47.5	12.0	0.4	0.5	22.9	21.9	0.2/25	0.2/30
140							1603	459	Stiff	1	27	28.4	29	16.3	2.7	21.5	5.4	0.6	0.3	7.8	8.3	0.2/25	0.2/20
141							1601	249	Soft	1	20.9	22.6	22.9	20.7	13.3	25.7	11.4	1.8	0.9	3.4	9.0	0.15/40	0.15/40
142	24/10/2006	Bursa	7.9	5.2	5.2	4.8	1606	274	Soft	1	10.7	12.2	12.7	13.4	4.9	11.4	4.8	13.2	15.0	7.2	8.7	0.1/20	0.2/30
143							1607	370	Stiff	1	7.3	9.3	9.4	19.2	7.5	15.1	8.2	14.4	10.8	5.8	3.2	0.1/20	0.2/30
144							1608	366	Stiff	1	13.7	14.9	15.8	15.7	6.3	14.4	4.6	3.0	4.3	7.6	4.8	0.15/20	0.1/25

Register Index	EARTHQUAKE INFORMATION						STATION INFORMATION							REGISTER INFORMATION									
	Date	Earthquake	Hypo central depth (km)	Magnitude			Station Code	$V_{s,30}$ (m/s)	Soil Type	Seismic Zone	Distance			Duration (NS)		Duration (EW)		Arias Intensity		ID		Filtering range f_1 / f_2 (Hz)	
				M_L	M_w	M_s					R_{jb} (km)	R_{rup} (km)	R_{epi} (km)	t_{br} (s)	t_{tf} (s)	t_{br} (s)	t_{tf} (s)	NS	EW	I_{D-NS}	I_{D-EW}	NS	EW
145							1609	228	Soft	1	12.7	13.9	14.7	26.7	10.7	19.9	10.4	5.0	5.8	14.4	7.4	0.1/20	0.1/25
146							1615	-	-	1	23.2	23.9	25.2	35.3	9.7	22.0	11.0	1.2	1.1	13.9	5.6	0.15/30	0.1/30
147							7701	375	Stiff	1	29.4	29.9	30.8	21.0	12.9	26.9	11.4	0.5	0.7	11.9	10.3	0.2/15	0.15/15
148							7702	359	Soft	1	28.5	29.1	29.7	18.1	3.3	18.5	7.3	0.9	0.6	7.4	10.5	0.2/25	0.25/20
149							1613	401	Stiff	2	57.8	58.7	59.8	48.3	21.7	48.8	23.9	0.1	0.1	28.5	31.7	0.2/25	0.2/25
150							302	198	Soft	1	-	-	151	95.0	42.7	95.5	50.1	0.5	0.3	14.9	21.8	0.1/20	0.1/20
151							1006	321	Soft	1	-	-	162	84.9	20.1	85.5	19.4	0.4	0.5	8.1	11.5	0.1/20	0.1/20
152							1009	561	Stiff	1	-	-	62.8	128.5	25.2	128.2	25.5	0.4	0.3	10.1	13.0	0.1/20	0.1/20
153							1102	407	Stiff	2	-	-	119	54.9	25.9	59.5	25.7	0.2	0.2	10.1	11.6	0.1/20	0.1/20
154							1613	401	Stiff	2	-	-	87.8	92.7	26.0	95.3	30.1	1.2	0.7	17.7	19.2	0.1/20	0.1/20
155							1614	265	Soft	1	-	-	116	48.9	16.7	40.2	9.6	1.1	2.6	9.9	7.4	0.1/20	0.1/20
156	19/05/2011	Kutahya-Simav	24.5	5.7	5.9	5.7	1618	-	-	1	-	-	136	95.9	25.6	95.8	23.5	0.4	0.3	15.1	16.1	0.1/20	0.1/20
157							2605	801	Rock	2	-	-	141	52.7	24.9	115.4	29.1	0.2	0.3	10.6	14.2	0.1/20	0.1/20
158							2610	-	-	2	-	-	138	113.0	30.7	97.6	32.6	0.4	0.3	12.9	13.1	0.1/20	0.1/20
159							2613	-	-	2	-	-	73.4	100.7	32.3	99.5	40.9	0.2	0.2	11.0	14.3	0.1/20	0.1/20
160							4108	-	-	1	-	-	195	164.0	67.2	160.9	75.3	0.9	1.0	30.0	15.2	0.1/20	0.1/20
161							4116	-	-	1	-	-	188	161.3	77.9	155.4	87.4	0.4	0.4	12.0	12.7	0.1/20	0.1/20
162							4301	267	Soft	2	-	-	85	90.8	19.7	92.9	26.3	1.8	1.4	17.9	18.3	0.1/20	0.1/20
163							4304	343	Soft	1	-	-	31.5	81.0	18.4	80.5	16.1	4.9	7.6	9.6	13.0	0.1/20	0.1/20
164	19/05/2011	Kutahya-Simav	24.5	5.7	5.9	5.7	4306	304	Soft	1	-	-	26.8	36.3	13.7	38.7	15.2	8.3	6.4	8.6	8.8	0.1/20	0.1/20
165							4502	292	Soft	1	-	-	11.8	95.8	33.1	94.7	35.2	0.8	0.8	10.7	9.2	0.1/20	0.1/20
166							6401	285	Soft	2	-	-	58.4	35.1	10.8	35.6	10.3	2.9	2.7	10.0	8.8	0.1/20	0.1/20
167							6503	293	Soft	1	-	-	42.2	57.0	19.2	57.1	22.3	78.5	50.9	10.5	12.8	0.1/20	0.1/20
168	23/10/2011	Van-Muradiye-Merkez	19.02	6.6	6.7	6.8	1302	-	-	2	-	-	117	116.7	12.6	117.8	16.1	10.4	14.9	8.3	11.8	0.1/20	0.1/20
169							4902	311	Soft	1	-	-	95.5	46.0	36.8	45.6	27.7	9.3	7.3	11.1	7.7	0.1/20	0.1/20

Table 3-2 PGA, PGV and PGD of the considered Turkish registers

Register Index	EARTHQUAKE INFORMATION			STATION INFORMATION			REGISTER INFORMATION											
							N-S Component						E-W Component					
							Uncorrected			Corrected			Uncorrected			Corrected		
	Date	Earthquake Location	M_w	Station - Code	Soil Type	Distance	PGA (cm/s^2)	PGV (cm/s)	PGD (cm)	PGA (cm/s^2)	PGV (cm/s)	PGD (cm)	PGA (cm/s^2)	PGV (cm/s)	PGD (cm)	PGA (cm/s^2)	PGV (cm/s)	PGD (cm)
1	19/08/1976	Denizli	6.1	2001	Soft Soil	9.9	348.51	40.05	77.0	348.68	25.61	2.2	260.06	28.75	125.1	266.90	17.10	1.3
2	16/12/1977	Izmir Guzelyali	5.6	3506	Stiff Soil	9.5	394.44	14.97	11.8	395.33	12.86	0.7	128.17	7.91	11.67	127.90	4.92	0.2
3	18/07/1979	Balikesir	5.3	1010	Stiff Soil	6.5	231.85	9.92	12.0	218.89	9.64	1.2	288.11	9.09	7.95	269.97	8.45	0.7
4	05/07/1983	Balikesir	6.1	1012	Stiff Soil	55.4	54.90	5.25	10.5	51.28	5.24	0.8	48.35	5.17	20.62	46.68	2.32	0.2
5				1014	Stiff Soil	44.1	49.36	8.90	38.7	47.04	3.92	0.7	46.40	8.49	29.50	44.76	2.37	0.4
6	05/05/1986	Adiyaman	6.0	203	Stiff Soil	29.2	115.92	15.69	13.2	116.43	14.43	4.8	77.45	7.93	7.39	76.80	5.56	1.5
7	06/06/1986	Adiyaman	5.8	203	Stiff Soil	34.4	68.88	9.13	3.8	69.31	8.37	1.3	33.83	8.67	15.97	33.57	4.20	0.6
8	13/03/1992	Erzincan	6.6	2402	Soft Soil	12.8	403.92	106.83	28.6	403.91	108.72	34.1	472.04	85.23	73.54	478.79	77.55	27.2
9				2403	Stiff Soil	76.4	66.77	6.11	16.5	66.54	4.20	0.6	84.92	4.90	12.31	80.60	3.61	0.6
10	15/03/1992	Erzincan	5.9	2402	Stiff Soil	45.4	32.72	3.54	5.1	32.21	3.37	1.1	39.28	4.48	7.60	39.03	4.67	1.5
11	06/11/1992	Aydin	6.0	905	Stiff Soil	38.7	83.00	9.01	20.7	82.59	4.36	0.5	71.25	9.27	33.84	70.32	3.40	0.4
12	13/11/1994	Mugla	5.3	4804	Stiff Soil	33.2	72.64	3.91	1.1	69.96	3.80	0.4	96.89	4.26	1.85	94.09	3.68	0.3
13	29/01/1995	Erzincan	5.2	2405	Soft Soil	21.7	45.19	4.06	13.5	44.86	2.31	0.3	48.28	5.32	13.11	47.77	3.74	0.5
14	01/10/1995	Afyon Dinar	6.4	1501	Soft Soil	39.1	40.15	6.96	23.7	34.49	4.61	0.95	42.13	5.97	23.18	39.18	4.31	1.2
15				2006	Soft Soil	49.6	65.78	7.04	37.8	62.63	3.12	0.36	61.15	7.13	18.93	57.97	4.08	0.5
16				302	Soft Soil	0.5	275.47	35.75	61.4	272.91	29.72	6.52	323.94	40.88	65.01	321.25	44.08	9.2
17				2002	Soft Soil	95.4	15.76	3.55	97.0	15.56	3.22	1.32	14.88	4.40	75.34	14.49	3.80	1.3
18	05/12/1995	Erzincan	5.8	2401	Soft Soil	61.6	28.27	2.27	10.7	28.01	2.11	0.47	24.02	2.11	51.58	23.79	1.18	0.3
19	14/08/1996	Amasya	5.7	502	Stiff Soil	47.8	27.02	1.40	5.7	26.81	1.28	0.26	53.58	2.48	26.66	53.90	2.27	0.1
20	14/08/1996	Amasya	5.7	6002	Soft Soil	118.7	10.72	1.42	17.0	10.51	1.06	0.11	7.24	0.74	5.31	7.22	0.64	0.1
21	14/08/1996	Amasya	5.6	502	Stiff Soil	47.9	20.02	1.30	3.9	19.48	1.18	0.12	33.08	2.11	25.90	33.34	1.46	0.1
22				6002	Soft Soil	119.8	15.22	1.38	5.7	15.30	1.38	0.13	12.26	1.05	3.52	11.94	0.94	0.1
23	22/01/1997	Hatay	5.7	3102	Soft Soil	19.8	136.16	5.89	29.7	133.39	5.54	1.00	150.45	6.54	52.27	148.89	6.16	0.9
24	28/02/1997	Amasya	5.2	502	Stiff Soil	42.1	21.49	1.17	8.4	21.41	1.06	0.07	21.36	0.76	3.73	21.36	0.73	0.0
25	14/11/1997	Canakkale	5.8	1701	Soft Soil	154.4	10.38	1.80	17.2	10.37	1.45	0.33	9.59	2.17	15.46	9.49	1.54	0.3
26	04/04/1998	Afyon Dinar	5.2	2006	Soft Soil	51.8	27.66	5.88	21.0	23.59	0.73	0.05	24.43	2.13	5.48	21.31	0.76	0.0
27				302	Soft Soil	4.4	135.48	7.76	18.3	135.46	6.24	0.85	129.92	12.44	8.29	128.03	12.38	1.8
28	13/04/1998	Bingol	5.2	1208	Stiff Soil	37.6	11.88	0.81	10.6	12.01	0.62	0.07	13.61	1.57	23.24	13.90	1.23	0.2
29	09/05/1998	Elazig	5.1	2301	Stiff Soil	49.2	25.97	1.83	14.7	26.12	2.03	0.15	15.01	1.39	16.77	15.13	1.04	0.1
30	27/06/1998	Adana Ceyhan	6.2	105	Soft Soil	48.2	223.40	28.15	27.2	222.04	29.94	7.16	273.78	26.50	29.47	273.50	22.78	5.8
31				3301	Stiff Soil	64.9	120.32	17.02	32.2	118.52	13.27	1.61	130.89	10.79	6.69	125.89	8.23	1.1
32				3102	Soft Soil	102.5	27.09	2.69	9.5	27.09	2.56	0.57	25.85	3.44	33.26	25.77	4.22	0.9
33	04/07/1998	Adana	5.4	107	-	42.2	28.29	1.80	1.4	28.30	1.80	0.64	20.80	1.02	2.94	20.86	1.04	0.2
34	04/07/1998	Adana	5.4	108	-	33.8	24.14	0.99	1.3	24.14	0.98	0.21	19.95	1.02	0.69	19.88	0.99	0.1
35	24/07/1999	Balikesir	5.0	1001	Stiff Soil	39.8	11.25	0.98	15.0	11.22	0.85	0.06	12.97	0.77	9.73	12.91	0.85	0.1

Register Index	EARTHQUAKE INFORMATION			STATION INFORMATION			REGISTER INFORMATION											
							N-S Component						E-W Component					
							Uncorrected			Corrected			Uncorrected			Corrected		
	Date	Earthquake Location	M_w	Station - Code	Soil Type	Distance	PGA (cm/s^2)	PGV (cm/s)	PGD (cm)	PGA (cm/s^2)	PGV (cm/s)	PGD (cm)	PGA (cm/s^2)	PGV (cm/s)	PGD (cm)	PGA (cm/s^2)	PGV (cm/s)	PGD (cm)
36	25/07/1999	Balikesir	5.2	1001	Stiff Soil	37.3	12.81	1.01	8.3	12.80	0.91	0.09	14.41	0.93	7.70	14.43	1.05	0.1
37	17/08/1999	Kocaeli	7.6	1604	-	94.7	54.34	9.53	31.3	54.26	9.25	5.48	45.30	8.84	279.1	45.08	7.98	4.2
38				8101	Soft Soil	101.2	373.67	53.42	71.0	365.59	58.29	22.97	314.79	60.67	57.23	311.35	59.84	42.0
39				4106	Stiff Soil	42.8	266.86	61.69	259.8	242.57	23.23	9.46	144.14	35.98	283.4	136.97	12.47	4.6
40				1404	Soft Soil	80.7	119.15	14.66	10.8	119.52	13.42	4.54	138.68	13.36	14.05	138.32	11.36	3.8
41				3401	Stiff Soil	86.5	60.68	10.03	18.8	60.39	8.89	9.08	42.69	7.81	11.11	42.87	7.38	5.0
42				1612	Soft Soil	40.3	91.89	17.89	112.8	91.84	19.85	12.16	123.26	30.97	73.61	123.79	26.48	20.4
43				4101	rock	3.4	169.38	42.77	578.8	164.87	22.42	8.89	226.30	52.68	527.4	230.82	37.64	19.3
44				4501	Soft Soil	324.5	12.08	3.45	56.2	12.14	2.84	1.32	6.01	2.39	28.98	6.08	2.41	2.2
45				301	Soft Soil	225.3	13.26	3.26	114.9	13.22	3.47	1.57	15.11	4.44	207.9	14.99	5.06	2.5
46				1001	Stiff Soil	216.7	17.79	5.55	73.8	17.55	4.76	3.92	18.17	6.55	42.45	17.88	4.99	4.3
47				1701	Soft Soil	309.2	24.56	9.86	42.4	24.37	8.52	8.68	28.63	6.40	18.96	28.72	5.90	3.7
48				4302	Soft Soil	148.4	2.34	0.36	16.1	2.27	0.19	0.06	3.09	0.38	7.76	3.10	0.28	0.1
49				3701	Stiff Soil	345.2	11.67	6.00	37.6	11.62	4.94	6.30	8.93	4.66	53.23	8.88	4.09	2.2
50	17/08/1999	Kocaeli	7.6	6401	Soft Soil	236.2	11.21	2.80	19.7	10.99	1.82	0.92	14.28	4.99	35.80	14.88	3.81	3.0
51	31/08/1999	Sakarya	5.1	5401	Stiff Soil	37.7	24.41	1.56	2.7	24.44	1.53	0.20	17.07	0.87	8.04	17.05	0.78	0.1
52	13/09/1999	Sakarya	5.8	3401	Stiff Soil	96.4	14.10	0.88	3.7	14.10	0.74	0.18	15.59	0.83	5.50	15.57	0.89	0.1
53				1612	Soft Soil	46	61.34	4.07	4.2	61.41	4.48	0.65	75.44	8.33	10.37	75.78	9.08	1.1
54				4302	Soft Soil	147.9	11.00	1.95	4.2	10.97	1.97	0.68	13.57	2.80	16.69	13.54	2.68	1.1
55				5401	Stiff Soil	25.5	42.22	2.40	11.1	42.18	2.50	0.76	50.64	1.96	8.66	51.62	1.99	0.6
56	29/09/1999	Sakarya	5.2	5401	Stiff Soil	88.6	11.90	0.80	1.7	11.86	0.81	0.07	13.67	0.75	5.47	13.72	0.64	0.0
57	11/11/1999	Sakarya	5.6	4302	Soft Soil	148.9	10.02	1.18	9.5	10.05	1.03	0.20	6.82	1.14	8.32	6.83	1.01	0.3
58				5401	Stiff Soil	11.2	206.53	15.16	395.9	198.13	14.49	2.51	345.30	9.52	154.7	351.23	9.68	1.1
59	12/11/1999	Duzce	7.1	1401	Soft Soil	36.1	739.44	58.64	44.4	744.73	56.23	23.28	805.86	66.43	46.11	806.57	66.85	11.8
60				8101	Soft Soil	5.3	514.22	89.34	275.6	515.03	81.78	56.35	407.57	65.88	92.19	406.14	68.25	44.1
61				4302	Soft Soil	184.4	17.11	5.00	26.6	17.07	5.08	2.76	20.70	9.81	22.97	20.67	9.91	5.4
62				1406	Soft Soil	37.5	58.80	24.62	355.6	59.41	16.75	14.13	121.03	17.09	74.33	120.39	10.37	7.8
63				5401	Stiff Soil	68.6	17.35	4.87	18.9	16.97	4.56	5.27	24.73	5.14	11.86	24.70	5.00	5.3
64	13/11/1999	Bolu	5.0	1401	Soft Soil	49.7	16.26	0.91	3.1	16.34	0.71	0.07	8.69	0.67	2.99	8.73	0.54	0.1
65	14/02/2000	Duzce	5.3	8101	Soft Soil	54	37.55	1.45	3.5	37.34	1.51	0.11	29.57	1.89	3.26	29.68	2.04	0.1
66	02/04/2000	Sakarya	4.5	5401	Stiff Soil	15.6	59.25	0.99	0.4	56.73	1.03	0.07	103.82	2.11	8.54	104.82	2.18	0.2
67	21/04/2000	Sakarya	5.4	2002	Soft Soil	23.4	27.56	2.58	8.0	27.51	2.53	0.52	17.68	2.94	46.74	17.67	2.27	0.7
68	06/06/2000	Cankiri Cerkes	6.0	1801	Soft Soil	15.2	62.47	8.10	9.5	62.44	8.02	2.84	63.15	6.84	58.09	63.21	6.27	2.9
69				3701	Stiff Soil	95.5	11.72	1.13	8.5	11.77	0.96	0.29	12.12	1.04	14.12	12.06	0.77	0.3
70	08/06/2000	Cankiri Cerkes	4.9	1801	Soft Soil	11.2	12.21	1.54	2.0	12.22	1.59	0.26	15.03	1.13	4.54	15.03	1.14	0.3
71	09/06/2000	Cankiri Cerkes	5.0	1801	Soft Soil	10.7	11.72	1.47	9.9	11.72	1.35	0.43	18.94	1.51	9.08	18.93	1.37	0.4
72	23/08/2000	Sakarya	5.3	5402	Soft Soil	17	79.02	16.67	7.9	79.06	16.57	5.62	96.72	18.92	19.06	96.65	18.76	5.4

Register Index	EARTHQUAKE INFORMATION			STATION INFORMATION			REGISTER INFORMATION											
							N-S Component						E-W Component					
							Uncorrected			Corrected			Uncorrected			Corrected		
	Date	Earthquake Location	M_w	Station - Code	Soil Type	Distance	PGA (cm/s^2)	PGV (cm/s)	PGD (cm)	PGA (cm/s^2)	PGV (cm/s)	PGD (cm)	PGA (cm/s^2)	PGV (cm/s)	PGD (cm)	PGA (cm/s^2)	PGV (cm/s)	PGD (cm)
73				8101	Soft Soil	33.5	23.28	1.30	2.8	23.19	1.20	0.21	17.52	1.16	3.71	17.53	1.03	0.2
74				1612	Soft Soil	96	21.69	2.75	4.2	21.69	2.71	0.98	16.20	2.13	3.26	16.24	1.99	0.4
75				5401	Stiff Soil	32.5	20.86	0.76	4.9	18.58	0.82	0.13	27.45	0.85	10.16	26.51	0.86	0.1
76	04/10/2000	Denizli	5.0	2002	Soft Soil	11.9	49.17	1.70	8.7	50.12	1.31	0.12	66.44	1.49	10.95	66.15	1.19	0.1
77	15/11/2000	Van	5.5	6501	Stiff Soil	40.6	13.32	0.98	6.8	13.35	0.84	0.15	11.69	0.82	3.65	11.70	0.73	0.1
78	16/01/2001	Istanbul	4.0	3401	Stiff Soil	18	10.94	0.34	0.5	10.82	0.31	0.02	15.93	0.44	1.48	14.13	0.36	0.0
79	22/03/2001	Cankiri	4.7	1801	Soft Soil	24	18.32	1.20	4.6	18.30	0.95	0.06	16.03	0.65	1.22	15.86	0.56	0.0
80	29/05/2001	Erzurum	4.9	2501	Stiff Soil	35.3	21.86	1.70	17.3	21.89	1.51	0.33	17.23	1.13	1.78	17.33	1.20	0.1
81	22/06/2001	Balikesir	5.2	1001	Soft Soil	34.8	11.76	0.52	3.5	11.78	0.51	0.08	11.01	0.45	1.81	10.98	0.40	0.1
82	25/06/2001	Kahramanmaras	5.4	4603	rock	75.8	11.78	1.10	25.1	11.72	0.77	0.16	14.32	1.37	34.95	14.07	0.78	0.2
83	10/07/2001	Erzurum	5.4	2501	Stiff Soil	34.1	19.54	1.97	23.3	19.59	2.45	0.48	21.93	1.98	6.65	21.85	1.92	0.3
84	26/08/2001	Bolu	5.2	1401	Soft Soil	24.2	189.09	3.37	0.6	189.53	3.27	0.08	131.68	1.77	0.26	129.63	1.88	0.0
85	02/12/2001	Van	4.8	6501	Stiff Soil	14.2	29.83	1.62	9.2	29.98	1.74	0.19	24.82	0.84	2.37	24.93	0.89	0.1
86	03/02/2002	Afyon	6.5	301	Soft Soil	64.7	113.32	14.29	42.7	113.35	13.06	2.05	94.29	9.11	37.72	94.34	8.37	2.7
87				4302	Soft Soil	144.4	23.12	3.53	16.7	23.19	3.29	1.14	20.79	4.01	15.62	20.79	3.70	1.5
88	03/02/2002	Afyon	5.8	301	Soft Soil	34	40.67	3.38	166.6	40.49	3.17	0.64	51.77	5.20	199.2	51.70	5.29	1.1
89	30/07/2002	Denizli	4.7	2002	Soft Soil	25.4	11.23	0.84	1.9	11.22	0.79	0.15	16.88	0.83	1.66	16.96	0.82	0.1
90	19/11/2002	Malatya	4.8	4401	Stiff Soil	35.9	16.26	0.46	2.1	16.08	0.43	0.04	19.32	1.18	7.33	19.29	0.96	0.1
91	14/12/2002	Kahramanmaras	4.8	4604	Stiff Soil	19.1	76.86	1.91	2.9	76.90	1.81	0.06	50.40	1.34	1.19	49.96	1.29	0.1
92	10/04/2003	Izmir	5.7	3502	Soft Soil	37.5	78.59	6.09	5.0	78.57	6.21	1.06	37.09	3.95	6.92	37.09	3.82	0.9
93				908	Soft Soil	132.8	11.00	1.08	7.5	11.02	0.96	0.24	6.64	0.88	1.60	6.67	0.93	0.2
94	01/05/2003	Bingol	6.3	1201	Stiff Soil	11.8	545.58	38.24	49.7	499.72	33.73	8.48	276.78	22.86	34.10	296.04	21.86	4.8
95	08/05/2003	Bingol	4.9	1202	-	14	23.89	1.51	0.3	23.88	1.50	0.17	20.02	1.04	0.27	20.06	1.04	0.1
96				1201	Stiff Soil	12.9	15.78	0.89	6.9	15.72	0.67	0.07	21.80	1.61	3.09	21.55	1.52	0.1
97				1205	Stiff Soil	12.9	18.29	1.31	4.0	18.29	1.22	0.15	28.47	2.46	6.91	28.47	2.57	0.3
98				1203	-	18	20.04	1.81	0.8	20.09	1.82	0.16	26.12	1.85	0.82	26.10	1.84	0.2
99	08/05/2003	Bingol	4.9	1204	-	14.3	12.29	0.46	0.3	12.28	0.48	0.05	7.40	0.49	0.80	7.32	0.49	0.1
100	10/05/2003	Bingol	4.8	1205	Stiff Soil	20.8	18.47	1.44	0.2	18.38	1.46	0.14	9.71	0.81	0.29	9.71	0.81	0.1
101	21/05/2003	Duzce	4.4	8101	Soft Soil	16.4	17.81	0.79	1.9	17.87	0.72	0.07	31.86	0.90	2.45	31.99	0.86	0.0
102	09/06/2003	Bandirma	4.8	1007	Stiff Soil	18.2	35.63	2.25	3.9	35.61	2.16	0.21	22.90	1.67	2.45	22.91	1.70	0.3
103	06/07/2003	Canakkale	5.7	1701	Soft Soil	45.9	26.20	2.33	6.6	26.21	2.42	0.56	15.54	2.00	3.90	15.56	2.02	0.5
104	13/07/2003	Malatya	5.5	4401	Stiff Soil	56.3	11.00	1.23	5.3	10.99	1.35	0.36	16.46	0.77	2.40	16.44	0.73	0.1
105	23/07/2003	Denizli	5.3	2007	Soft Soil	13.3	90.17	4.81	18.3	90.73	4.95	0.74	123.24	4.89	15.85	122.16	4.79	1.1
106				907	Soft Soil	39.9	21.73	1.35	1.4	21.76	1.37	0.28	19.91	1.24	2.15	19.99	1.24	0.2
107				908	Soft Soil	49.9	23.07	1.52	1.4	23.07	1.49	0.38	25.95	1.58	8.28	25.99	1.51	0.3
108				2002	Soft Soil	32.9	22.20	1.06	14.2	22.19	0.88	0.20	45.87	1.19	3.27	46.00	1.18	0.2
109	26/07/2003	Denizli	4.9	2007	Soft Soil	20	47.53	1.29	11.5	47.62	1.19	0.14	34.47	1.31	5.22	34.47	1.27	0.2

Register Index	EARTHQUAKE INFORMATION			STATION INFORMATION			REGISTER INFORMATION											
							N-S Component						E-W Component					
							Uncorrected			Corrected			Uncorrected			Corrected		
	Date	Earthquake Location	M_w	Station - Code	Soil Type	Distance	PGA (cm/s^2)	PGV (cm/s)	PGD (cm)	PGA (cm/s^2)	PGV (cm/s)	PGD (cm)	PGA (cm/s^2)	PGV (cm/s)	PGD (cm)	PGA (cm/s^2)	PGV (cm/s)	PGD (cm)
110				907	Soft Soil	43.2	10.54	0.84	0.1	10.53	0.84	0.10	11.22	0.60	1.00	11.22	0.61	0.1
111				908	Soft Soil	52.6	10.23	0.53	0.8	10.23	0.53	0.08	16.83	0.60	0.44	16.83	0.59	0.1
112				2007	Soft Soil	13.8	107.51	5.42	18.0	107.91	5.37	1.55	121.12	4.20	16.75	121.48	4.12	1.0
113				2002	Soft Soil	32.2	23.74	1.66	13.4	23.14	1.47	0.37	25.78	1.58	8.60	24.73	1.63	0.4
114	26/07/2003	Denizli	5.4	907	Soft Soil	42.5	26.29	2.08	2.1	26.32	2.11	0.35	19.95	1.27	12.87	19.98	1.11	0.2
115				908	Soft Soil	52.5	26.97	1.49	4.3	26.86	1.52	0.46	27.16	1.72	5.53	27.18	1.67	0.4
116				904	Stiff Soil	79	10.45	0.41	0.5	10.42	0.39	0.09	8.48	0.49	0.10	8.53	0.49	0.1
117	26/07/2003	Denizli	4.9	2007	Soft Soil	18.5	14.30	0.81	10.5	14.22	0.82	0.19	17.33	0.90	10.22	17.18	1.04	0.3
118				908	Soft Soil	49.9	14.67	1.10	1.2	14.67	1.09	0.19	18.40	1.25	6.71	18.41	1.16	0.1
119	26/02/2004	Malatya	4.9	4401	Stiff Soil	45.6	16.23	0.83	8.6	16.20	0.72	0.04	7.95	0.41	1.21	7.93	0.39	0.0
120	03/03/2004	Malatya	4.6	1201	Stiff Soil	18.7	15.96	1.14	5.0	15.94	0.97	0.09	9.20	0.40	2.75	9.21	0.33	0.0
121	13/04/2004	Bolu	4.4	1401	Soft Soil	7.4	64.86	3.42	3.2	64.65	3.45	0.29	53.05	1.84	6.76	51.85	1.62	0.1
122	04/08/2004	Mugla	5.5	4802	Stiff Soil	36.5	17.42	1.79	2.2	17.40	1.79	0.27	27.38	1.57	0.32	27.35	1.68	0.2
123				4802	Stiff Soil	37	28.11	1.76	3.6	28.09	1.73	0.30	21.21	1.00	2.73	21.24	1.09	0.1
124	11/08/2004	Elazig	5.6	2301	Stiff Soil	37	19.58	2.63	34.1	19.59	2.28	0.43	18.92	5.05	41.94	18.78	4.01	1.2
125	20/12/2004	Mugla	5.3	4804	Stiff Soil	36.7	27.39	0.86	2.7	27.38	0.95	0.11	15.04	0.65	0.62	15.05	0.62	0.1
126				4805	Stiff Soil	18.7	33.90	1.96	15.8	33.39	1.63	0.39	31.05	2.23	0.77	31.47	2.11	0.3
127	10/01/2005	Mugla	5.4	4805	Stiff Soil	43.3	16.56	1.61	7.4	16.53	1.40	0.38	15.12	1.14	2.39	14.96	1.14	0.3
128	11/01/2005	Mugla	5.0	4802	Stiff Soil	27.4	6.96	0.29	1.6	6.95	0.25	0.05	7.82	0.29	1.40	7.85	0.33	0.0
129	23/01/2005	Antalya	5.8	703	Soft Soil	80	25.03	3.31	44.7	25.08	3.32	0.82	23.95	2.77	17.94	23.64	3.17	0.6
130	06/06/2005	Bingol	5.6	1208	Stiff Soil	48.5	14.73	0.94	19.7	14.80	0.76	0.12	14.47	0.96	7.99	14.53	0.78	0.2
131	17/10/2005	Izmir	5.5	3502	Soft Soil	56.2	15.03	1.07	3.3	15.04	1.19	0.15	16.52	1.23	1.45	16.54	1.28	0.1
132	17/10/2005	Izmir	5.8	3502	Soft Soil	56.1	22.48	1.73	6.7	22.51	1.65	0.22	19.13	1.54	10.73	19.13	1.30	0.7
133	17/10/2005	Izmir	5.2	3502	Soft Soil	58.3	13.14	1.25	1.6	13.14	1.14	0.20	9.64	0.80	2.02	9.60	0.77	0.1
134	20/10/2005	Izmir	5.8	3502	Soft Soil	59	23.66	1.93	14.0	23.66	2.16	0.51	31.92	2.69	1.81	31.93	2.74	0.6
135				4501	Soft Soil	80.3	12.44	1.48	30.8	12.52	0.91	0.20	22.01	1.94	11.48	22.21	1.67	0.2
136	26/11/2005	Malatya	5.1	4401	Stiff Soil	49.2	11.85	0.95	1.6	11.86	0.89	0.07	11.43	0.62	2.00	11.46	0.57	0.1
137				2007	Soft Soil	15.8	22.86	1.74	6.0	22.81	1.83	0.15	19.61	1.01	7.10	19.61	0.91	0.1
138	05/06/2006	Denizli	4.8	907	Soft Soil	24.5	45.12	1.05	0.6	45.67	1.02	0.07	66.80	1.61	4.14	66.14	1.76	0.1
139				908	Soft Soil	35.2	16.75	0.70	1.6	16.48	0.67	0.06	20.89	0.70	0.57	21.10	0.68	0.1
140				1603	Stiff Soil	29	36.57	1.22	4.3	36.43	1.29	0.12	28.38	0.90	2.42	28.35	0.82	0.1
141				1601	Soft Soil	22.9	77.40	4.24	4.8	77.36	4.22	0.38	37.00	1.71	0.46	36.98	1.68	0.3
142				1606	Soft Soil	12.7	159.25	7.17	2.8	159.43	7.18	0.74	179.77	6.05	1.21	179.31	6.02	0.6
143	24/10/2006	Bursa	5.2	1607	Stiff Soil	9.4	177.14	8.72	9.4	175.10	8.79	1.35	206.20	9.85	12.14	206.20	10.07	1.0
144				1608	Stiff Soil	15.8	69.54	3.62	0.5	68.97	3.61	0.38	100.42	5.46	1.60	100.17	5.49	0.5
145				1609	Soft Soil	14.7	65.95	3.27	0.8	66.01	3.29	0.34	95.34	5.21	4.73	94.42	5.16	0.4
146				1615	-	25.2	29.86	1.82	0.8	29.83	1.84	0.31	45.24	2.73	0.46	45.15	2.74	0.4

Register Index	EARTHQUAKE INFORMATION			STATION INFORMATION			REGISTER INFORMATION											
							N-S Component						E-W Component					
							Uncorrected			Corrected			Uncorrected			Corrected		
	Date	Earthquake Location	M_w	Station - Code	Soil Type	Distance	PGA (cm/s^2)	PGV (cm/s)	PGD (cm)	PGA (cm/s^2)	PGV (cm/s)	PGD (cm)	PGA (cm/s^2)	PGV (cm/s)	PGD (cm)	PGA (cm/s^2)	PGV (cm/s)	PGD (cm)
147				7701	Stiff Soil	30.8	28.46	1.01	0.5	26.73	0.96	0.10	29.34	1.64	0.80	26.48	1.62	0.1
148	24/10/2006	Bursa	5.2	7702	Soft Soil	29.7	37.78	1.88	0.4	37.68	1.94	0.19	25.66	1.40	1.54	25.72	1.35	0.1
149				1613	Stiff Soil	59.8	10.05	0.32	6.1	10.05	0.30	0.02	6.68	0.30	3.44	6.58	0.26	0.0
150				302	Soft Soil	151.33	10.66	2.07	3.1	10.64	2.02	0.56	6.77	1.21	1.08	6.77	1.20	0.3
151				1006	Soft Soil	162.4	18.31	1.87	4.1	18.30	1.85	0.43	16.00	1.62	3.49	15.98	1.54	0.3
152				1009	Stiff Soil	62.809	16.44	1.35	3.1	16.89	1.34	0.39	16.32	0.92	1.42	15.55	0.88	0.3
153				1102	Stiff Soil	119.28	14.65	1.00	0.6	14.69	0.92	0.22	11.59	0.89	1.17	11.60	0.86	0.2
154				1613	Stiff Soil	87.815	24.63	1.70	1.0	24.47	1.67	0.37	17.24	1.28	2.22	16.95	1.25	0.2
155				1614	Soft Soil	116.28	29.40	2.31	1.2	29.18	2.37	0.51	61.91	3.63	3.43	62.23	3.54	0.5
156				1618	-	135.89	13.65	1.06	1.3	13.65	1.11	0.26	15.11	0.81	2.04	15.10	0.80	0.2
157				2605	rock	141.1	12.23	0.98	1.6	12.22	0.92	0.28	14.46	0.84	0.70	14.37	0.86	0.2
158	19/05/2011	Kutahya Simav	5.85	2610	-	138.35	11.74	1.49	1.8	11.67	1.49	0.20	10.64	1.39	11.39	10.62	1.50	0.3
159				2613	-	73.362	11.63	1.20	1.7	11.62	1.17	0.22	8.41	1.14	7.54	8.40	1.08	0.3
160				4108	-	194.78	12.57	1.48	7.1	12.57	1.52	0.54	14.71	2.87	34.00	14.71	2.71	0.6
161				4116	-	188.49	11.12	1.73	38.2	11.15	1.83	0.65	10.80	1.73	37.55	10.80	1.89	0.6
162				4301	Soft Soil	85.038	33.62	1.90	1.6	33.74	1.87	0.36	25.13	1.96	2.92	24.99	1.89	0.4
163				4304	Soft Soil	31.53	92.33	3.96	6.7	81.80	3.91	1.01	103.92	3.46	8.72	108.01	3.37	0.6
164				4306	Soft Soil	26.787	74.69	7.97	1.8	75.28	7.99	1.36	73.13	6.17	3.57	71.19	6.31	1.1
165				4502	Soft Soil	11.75	18.00	2.55	6.0	18.01	2.58	0.74	17.32	3.24	3.11	17.32	3.21	0.7
166				6401	Soft Soil	58.355	47.87	3.87	2.0	47.86	3.79	0.59	46.91	4.19	5.74	45.60	4.19	0.5
167		Van-Muradiye	6.8	6503	Soft Soil	42.23	178.53	25.91	19.7	178.51	26.26	5.59	169.48	14.69	12.21	168.54	14.74	3.8
168	23/10/2011	Van-Muradiye	6.8	1302	-	117.3	89.67	8.35	7.1	89.56	8.78	1.93	102.24	7.59	17.57	102.62	7.69	1.1
169		Van-Muradiye	6.8	4902	Soft Soil	95.528	44.37	11.61	14.9	44.31	11.83	5.25	56.21	11.15	7.56	55.83	10.57	5.0

4 Proposal of Design Input Energy Spectra

4.1 Introduction

This section describes the proposal of design input energy spectra in terms of velocity, V_E. These spectra are intended for structures with both linear and nonlinear behavior; section 4.2 describes the linear spectra while section 4.3 describes the nonlinear spectra. The linear spectra are derived from linear dynamic analyses for the registers listed in Table 3-1. As indicated in the Introduction, in the mid and long period ranges the input energy is a rather stable quantity that is primarily governed by the total mass and fundamental period T of the structure, being scarcely affected by its strength, degree of plastification, or hysteretic properties; therefore, in these period ranges the linear spectra can be also used for nonlinear design. Conversely, in the short period range the energy spectral ordinates are not as clearly independent on the resistance and the hysteretic behavior; therefore, nonlinear dynamic analyses must be carried out. The nonlinear spectra are proposed to be roughly equal to the linear ones in the mid and long period ranges while in the short period range their ordinates are obtained by modifying those of the linear spectra with convenient factors.

The linear and nonlinear spectra are proposed for each of the aforementioned eight groups (stiff soil / soft soil, impulsive / vibratory, $M_s > 5.5$ / $M_s \leq 5.5$); given the scarcity of registers out of the seismic zone 1 (see Figure 3-3) and their rather low intensity (see Table 3-1), only inputs from zone 1 are considered. For each of these eight groups, median and characteristic spectra are proposed; such levels are intended to correspond to 50% and to 95% percentiles, respectively. The observation of the obtained spectra [Yazgan 2012] shows that they do not fit any statistical distribution; therefore, the median and characteristic values are determined regardless of the statistical distribution.

4.2 Linear Spectra

Given the similarity between the relative velocity spectra and the V_D spectra and the little sensitivity of the ratio V_D / V_E on the period [Decanini, Mollaioli 2001; Benavent et al. 2010], the proposed spectra are expected to be basically shaped as the result of multiplying the design acceleration spectra proposed by the Eurocode 8 [EN-1998 2004] by factor $T / 2\,\pi$. Therefore, these spectra have three branches, corresponding roughly to the short, medium and long period ranges, respectively; the first branch is linear starting from zero, the second branch is constant, and the third branch is decreasing. Figure 4-1 shows a sketch of such a spectrum; T_C and T_D are the corner periods separating the aforementioned three branches.

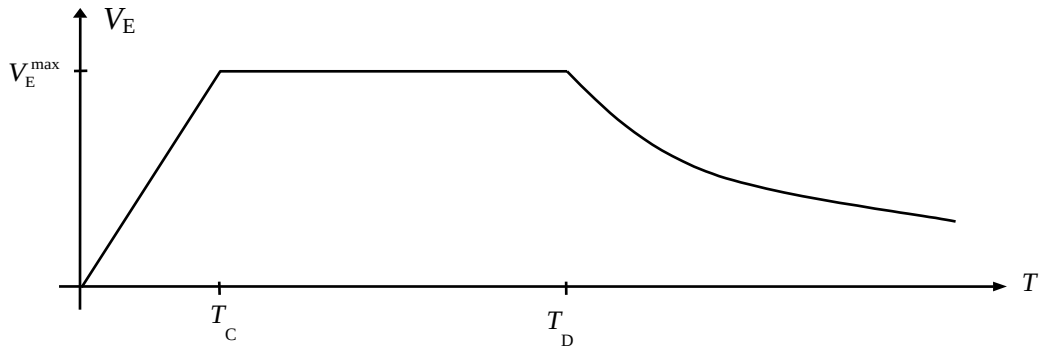

Figure 4-1 Proposed linear V_E design spectra

In Figure 4-1 the descending branch (for $T \geq T_D$) follows the equation

$$V_E = V_E^{max} \left(\frac{T_D}{T} \right)^a \tag{4-1}$$

In equation (4-1), V_E^{max} is the spectral ordinate of the plateau and a is an exponent. Figure 4-1 and equation (4-1) show that every linear proposed spectrum is characterized by the periods T_C and T_D, by the plateau ordinate V_E^{max} and by the exponent a.

The proposal of the linear design input energy spectra in terms of equivalent velocity (V_E) in the range of periods $0 - T$ consists of deriving separately normalized spectra ($V_E / \|V_E\|_T$) and spectral factors $\|(V_E\|_T)$; the proposed V_E design spectra are obtained by multiplying the normalized spectra by the spectral factors. The spectral factor $\|V_E\|_T$ is defined as the integral of the V_E spectrum:

$$\left\| V_E \right\|_T = \int_0^T V_E \, dT \tag{4-2}$$

Remarkably, $\|V_E\|_T$ can be considered as a norm even it does not have the dimension of velocity since the integral has not been divided by the period range; it should be kept in mind that such period is the same in all the considered cases. Therefore dividing the integral of the second member of equation (4-2) by a constant value T does not affect the proposed design spectra V_E-T. The normalized spectra are obtained from the linear analyses carried out on the Turkish registers listed in Table 3-1. However, given the scarcity of available strong inputs, the spectral factors are obtained from the Turkish recordings only in the group where the inputs are more demanding ("Soft Soil / M_s > 5.5 / Impulsive"); in the other groups the available registers are too small, and this lack of seismic information is complemented with the information provided by other studies [Decanini, Mollaioli 1998] and by some of the major design codes [EN-1998 2004; BSL 2009; UBC 1997]. The linear analyses consist of determining the value of E_I in equation (2-22) for SDOF systems with damping factor $\zeta = 0.10$ and for natural periods T ranging in between 0.02 and 8 s , and expressing E_I in terms of the equivalent velocity V_E defined by equation (2-10) or (2-30).

The criteria for estimating, for each of the aforementioned eight groups (section 3.5), the values of the parameters T_C, T_D, $V^{max}_E / \|V_E\|_T$ and a that characterize every normalized spectrum are described next. In these operations the spectra with smallest norms are disregarded since they correspond to small registers.

- **Period T_C**. For each of the aforementioned eight groups, the procedure to estimate the median and characteristic values of the corner period T_C consists of the following

consecutive steps: (i) for each individual normalized $\|V_E\|_T - T$ spectrum of the group, T_C is initially defined as the intersection between their initial (linear, starting from the origin) and maximum (horizontal) envelopes; (ii) for all the individual normalized spectra considered in this group, the median and characteristic values (50% and 95% percentiles, respectively) of such T_C periods are determined; (iii) the initial median and characteristic branches are finally obtained by joining the origin and the points of the abovementioned maximum linear envelopes that correspond to the median and characteristic values of T_C, respectively.

- **Period T_D**. Given that the Eurocode 8 proposes separate design spectra for registers corresponding to $M_s > 5.5$ and to $M_s \leq 5.5$ (Type 1 and Type 2, respectively) and that in both cases the values of T_D do not depend on the soil type, we have tried to preserve these features in this study. Eurocode 8 states $T_D = 2$ s and $T_D = 1.2$ s for Type 1 and Type 2 spectra, respectively; in this study values $T_D = 1.6$ s and $T_D = 0.9$ s have provided better fits and are adopted for registers corresponding to $M_s > 5.5$ and to $M_s \leq 5.5$, respectively. Remarkably, these values are considered regardless of the soil type and the near-source effects; as well, no distinction is made between median and characteristic spectra.
- **Normalized plateau ordinate $V^{max}_E / \|V_E\|_T$**. For each of the aforementioned eight groups (section 3.5), the median and characteristic values of the normalized maximum spectral ordinates are estimated, in the range $T_C - T_D$, as the average of the median and characteristic values of the individual normalized spectra. In this operation the spectra that came from individual spectra with smallest norms have been disregarded.
- **Exponent a**. For each of the aforementioned eight groups (section 3.5), the exponent a is determined as providing the best fit, in the range $T_D - T$.

Since most of the civil engineering constructions correspond to periods not exceeding 4 s, in this study $T = 4$ s, i.e. the proposed design spectra are limited to the range 0 – 4 seconds. Also, $T = 4$ s is adopted in equation (4-2) for calculating the norm $\|V_E\|_T$. However, the linear dynamic analyses have been carried out along the interval 0 – 8 seconds; when relevant peaks have been detected for periods $4 < T < 8$ seconds, this information has been considered for determining the descending branch (i.e. the value of paramenter a). For each of the aforementioned eight groups (section 3.5), Table 4-1 shows the actual number of the considered registers (n) and the values of the parameters T_C, T_D, $V^{max}_E / \|V_E\|_T$ and a for the median / characteristic $V_E / \|V_E\|_4$ normalized spectra; Figure 4-2 to Figure 4-9 display those spectra with thick black lines. Each of the eight groups of plots from Figure 4-2 to Figure 4-9 contains also the individual normalized spectra (thin gray lines), the median and characteristic ones and the proposed (smoothed) median and characteristic normalized spectra.

Table 4-1 Parameters for the median / characteristic normalized spectra $V_E / \|V_E\|_4$

Soil type	Magnitude	Pulses	n	T_C (s)	T_D (s)	$V^{max}_E / \|V_E\|_4$ (s^{-1})	a
Stiff Soil	$M_s > 5.5$	Impulsive	12	0.41 / 0.18	1.60 / 1.60	0.28 / 0.46	0.55 / 0.5*
		Vibratory	5	0.22 / 0.17	1.60 / 1.60	0.35 / 0.47	1.0 / 1.2
	$M_s \leq 5.5$	Impulsive	8	0.30 / 0.20	0.90 / 0.90	0.52 / 0.85	1.3 / 1.5
		Vibratory	9	0.27 / 0.19	0.90 / 0.90	0.49 / 0.78	1.2 / 1.2
Soft Soil	$M_s > 5.5$	Impulsive	19	0.54 / 0.32	1.60 / 1.60	0.34 / 0.53	1.0 / 0.8*
		Vibratory	13	0.53 / 0.28	1.60 / 1.60	0.33 / 0.50	0.9 / 0.65
	$M_s \leq 5.5$	Impulsive	11	0.29 / 0.21	0.90 / 0.90	0.46 / 0.70	0.9 / 1.0
		Vibratory	18	0.26 / 0.18	0.90 / 0.90	0.41 / 0.69	0.7 / 0.9

(*) These values have been modified to fit the peaks inside the range from 4 to 8 s.

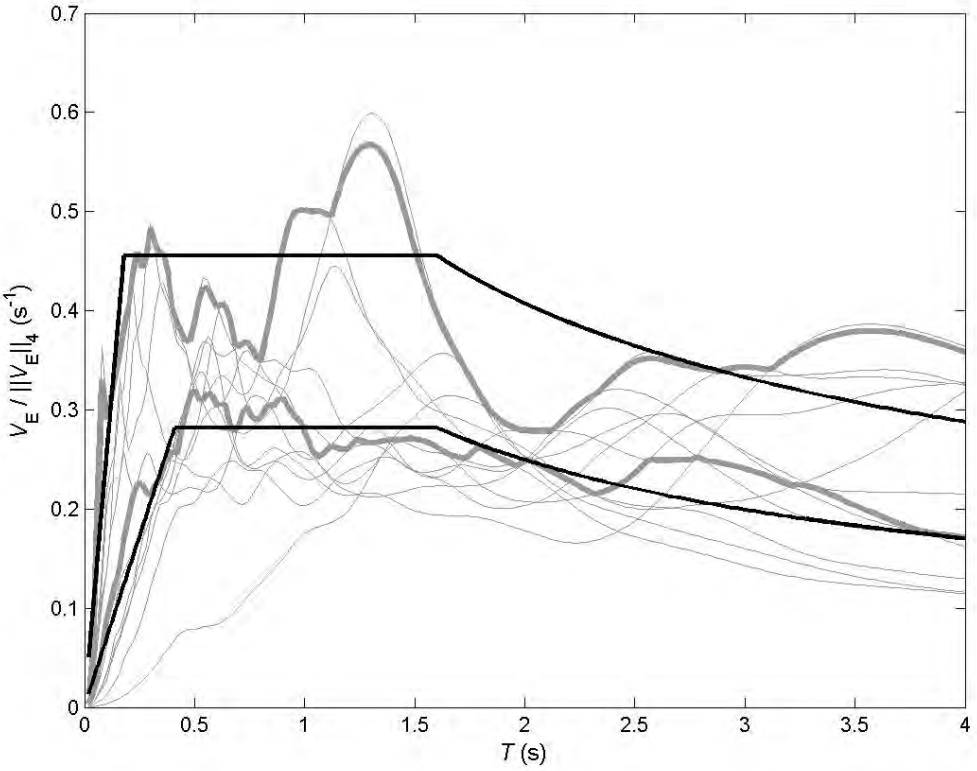

Figure 4-2 Proposed normalized V_E / $\|V_E\|_4$ design spectra. Stiff soil. M_s > 5.5. Impulsive

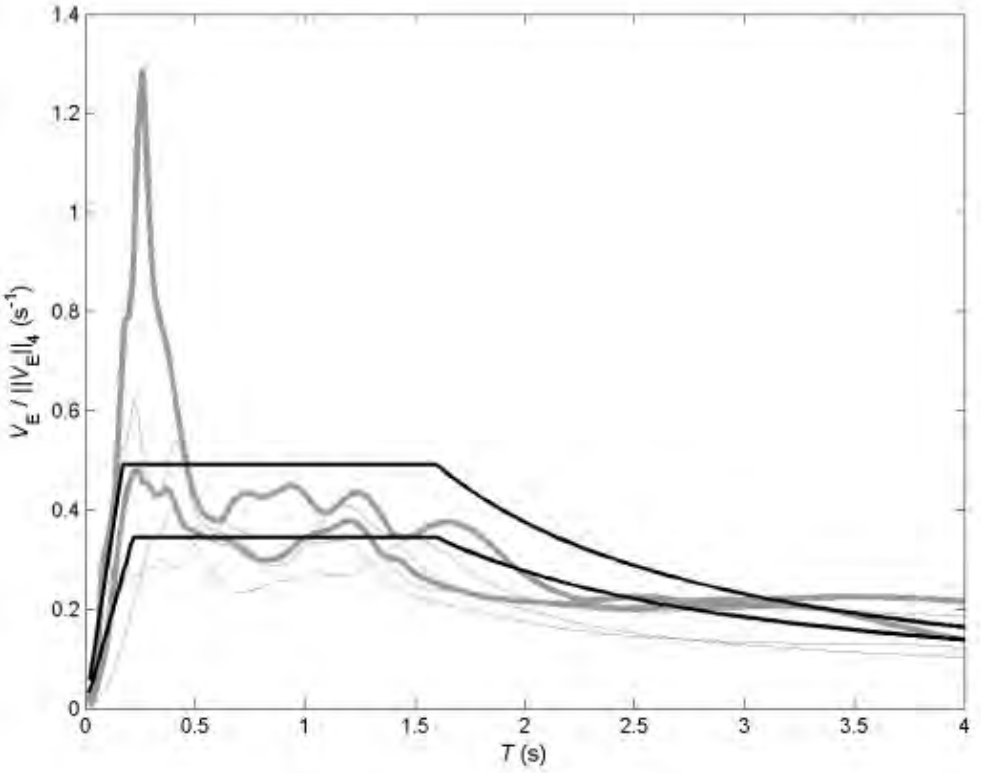

Figure 4-3 Proposed normalized V_E / $\|V_E\|_4$ design spectra Stiff soil. M_s > 5.5. Vibratory

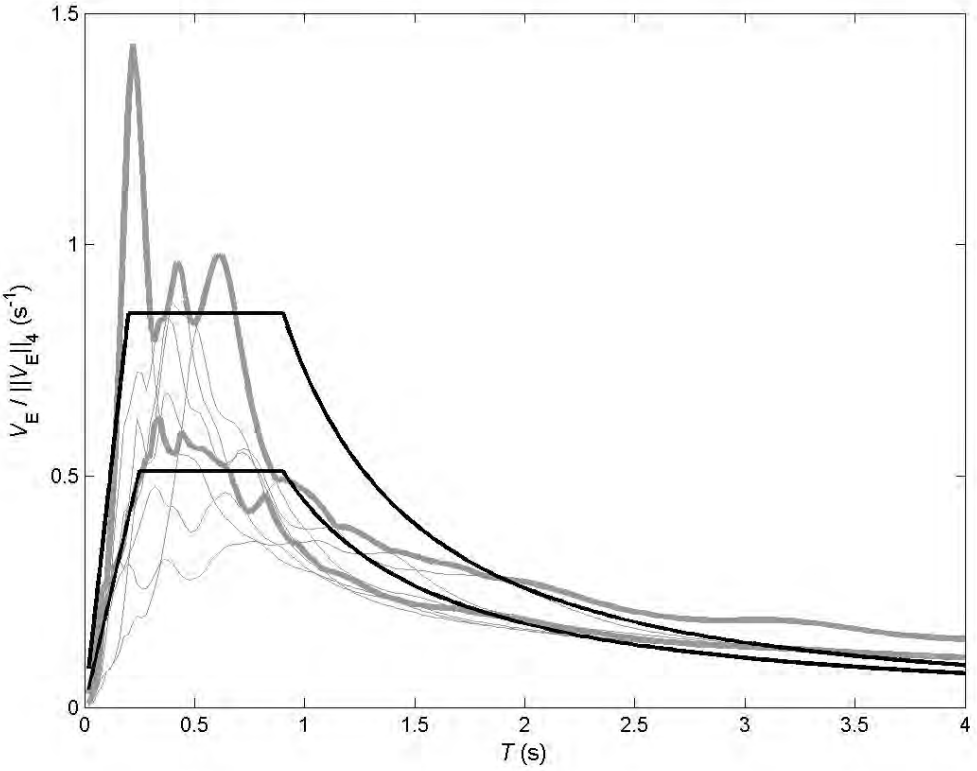

Figure 4-4 Proposed normalized V_E / $\|V_E\|_4$ design spectra Stiff soil. $M_s \leq 5.5$. Impulsive

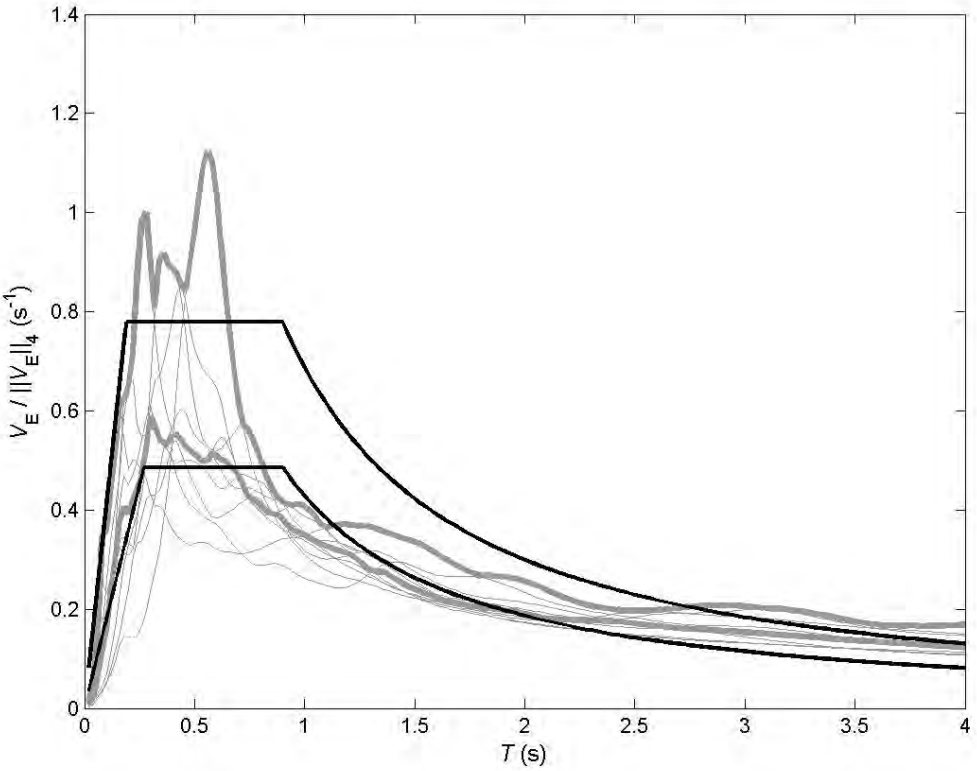

Figure 4-5 Proposed normalized V_E / $\|V_E\|_4$ design spectra Stiff soil. $M_s \leq 5.5$. Vibratory

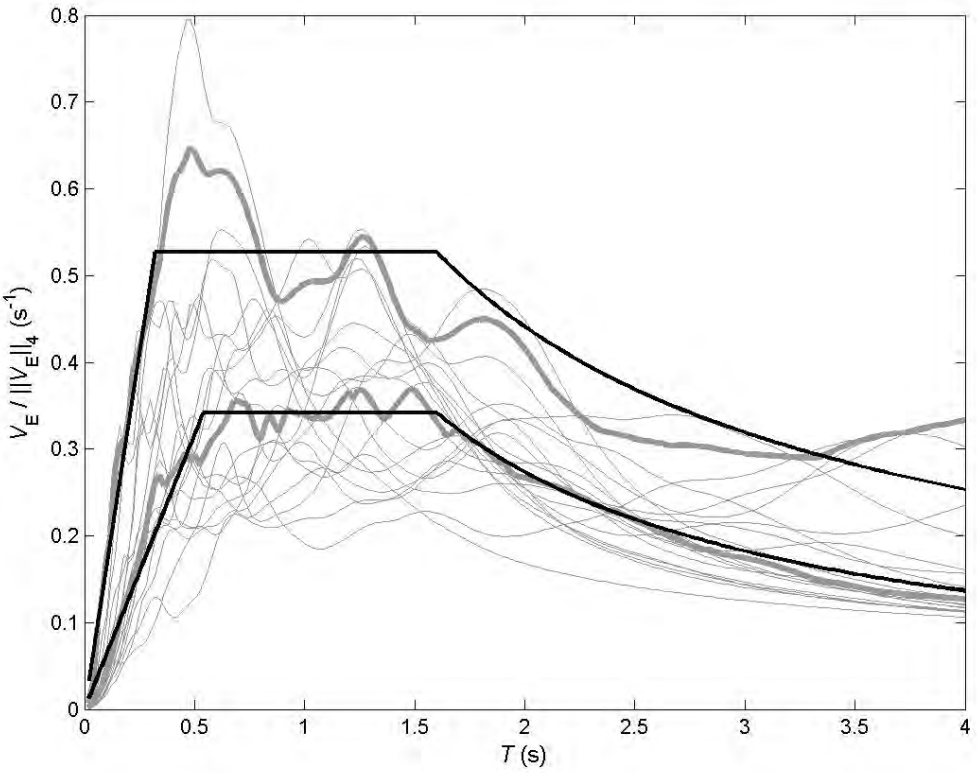

Figure 4-6 Proposed normalized V_E / $\|V_E\|_4$ design spectra Soft soil. M_s > 5.5. Impulsive

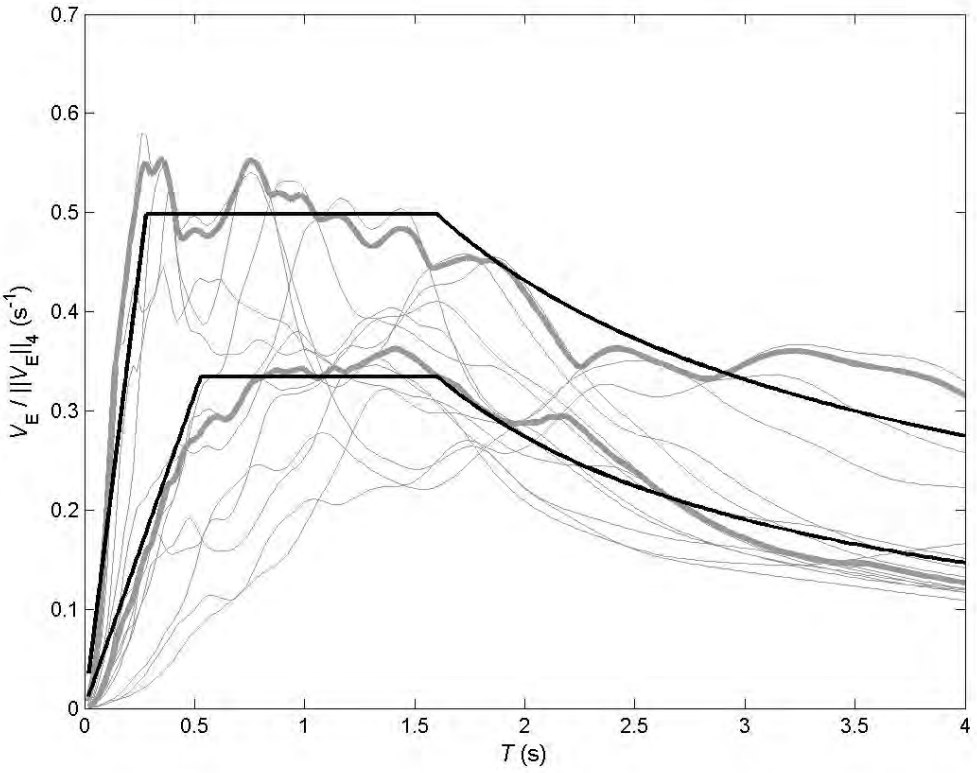

Figure 4-7 Proposed normalized V_E / $\|V_E\|_4$ design spectra Soft soil. M_s > 5.5. Vibratory

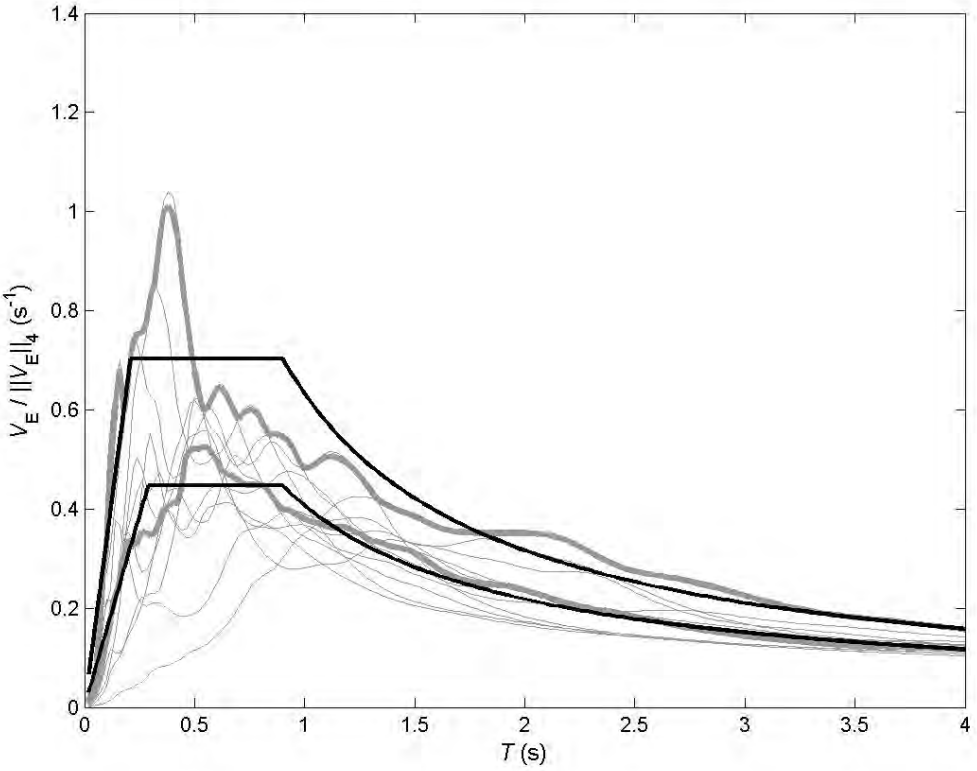

Figure 4-8 Proposed normalized V_E / $\|V_E\|_4$ design spectra Soft soil. $M_s \leq 5.5$. Impulsive

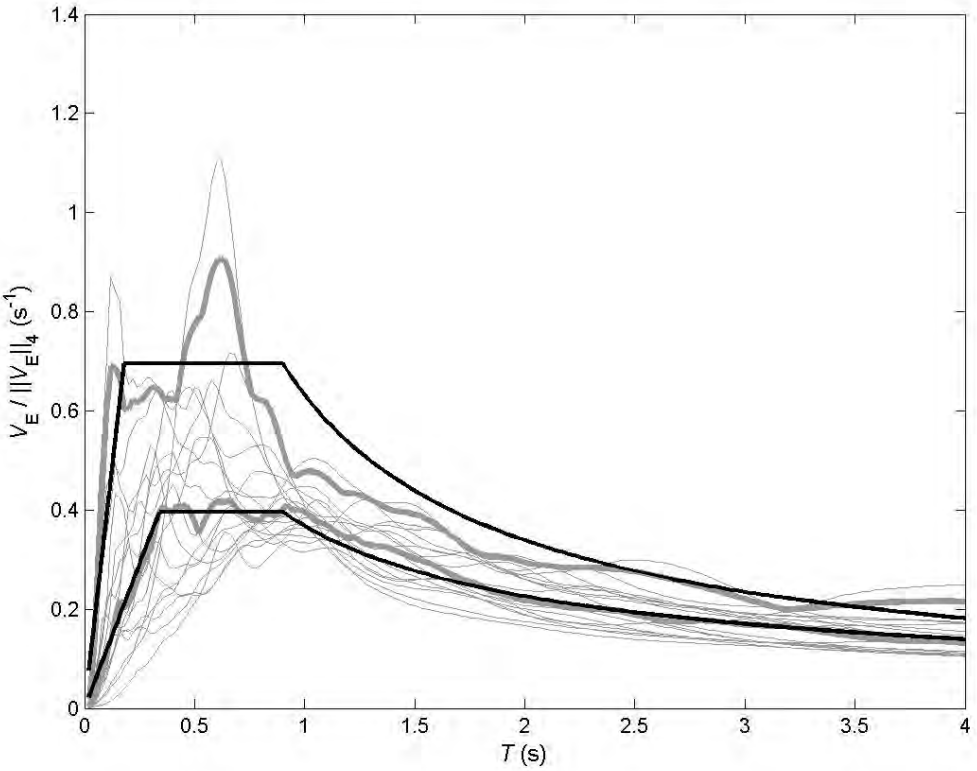

Figure 4-9 Proposed normalized V_E / $\|V_E\|_4$ design spectra Soft soil. $M_s \leq 5.5$. Vibratory

As discussed previously, the proposed V_E design linear spectra are determined by multiplying the smoothed (three-branched) normalized spectra shown in Figure 4-2 to Figure 4-9 by the spectral factors $\|V_E\|_4$. In this study, the values of $\|V_E\|_4$ are determined so that the resulting V_E^{max} are consistent with the values obtained in the analyses conducted with the Turkish registers. In some cases (i.e. for some combinations of soil type, earthquake magnitude and type of earthquake) the number and level of the available Turkish registers is too small to derive values of V_E^{max} that represent the actual seismicity. In these cases, the information obtained from the Turkish registers has been completed with the results of past research and relevant seismic codes as explained next.

Columns four to seven of Table 4-2 display the ordinate values of the constant-velocity branches of several V_E spectra, i.e. the plateau ordinates V_E^{max} proposed in previous studies and those inherent or proposed in several seismic codes. Fourth column contains the spectral values described in the reference [Decanini, Mollaioli 1998] and fifth, sixth and seventh columns contain the design quantities according to the Eurocode 8 [EN-1998 2004], the Japanese code [BSL 2009] and the UBC-97 [UBC 1997], respectively. In all these codes, the design ground acceleration is 0.4 g. The eigth column exhibits the values of V_E^{max} obtained in this study, the ninth column shows the proposed values of V_E^{max} and the tenth column contains the corresponding values of $\|V_E\|_4$ calculated by dividing by the value of $V^{max}{}_E / \|V_E\|_4$ given by the seventh column of Table 4-1. In case of rock, the values of $\|V_E\|_4$ are estimated by dividing those for stiff soil by 1.4 as indicated by the UBC-97.

Deeper descriptions of the criteria considered to select the figures shown in the columns four in Table 4-2 are listed next.

- **Decanini, Mollaioli 1998**. These researchers aimed to propose design spectra in terms of input energy normalized with respect to the mass (E_I / m); in this work, the corresponding V_E value has been determined by equation (2-30). Those spectra were proposed after linear analyses on an important number of world-wide seismic strong motions. Such inputs were classified according to soil conditions, earthquake magnitude and source-to-site distance. Values in Table 4-2 have been selected to correspond to conditions similar to those in this study. About the soil type, three categories were considered, namely S1, S2 and S3; "rock" and "stiff soil", as considered in this work, match the conditions of S1 and "soft soil" matches those of S2. Since the values for soil S1 should match the most demanding situation inside this soil category, they have been assigned to "stiff soil". About the earthquake magnitude, values in Table 4-2 for $M_s > 5.5$ and for $M_s \leq 5.5$ have been assigned to the M_s intervals 6.5 – 7.1 and 4.2 – 5.2, respectively. About the source-to-site distance, the values in Table 4-2 for impulsive and vibratory registers are consistent with distances smaller than 5 km and comprised in between 12 and 30 km, respectively. In Table 4-2, left / right figures correspond to mean values and to mean + standard deviation values, respectively.
- **Eurocode 8**. The Eurocode 8 does not propose energy spectra, the V_E values have been estimated by identifying the V_D spectra with the pseudo-velocity design spectra (S_v); their ordinates have been determined by multiplying those of the acceleration design spectra by $T / 2\,\pi$. The input energy in terms of velocity (V_E) is obtained from V_D according to equation $\frac{V_D}{V_E} = \frac{1}{1+3\zeta+1.2\sqrt{\zeta}}$ [Akiyama, 1985]. The cases for magnitude higher than 5.5 correspond to Type 1 spectra while those for magnitude smaller than 5.5 are consistent with Type 2 spectra. Since the Eurocode 8 does not contain any specific indication neither about the directivity effects nor about the probability of exceeding the spectral ordinate, the obtained quantities have been assigned to vibratory registers and to characteristic values.

- **BSL 2009**. The spectral ordinates have been derived from the input energy design spectra V_D proposed by the Japanese code; the V_E spectra have been obtained as in the Eurocode 8. The soil is classified in three types, namely 1, 2 and 3; "soil 1" is considered to be equivalent to "rock" and "soil 2" matches the conditions of both "stiff soil" and "soft soil". Since the values for soil 2 should correspond to the most demanding situation inside this soil category, they have been assigned to "soft soil".
- **UBC 1997**. The input energy in terms of velocity (V_E) has been determined following basically the same approach than in the Eurocode 8. The soil is classified in six types, namely S_A to S_F; S_B is considered to be equivalent to "rock", S_C corresponds to "stiff soil" and S_D matches the conditions of "soft soil". Registers generated by earthquakes with $M_s > 5.5$ and with $M_s \leq 5.5$ are identified with sources type A and C, respectively. For earthquakes with $M_s > 5.5$ the values for the impulsive registers are obtained by multiplying those from the vibratory ones by factor N_v; it is assumed that $N_v = 1.6$.

Table 4-2 Proposed design values of V_E^{max} (cm/s) and of $\|V_E\|_4$ (cm)

Soil type	Magn.	Pulses	V_E^{max} (cm/s)						$\|V_E\|_4$ (cm)
			Decanini, Mollaioli (1998)	Eurocode 8	Japanese code	UBC-97	This study	Proposal	Proposal
Rock	$M_s > 5.5$	Imp.	– / –	– / –	– / –	– / 142	– / –	168 / 260	599 / 565
		Vibr.	– / –	– / 89	– / 234	– / 88	– / –	84 / 129	239 / 275
	$M_s \leq 5.5$	Imp.	– / –	– / –	– / –	– / 88	– / –	51 / 80	99 / 94
		Vibr.	– / –	– / 56	– / 234	– / 88	– / –	28 / 43	57 / 55
Stiff Soil	$M_s > 5.5$	Imp.	312 / 361	– / –	– / –	– / 199	56 / 93	235 / 364	839 / 791
		Vibr.	155 / 179	– / 133	– / –	– / 123	17 / 22	117 / 181	334 / 385
	$M_s \leq 5.5$	Imp.	95 / 110	– / –	– / –	– / 123	37 / 60	72 / 112	138 / 132
		Vibr.	52 / 60	– / 75	– / –	– / 123	11 / 17	39 / 60	80 / 77
Soft Soil	$M_s > 5.5$	Imp.	338 / 419	– / –	– / –	– / 227	**255 / 395**	255 / 395	750 / 745
		Vibr.	228 / 283	– / 153	– / 312	– / 142	69 / 104	172 / 266	521 / 532
	$M_s \leq 5.5$	Imp.	129 / 160	– / –	– / –	– / 142	27 / 41	97 / 150	211 / 214
		Vibr.	72 / 89	– / 83	– / 312	– / 142	21 / 34	54 / 84	132 / 122

Eigth column in Table 4-2 contains the constant-velocity spectral ordinates obtained in this study for seismic zone 1 in Turkey (design ground acceleration 0.4 g); left / right figures correspond to median / characteristic values, respectively. Comparison among these quantities and the figures indicated in columns four to seven shows that only in the group "Soft Soil / M_s > 5.5 / Impulsive" the number of available strong registers is enough to provide highly demanding results; in the other groups, the obtained spectral ordinates are too small to represent the actual seismicity. Therefore, this lack of data has to be compensated with the information provided by the previous four columns, mainly the fifth one. According to this approach, ninth column in Table 4-2 displays the constant-velocity median and characteristic spectral ordinates (V_E^{max}) proposed in this study for seismic zone 1 in Turkey. The proposed median values have been determined taking into account columns four to seven of Table 4-2 while the characteristic values are obtained from the median ones by assuming that the median / characteristic ratios are the same than in the group "Soft Soil / M_s > 5.5 / Impulsive"; this assumption stems from the consideration that the statistical properties are basically independent on the soil type, the earthquake magnitude and the source-to-site distance. For stiff and soft soil the median values are determined according to the mean values obtained by Decanini and Mollaioli; for rock, such values are estimated by dividing those for stiff soil by 1.4 as indicated by the UBC-97 (seventh column) for earthquakes with $M_s > 5.5$. A more detailed description of the procedure to derive the figures the last column in Table 4-2 is presented in the next paragraph.

Since the group "Soft Soil / M_s > 5.5 / Impulsive" is the one that contain the most demanding inputs, the proposed median and characteristic spectral ordinates are taken equal to those arising from the analyses on the Turkish registers. In the other groups, the median spectral ordinates are obtained as keeping the same proportion as in the study by Decanini and Mollaioli [1998]; for

instance, for the group "Soft Soil / $M_s > 5.5$ / Vibratory" the spectral ordinate is (228 / 338) 255 = 172. The characteristic spectral ordinates are stated as keeping the same ratio as in the group "Soft Soil / $M_s > 5.5$ / Impulsive"; for instance, for the group "Soft Soil / $M_s > 5.5$ / Vibratory" the spectral ordinate is (395 / 255) 172= 266.

The proposed V_E design linear spectra are obtained by multiplying the abscissas of the normalized spectra shown in Figure 4-2 to Figure 4-9 by the spectral factors $\|V_E\|_4$ listed in the last column of Table 4-2. Figure 4-10 to Figure 4-17 display the proposed V_E linear spectra corresponding to stiff soil and to soft soil. For the sake of comparison with the unscaled individual spectra that have been used to derive the design ones, they are also plotted. For rock, the lack of available information does not allow deriving V_E design spectra apart from the plateau ordinates indicated in Table 4-2.

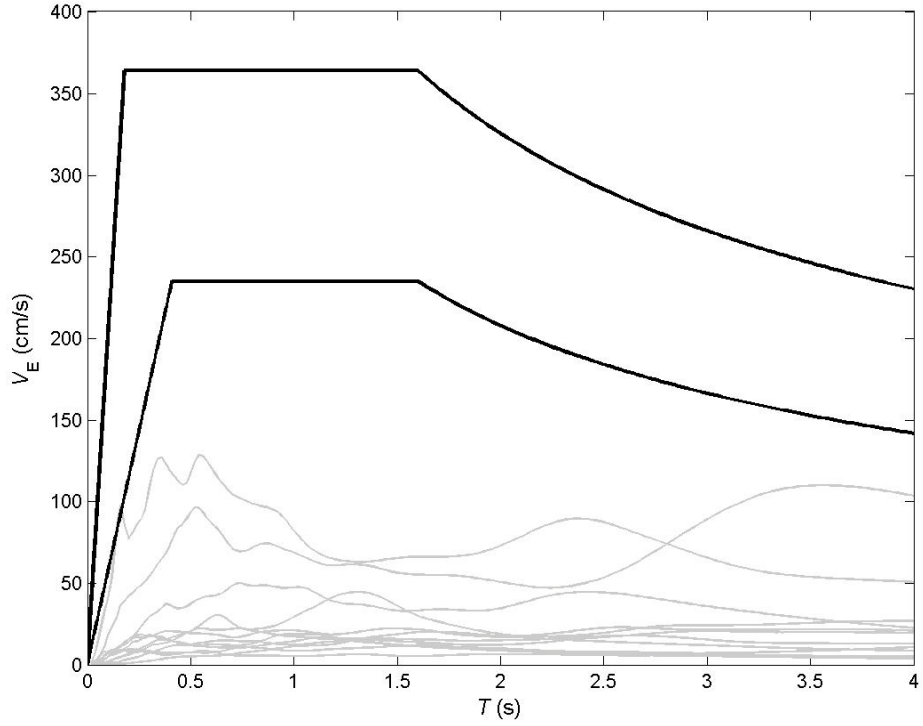

Figure 4-10 Linear V_E design spectra proposed for design acceleration 0.4 g. Stiff soil. $M_s > 5.5$. Impulsive

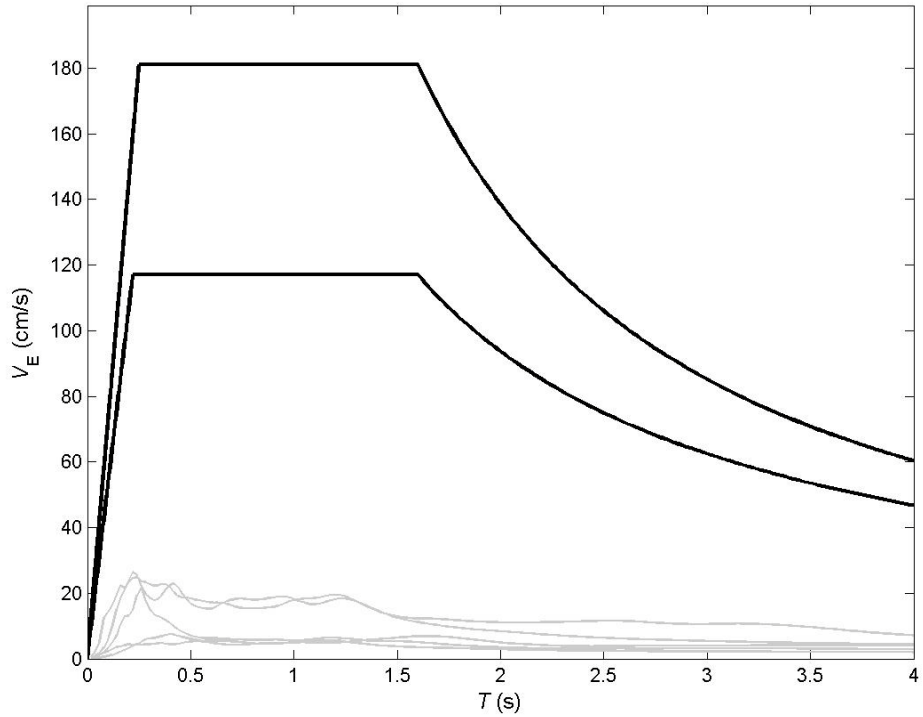

Figure 4-11 Linear V_E design spectra proposed for design acceleration 0.4 g. Stiff soil. $M_s > 5.5$. Vibratory

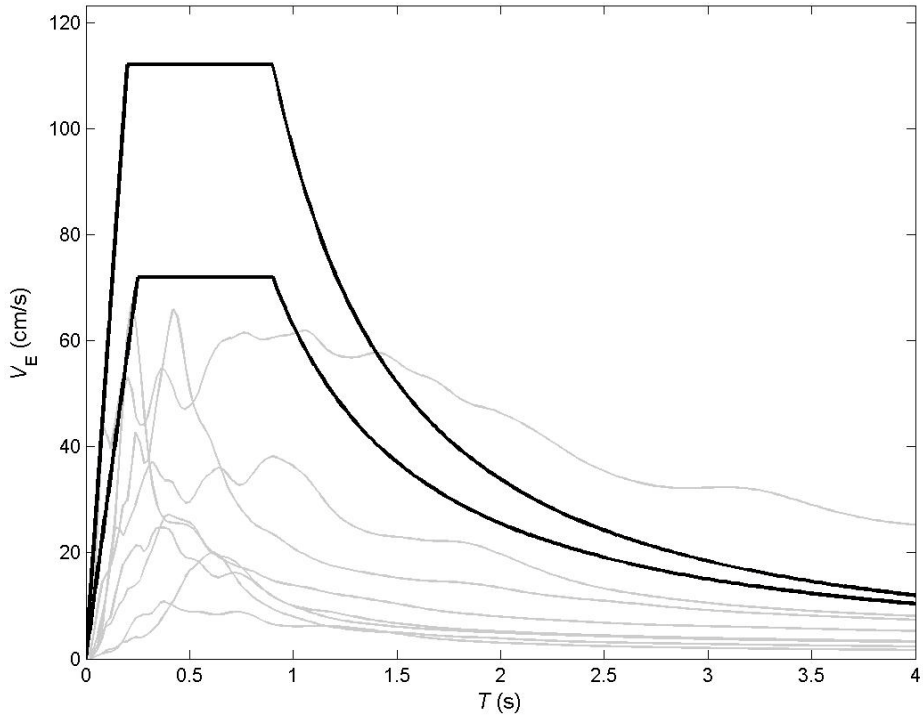

Figure 4-12 Linear V_E design spectra proposed for design acceleration 0.4 g. Stiff soil. $M_s \leq 5.5$. Impulsive

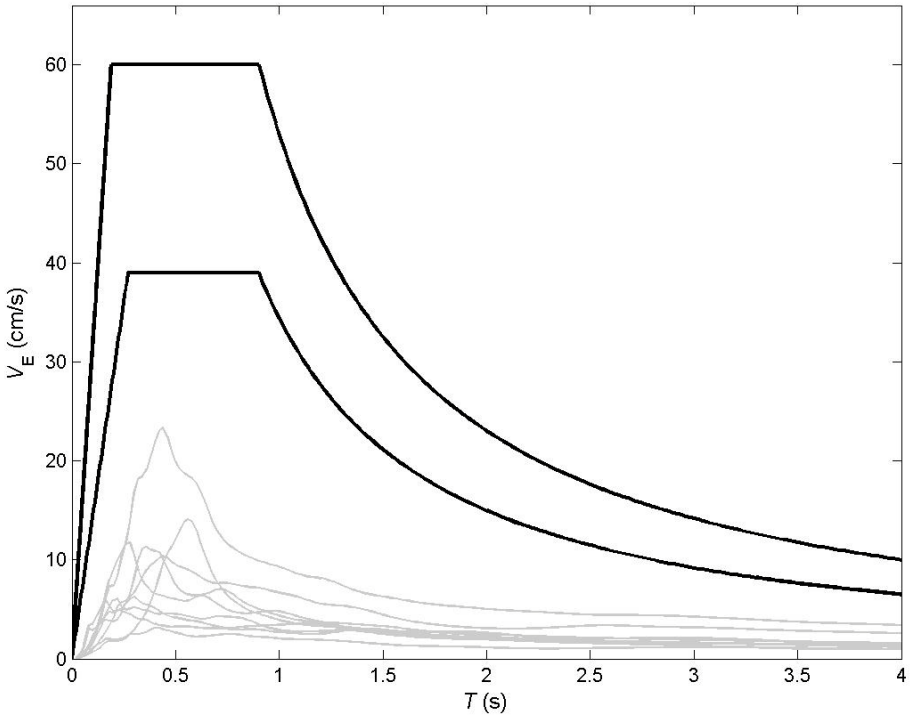

Figure 4-13 Linear V_E design spectra proposed for design acceleration 0.4 g. Stiff soil. $M_s \leq 5.5$. Vibratory

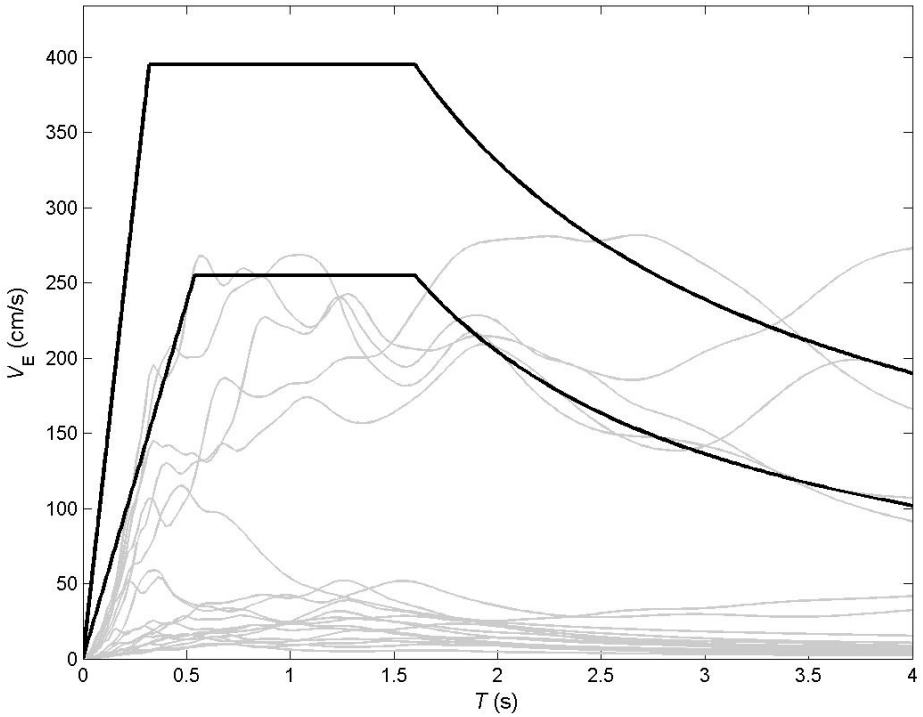

Figure 4-14 Linear V_E design spectra proposed for design acceleration 0.4 g. Soft soil. $M_s > 5.5$. Impulsive

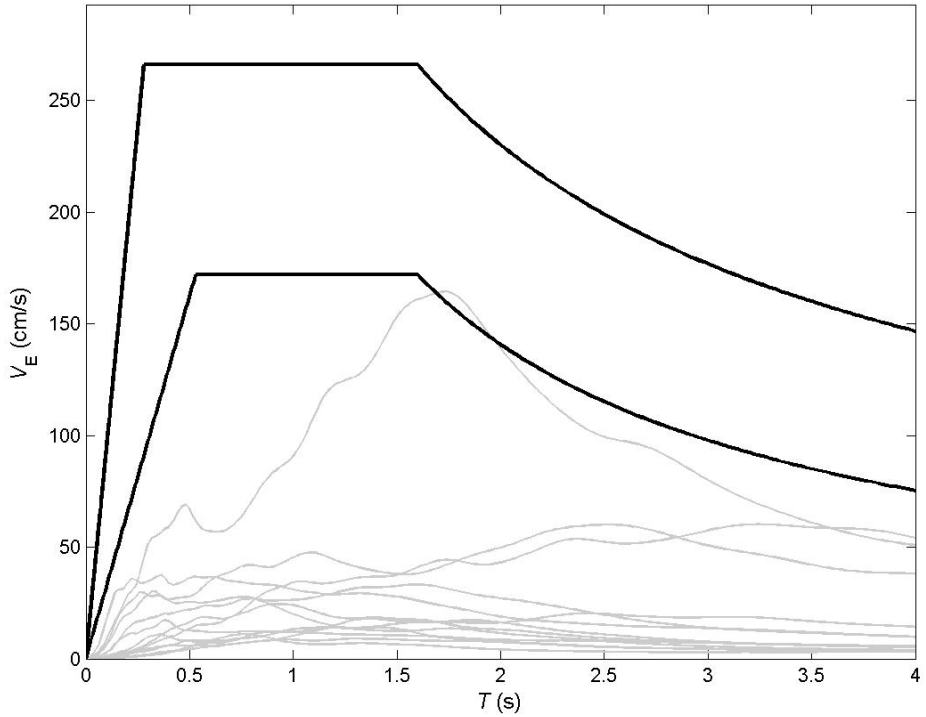

Figure 4-15 Linear V_E design spectra proposed for design acceleration 0.4 g. Soft soil. M_s > 5.5. Vibratory

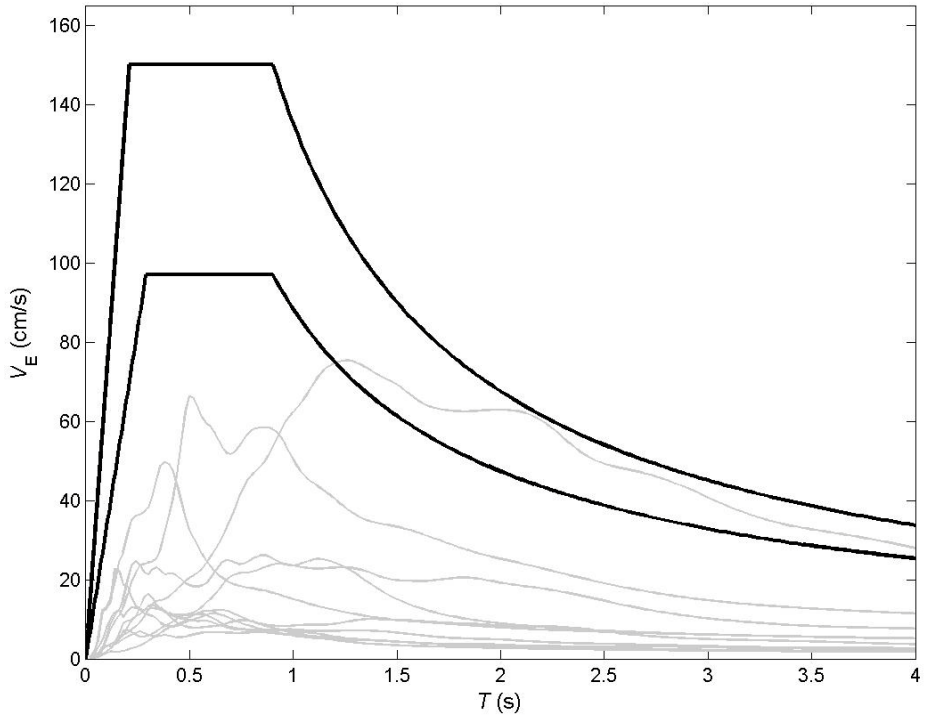

Figure 4-16 Linear V_E design spectra proposed for design acceleration 0.4 g. Soft soil. $M_s \leq 5.5$. Impulsive

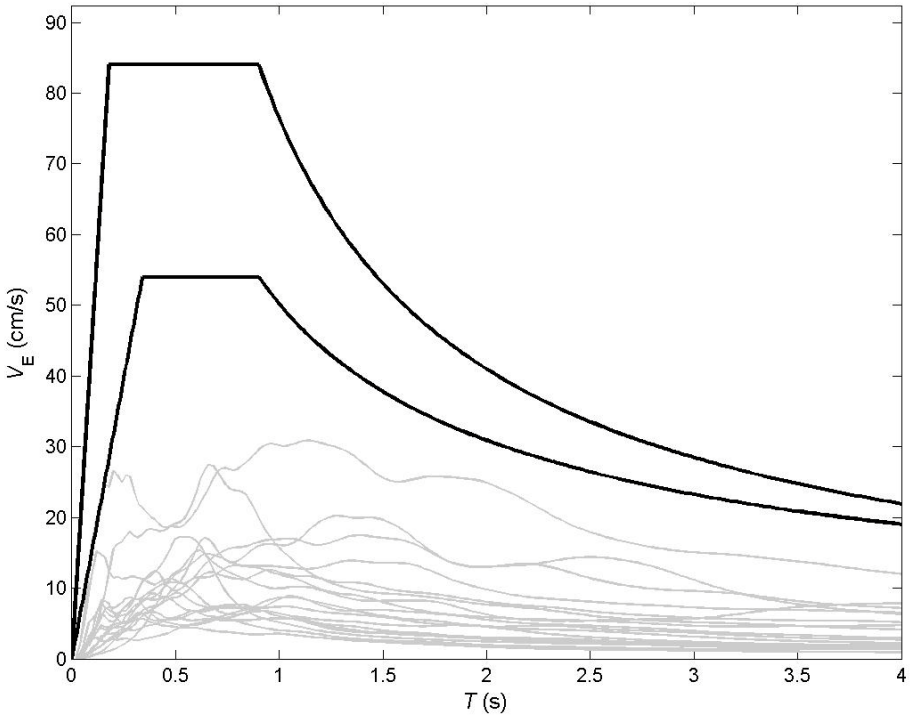

Figure 4-17 Linear V_E design spectra proposed for design acceleration 0.4 g. Soft soil. $M_s \leq 5.5$. Vibratory

The spectra drawn in Figure 4-10 to Figure 4-17 correspond to seismic zone 1 in Turkey, whose design input acceleration is 0.4 g; in the other seismic zones of Turkey and of other countries, the design spectra can be obtained by multiplying the spectral ordinates by the ratio among the actual design acceleration and 0.4 g. This approach requires the additional assumption that the ratio among the design peak ground acceleration (PGA) and the input energy in terms of equivalent velocity V_E is constant. This assumption is a rought approximation and a matter of future research.

4.3 Non-Linear Spectra

As discussed in section 2.1, the proposed V_E nonlinear spectra are similar to the linear ones; in fact, the only difference is a shortening of the corner period T_C. In other words, the slope of the initial branch is augmented to take into account the dependency of the spectral ordinates on the resistance and the hysteretic behavior of the structure and the elongation of the fundamental period of the structure generated by its nonlinear behavior. Akiyama [1985] suggested deriving the slope of the initial branch of the nonlinear spectra by multiplying the slope of the linear spectra by 1.2; such factor was derived only from a limited number of records and the authors believe that a more precise evaluation is required mainly because many low-to-medium rise buildings have fundamental periods in the range $0 - T_C$. The nonlinear time history analyses consist of determining the value of E_I (equation (2-12)) in the range 0 – 4 seconds for the inputs listed in Table 3-1. The considered nonlinear SDOF systems have an elastic-perfectly plastic behavior and, hence, they are characterized by their damping ratio ζ, by their initial (elastic) natural period T and by the displacement ductility μ. In this study, three values of ζ are considered (0.02, 0.05, 0.10) and six values of μ are considered (2, 3, 5, 10, 15, 20). Obtaining the spectrum of each acceleration record for a given fixed value of μ requires performing iterative analyses in which the yield strength of the SDOF system, Q_y, is varied until the resulting μ reaches the prescribed target value with 10% tolerance. Since the accelerograms corresponding to NS and EW directions are considered separately, the total number of obtained

spectra is 338 × 3 × 6 = 6084. As discussed in the next section, these spectra are also used for estimating the ratio V_D / V_E.

For each nonlinear analysis the slope of the initial smoothed branch is obtained as the best linear fit in the range 0 – T_C; such slope is termed m_μ. Figure 4-18 to Figure 4-41 displays, in thin dashed lines, the values of the ratio m_μ / m_1 corresponding to ζ = 0.02, ζ = 0.05 and ζ = 0.10 respectively; m_1 is the linear slope, i.e. corresponding to μ = 1. Given the high scattering of the values shown in Figure 4-18 to Figure 4-41, these ratios cannot be used to modify the linear spectra; conversely they have to be averaged and smoothed. About averaging, the thick dashed lines in Figure 4-18 to Figure 4-41 represent the median values, i.e. corresponding to the 50% percentile. Since these lines are too abrupt, they have to be smoothed; the following equation [Benavent et al. 2010] is considered:

$$\frac{m_\mu}{m_1} = p\,(\mu - 1) + \frac{(1+r)\mu^s}{r+\mu^s} \tag{4-3}$$

In this study, parameter r is chosen as r = 0.3 and the values of parameters p and s are determined to provide the best fit with the median values (thick dashed lines in Figure 4-18 to Figure 4-41); the obtained values are indicated in Table 4-3. The smoothed ratios m_μ / m_1 are drawn with thick solid lines in Figure 4-18 to Figure 4-41. Table 4-4 displays the smoothed factors m_μ / m_1 that will modify the slopes of the initial branches of the linear V_E spectra for a damping factor ζ = 0.10.

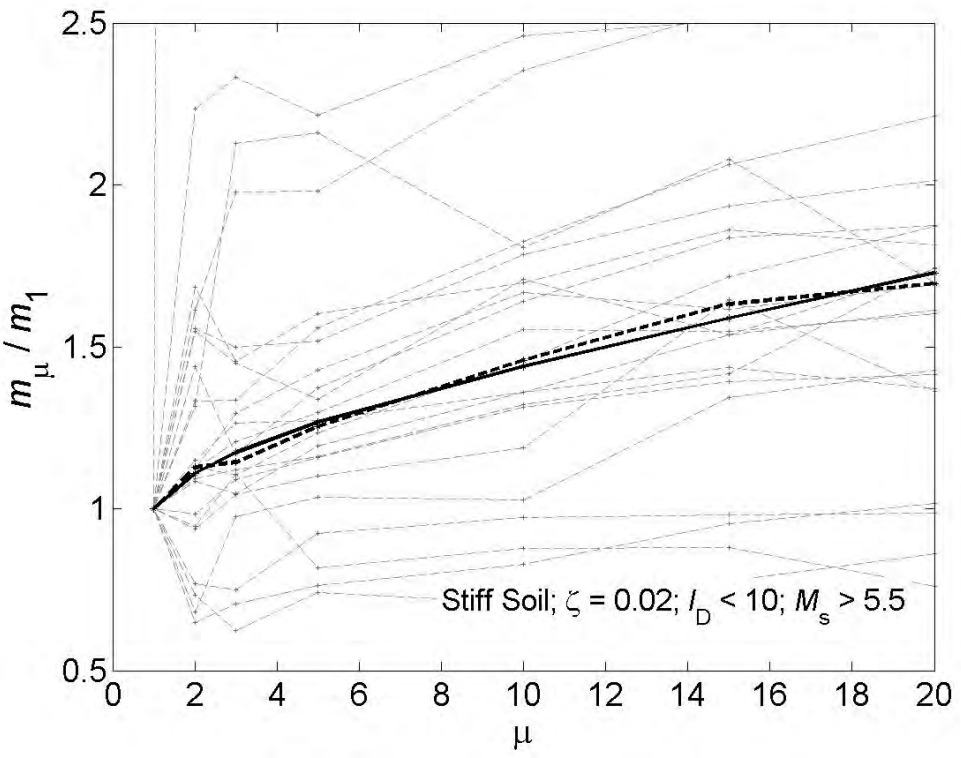

Figure 4-18 Factor modifying the slope of the initial branch of the linear V_E spectra. ζ = 0.02. Stiff soil. M_s > 5.5. Impulsive

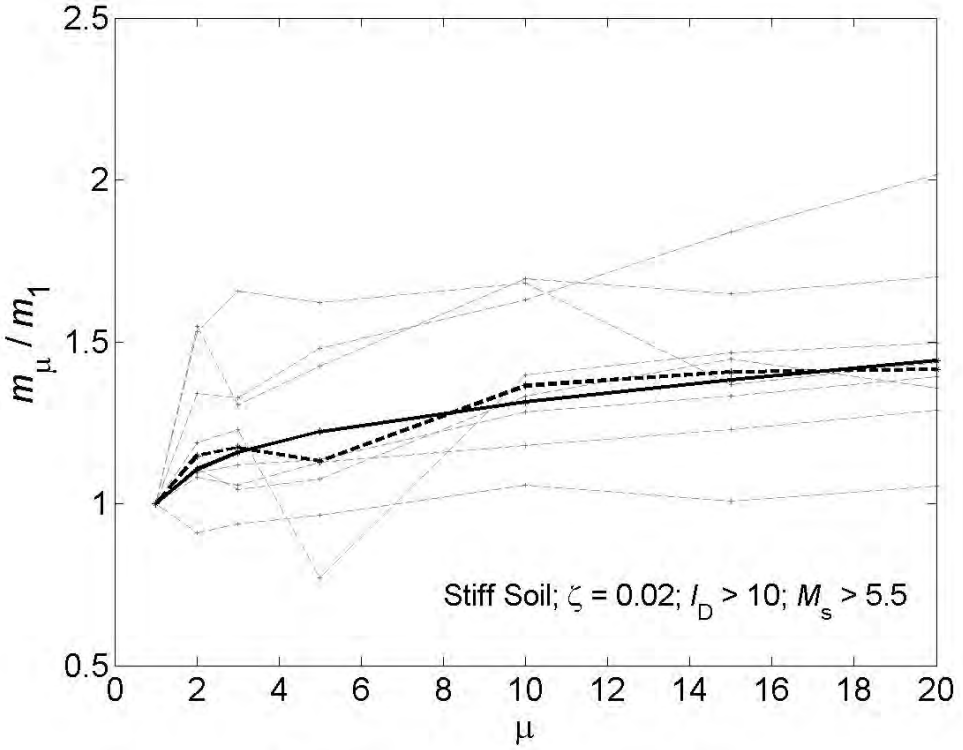

Figure 4-19 Factor modifying the slope of the initial branch of the linear V_E spectra. $\zeta = 0.02$. Stiff soil. $M_s > 5.5$. Vibratory

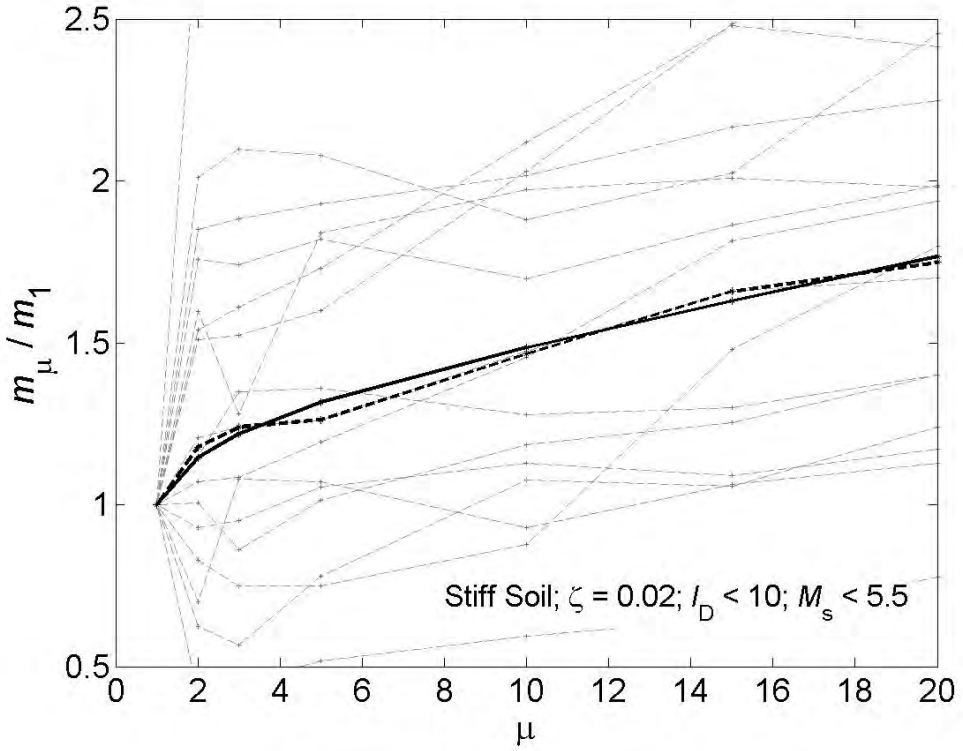

Figure 4-20 Factor modifying the slope of the initial branch of the linear V_E spectra. $\zeta = 0.02$. Stiff soil. $M_s \leq 5.5$. Impulsive

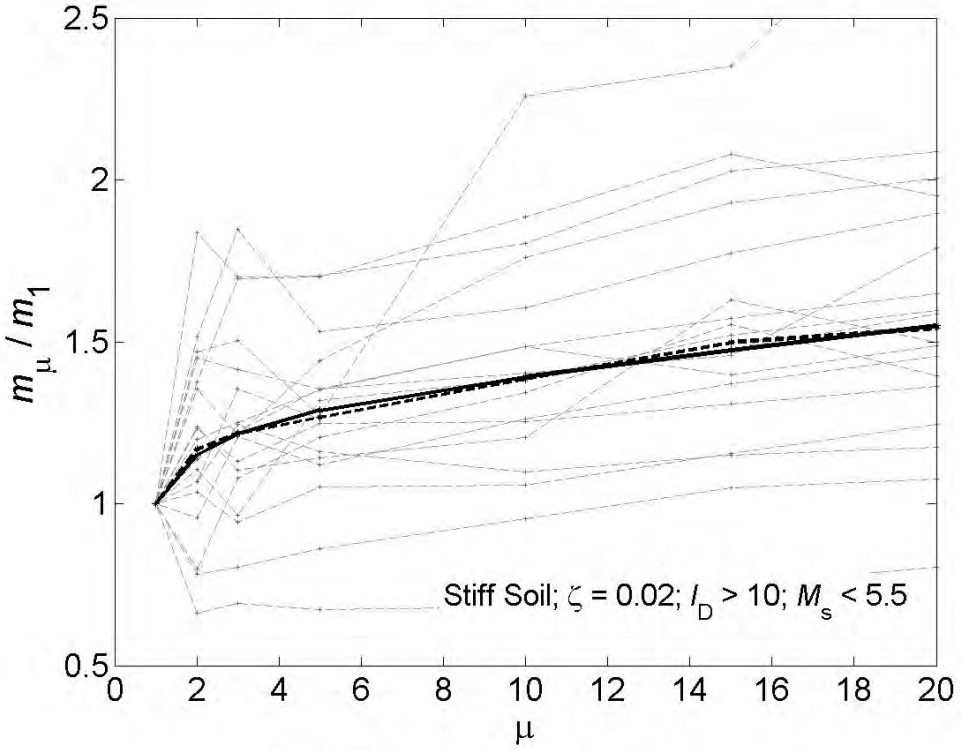

Figure 4-21 Factor modifying the slope of the initial branch of the linear V_E spectra. $\zeta = 0.02$. Stiff soil. $M_s \leq 5.5$. Vibratory

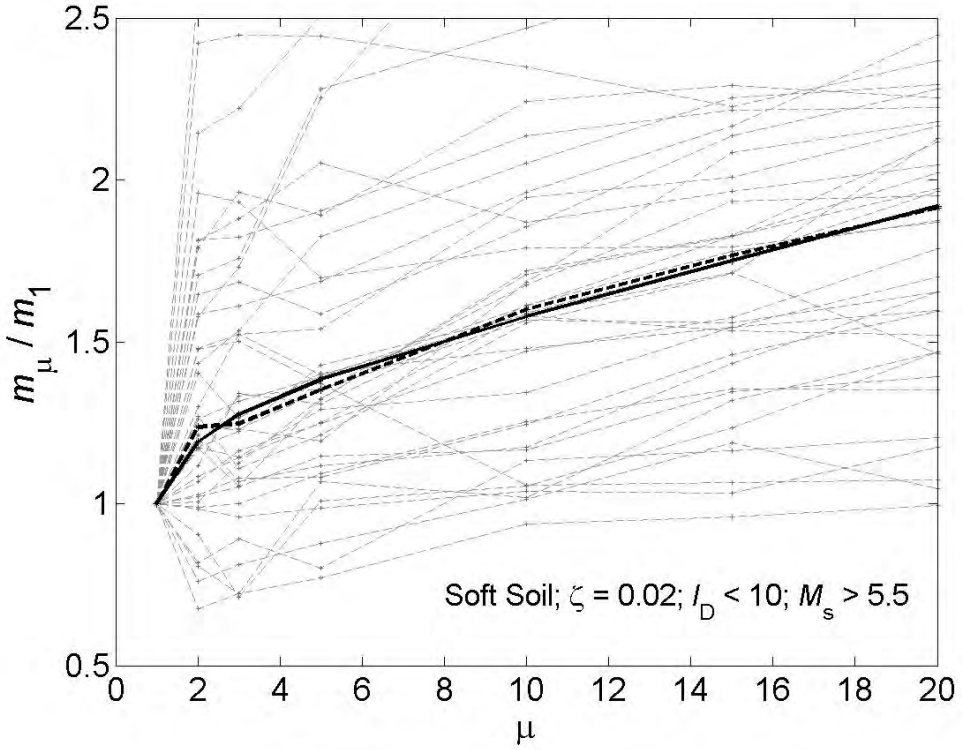

Figure 4-22 Factor modifying the slope of the initial branch of the linear V_E spectra. $\zeta = 0.02$. Soft soil. $M_s > 5.5$. Impulsive

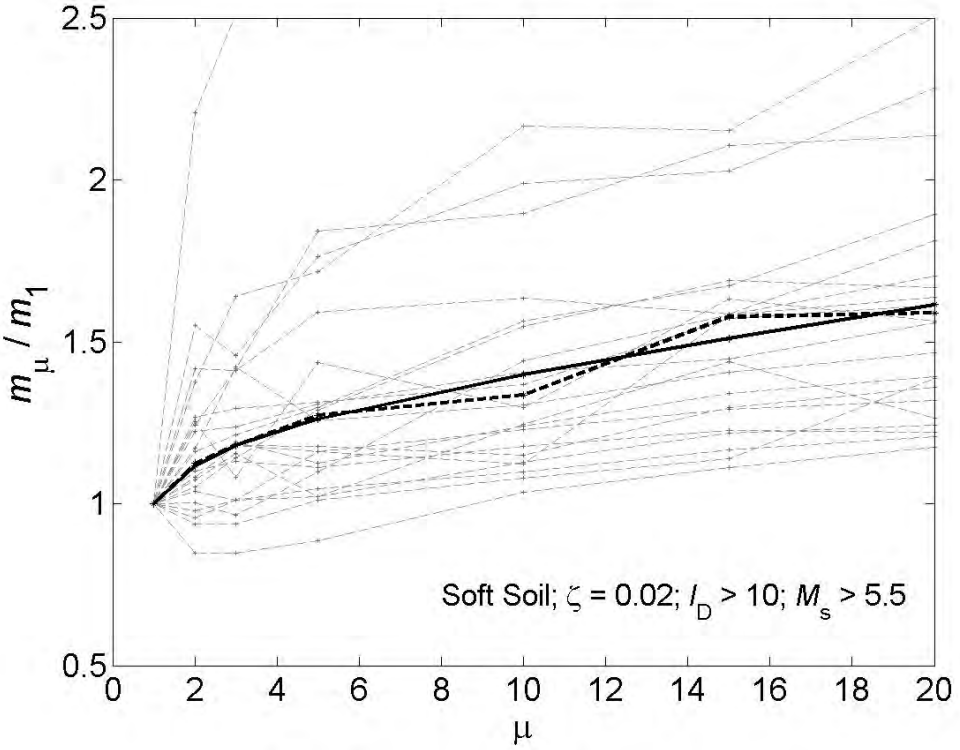

Figure 4-23 Factor modifying the slope of the initial branch of the linear V_E spectra. $\zeta = 0.02$. Soft soil. $M_s > 5.5$. Vibratory

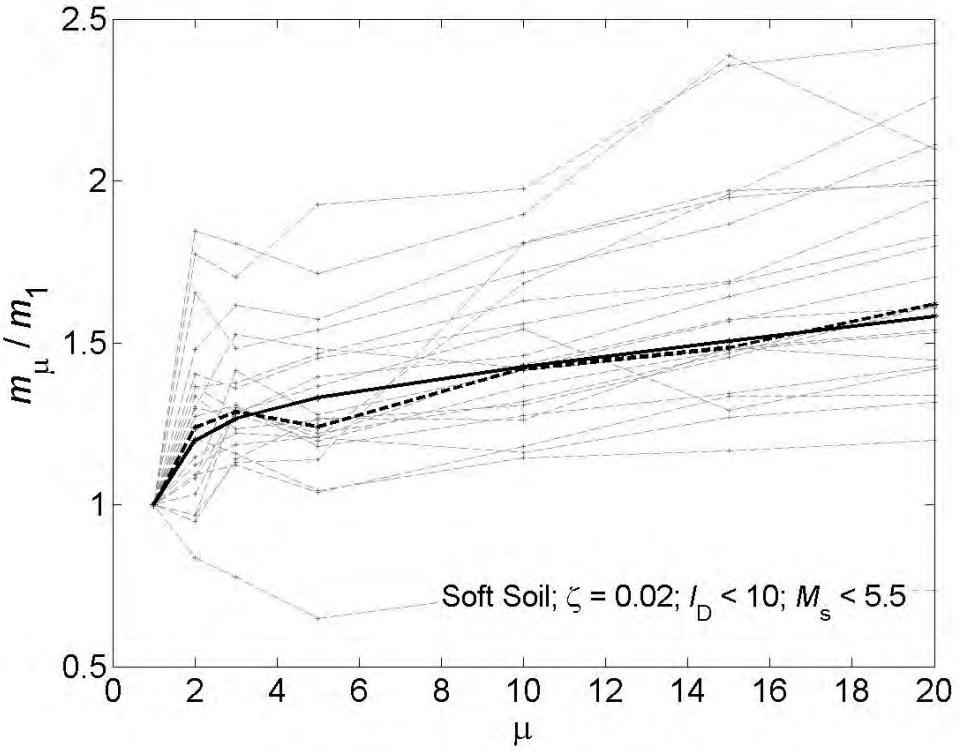

Figure 4-24 Factor modifying the slope of the initial branch of the linear V_E spectra. $\zeta = 0.02$. Soft soil. $M_s \leq 5.5$. Impulsive

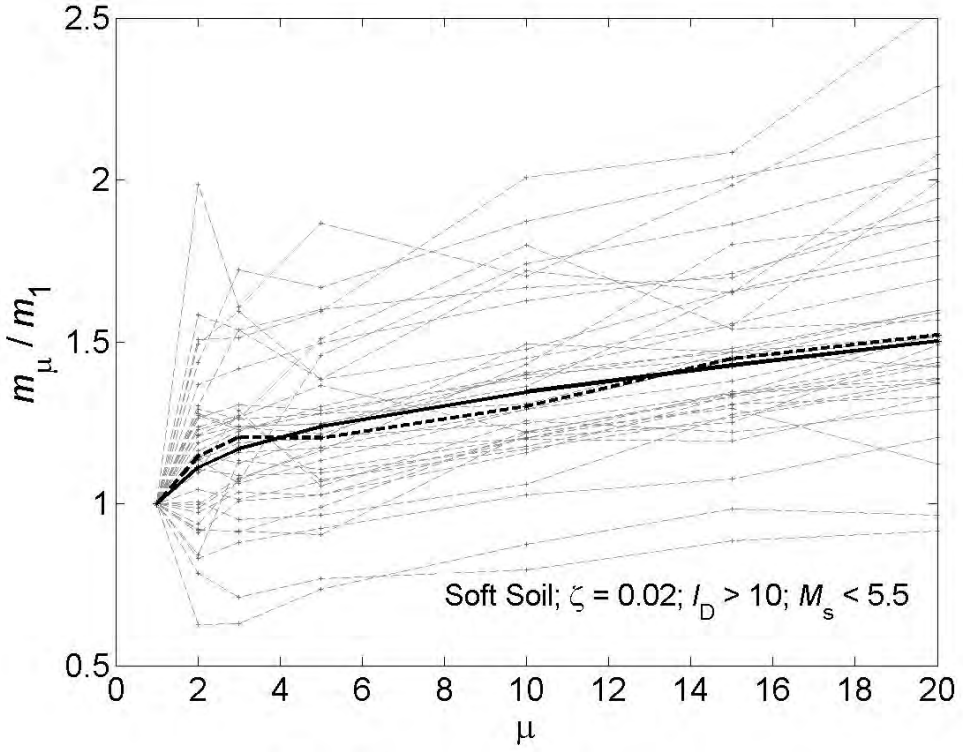

Figure 4-25 Factor modifying the slope of the initial branch of the linear V_E spectra. $\zeta = 0.02$. Soft soil. $M_s \leq 5.5$. Vibratory

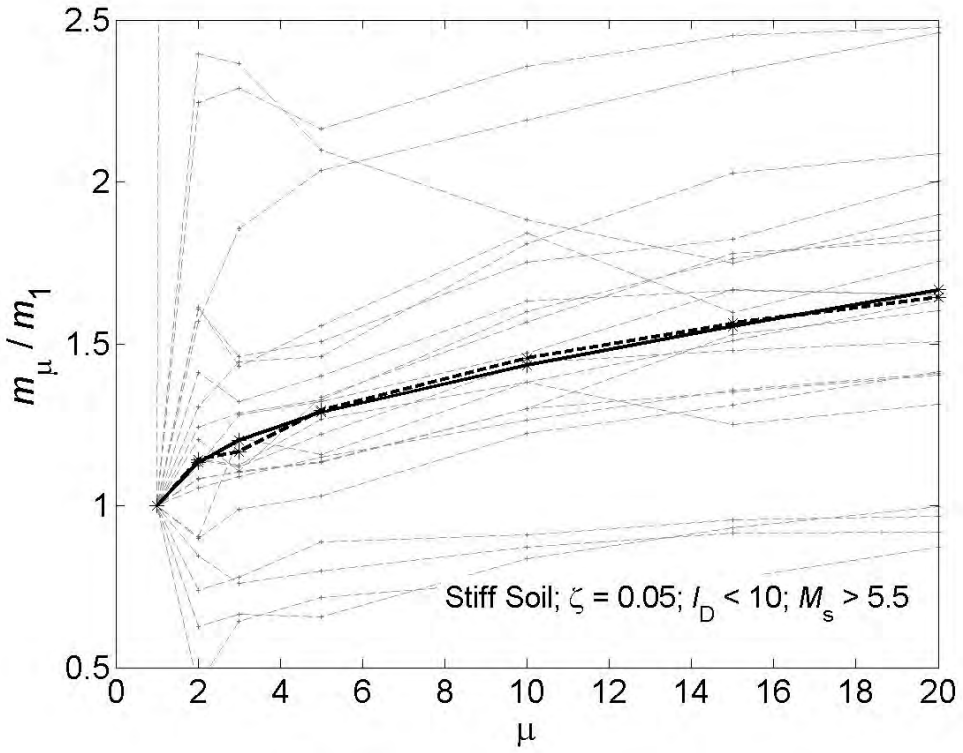

Figure 4-26 Factor modifying the slope of the initial branch of the linear V_E spectra. $\zeta = 0.05$. Stiff soil. $M_s > 5.5$. Impulsive

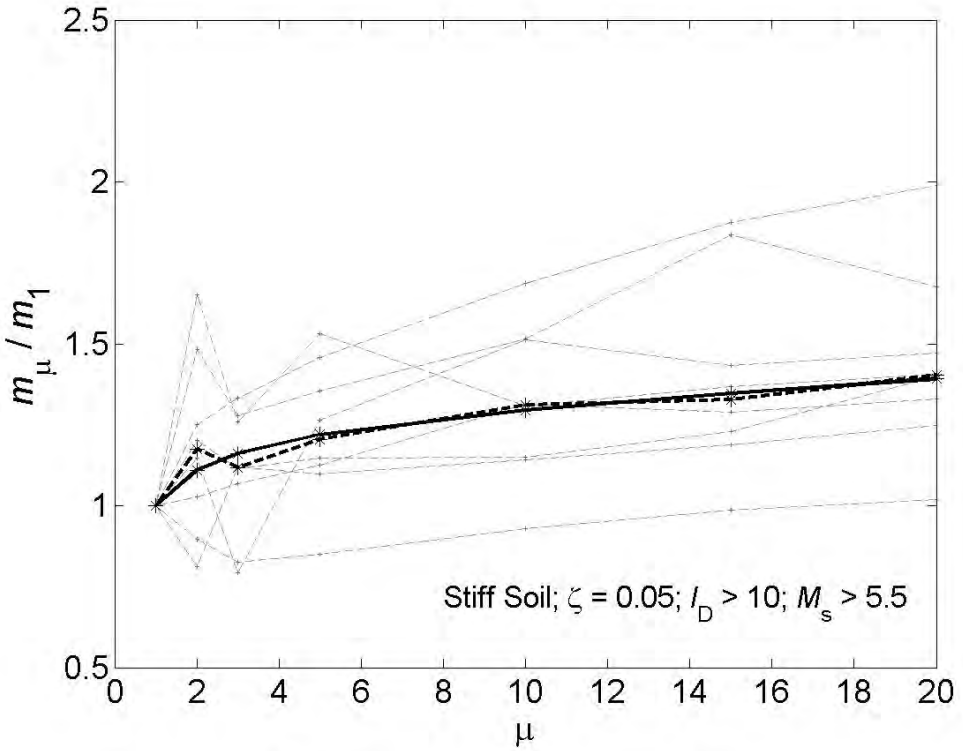

Figure 4-27 Factor modifying the slope of the initial branch of the linear V_E spectra. $\zeta = 0.05$ Stiff soil. $M_s > 5.5$. Vibratory.

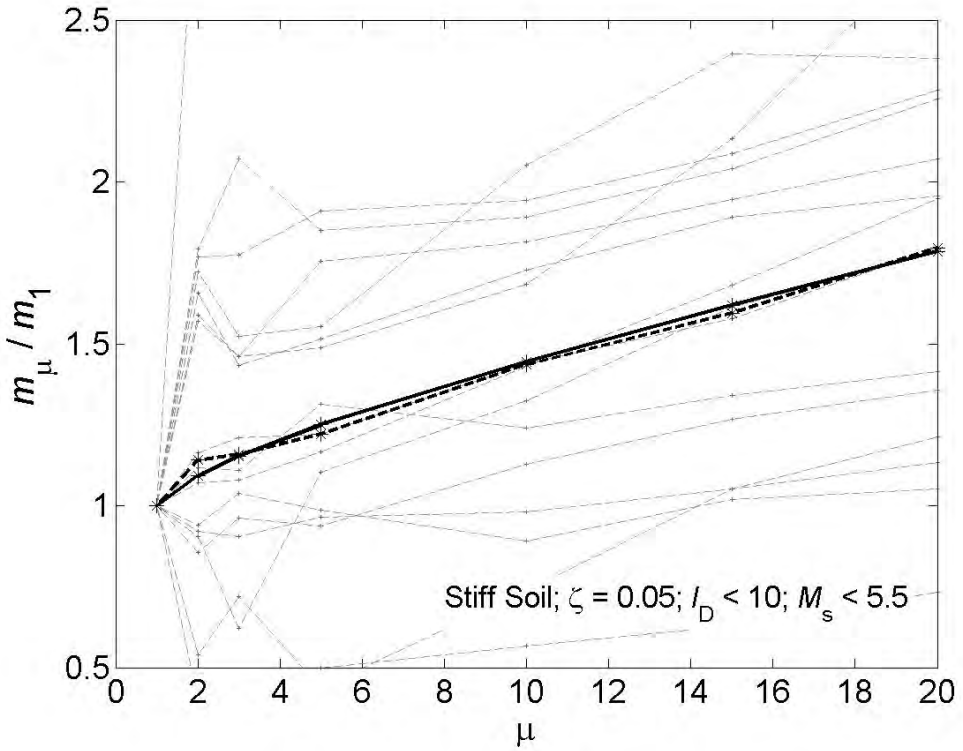

Figure 4-28 Factor modifying the slope of the initial branch of the linear V_E spectra. $\zeta = 0.05$. Stiff soil. $M_s \leq 5.5$. Impulsive

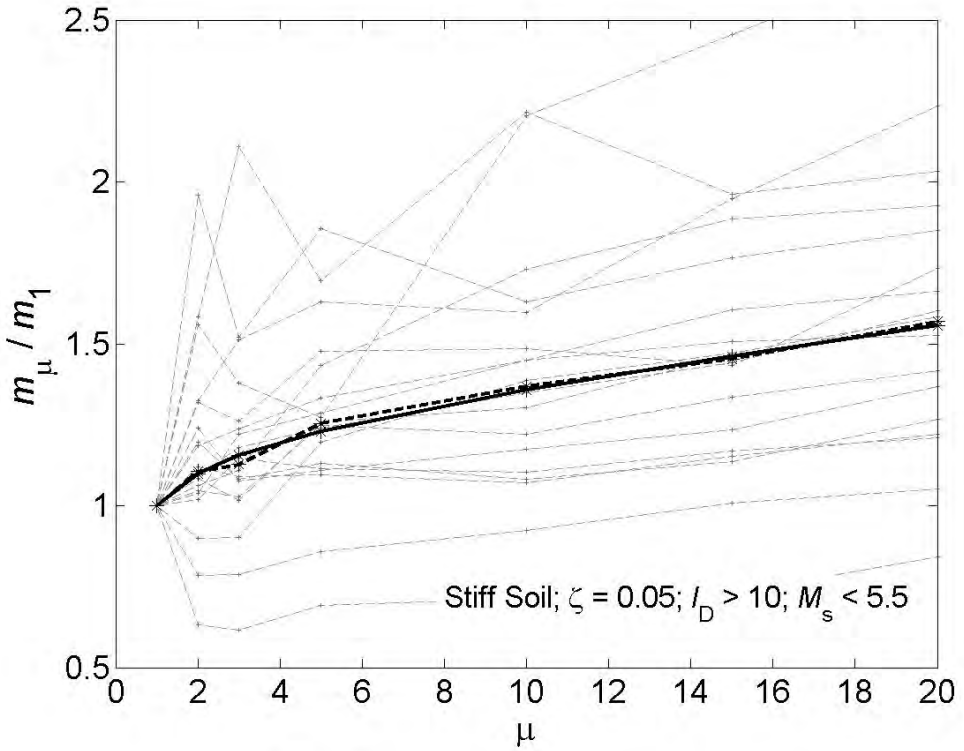

Figure 4-29 Factor modifying the slope of the initial branch of the linear V_E spectra. $\zeta = 0.05$ Stiff soil. $M_s \leq 5.5$. Vibratory.

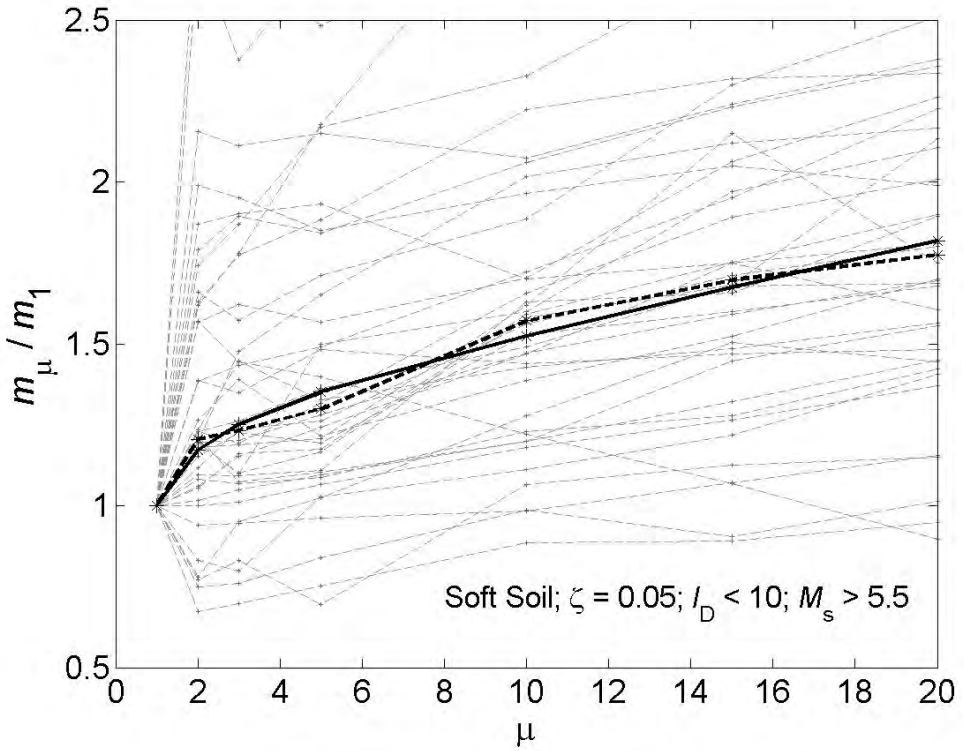

Figure 4-30 Factor modifying the slope of the initial branch of the linear V_E spectra. $\zeta = 0.05$. Soft soil. $M_s > 5.5$. Impulsive

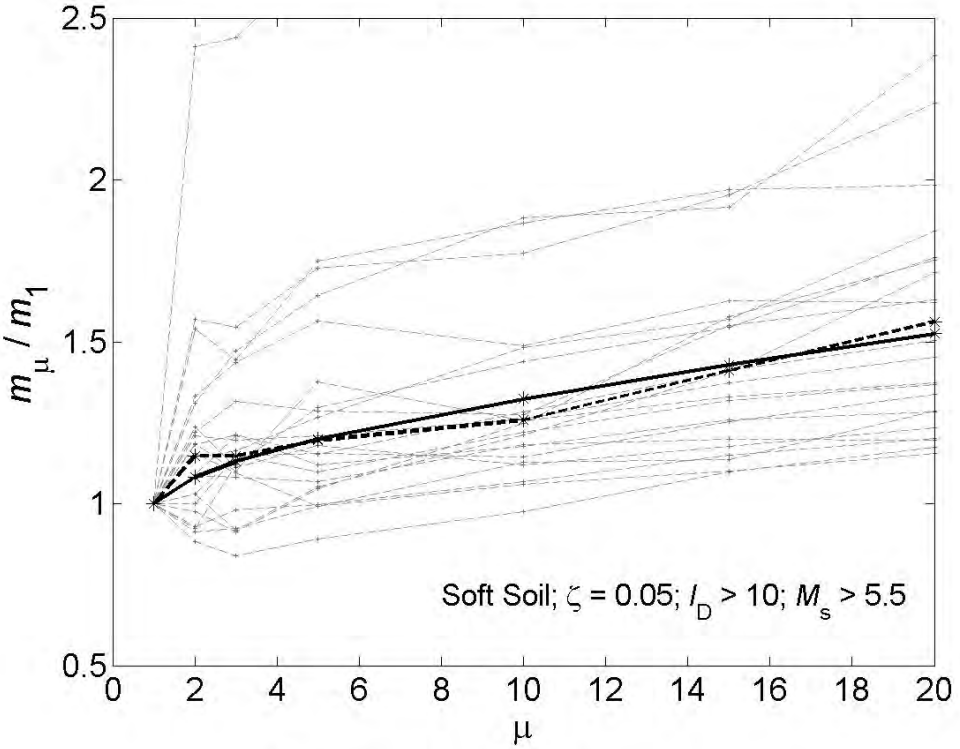

Figure 4-31 Factor modifying the slope of the initial branch of the linear V_E spectra. $\zeta = 0.05$. Soft soil. $M_s > 5.5$. Vibratory

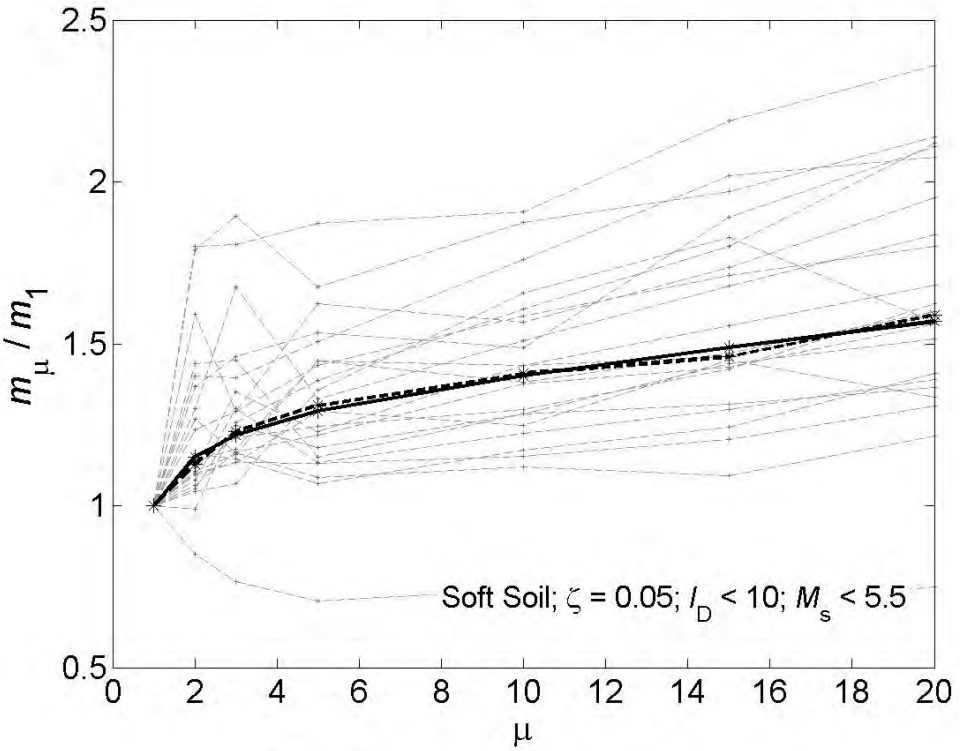

Figure 4-32 Factor modifying the slope of the initial branch of the linear V_E spectra. $\zeta = 0.05$ Soft soil. $M_s \leq 5.5$. Impulsive.

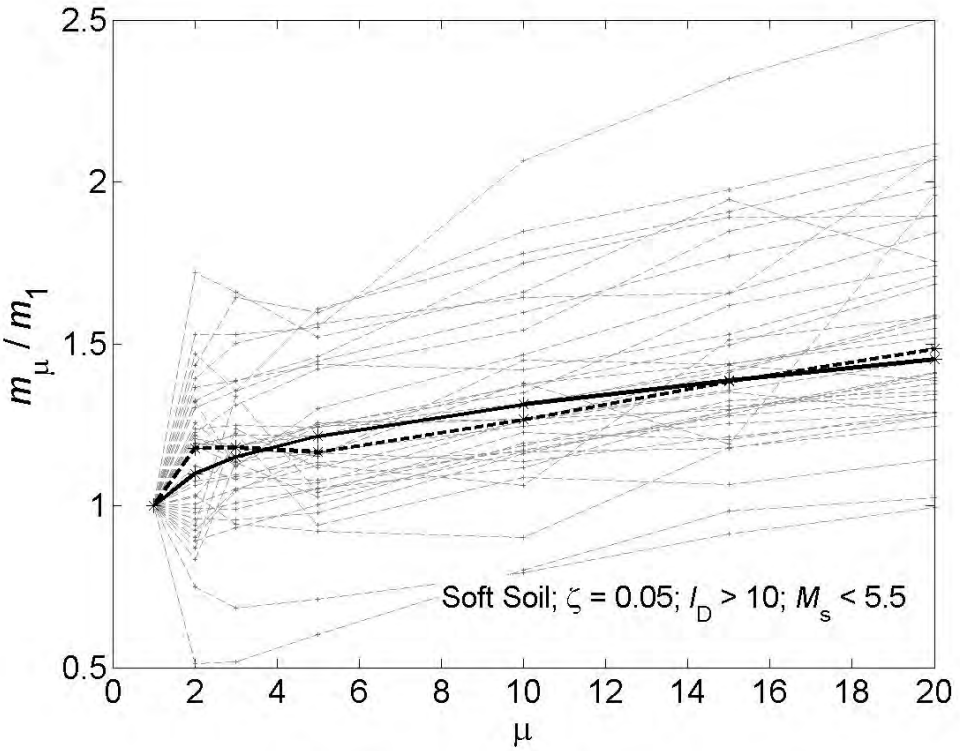

Figure 4-33 Factor modifying the slope of the initial branch of the linear V_E spectra. $\zeta = 0.05$. Soft soil. $M_s \leq 5.5$. Vibratory

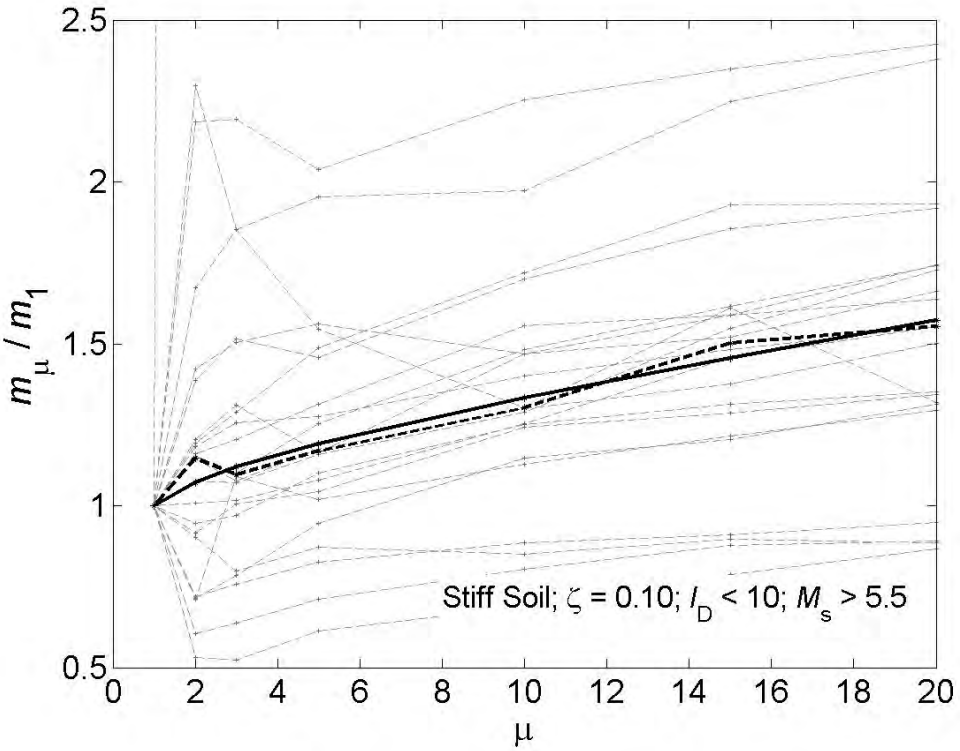

Figure 4-34 Factor modifying the slope of the initial branch of the linear V_E spectra. $\zeta = 0.10$ Stiff soil. $M_s > 5.5$. Impulsive.

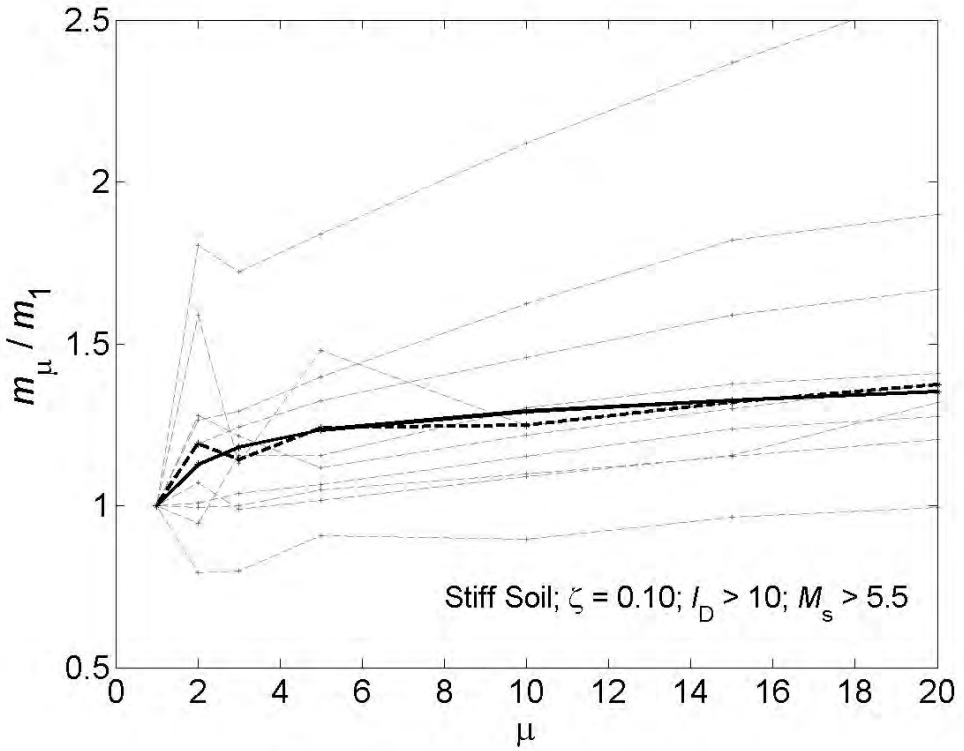

Figure 4-35 Factor modifying the slope of the initial branch of the linear V_E spectra. $\zeta = 0.10$ Stiff soil. $M_s > 5.5$. Vibratory.

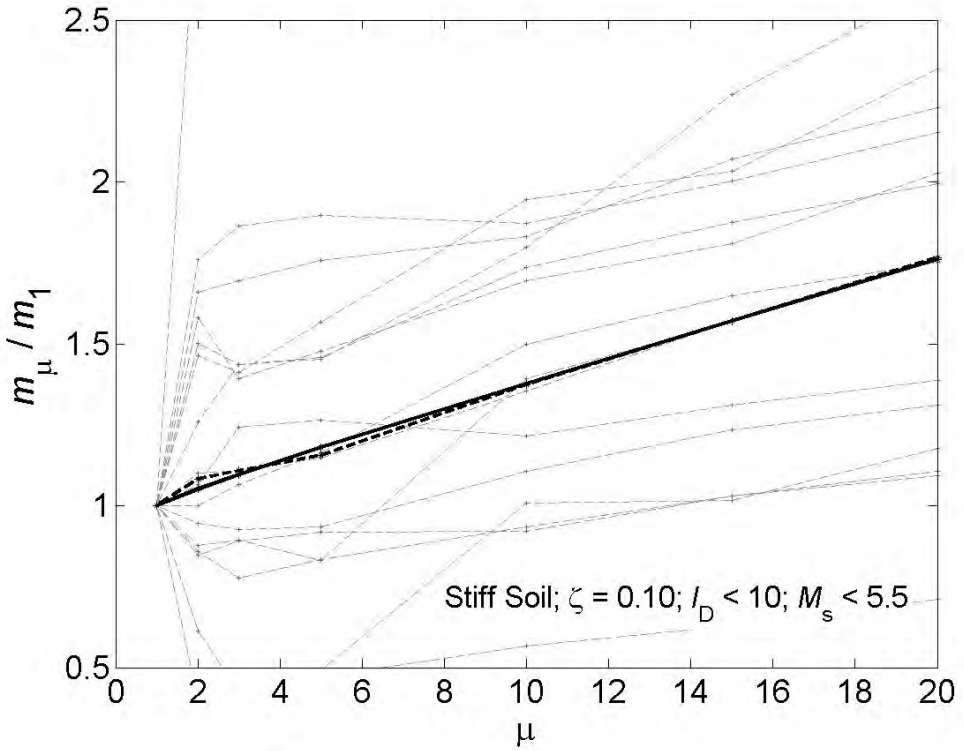

Figure 4-36 Factor modifying the slope of the initial branch of the linear V_E spectra. $\zeta = 0.10$. Stiff soil. $M_s \leq 5.5$. Impulsive

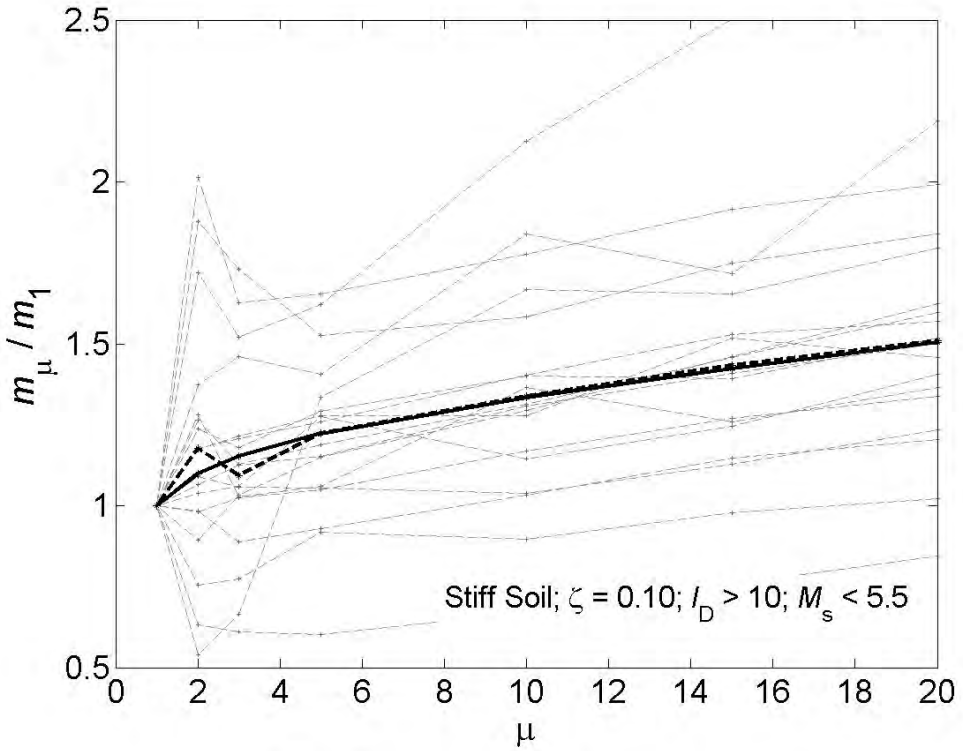

Figure 4-37 Factor modifying the slope of the initial branch of the linear V_E spectra. $\zeta = 0.10$. Stiff soil. $M_s \leq 5.5$. Vibratory

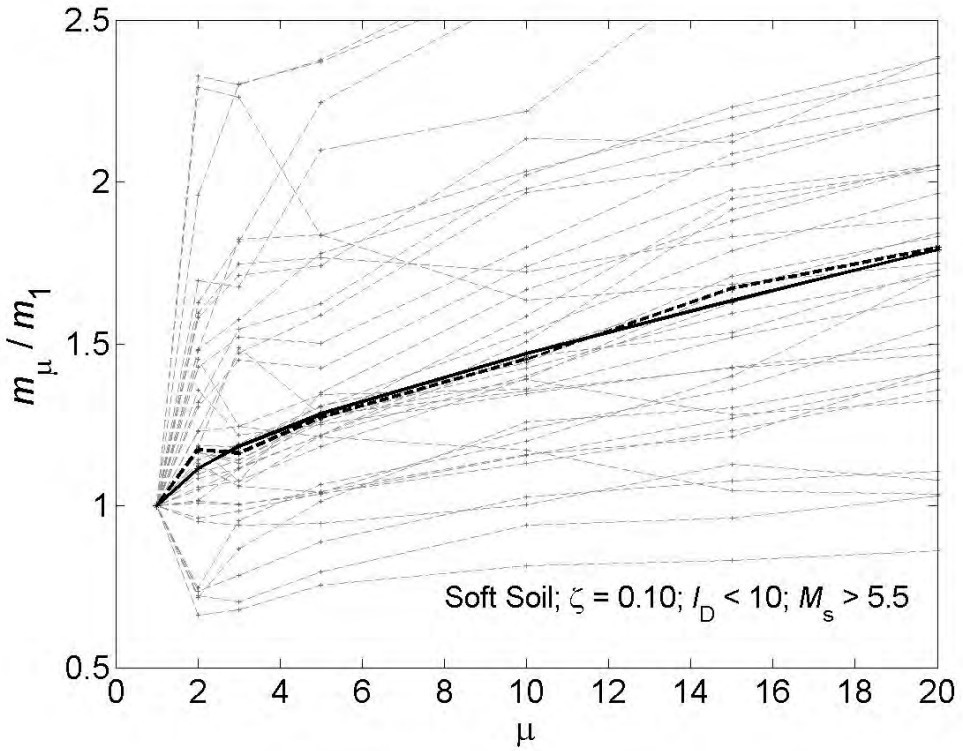

Figure 4-38 Factor modifying the slope of the initial branch of the linear V_E spectra. $\zeta = 0.10$. Soft soil. $M_s > 5.5$. Impulsive

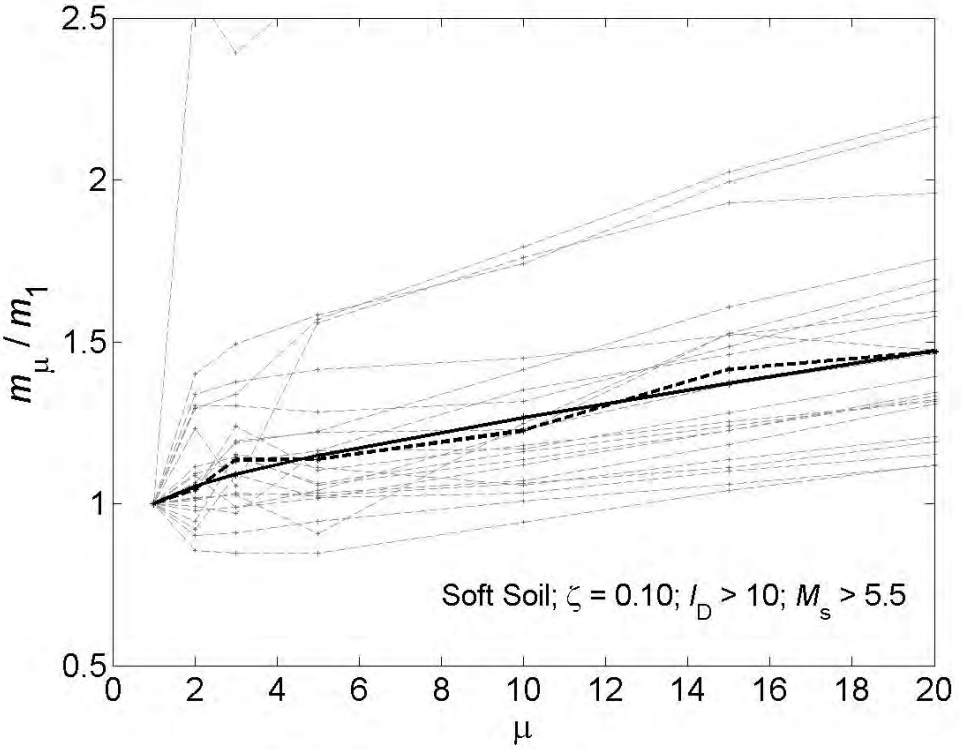

Figure 4-39 Factor modifying the slope of the initial branch of the linear V_E spectra. ζ = 0.10. Soft soil. M_s > 5.5. Vibratory

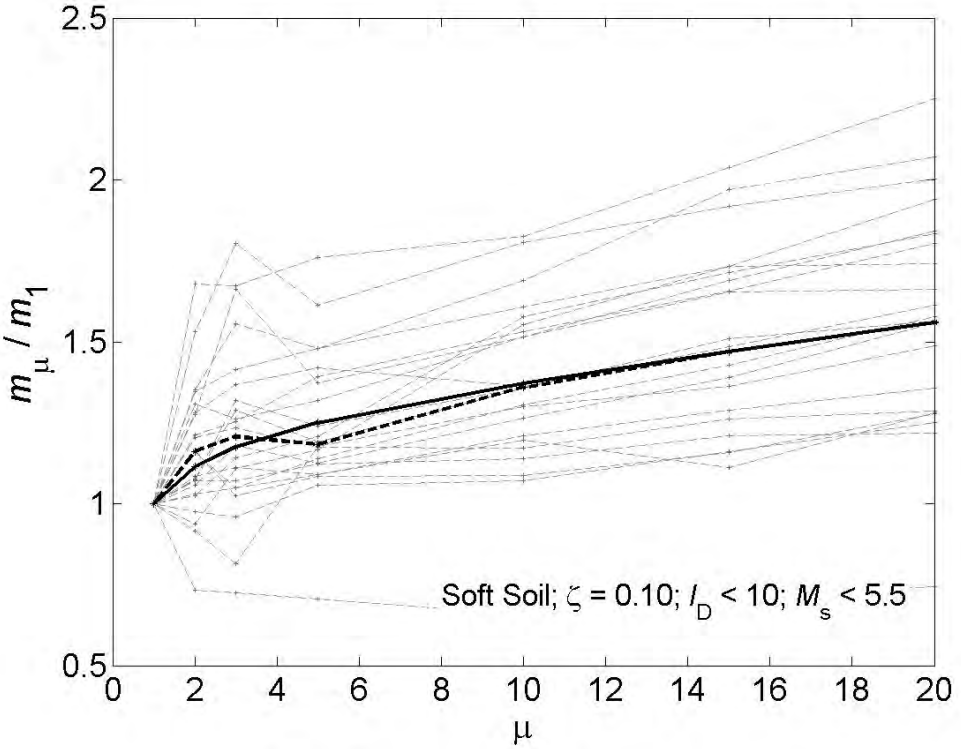

Figure 4-40 Factor modifying the slope of the initial branch of the linear V_E spectra. ζ = 0.10. Soft soil. $M_s \leq$ 5.5. Impulsive

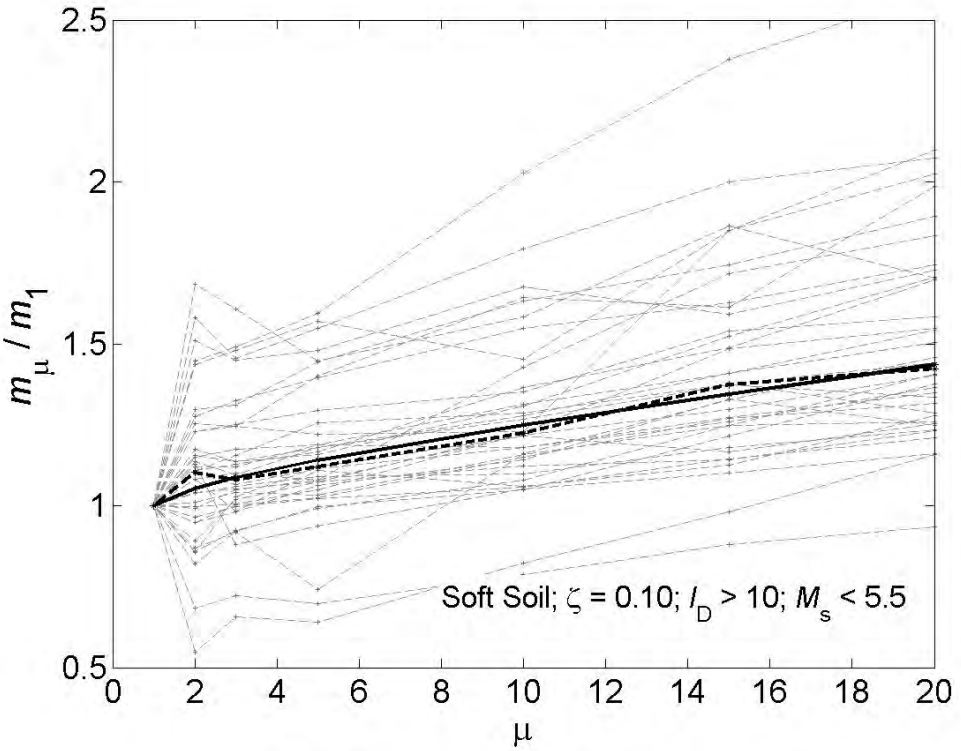

Figure 4-41 Factor modifying the slope of the initial branch of the linear V_E spectra. $\zeta = 0.10$. Soft soil. $M_s \leq 5.5$. Vibratory

Table 4-3 Coefficients *p* and *s* for the correction of the slopes of the initial branches of the linear V_E spectra. $r = 0.3$

Soil type	Magnitude	Velocity pulses	$\zeta = 0.02$		$\zeta = 0.05$		$\zeta = 0.10$	
			p	*s*	*p*	*s*	*p*	*s*
Stiff Soil	$M_s > 5.5$	Impulsive	0.026	0.58	0.020	0.82	0.020	0.34
		Vibratory	0.010	0.687	0.007	0.741	0.012	0.204
	$M_s \leq 5.5$	Impulsive	0.025	0.88	0.030	0.41	0.037	0.088
		Vibratory	0.014	1.052	0.017	0.58	0.014	0.60
Soft Soil	$M_s > 5.5$	Impulsive	0.033	1.273	0.028	1.124	0.029	0.60
		Vibratory	0.019	0.70	0.016	0.43	0.018	0.23
	$M_s \leq 5.5$	Impulsive	0.015	1.59	0.015	1.052	0.015	0.70
		Vibratory	0.013	0.70	0.011	0.62	0.015	0.23

Figure 4-18 to Figure 4-41 and Table 4-4 show that the m_μ / m_1 ratios are bigger for higher values of μ, and that, for mid and big values of μ, the ratios m_μ / m_1 tend to be higher for impulsive registers than for vibratory ones. Comparison among the constant value 1.2 suggested by Akiyama and the factors drawn in Figure 4-18 to Figure 4-40 and displayed in Table 4-4 show that for displacement ductility larger than about 5, the value proposed by Akiyama might be clearly unconservative.

Table 4-4. Factors m_μ / m_1 correcting the slopes of the initial branches of the linear V_E spectra

Damping	Soil type	Magnitude	Pulses	m_μ / m_1					
				$\mu = 2$	$\mu = 3$	$\mu = 5$	$\mu = 10$	$\mu = 15$	$\mu = 20$
$\zeta = 0.02$	Stiff Soil	$M_s > 5.5$	Impulsive	1.13	1.14	1.25	1.46	1.63	1.70
			Vibratory	1.34	1.27	1.43	1.51	1.43	1.46
		$M_s \leq 5.5$	Impulsive	1.18	1.24	1.26	1.46	1.66	1.75
			Vibratory	1.17	1.22	1.27	1.39	1.50	1.54
	Soft Soil	$M_s > 5.5$	Impulsive	1.24	1.25	1.35	1.60	1.77	1.91
			Vibratory	1.12	1.18	1.27	1.34	1.58	1.59
		$M_s \leq 5.5$	Impulsive	1.24	1.29	1.24	1.41	1.48	1.62
			Vibratory	1.11	1.16	1.22	1.31	1.38	1.44
$\zeta = 0.05$	Stiff Soil	$M_s > 5.5$	Impulsive	1.14	1.17	1.29	1.46	1.56	1.64
			Vibratory	1.23	1.19	1.36	1.31	1.37	1.41
		$M_s \leq 5.5$	Impulsive	1.14	1.16	1.22	1.44	1.59	1.80
			Vibratory	1.11	1.13	1.25	1.37	1.45	1.57
	Soft Soil	$M_s > 5.5$	Impulsive	1.21	1.23	1.30	1.57	1.70	1.78
			Vibratory	1.15	1.15	1.20	1.26	1.41	1.56
		$M_s \leq 5.5$	Impulsive	1.13	1.23	1.31	1.41	1.46	1.59
			Vibratory	1.11	1.16	1.22	1.30	1.35	1.39
$\zeta = 0.10$	Stiff Soil	$M_s > 5.5$	Impulsive	1.15	1.10	1.17	1.30	1.50	1.55
			Vibratory	1.19	1.14	1.24	1.25	1.32	1.37
		$M_s \leq 5.5$	Impulsive	1.08	1.11	1.16	1.37	1.57	1.77
			Vibratory	1.18	1.09	1.22	1.34	1.43	1.51
	Soft Soil	$M_s > 5.5$	Impulsive	1.17	1.16	1.27	1.45	1.67	1.80
			Vibratory	1.04	1.14	1.14	1.23	1.41	1.47
		$M_s \leq 5.5$	Impulsive	1.17	1.21	1.18	1.36	1.47	1.56
			Vibratory	1.04	1.07	1.12	1.20	1.28	1.35

The proposed design nonlinear V_E spectra are based on modifying the slopes of the initial branches of the linear spectra (shown in Figure 4-2 to Figure 4-9) with the factors listed in Table 4-4; the same factors are used to multiply the median and characteristic branches. Figure 4-42 to Figure 4-65 display the initial median and characteristic branches of the proposed nonlinear spectra for $\zeta = 0.02$, $\zeta = 0.05$, $\zeta = 0.10$ and $1 \leq \mu \leq 20$; obviously, the right branches (those with smallest slopes) correspond to $\mu = 1$ while the left ones (those with highest slopes) correspond to $\mu = 20$.

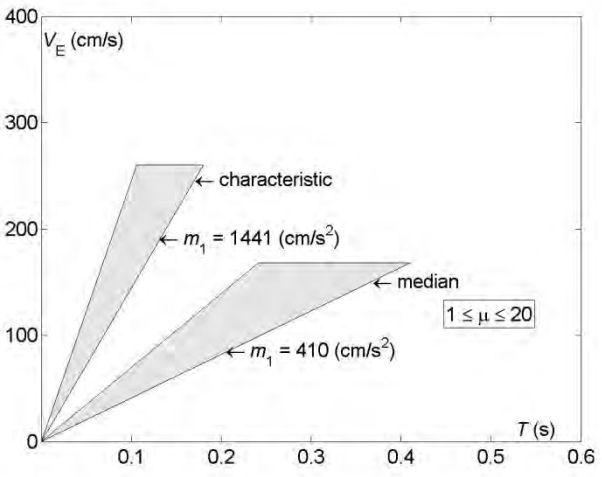

Figure 4-42 Initial branch of the nonlinear V_E spectra. Stiff soil. $M_s > 5.5$. Impulsive. $\zeta = 0.02$

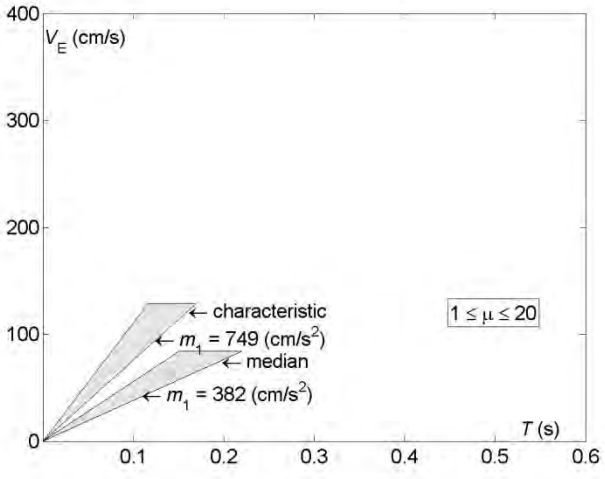

Figure 4-43 Initial branch of the nonlinear V_E spectra. Stiff soil. M_s > 5.5. Vibratory. ζ = 0.02

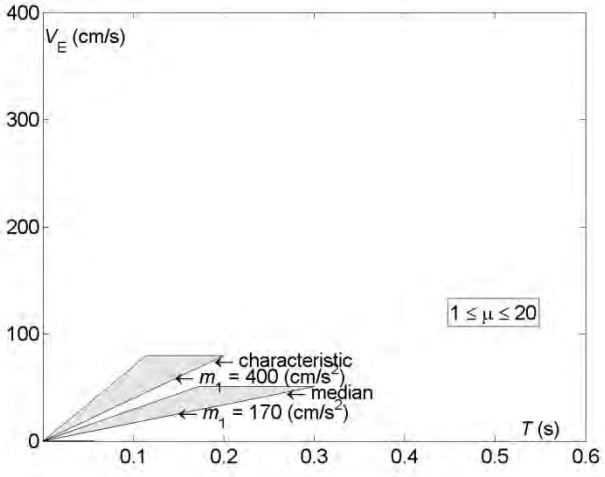

Figure 4-44 Initial branch of the nonlinear V_E spectra. Stiff soil. $M_s \leq$ 5.5.Impulsive. ζ = 0.02

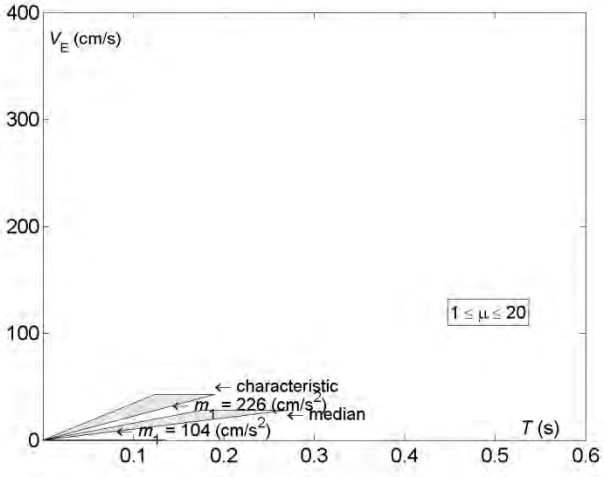

Figure 4-45 Initial branch of the nonlinear V_E spectra. Stiff soil. $M_s \leq$ 5.5.Vibratory. ζ = 0.02

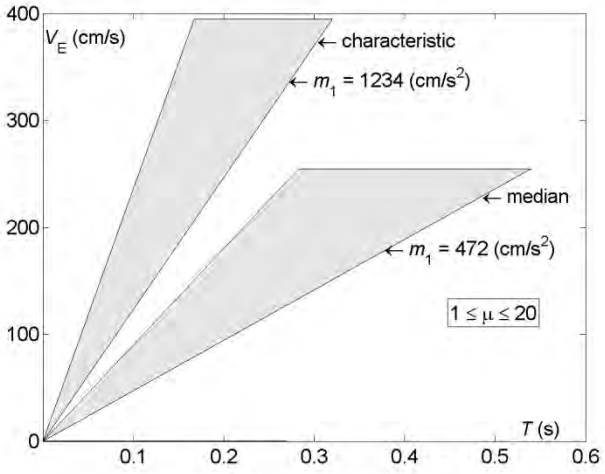

Figure 4-46 Initial branch of the nonlinear V_E spectra. Soft soil. M_s > 5.5. Impulsive. ζ = 0.02

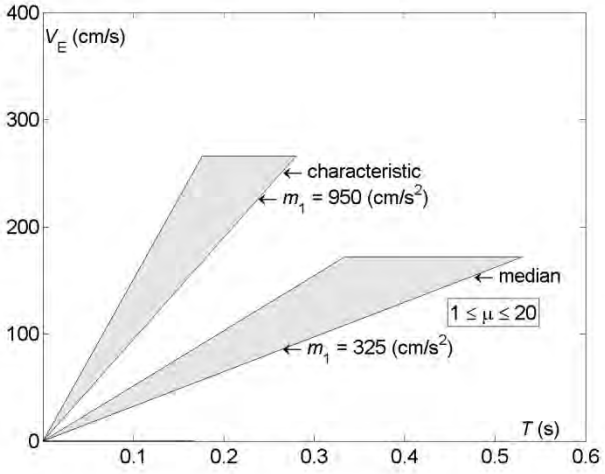

Figure 4-47 Initial branch of the nonlinear V_E spectra. Soft soil. M_s > 5.5. Vibratory. ζ = 0.02

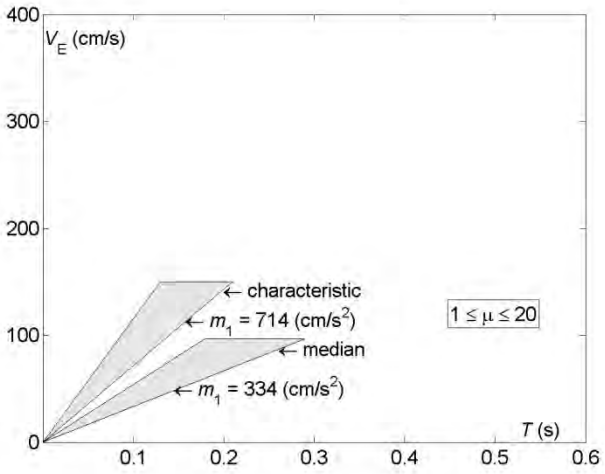

Figure 4-48 Initial branch of the nonlinear V_E spectra. Soft soil. $M_s \leq$ 5.5.Impulsive. ζ = 0.02

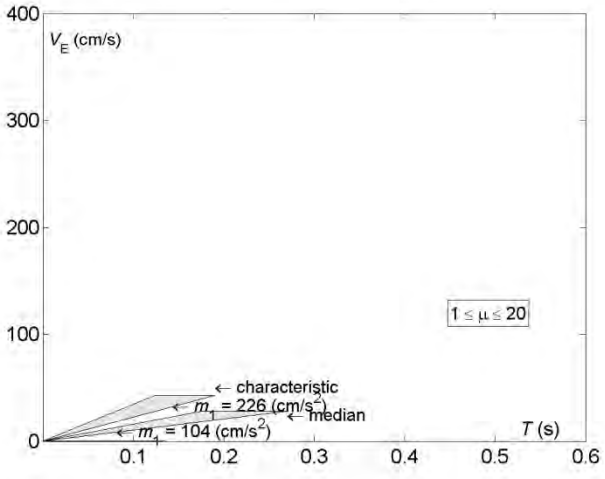

Figure 4-49 Initial branch of the nonlinear V_E spectra. Soft soil. $M_s \le 5.5$.Vibratory. $\zeta = 0.02$

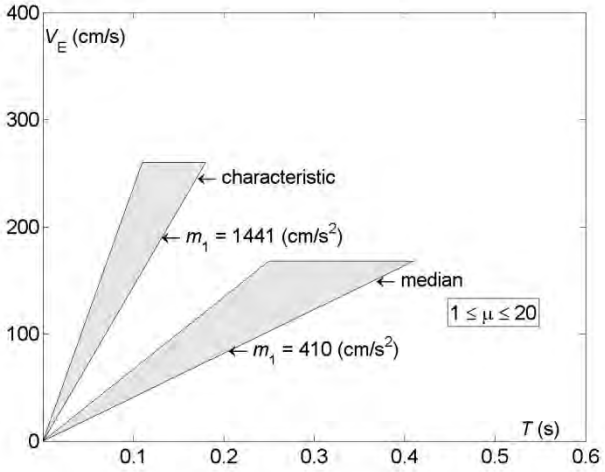

Figure 4-50 Initial branch of the nonlinear V_E spectra. Stiff soil. $M_s > 5.5$. Impulsive. $\zeta = 0.05$

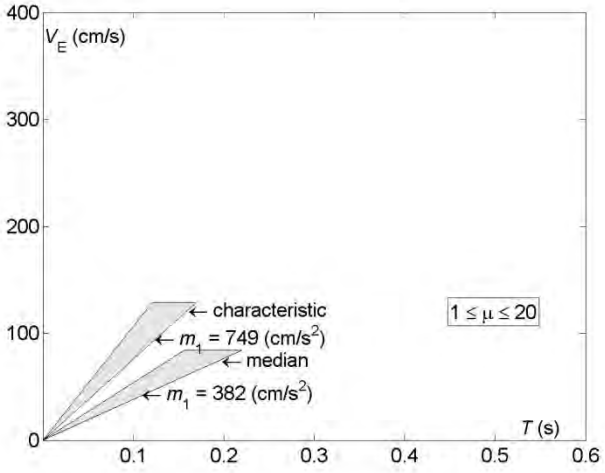

Figure 4-51 Initial branch of the nonlinear V_E spectra. Stiff soil. $M_s > 5.5$. Vibratory. $\zeta = 0.05$

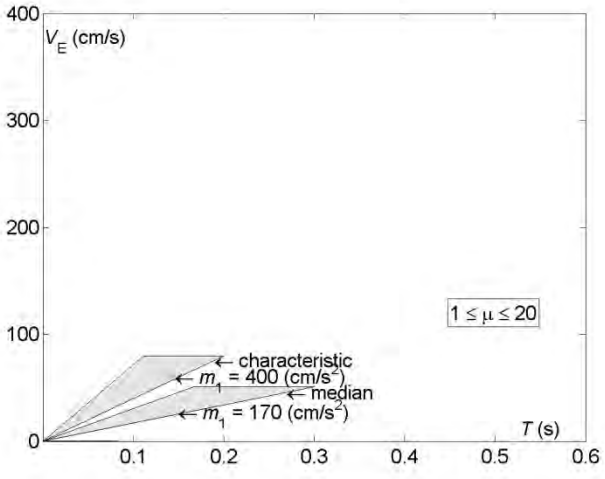

Figure 4-52 Initial branch of the nonlinear V_E spectra. Stiff soil. $M_s \leq 5.5$.Impulsive. $\zeta = 0.05$

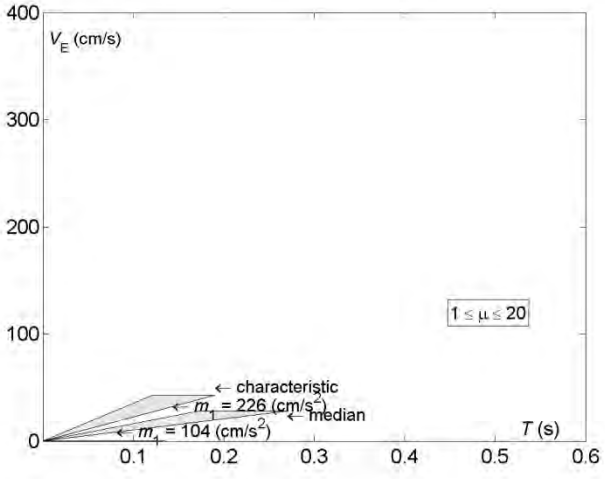

Figure 4-53 Initial branch of the nonlinear V_E spectra. Stiff soil. $M_s \leq 5.5$.Vibratory. $\zeta = 0.05$

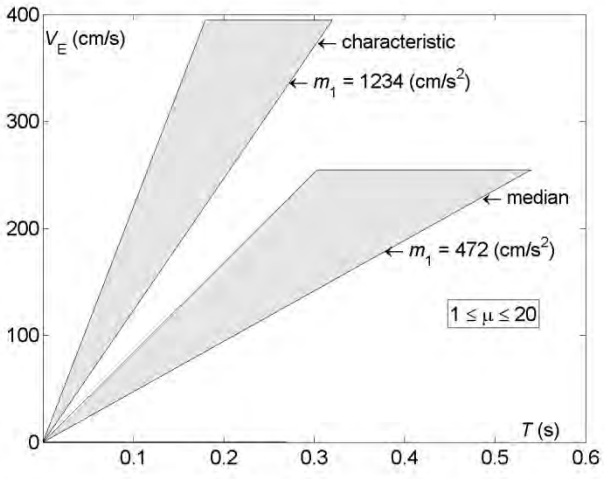

Figure 4-54 Initial branch of the nonlinear V_E spectra. Soft soil. $M_s > 5.5$. Impulsive. $\zeta = 0.05$

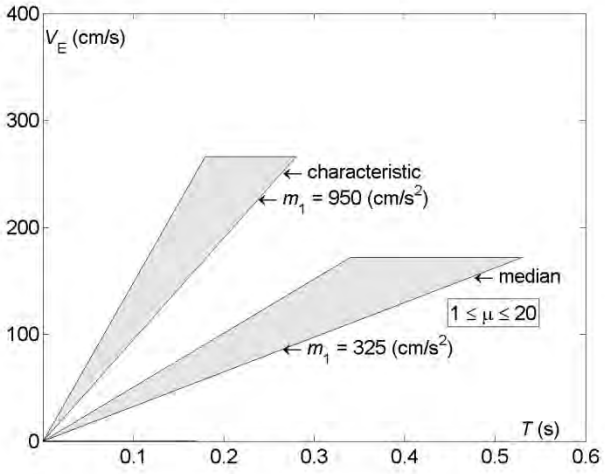

Figure 4-55 Initial branch of the nonlinear V_E spectra. Soft soil. M_s > 5.5. Vibratory. ζ = 0.05

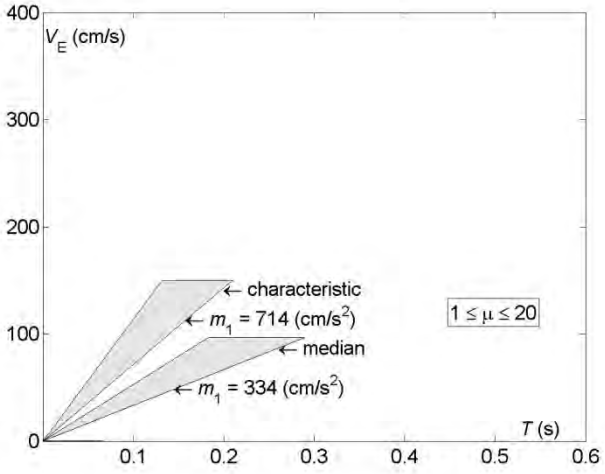

Figure 4-56 Initial branch of the nonlinear V_E spectra. Soft soil. $M_s \leq$ 5.5.Impulsive. ζ = 0.05

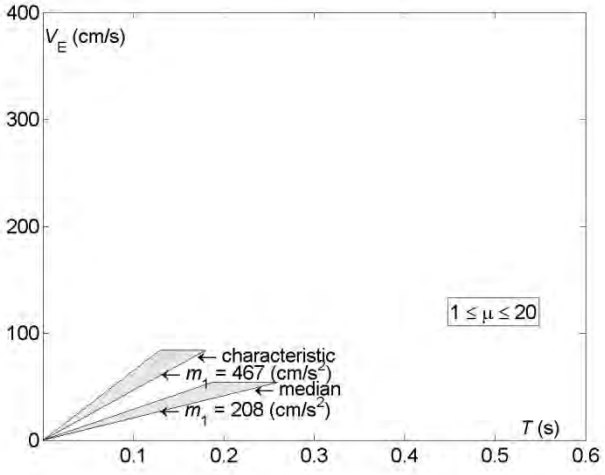

Figure 4-57 Initial branch of the nonlinear V_E spectra. Soft soil. $M_s \leq$ 5.5.Vibratory. ζ = 0.05

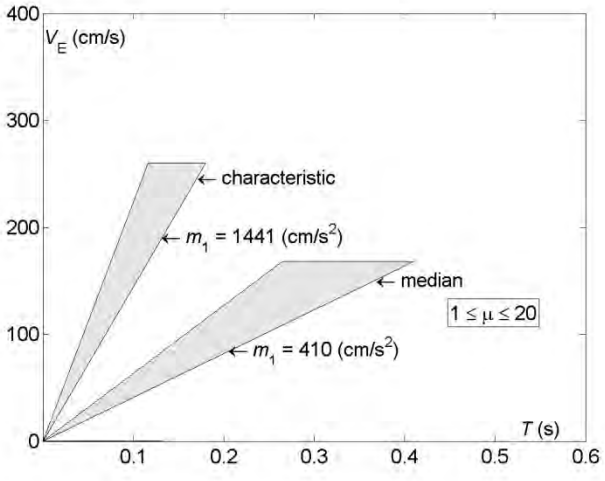

Figure 4-58 Initial branch of the nonlinear V_E spectra. Stiff soil. $M_s > 5.5$. Impulsive. $\zeta = 0.10$

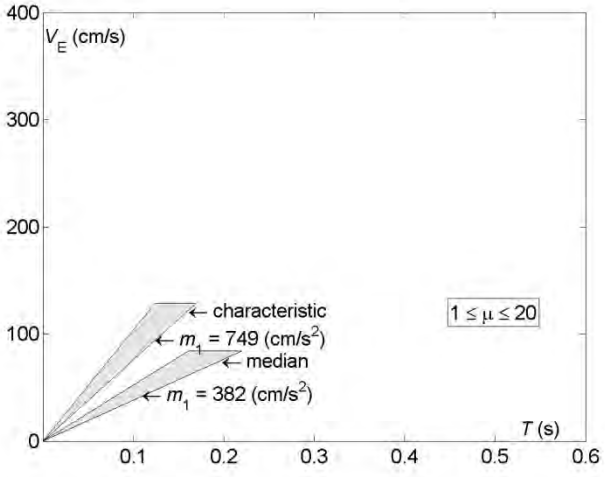

Figure 4-59 Initial branch of the nonlinear V_E spectra. Stiff soil. $M_s > 5.5$. Vibratory. $\zeta = 0.10$

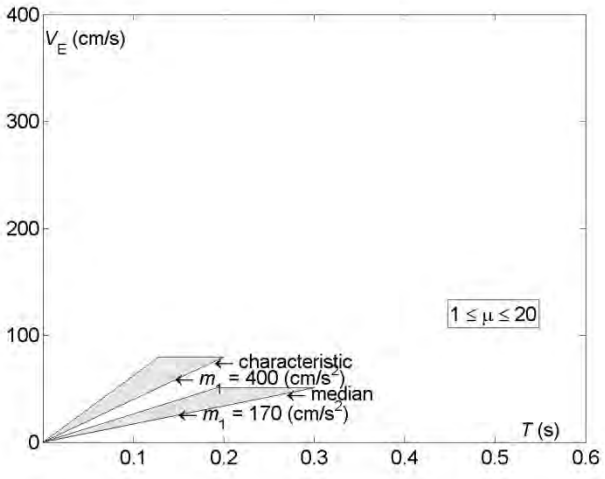

Figure 4-60 Initial branch of the nonlinear V_E spectra. Stiff soil. $M_s \leq 5.5$.Impulsive. $\zeta = 0.10$

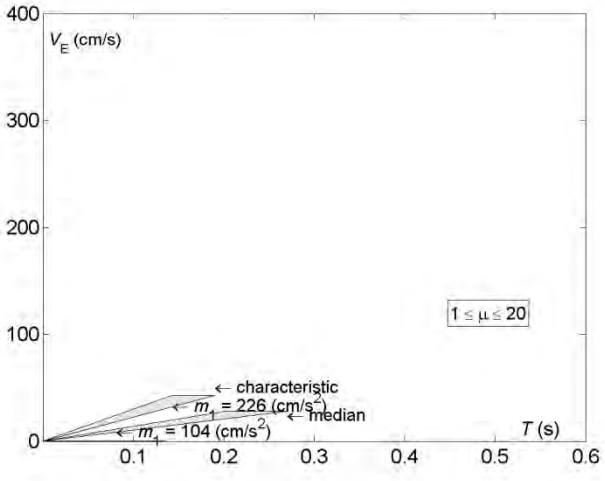

Figure 4-61 Initial branch of the nonlinear V_E spectra. Stiff soil. $M_s \le 5.5$.Vibratory. $\zeta = 0.10$

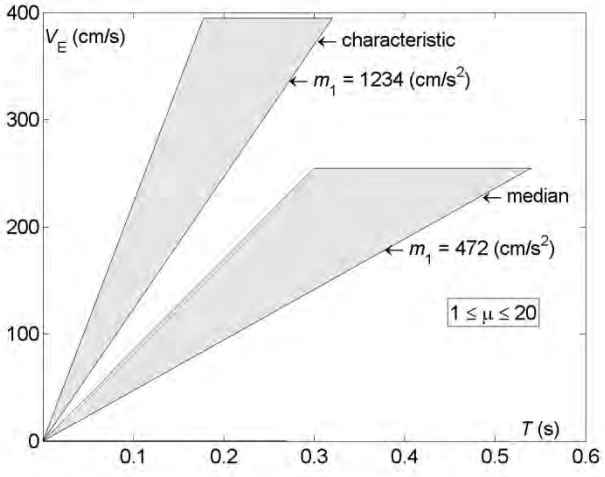

Figure 4-62 Initial branch of the nonlinear V_E spectra. Soft soil. $M_s > 5.5$. Impulsive. $\zeta = 0.10$

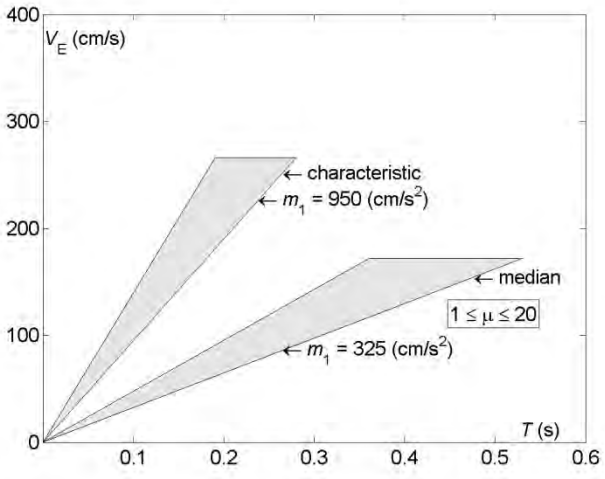

Figure 4-63 Initial branch of the nonlinear V_E spectra. Soft soil. $M_s > 5.5$. Vibratory. $\zeta = 0.10$

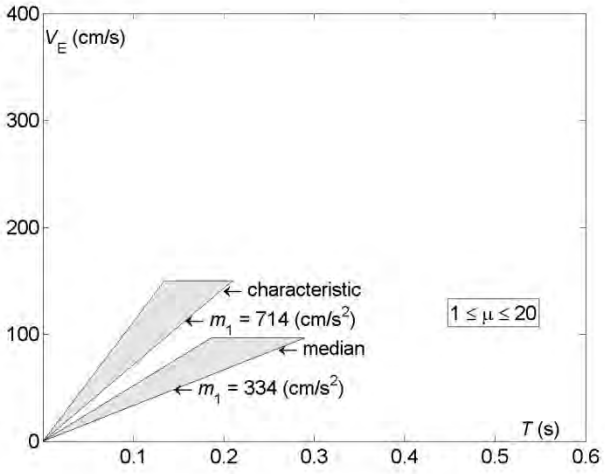

Figure 4-64 Initial branch of the nonlinear V_E spectra. Soft soil. $M_s \le 5.5$.Impulsive. $\zeta = 0.10$

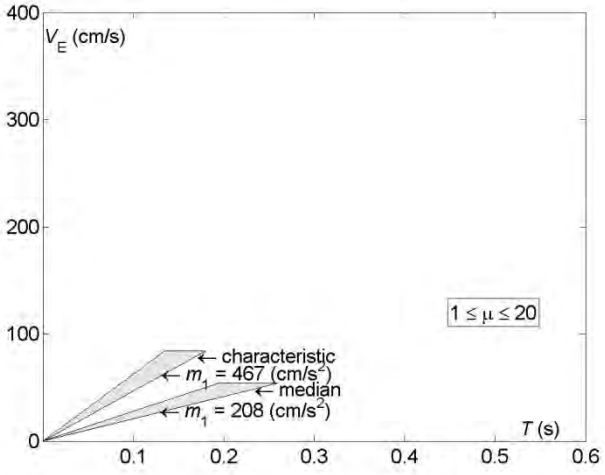

Figure 4-65 Initial branch of the nonlinear V_E spectra. Soft soil. $M_s \le 5.5$.Vibratory. $\zeta = 0.10$

5 Design hysteretic energy to input energy ratio V_D / V_E

5.1 Introductory remarks

The evaluation of the input energy E_I is an acceptable starting point to develop and to apply the seismic energy-based design methods; however, only the hysteretic energy E_H (which is alike to E_D, according to equation (2-17), is directly related to the seismic structural damage and, hence, it needs to be evaluated [Manfredi 2001]. Since V_D and E_H are directly related by equation (2-30), the estimation of the ratio V_D / V_E, after the non-linear analyses presented in section 4.3, is described in this section.

5.2 Previous studies

As discussed in section 2.2, V_D / V_E depends mainly on the structural damping and on the demanded ductility; the latter can be formulated in terms of the displacement ductility μ, or in terms of the cumulative ductility η:

$$\mu = \frac{y_{max}}{y_y} \qquad \eta = \frac{E_H}{Q_y\, y_y} \tag{5-1}$$

In equation (5-1), y_{max} is the maximum displacement and Q_y and y_y are the restoring force and the displacement at yielding, respectively. Several empirical equations have been proposed in the literature to estimate V_D / V_E. Based on analyses of SDOF systems with elastic-perfectly-plastic restoring force characteristics, Akiyama [1985] and Kuwamura and Galambos [1989] proposed, respectively, the following equations:

$$\frac{V_D}{V_E} = \frac{1}{1+3\zeta+1.2\sqrt{\zeta}} \qquad \frac{V_D}{V_E} = \frac{\sqrt{\frac{\eta}{\eta+0.15}}}{1+\frac{20(3\zeta+1.2\sqrt{\zeta})}{\eta+10}} \tag{5-2}$$

Benavent et al. [2002, 2010] suggested, respectively, the following modifications of Akiyama's equation (5-2) to account for the level of plastification:

$$\frac{V_D}{V_E} = \frac{1.15\eta}{(0.75+\eta)(1+3\zeta+1.2\sqrt{\zeta})} \qquad \frac{V_D}{V_E} = \frac{1}{\sqrt{1+4\pi\zeta\, n}}\frac{\eta^c}{(8.75\zeta+k^c+\eta^c)} \tag{5-3}$$

In the last equation (5-3), n, k and c are dimensionless coefficients whose values are n = 0.9, k = 0.33 and c = 0.57 for rock, and n = 0.15, k = 0.02 and c = 0.37 for soil.

From parametric studies with non-linear elastic-perfectly-plastic SDOF systems, Fajfar and Vidic [1994] proposed an expression valid for systems with ζ = 0.05:

Lawson and Krawinkler [1995] confirmed that V_D / V_E constitutes a highly stable parameter, and proposed adopting $V_D / V_E = 0.63$ for $\mu = 2$ and $V_D / V_E = 0.77$ for $4 \leq \mu \leq 8$, except for the shortest periods. Decanini and Mollaioli [2001] investigated the ratio $E_H / E_{I,abs}$ in relation with the period T, the type of soil, and the ductility μ for elastic-perfectly-plastic SDOF systems with $\zeta = 5\%$; Although Akiyama used the relative input energy and Decanini and Mollaioli the absolute input energy, the design values of the ratio of hysteretic energy to total input energy proposed by both approaches can be compared. Decanini and Mollaioli investigated also the effects of the hysteretic model, the vibration period, and the soil type.

5.3 Influence of damping and ductility

In this study, the registers have been classified in the aforementioned eight groups, depending on the soil type, the earthquake magnitude and the relevance of the velocity pulses (section 3.5); mainly for this reason, a new empirical approximation of V_D / V_E whose parameters take into account this diversity is proposed. This expression is intended to be used together with the spectra proposed in chapter 4. To obtain the new approximation of V_D / V_E, the linear and nonlinear analyses carried out in section 4.3 are examined; three major conclusions are derived: (i) the results for seismic zones 1 and 2 are similar, (ii) the results for $M_s > 5.5$ and for $M_s \leq 5.5$ are rather equivalent, and, (iii) no significant changes occur for $\eta > 150$. This value of η is very large for a plastic hinge developped at the end of a beam of a typical reinforced concrete or even a steel frame structure, but it is a realistic value for special devices such as hysteretic-type energy dissipators. These observations indicate that the results of the analyses should be grouped only according to the soil type and to the earthquake magnitude and that only the points corresponding to $0 < \eta < 150$ are of interest. Figure 5-1 to Figure 5-12 display the relationship between V_D / V_E and the cumulative ductility η, for stiff and soft soil, and for different damping ratios ζ; Figure 5-1 to Figure 5-6 correspond to impulsive registers while Figure 5-7 to Figure 5-12 correspond to vibratory ones. Every point in Figure 5-1 to Figure 5-12 corresponds to a spectral ordinate obtained from the NS and EW, linear and nonlinear analyses performed in chapter 4 for the registers in Table 3-1; equation (5-1) shows that in the linear analyses $\eta = 0$ while in the nonlinear analyses $\eta \neq 0$. Also plotted in Figure 5-1 to Figure 5-12 are the upper and lower bounds proposed in [Lawson, Krawinkler 1995] and in equations (5-2) and (5-3).

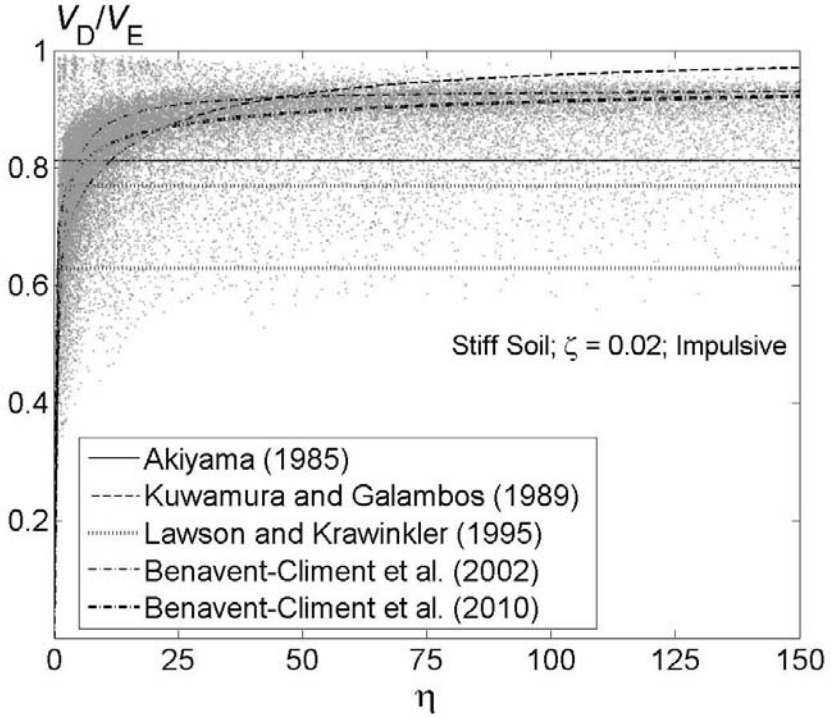

Figure 5-1 Ratio V_D / V_E for impulsive registers. Stiff soil. $\zeta = 0.02$

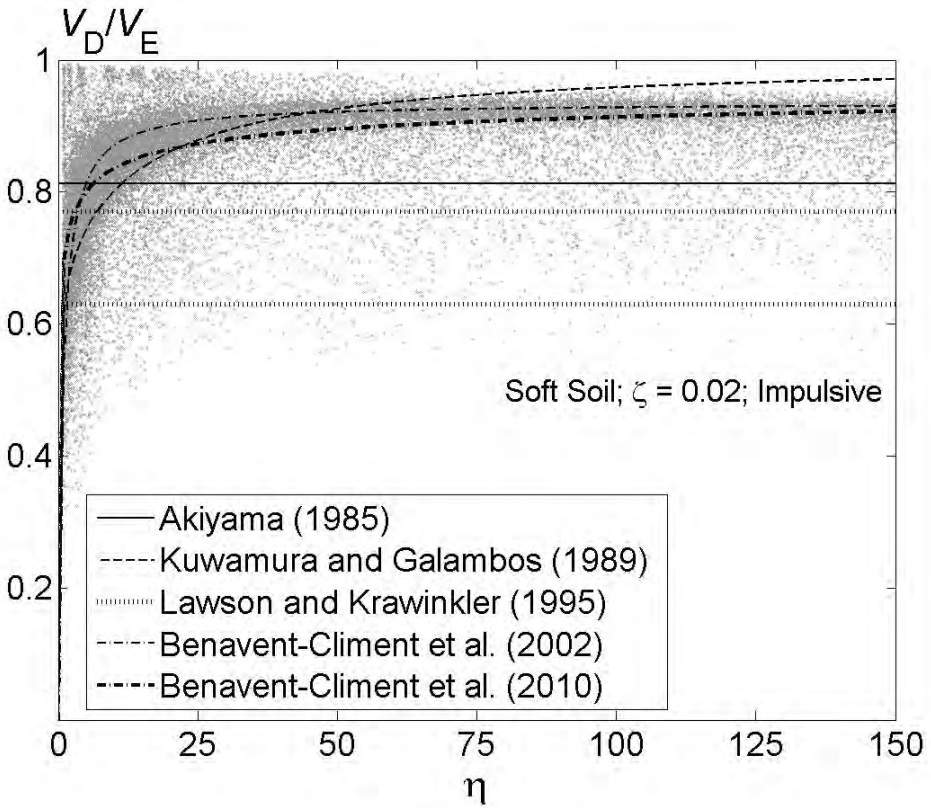

Figure 5-2 Ratio V_D / V_E for impulsive registers. Soft soil. ζ = 0.02

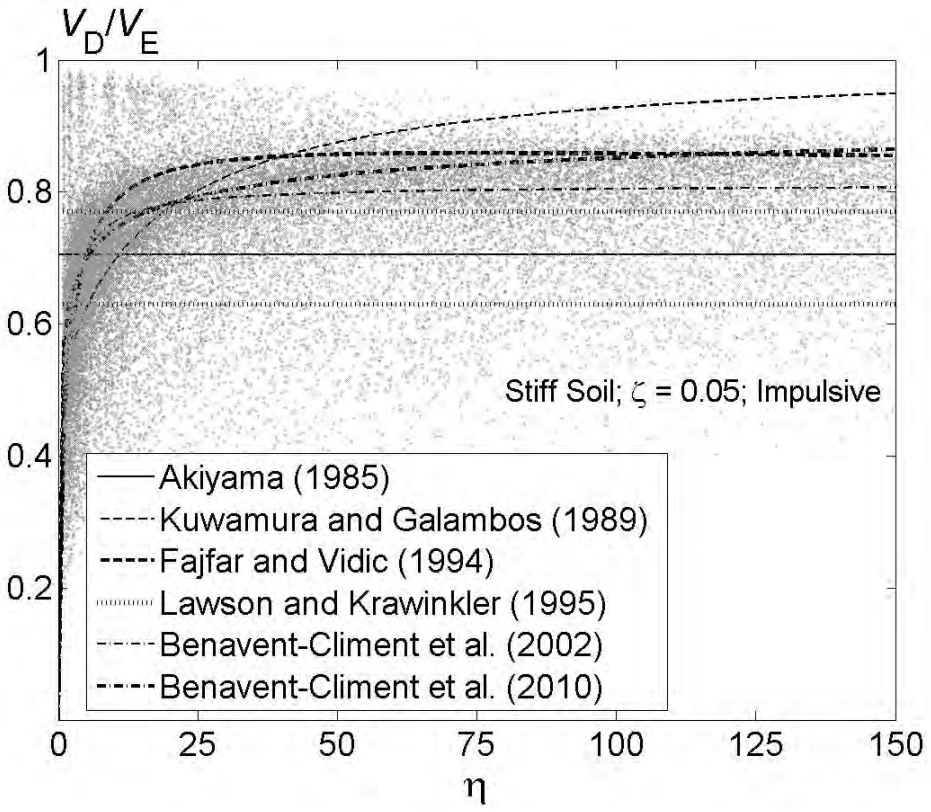

Figure 5-3 Ratio V_D / V_E for impulsive registers. Stiff soil. ζ = 0.05

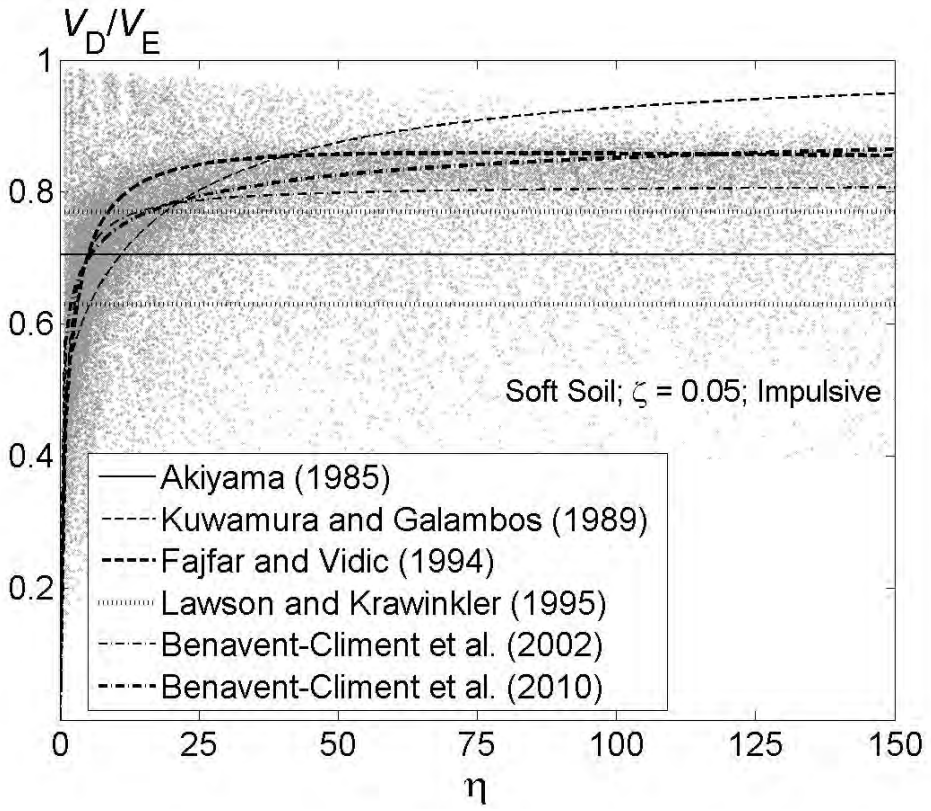

Figure 5-4 Ratio V_D / V_E for impulsive registers. Soft soil. ζ = 0.05

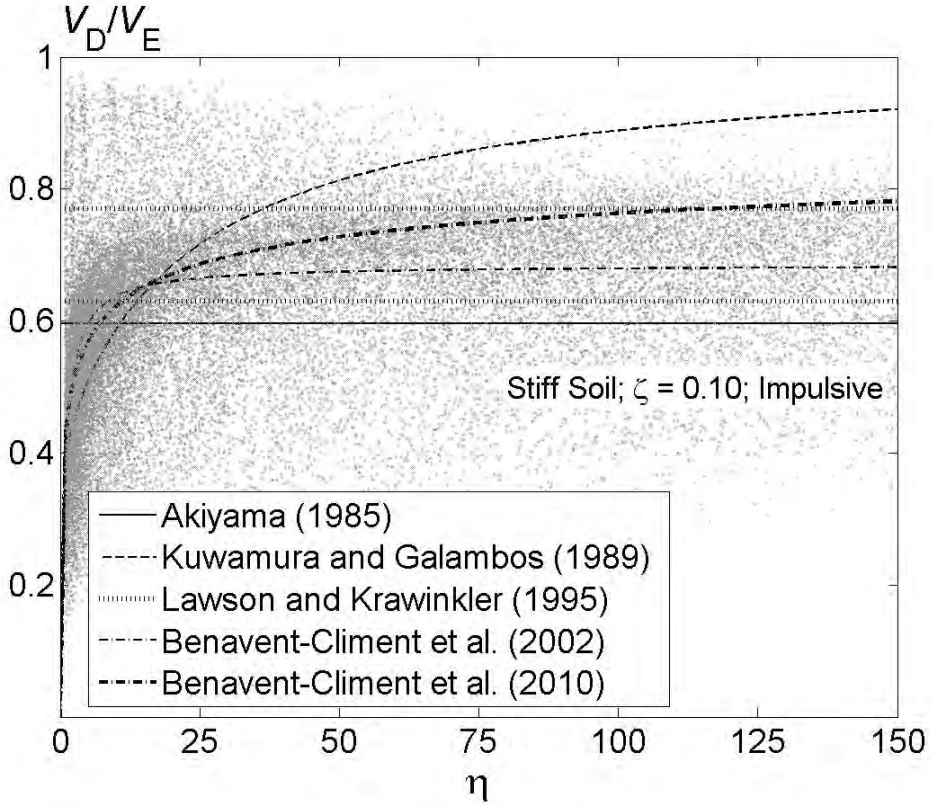

Figure 5-5 Ratio V_D / V_E for impulsive registers. Stiff soil. ζ = 0.10

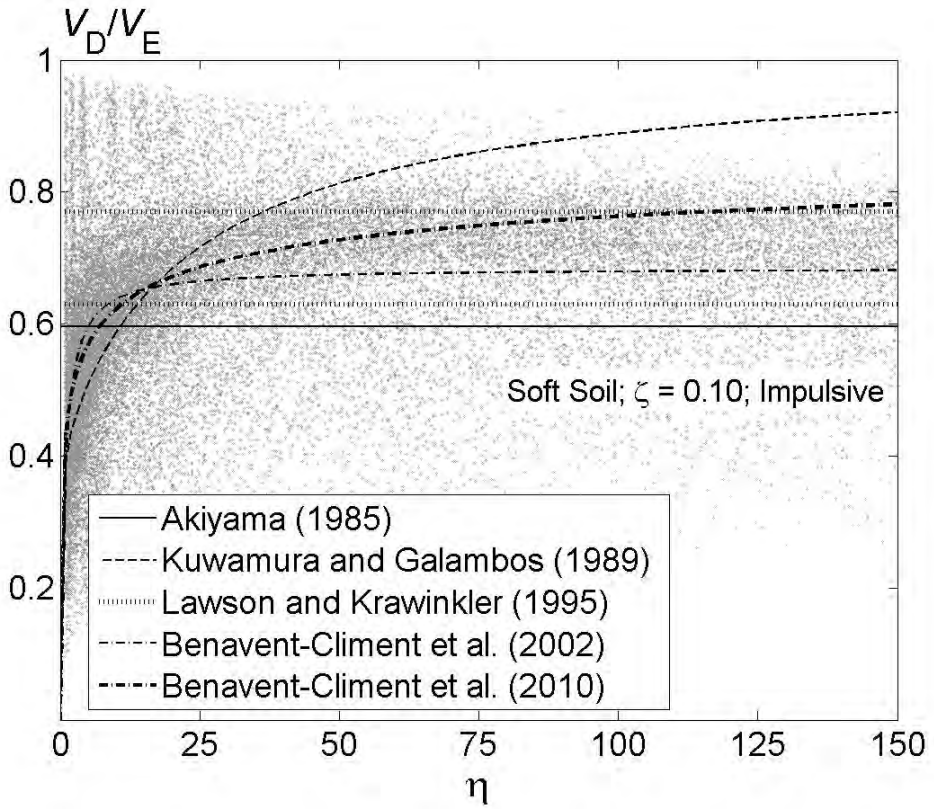

Figure 5-6 Ratio V_D / V_E for impulsive registers. Soft soil. ζ = 0.10

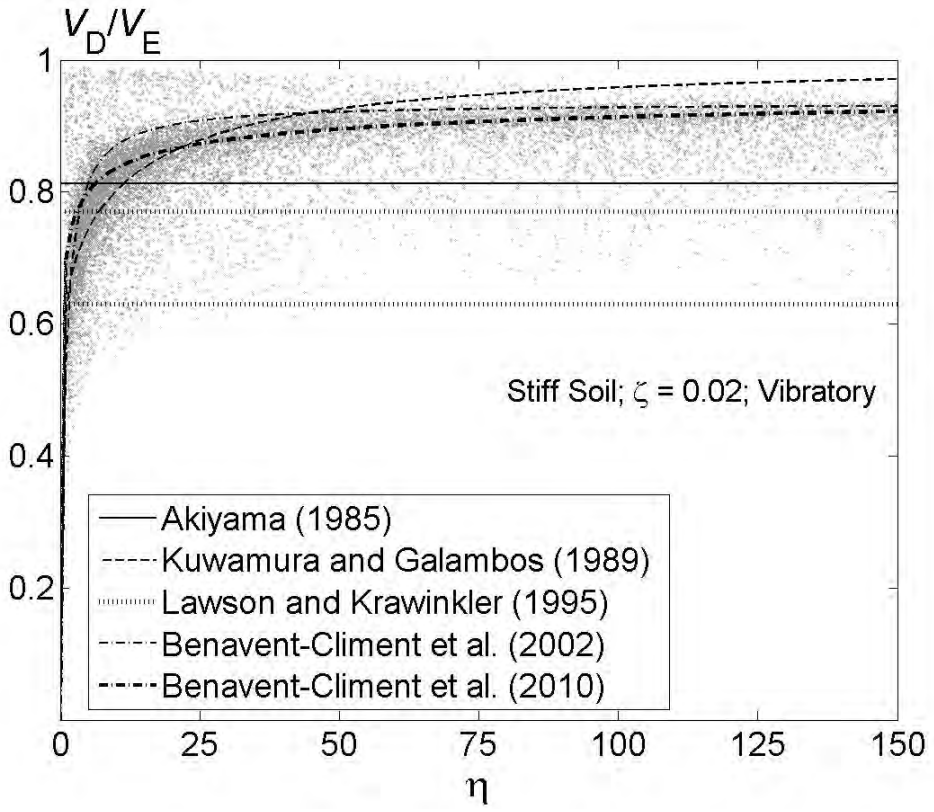

Figure 5-7 Ratio V_D / V_E for vibratory registers. Stiff soil. ζ = 0.02

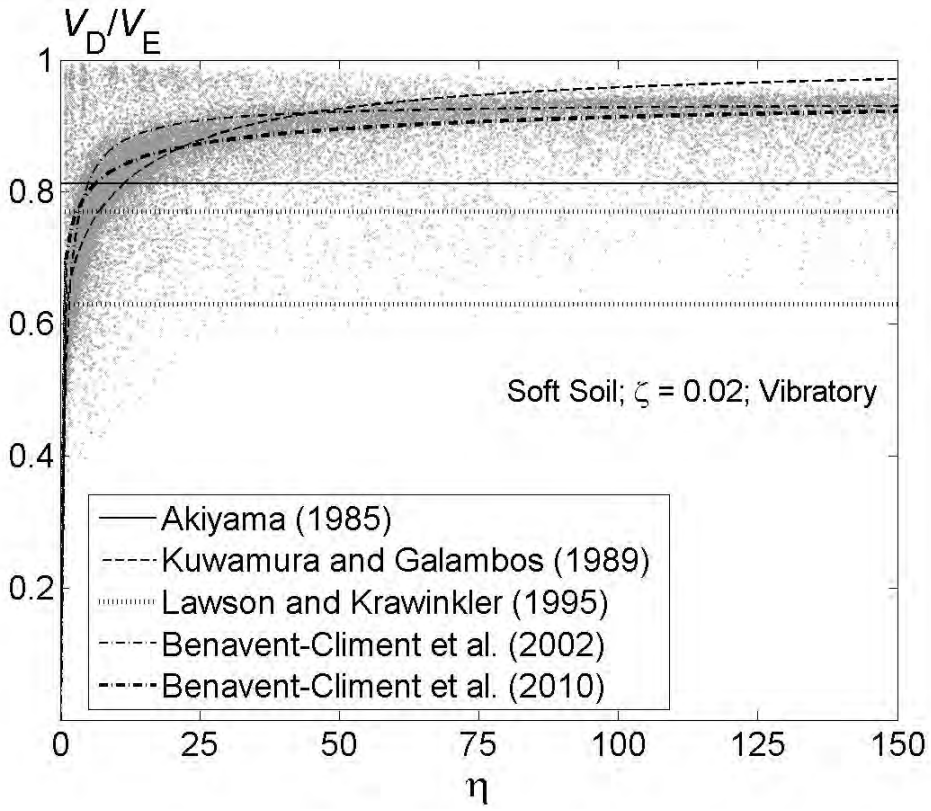

Figure 5-8 Ratio V_D / V_E for vibratory registers. Soft soil. ζ = 0.02

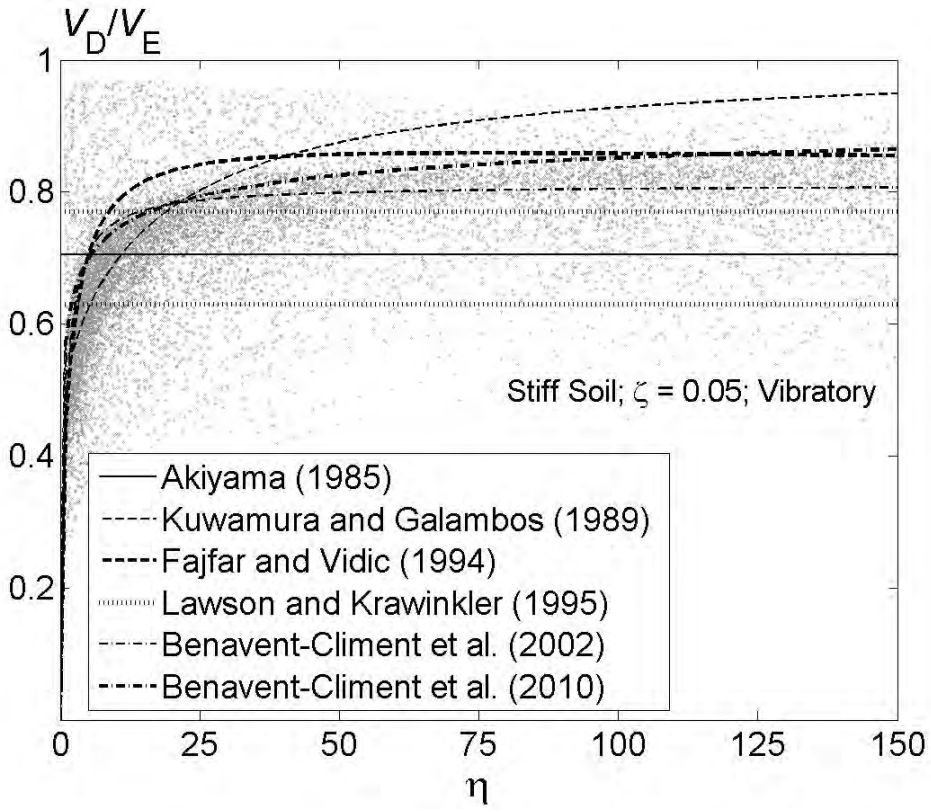

Figure 5-9 Ratio V_D / V_E for vibratory registers. Stiff soil. ζ = 0.05

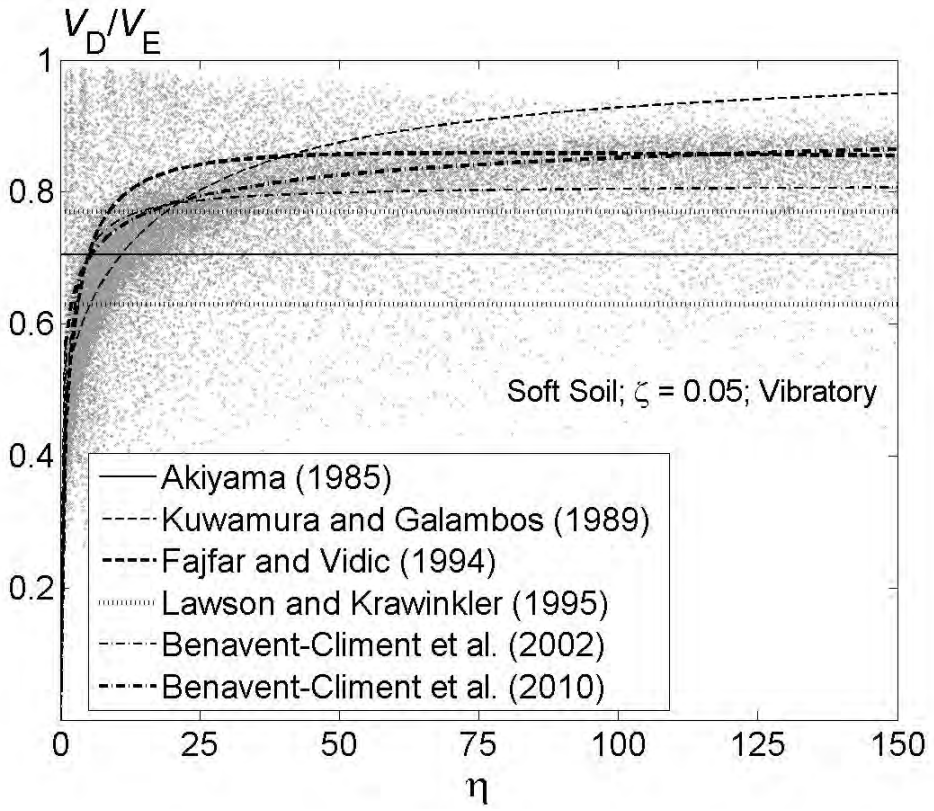

Figure 5-10 Ratio V_D / V_E for vibratory registers. Soft soil. ζ = 0.05

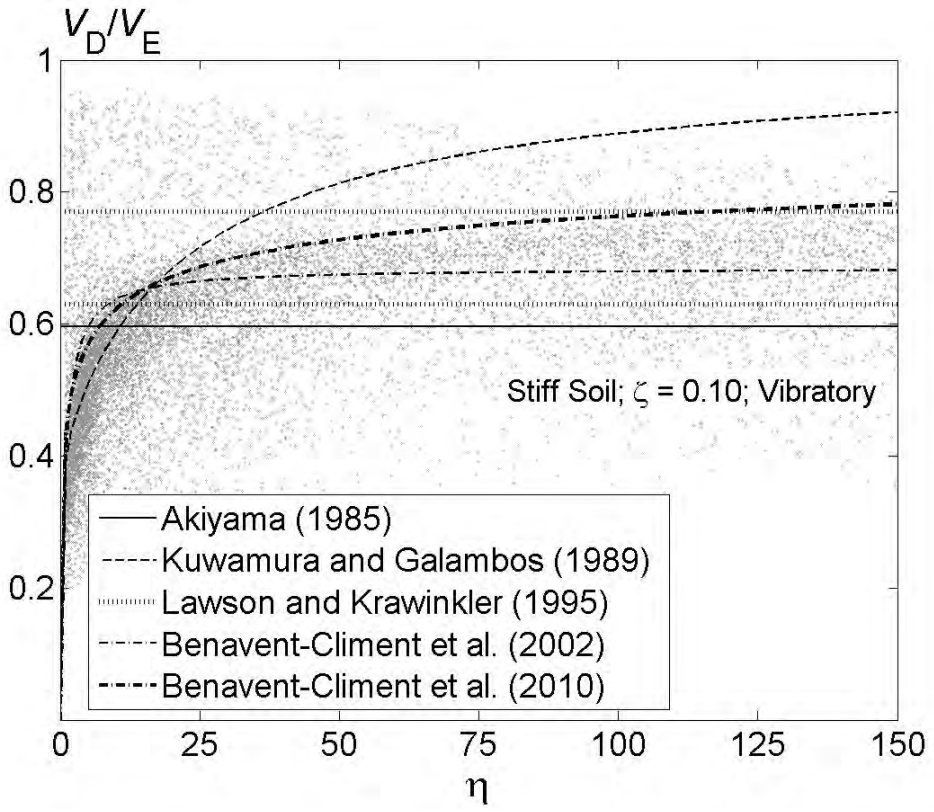

Figure 5-11 Ratio V_D / V_E for vibratory registers. Stiff soil. ζ = 0.02

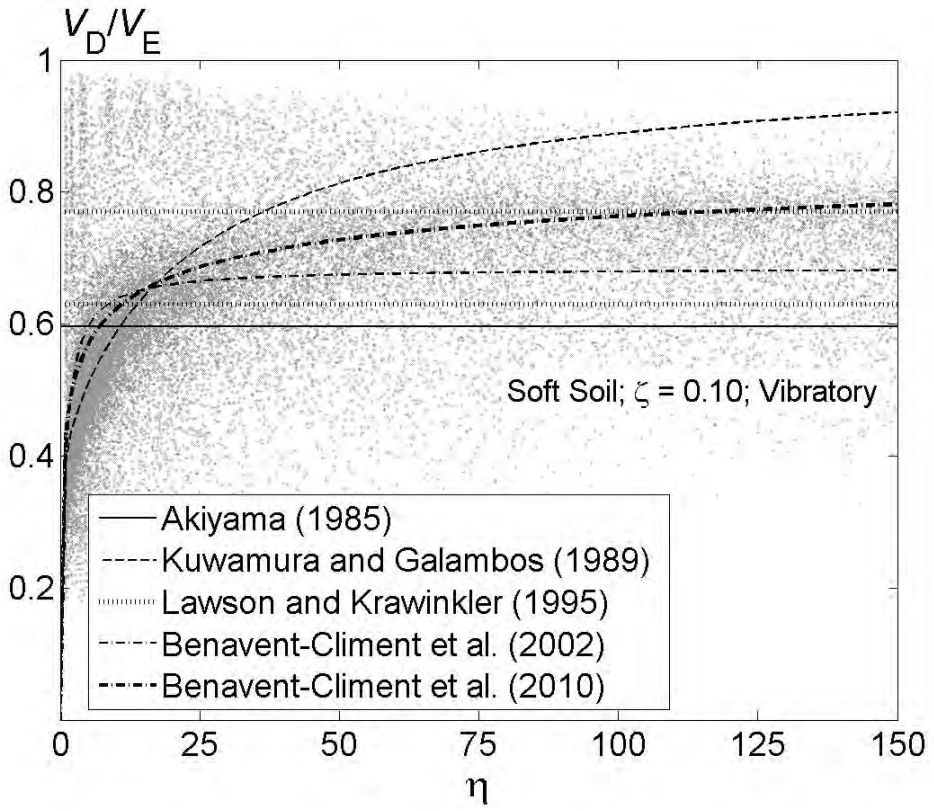

Figure 5-12 Ratio V_D / V_E for vibratory registers. Soft soil. $\zeta = 0.10$

The observation of Figure 5-1 to Figure 5-12 shows that the agreement among the obtained points and the previously suggested fits is reasonable, particularly in the latest study by Benavent et al. [2010]. However, the fit can be further improved and, moreover, none of the previous studies has discussed deeply the influence of soil type, earthquake magnitude, velocity pulses and period; for this reason, another fitting criterion is proposed in this paper. To derive such criterion, Figure 5-13 to Figure 5-44 show the obtained points for damping 2%, 5% and 10%, respectively. Such points are plotted together with the best fit curve using a two-term exponential expression:

$$\frac{V_D}{V_E} = a e^{b\eta} + c e^{d\eta} \tag{5-4}$$

This expression is chosen given its suitability of the characteristics of the clouds of points to be fitted. In the second term of equation (5-4) coefficients *c* ("amplitude") and *d* ("exponent") are intended to be negative and provide the trend of the fitting curves to be horizontal for $\eta > 100$; in the first term amplitude *a* is positive and exponent *b* can be either negative or positive. The absolute values of the exponent *b* are significantly smaller than those of *d* while this trend is inverted for the amplitudes. Roughly, the first term governs the behavior for small values of η while the second term controls the values for higher values of η.

Table 5-1 shows the values of the coefficients *a*, *b*, *c* and *d* that provide the best fit in the sense of the least value of the sum of the squares of the differences between the ordinates of the obtained points and those of the fitting curves. For better clarity, Figure 5-46 to Figure 5-48 display the fitted curves for all the considered damping ratios.

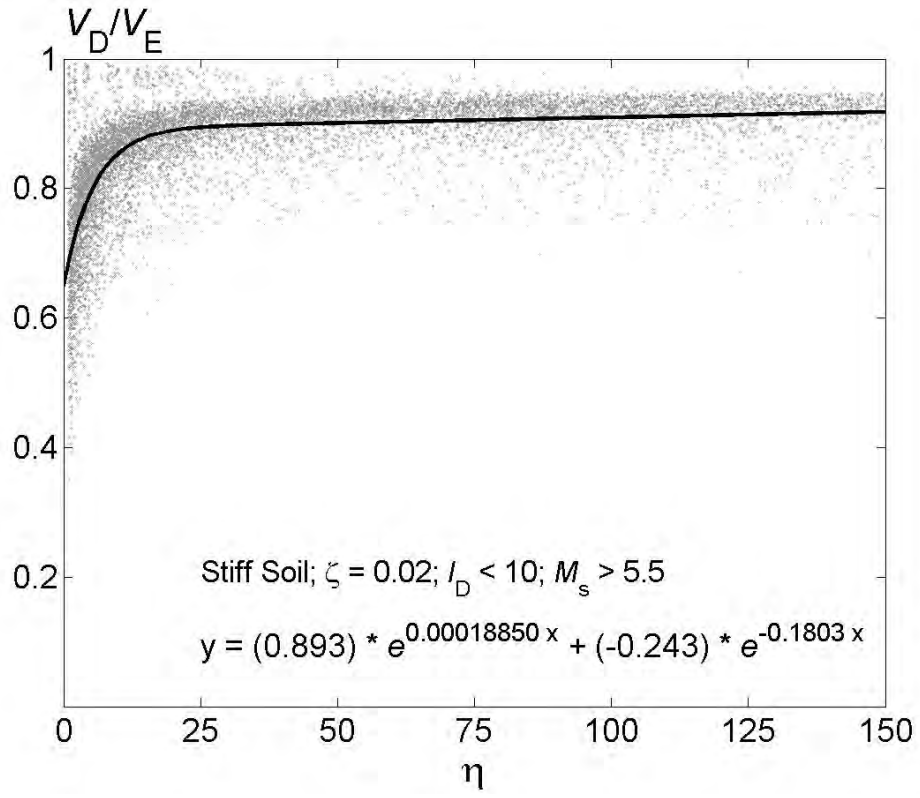

Figure 5-13 Proposed empirical approximations of the ratio V_D / V_E for damping ζ = 0.02. Stiff soil. M_s > 5.5. Impulsive

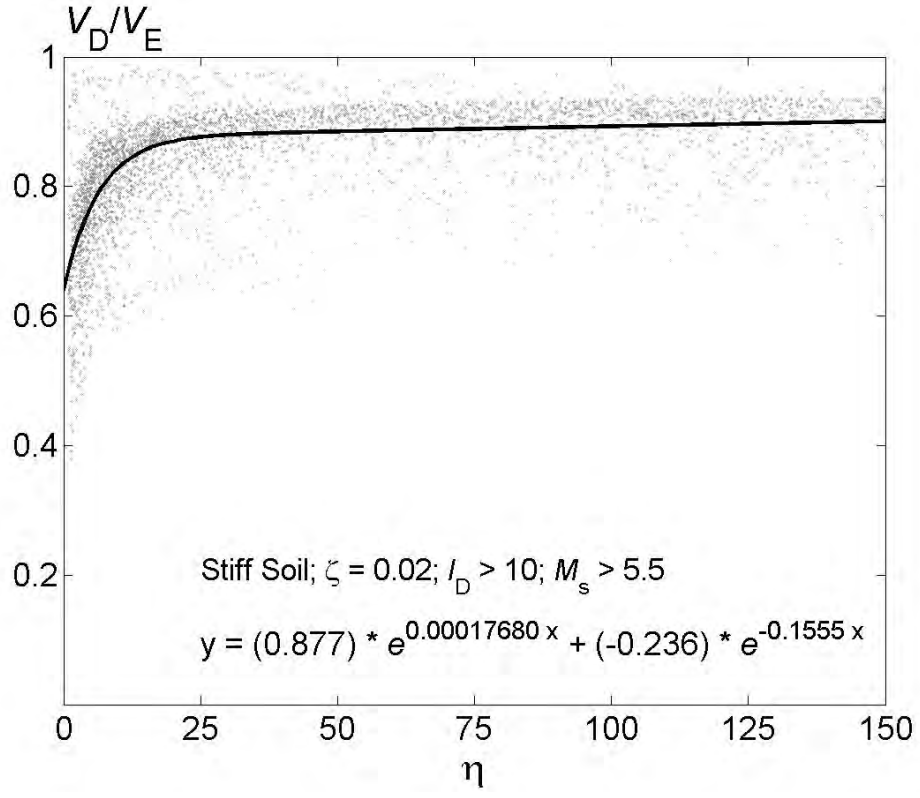

Figure 5-14 Proposed empirical approximations of the ratio V_D / V_E for damping ζ = 0.02. Stiff soil. M_s > 5.5. Vibratory

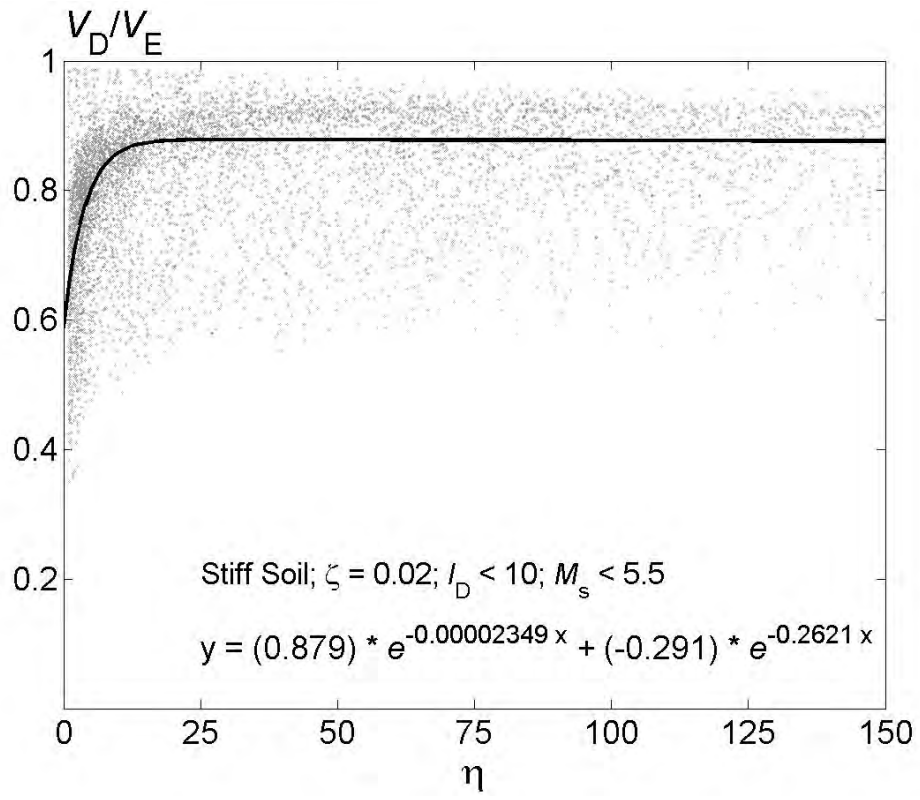

Figure 5-15 Proposed empirical approximations of the ratio V_D / V_E for damping ζ = 0.02. Stiff soil. $M_s \leq$ 5.5. Impulsive

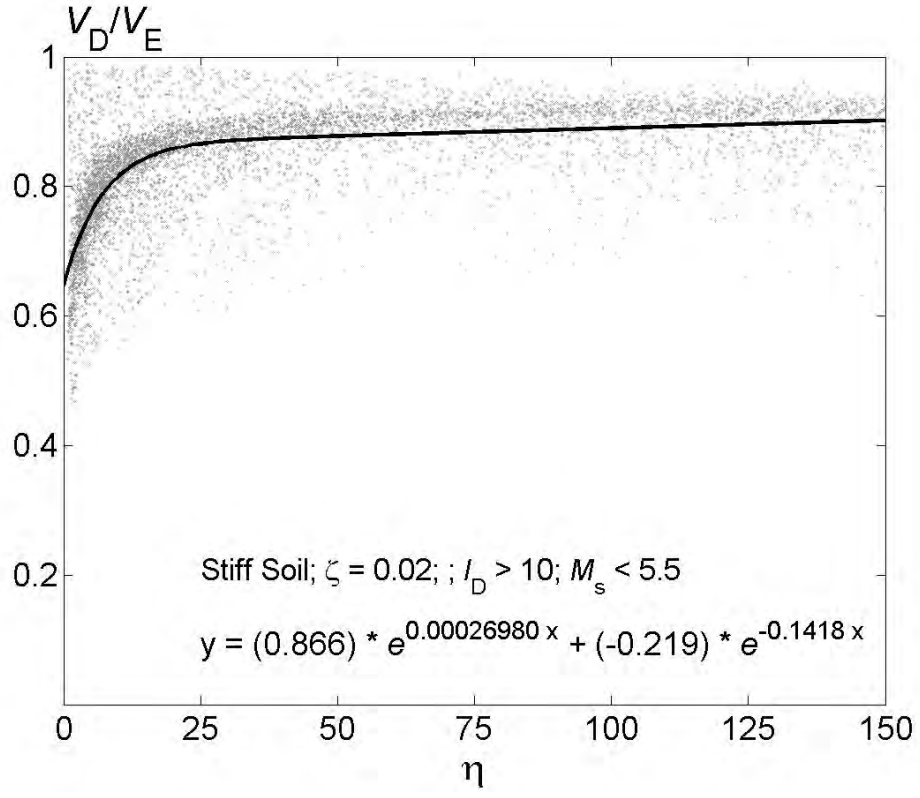

Figure 5-16 Proposed empirical approximations of the ratio V_D / V_E for damping ζ = 0.02. Stiff soil. $M_s \leq$ 5.5. Vibratory

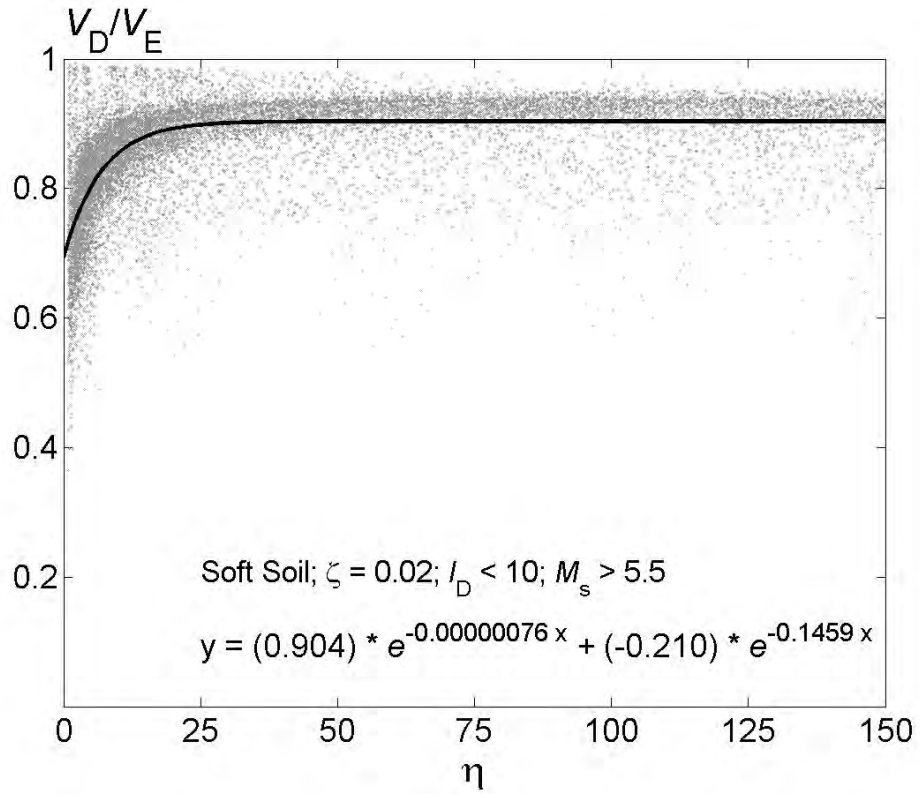

Figure 5-17 Proposed empirical approximations of the ratio V_D / V_E for damping ζ = 0.02. Soft soil. M_s > 5.5. Impulsive

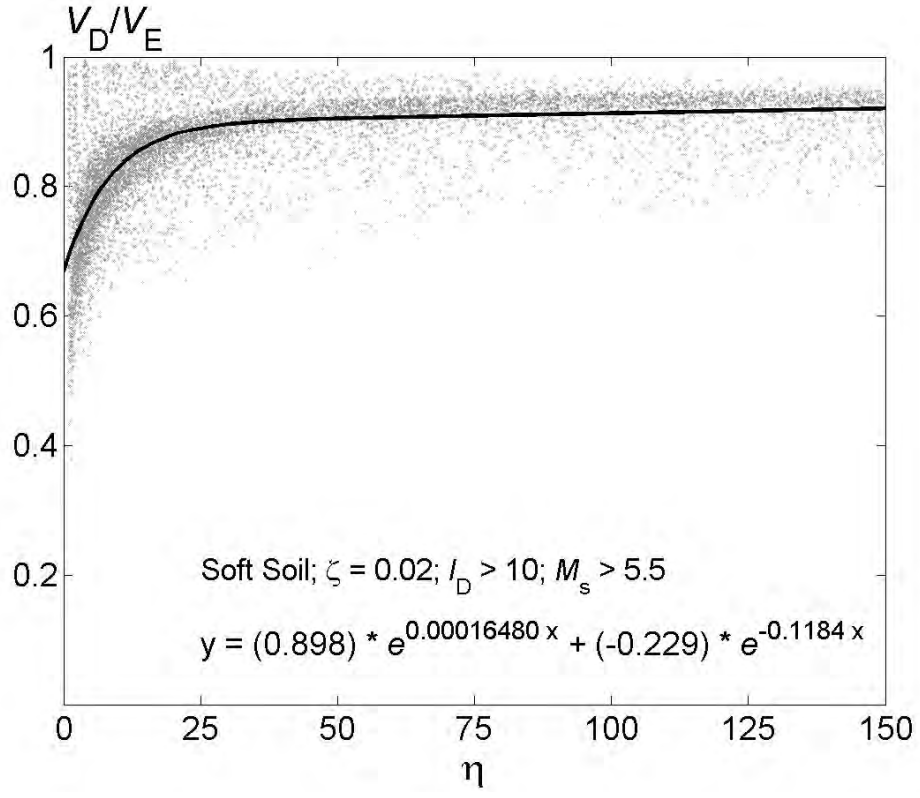

Figure 5-18 Proposed empirical approximations of the ratio V_D / V_E for damping ζ = 0.02. Soft soil. M_s > 5.5. Vibratory

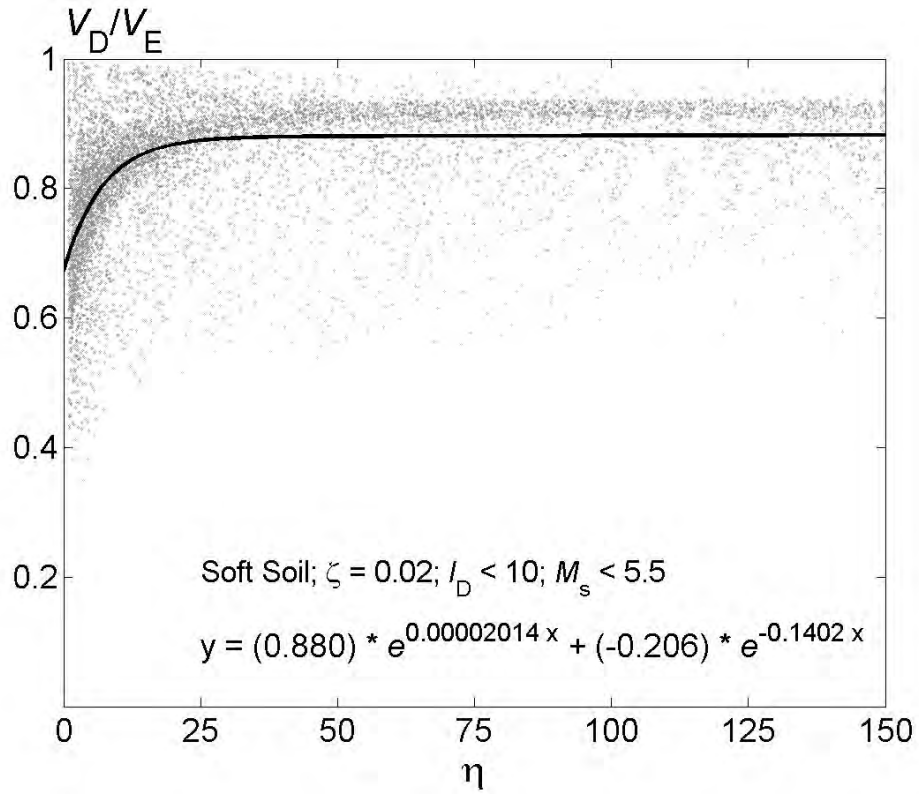

Figure 5-19 Proposed empirical approximations of the ratio V_D / V_E for damping ζ = 0.02. Soft soil. $M_s \leq$ 5.5. Impulsive

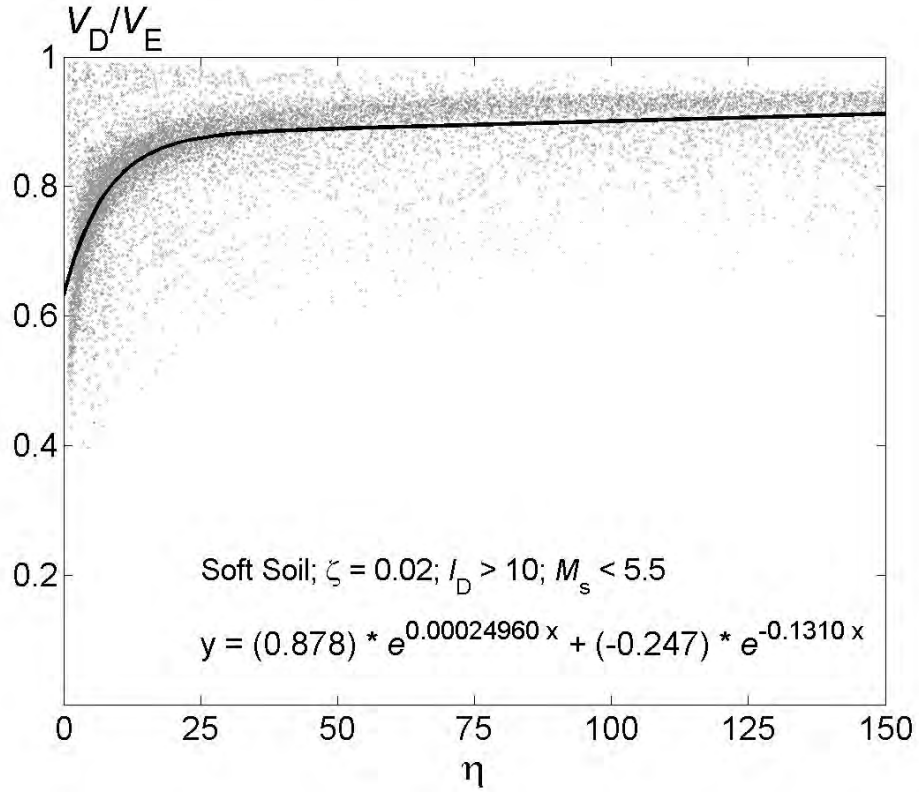

Figure 5-20 Proposed empirical approximations of the ratio V_D / V_E for damping ζ = 0.02. Soft soil. $M_s \leq$ 5.5. Vibratory

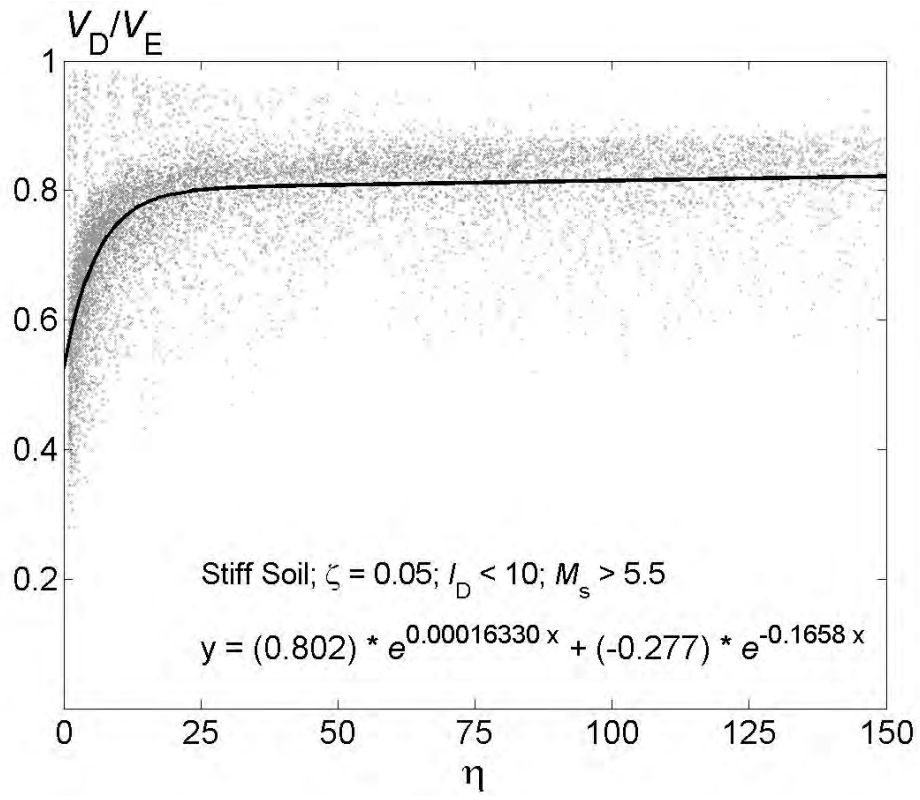

Figure 5-21 Proposed empirical approximations of the ratio V_D / V_E for damping ζ = 0.05. Stiff soil. M_s > 5.5. Impulsive

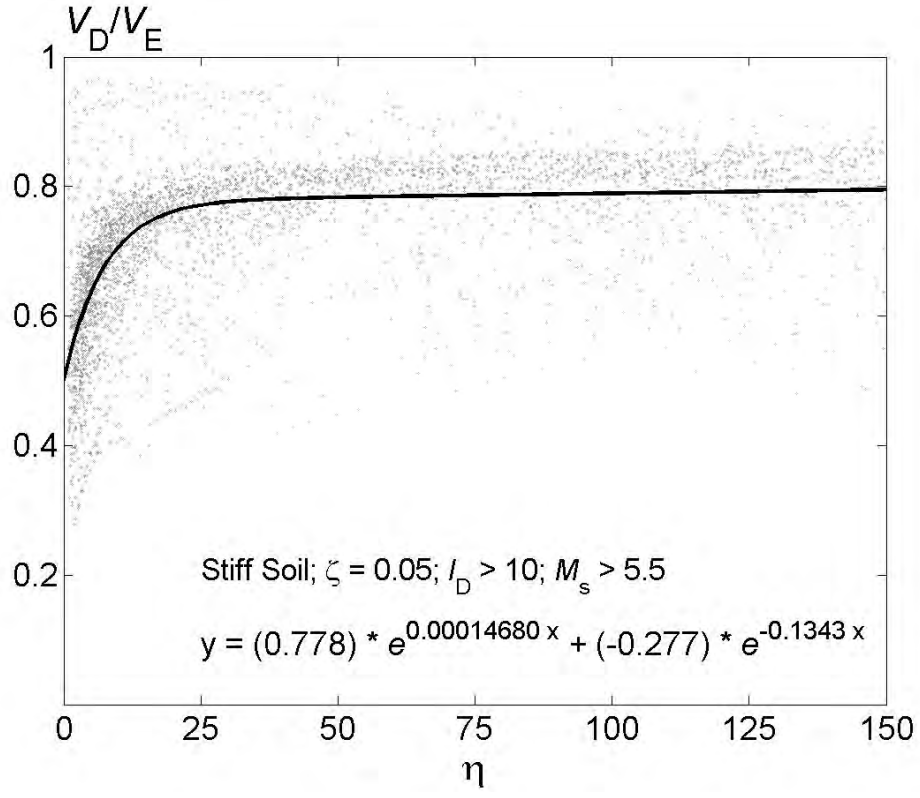

Figure 5-22 Proposed empirical approximations of the ratio V_D / V_E for damping ζ = 0.05. Stiff soil. M_s > 5.5. Vibratory

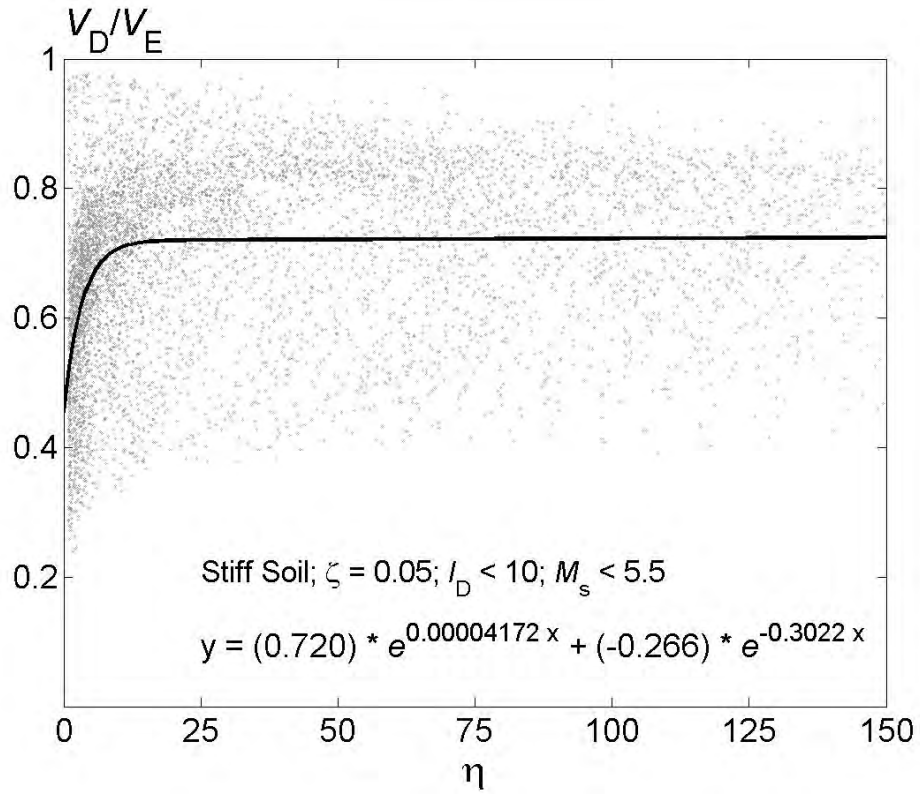

Figure 5-23 Proposed empirical approximations of the ratio V_D / V_E for damping ζ = 0.05. Stiff soil. $M_s \leq$ 5.5. Impulsive

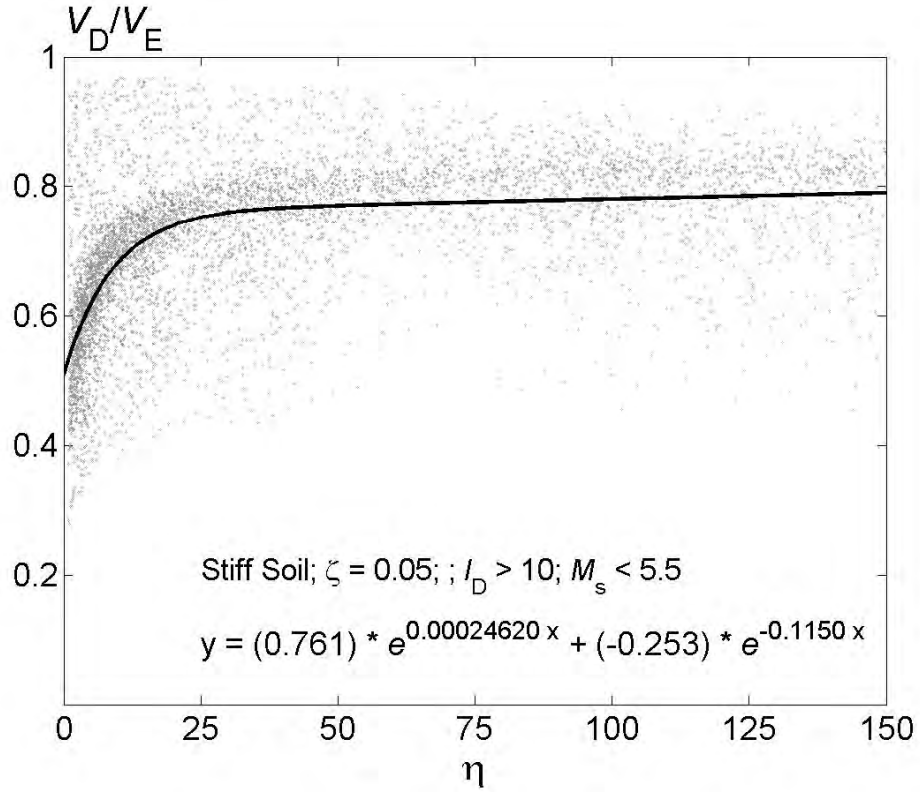

Figure 5-24 Proposed empirical approximations of the ratio V_D / V_E for damping ζ = 0.05. Stiff soil. $M_s \leq$ 5.5. Vibratory

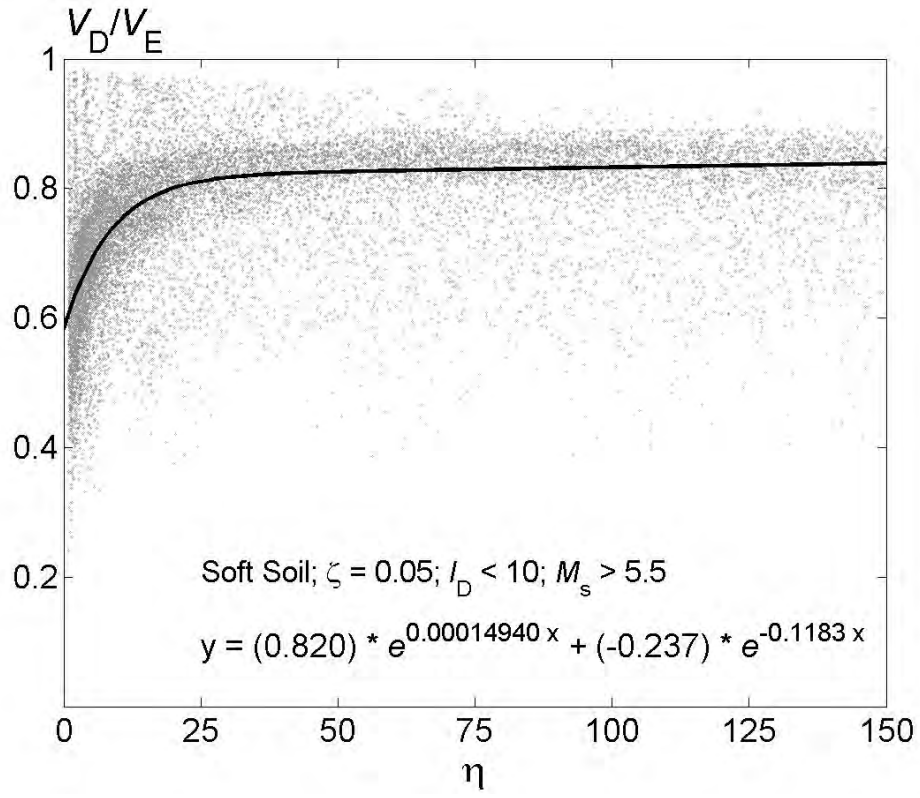

Figure 5-25 Proposed empirical approximations of the ratio V_D / V_E for damping ζ = 0.05. Soft soil. M_s > 5.5. Impulsive

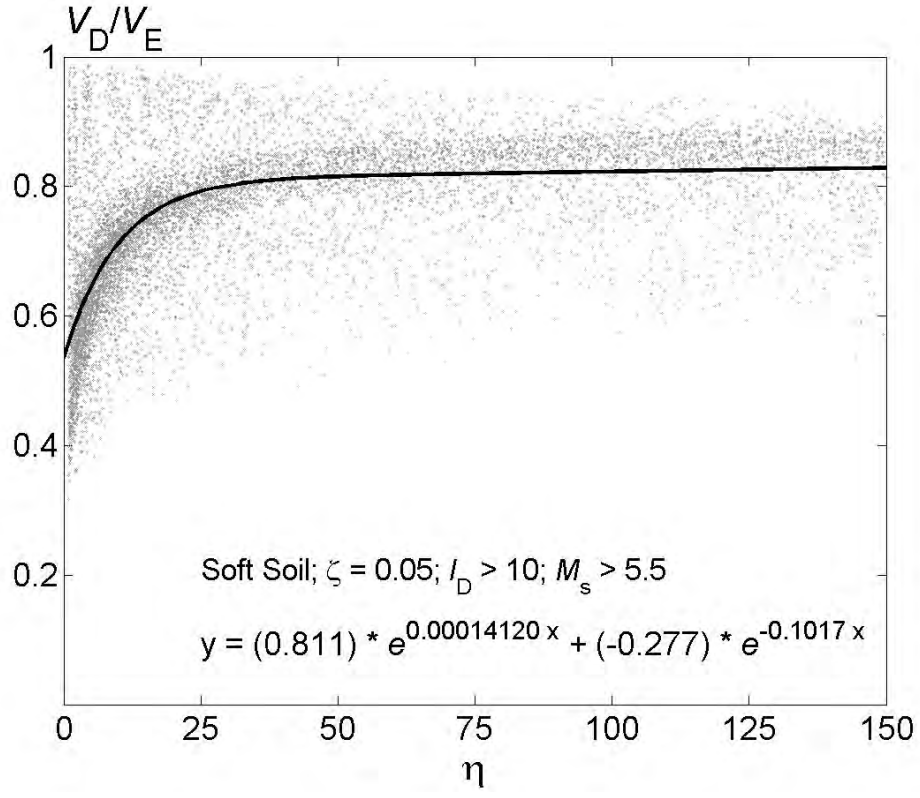

Figure 5-26 Proposed empirical approximations of the ratio V_D / V_E for damping ζ = 0.05. Soft soil. M_s > 5.5. Vibratory

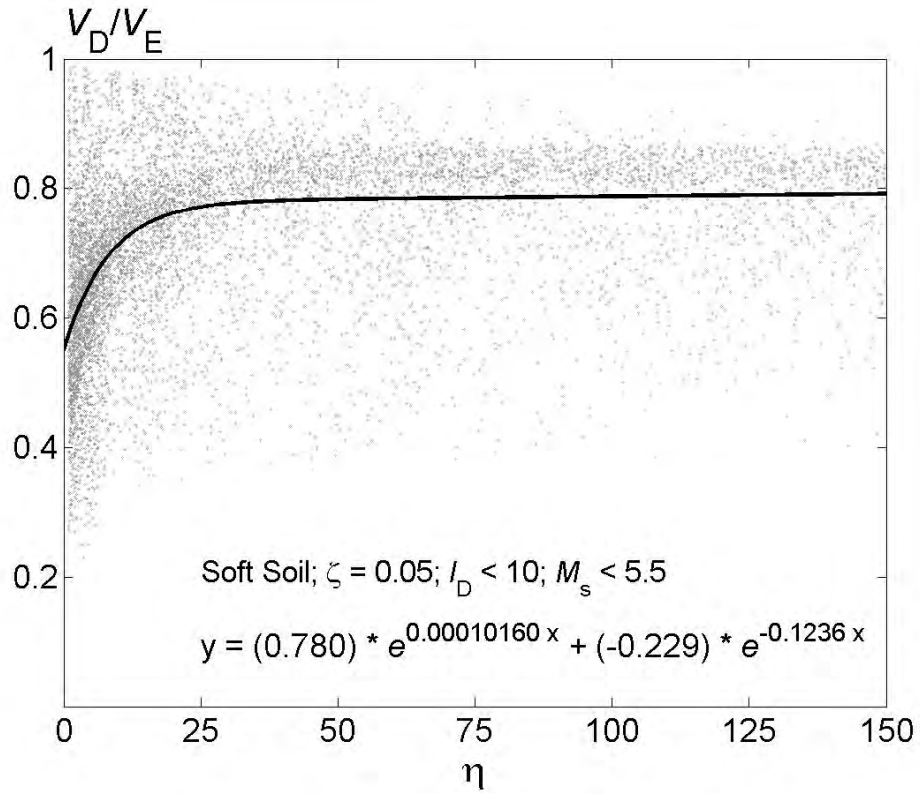

Figure 5-27 Proposed empirical approximations of the ratio V_D / V_E for damping ζ = 0.05. Soft soil. $M_s \leq$ 5.5. Impulsive

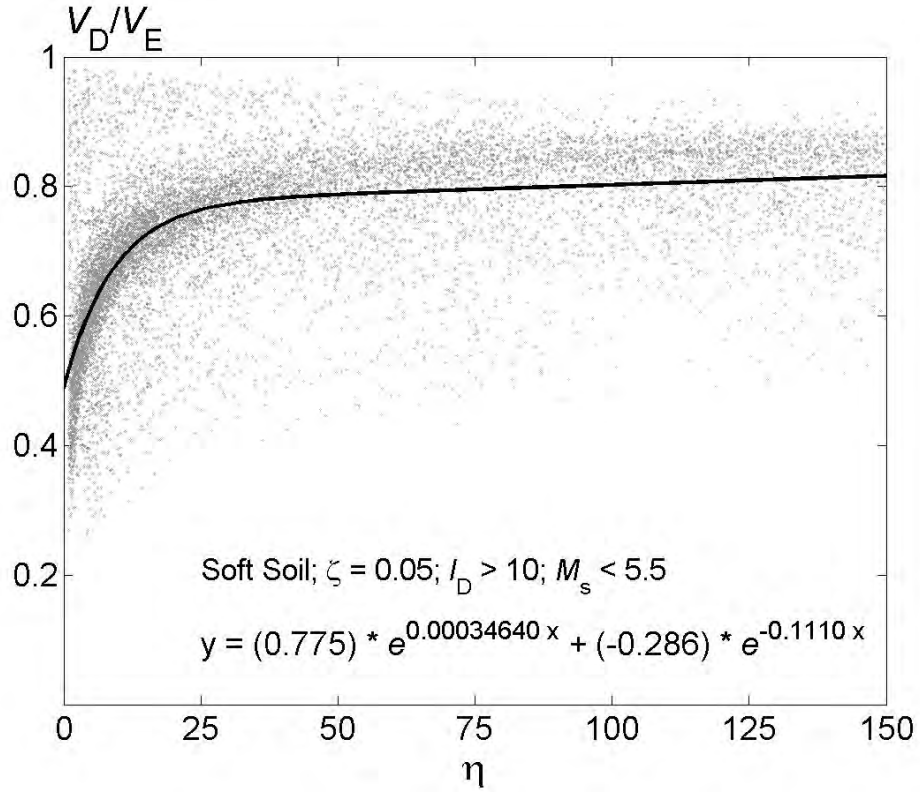

Figure 5-28 Proposed empirical approximations of the ratio V_D / V_E for damping ζ = 0.05. Soft soil. $M_s \leq$ 5.5. Vibratory

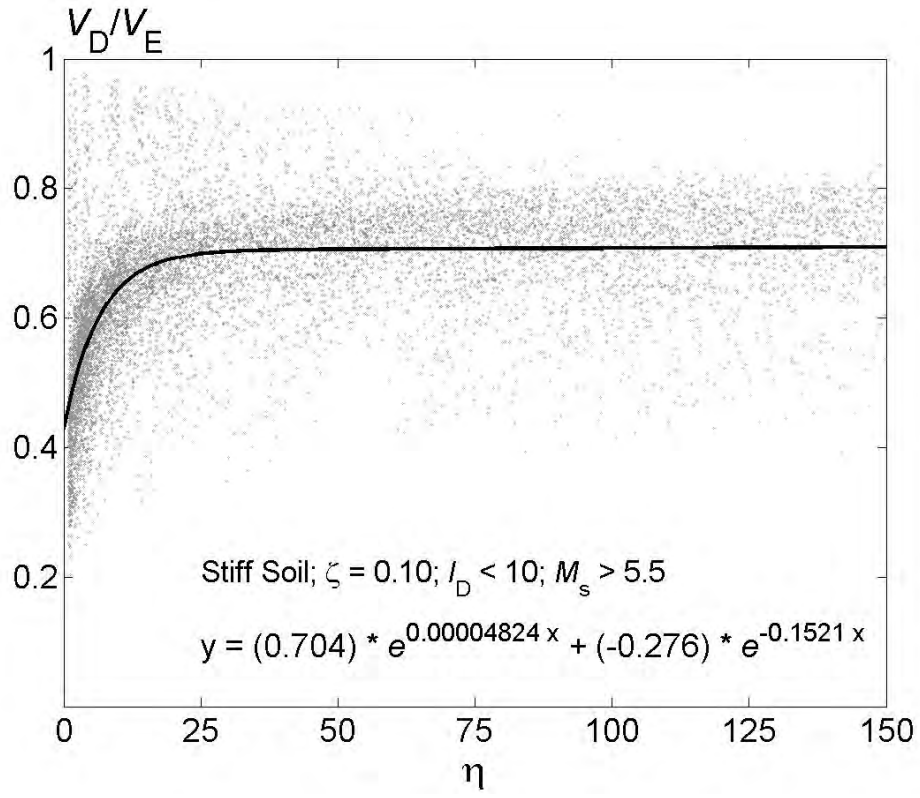

Figure 5-29 Proposed empirical approximations of the ratio V_D / V_E for damping ζ = 0.10. Stiff soil. M_s > 5.5. Impulsive

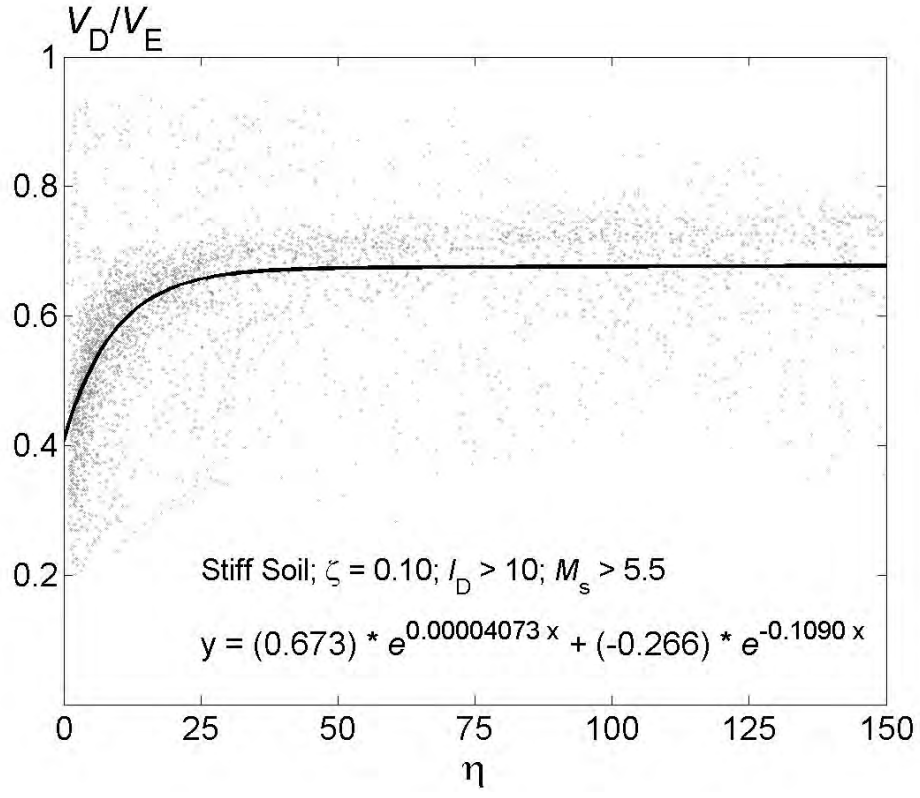

Figure 5-30 Proposed empirical approximations of the ratio V_D / V_E for damping ζ = 0.10. Stiff soil. M_s > 5.5. Vibratory

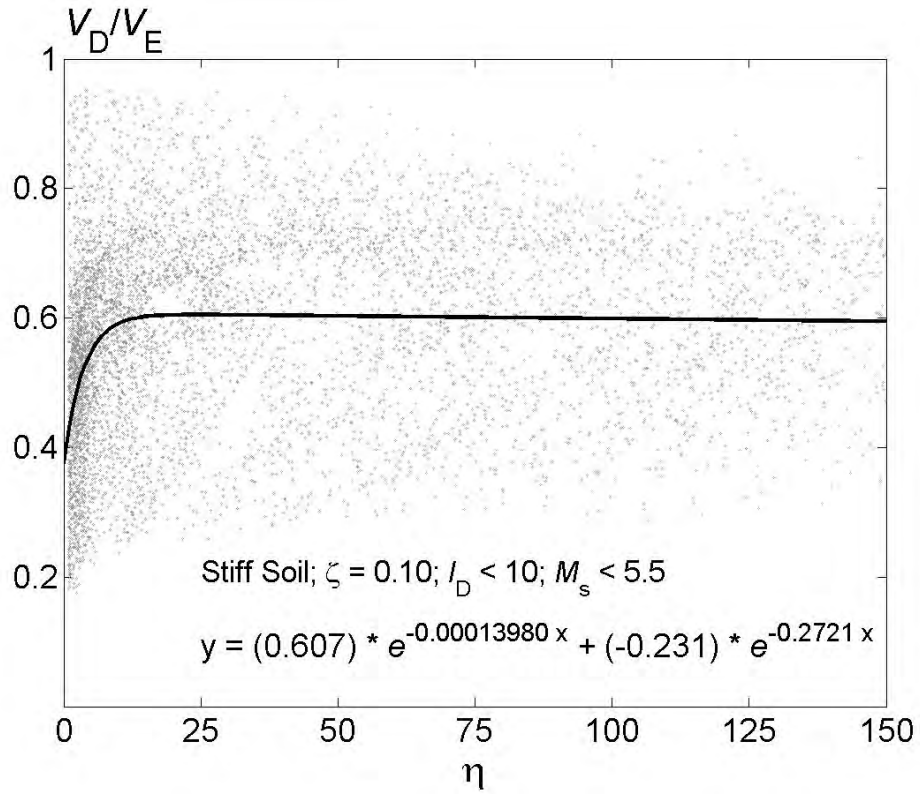

Figure 5-31 Proposed empirical approximations of the ratio V_D / V_E for damping ζ = 0.10. Stiff soil. $M_s \leq$ 5.5. Impulsive

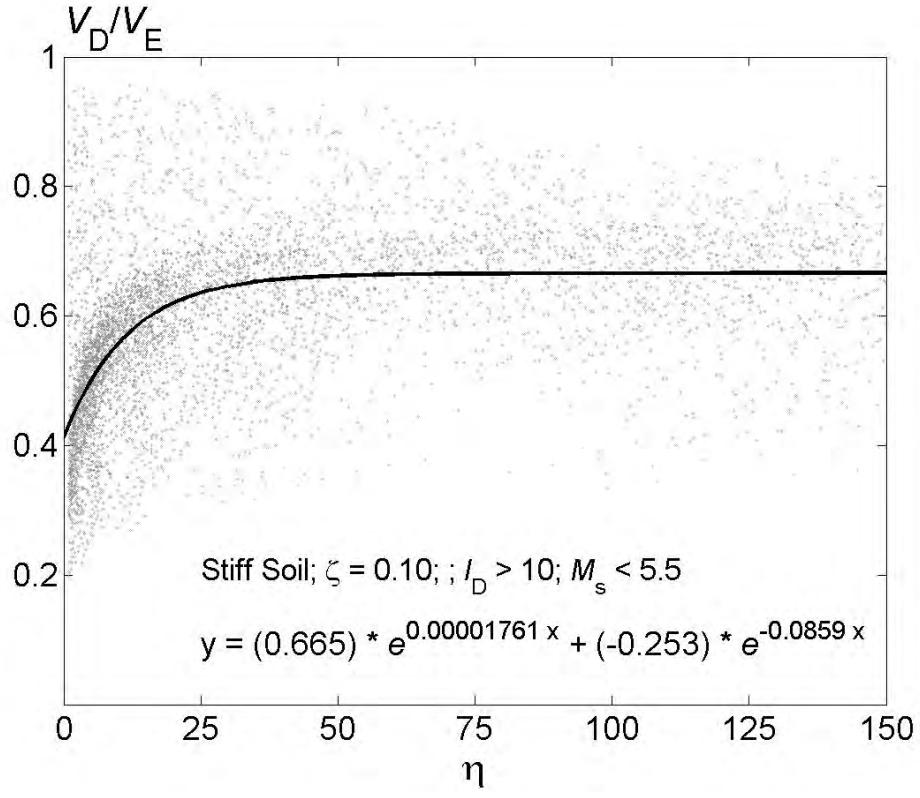

Figure 5-32 Proposed empirical approximations of the ratio V_D / V_E for damping ζ = 0.10. Stiff soil. $M_s \leq$ 5.5. Vibratory

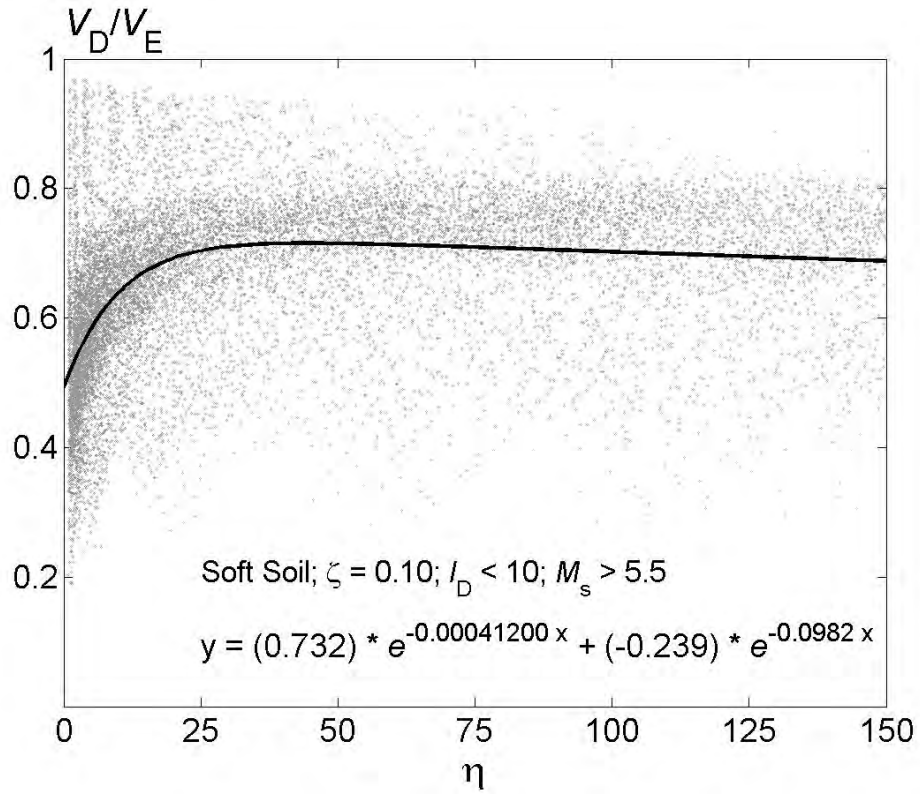

Figure 5-33 Proposed empirical approximations of the ratio V_D / V_E for damping ζ = 0.10. Soft soil. M_s > 5.5. Impulsive

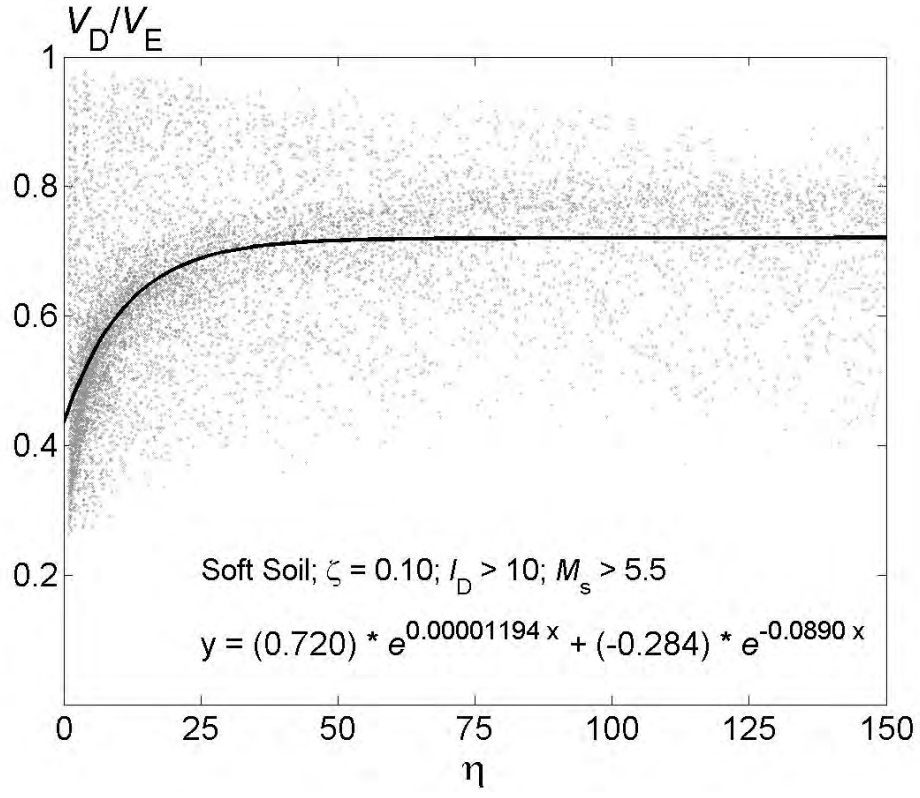

Figure 5-34 Proposed empirical approximations of the ratio V_D / V_E for damping ζ = 0.10. Soft soil. M_s > 5.5. Vibratory

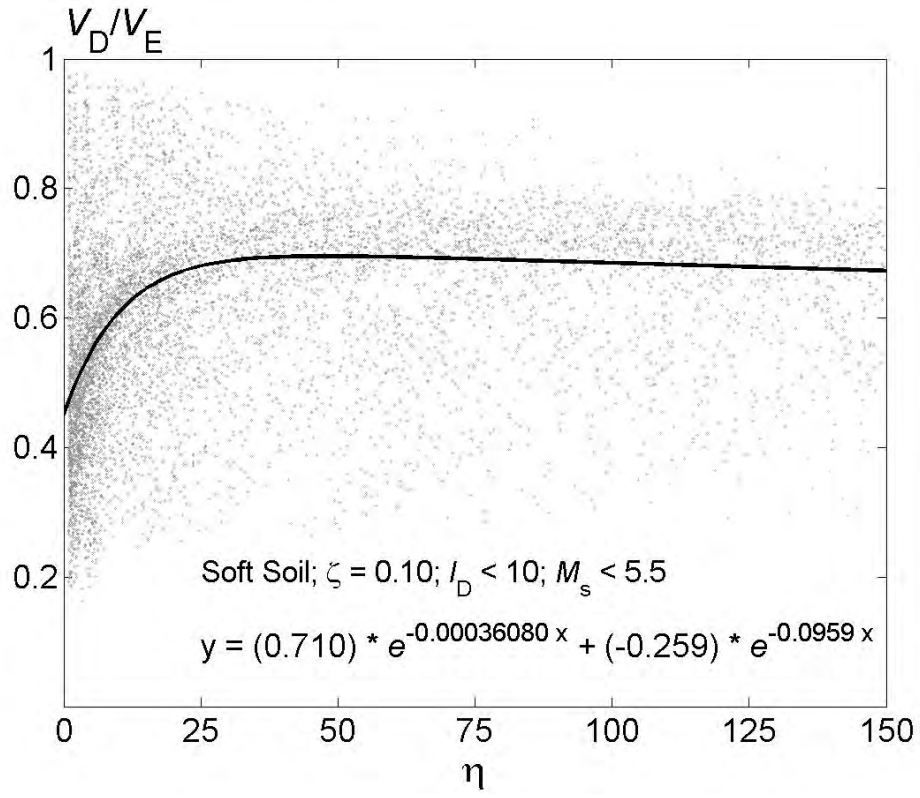

Figure 5-35 Proposed empirical approximations of the ratio V_D / V_E for damping ζ = 0.10. Soft soil. $M_s \leq$ 5.5. Impulsive

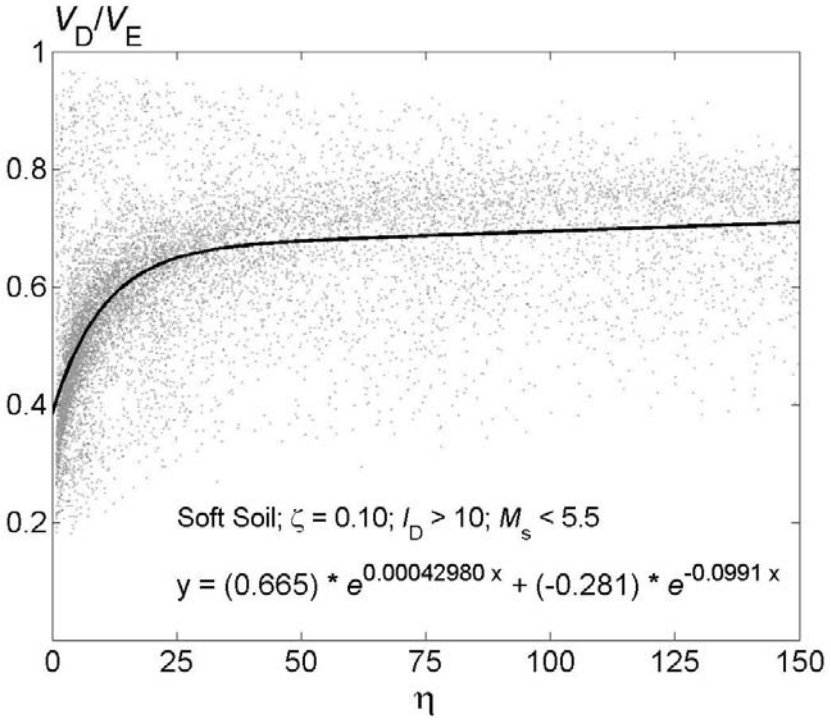

Figure 5-36 Proposed empirical approximations of the ratio V_D / V_E for damping ζ = 0.10. Soft soil. $M_s \leq$ 5.5. Vibratory

Table 5-1 Coefficients of the best exponential fit curve of the V_D / V_E ratio for each group

Dampin g	Soil Type	Magnitu de	Pulses	Coefficient				Goodness of Fit	
				a	*b*	*c*	*d*	SSE	R-Square
ζ = 0.02	Stiff Soil	$M_s > 5.5$	Imp.	0.893	0.0001885	– 0.243	– 0.180	33.31	0.5488
			Vibr.	0.877	0.0001867	– 0.236	– 0.156	16.84	0.4693
		$M_s \leq 5.5$	Imp.	0.879	– 0.0000235	– 0.291	– 0.262	0.04	0.7697
			Vibr.	0.866	0.0002698	– 0.219	– 0.142	26.02	0.4844
	Soft Soil	$M_s > 5.5$	Imp.	0.904	– 0.000000757	– 0.219	– 0.146	50.11	0.457
			Vibr.	0.898	0.0001648	– 0.229	– 0.118	29.22	0.5756
		$M_s \leq 5.5$	Imp.	0.880	0.0000201	– 0.206	– 0.140	55.49	0.3242
			Vibr.	0.878	0.0002496	– 0.247	– 0.131	49.18	0.5324
ζ = 0.05	Stiff Soil	$M_s > 5.5$	Imp.	0.802	0.0001633	– 0.277	– 0.166	62.49	0.4843
			Vibr.	0.777	0.0001467	– 0.277	– 0.134	31.62	0.4192
		$M_s \leq 5.5$	Imp.	0.720	0.0000417	– 0.266	– 0.302	118.2	0.1555
			Vibr.	0.761	0.0002462	– 0.252	– 0.115	54.53	0.4045
	Soft Soil	$M_s > 5.5$	Imp.	0.820	– 0.0001494	– 0.273	– 0.118	109.4	0.3526
			Vibr.	0.811	0.0001412	– 0.277	– 0.102	67.77	0.492
		$M_s \leq 5.5$	Imp.	0.780	– 0.0001016	– 0.229	– 0.124	109.9	0.2424
			Vibr.	0.775	0.0003464	– 0.286	– 0.111	99.01	0.4811
ζ = 0.10	Stiff Soil	$M_s > 5.5$	Imp.	0.704	0.00004824	– 0.276	– 0.152	83.75	0.4212
			Vibr.	0.673	0.00004073	– 0.266	– 0.109	40.71	0.3653
		$M_s \leq 5.5$	Imp.	0.607	– 0.0001398	– 0.231	– 0.272	142.7	0.1066
			Vibr.	0.665	0.0000176	– 0.252	– 0.086	75.09	0.3299
	Soft Soil	$M_s > 5.5$	Imp.	0.732	– 0.0000412	– 0.239	– 0.098	159.7	0.2715
			Vibr.	0.702	0.00001194	– 0.284	– 0.089	109.5	0.3947
		$M_s \leq 5.5$	Imp.	0.710	– 0.0003608	– 0.259	– 0.096	0.076	0.7456
			Vibr.	0.665	0.0004298	– 0.281	– 0.099	137.1	0.4173

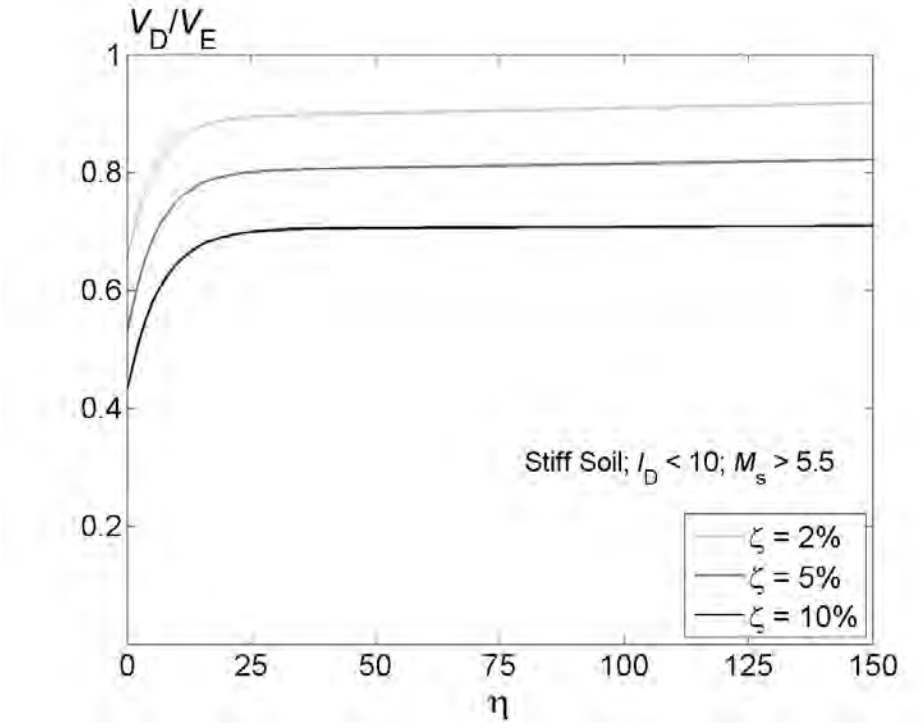

Figure 5-37 Proposed empirical approximations of the ratio V_D / V_E for damping ζ = 0.02, 0.05, 0.10. Stiff soil. M_s > 5.5. Impulsive

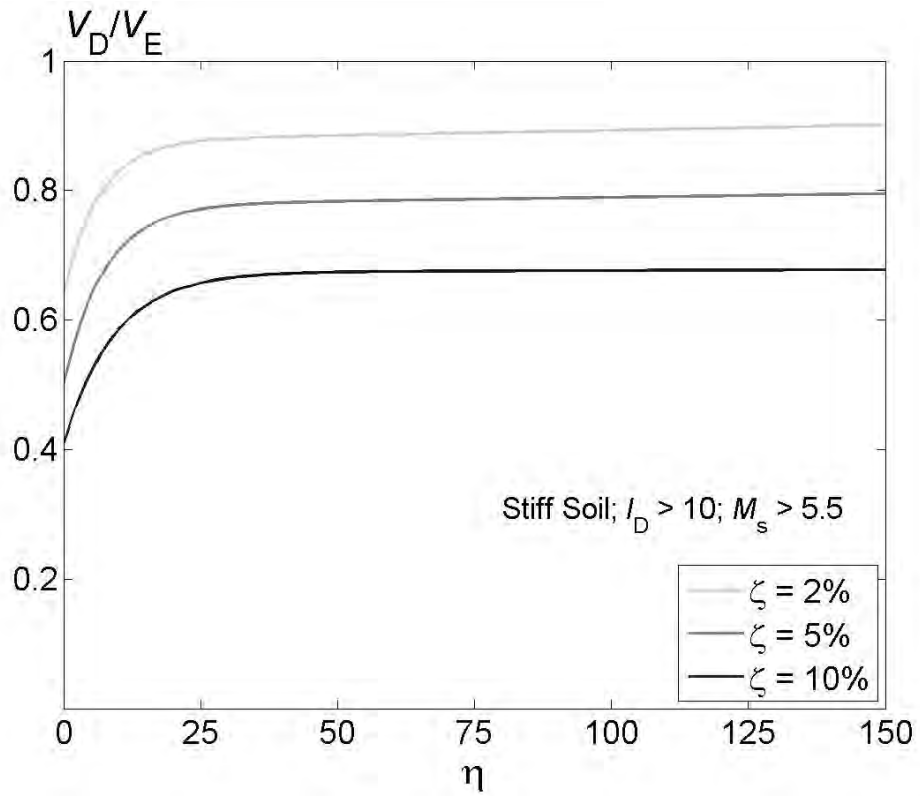

Figure 5-38 Proposed empirical approximations of the ratio V_D / V_E for damping ζ = 0.02, 0.05, 0.10. Stiff soil. M_s > 5.5. Vibratory

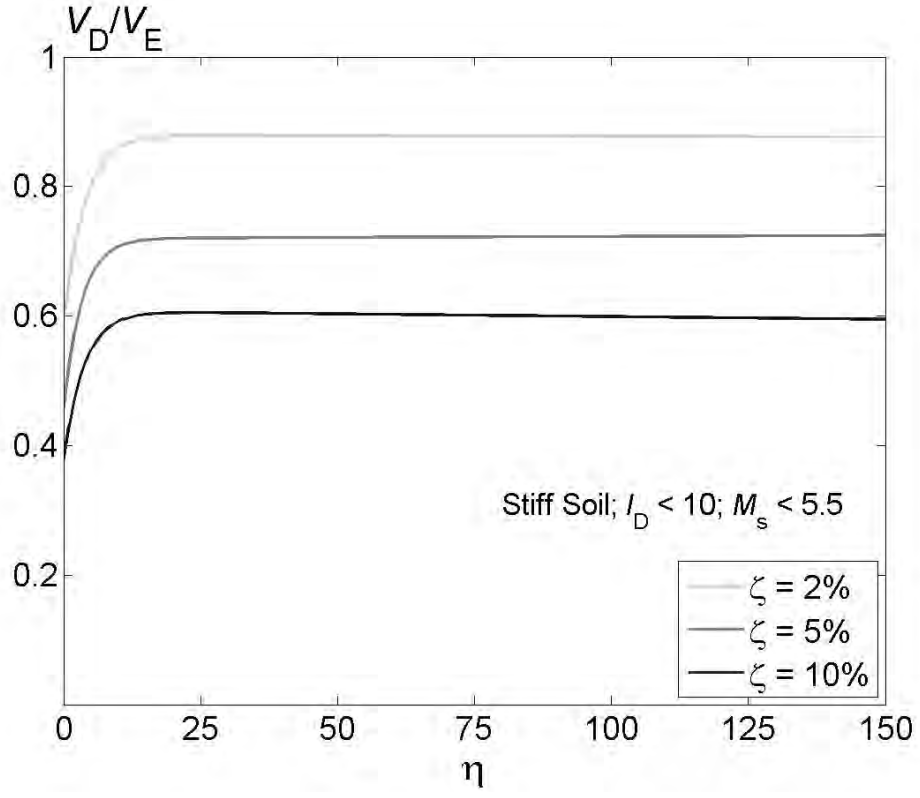

Figure 5-39 Proposed empirical approximations of the ratio V_D / V_E for damping ζ = 0.02, 0.05, 0.10. Stiff soil. $M_s \leq 5.5$. Impulsive

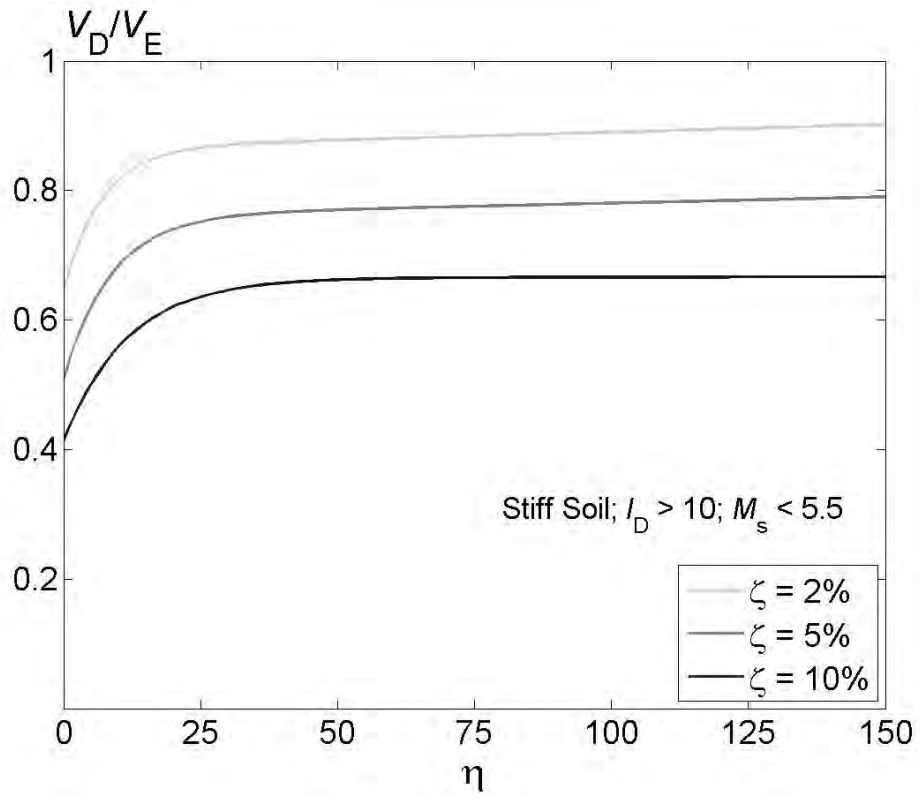

Figure 5-40 Proposed empirical approximations of the ratio V_D / V_E for damping ζ = 0.02, 0.05, 0.10. Stiff soil. $M_s \leq 5.5$. Vibratory

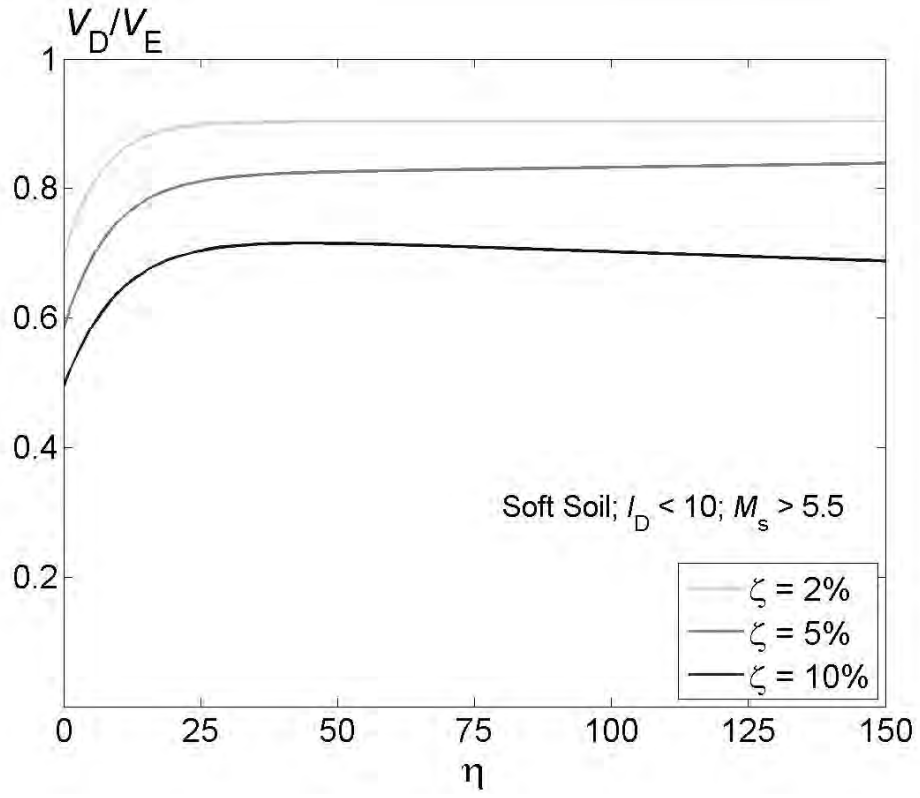

Figure 5-41 Proposed empirical approximations of the ratio V_D / V_E for damping ζ = 0.02, 0.05, 0.10. Soft soil. $M_s > 5.5$. Impulsive

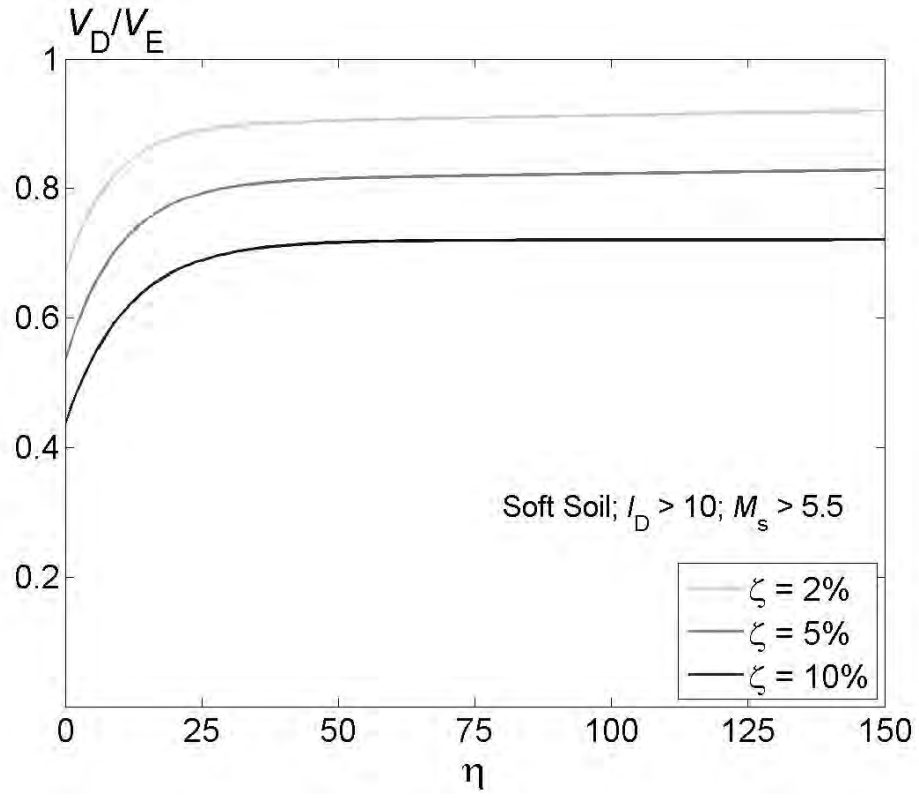

Figure 5-42 Proposed empirical approximations of the ratio V_D / V_E for damping ζ = 0.02, 0.05, 0.10. Soft soil. M_s > 5.5. Vibratory

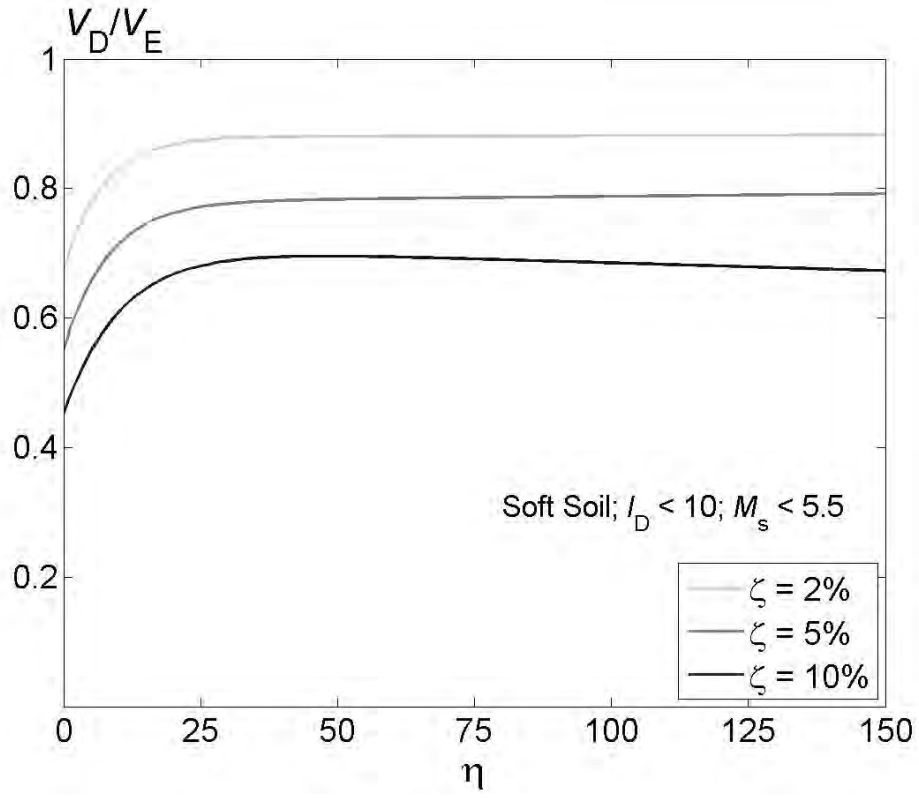

Figure 5-43 Proposed empirical approximations of the ratio V_D / V_E for damping ζ = 0.02, 0.05, 0.10. Soft soil. $M_s \leq 5.5$. Impulsive

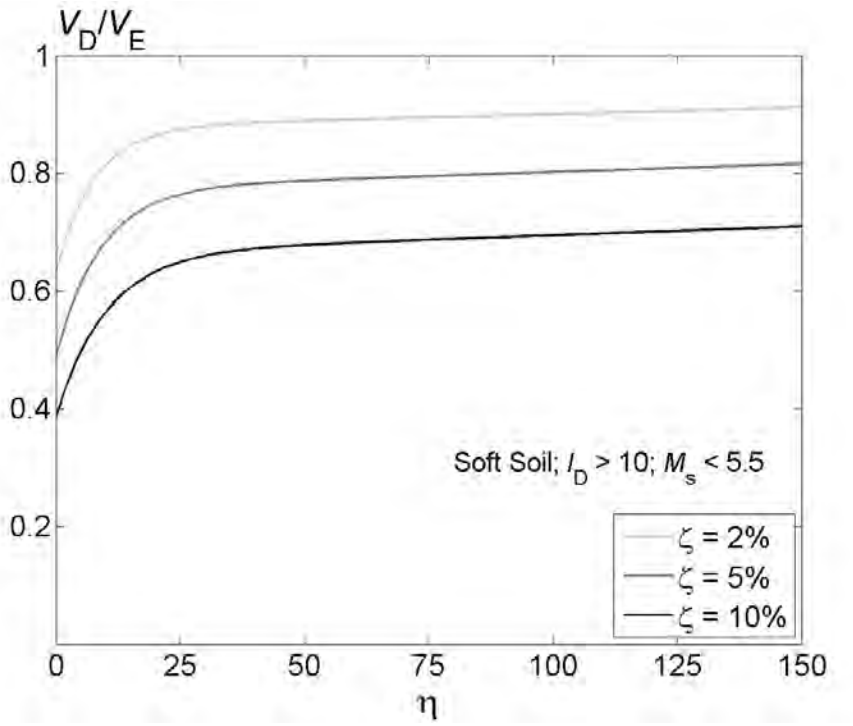

Figure 5-44 Proposed empirical approximations of the ratio V_D / V_E for damping ζ = 0.02, 0.05, 0.10. Soft soil. $M_s \leq 5.5$. Vibratory

Figure 5-13 to Figure 5-48, and Table 5-1 show the following general trends: (i) V_D / V_E increases with the increase of η but such dependency tends to disappear as such parameter reaches about 100; (ii) V_D / V_E decreases with the increase of ζ; (iii) for a given value of η, the dispersion of V_D / V_E increases with ζ and, for a given value of ζ, the dispersion of V_D / V_E decreases with η; (iv) the overall behavior of V_D / V_E for impulsive and vibratory registers is rather similar, although for smaller η the values of V_D / V_E are slightly higher for impulsive registers than for vibratory ones; (v) the results for $M_s > 5.5$ and for $M_s \leq 5.5$ are rather equivalent; and (vi) V_D / V_E is similar on stiff soil and on soft soil. These last three conclusions show that the ratio V_D / V_E is analogous in the eight aforementioned groups (section 3.5; therefore, the proposal of approximate expressions for estimating V_D / V_E has to be made irrespectively of the soil type, the impulsivity of the register and the magnitude of the earthquake. Figure 5-45 to Figure 5-47 display the clouds of points corresponding to all the considered registers (Table 3-1) for damping factors ζ = 0.02, 0.05 and 0.10 together with the best fit curves according to the two-term exponential expression (5-4);Figure 5-45, Figure 5-46 and Figure 5-47 show the cases for ζ = 0.02, 0.05 and 0.10, respectively, while Figure 5-48 shows jointly the three exponential fitting curves alone (e.g. without the fitted points). As well, Table 5-2 displays the values of the coefficients *a*, *b*, *c* and *d* that provides the best fit for ζ = 0.02, 0.05 and 0.10.

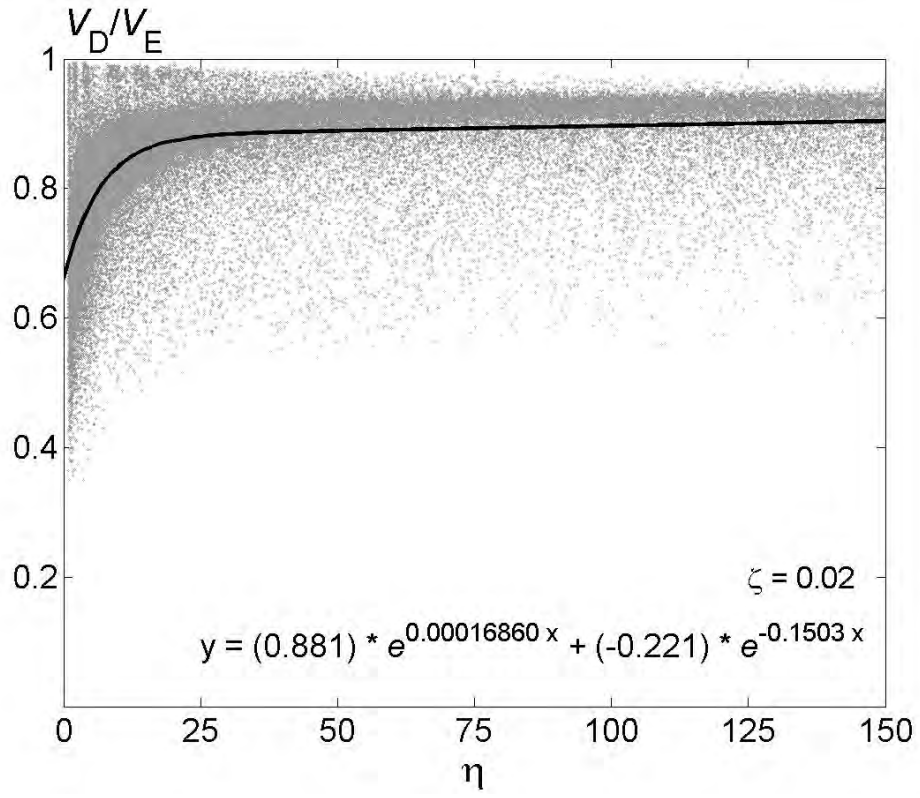

Figure 5-45 Proposed empirical approximations of the ratio V_D / V_E regardless of the group. $\zeta = 0.02$

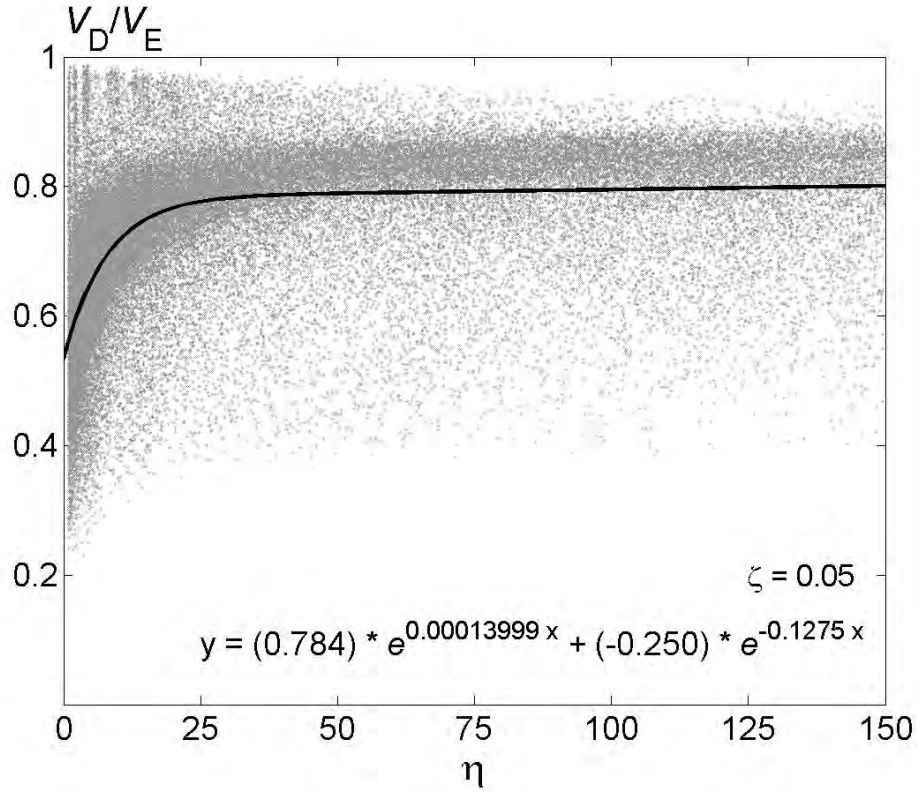

Figure 5-46 Proposed empirical approximations of the ratio V_D / V_E regardless of the group $\zeta = 0.05$

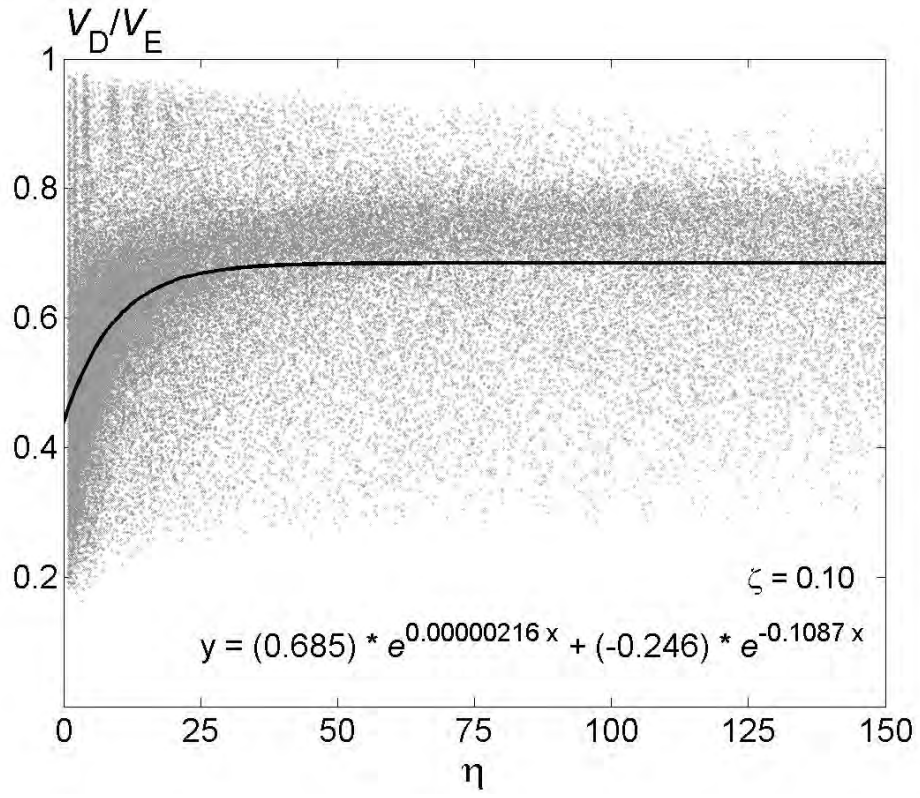

Figure 5-47 Proposed empirical approximations of the ratio V_D / V_E regardless of the group. ζ = 0.10

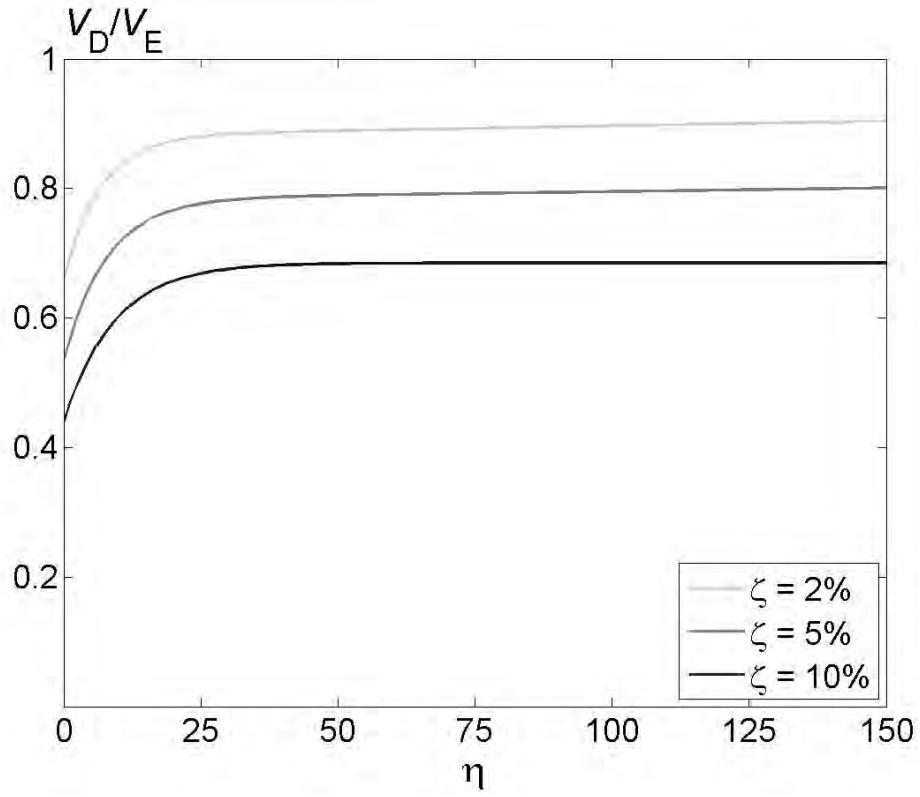

Figure 5-48 Proposed empirical approximations of the ratio V_D / V_E regardless of the group. ζ = 0.02, 0.05 and 0.10

Table 5-2 Coefficients of the best exponential fit curve of the V_D / V_E ratio for all the groups

Damping	*a*	*b*	*c*	*d*
$\zeta = 0.02$	0.881	0.00016860	– 0.221	– 0.1503
$\zeta = 0.05$	0.784	– 0.00013999	– 0.250	– 0.1275
$\zeta = 0.10$	0.685	0.00000216	– 0.246	– 0.1087

5.4 Influence of Period

Aiming to investigate the variation of the ratio V_D / V_E with period *T*, Figure 5-49 to Figure 5-66 show the spectra of V_D / V_E for different values of the damping factor (ζ = 0.02, 0.05 and 0.10) and of the displacement ductility (μ = 2, 3, 5, 10, 15 and 20). Since the previous study about the influence of ζ and η in the ratio V_D / V_E (section 5.3) has shown little influence of the soil type, the impulsive / vibratory character and the earthquake magnitude, the V_D / V_E spectra are presented herein regardless of such issues; i.e. each set of plots in Figure 5-49 to Figure 5-66 correspond to all the considered registers in Table 3-1. Each set of plots (Figure 5-49 to Figure 5-66) contain the individual spectra, the median one and a linear fit of such median spectrum. Remarkably, a bilinear approximation (where the initial branch starts from $V_D / V_E = 1$ for $T = 0$) would provide a better match; however, since that branch corresponds only to extremely short periods (e.g. shorter than 0.06 s), it is neglected in this study. Table 5-3 displays the parameters of the chosen linear fit; such parameters are the slope, the spectral ordinate that corresponds to T = 4 s, and the average spectral ordinate, e.g. the one that corresponds to T = 2 s.

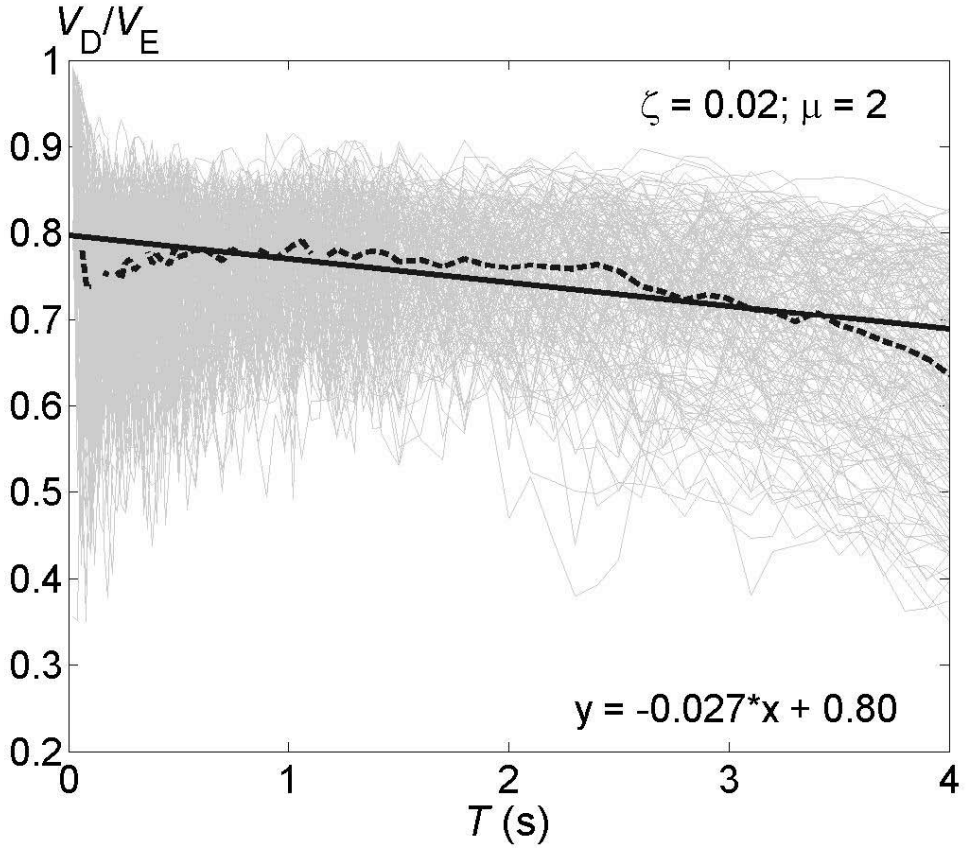

Figure 5-49 Spectra of the ratio V_D / V_E. ζ = 0.02; μ = 2

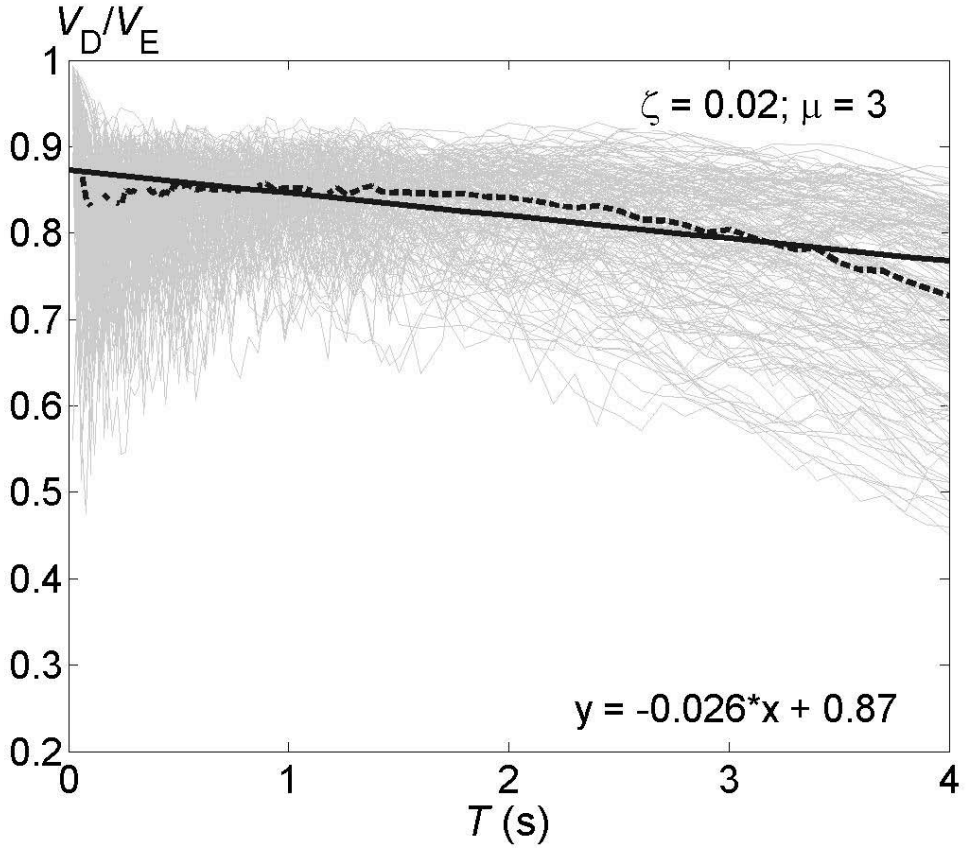

Figure 5-50 Spectra of the ratio V_D / V_E. ζ = 0.02; μ = 3

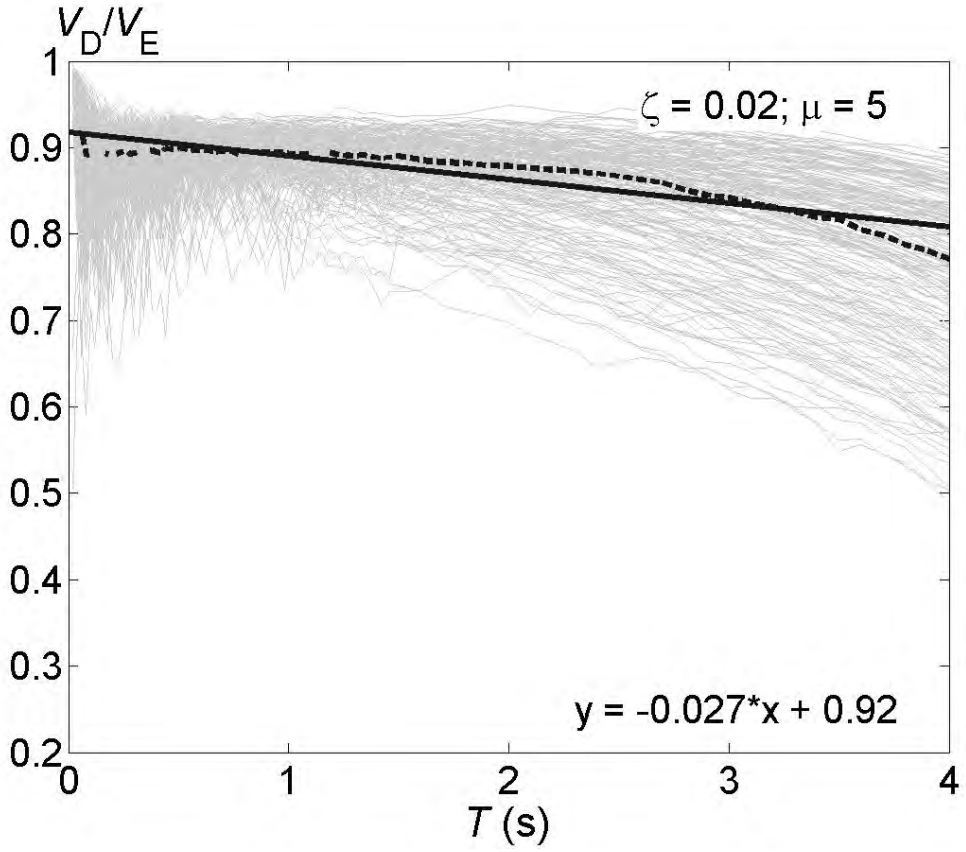

Figure 5-51 Spectra of the ratio V_D / V_E. ζ = 0.02; μ = 5

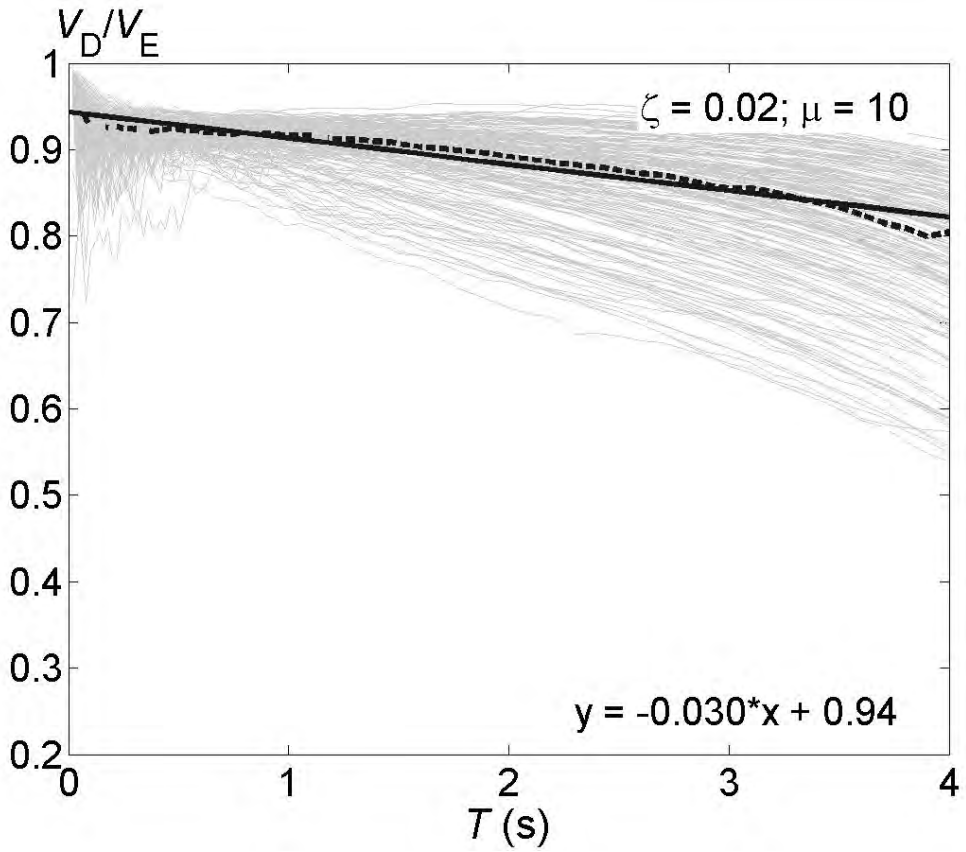

Figure 5-52 Spectra of the ratio V_D / V_E. ζ = 0.02; μ = 10

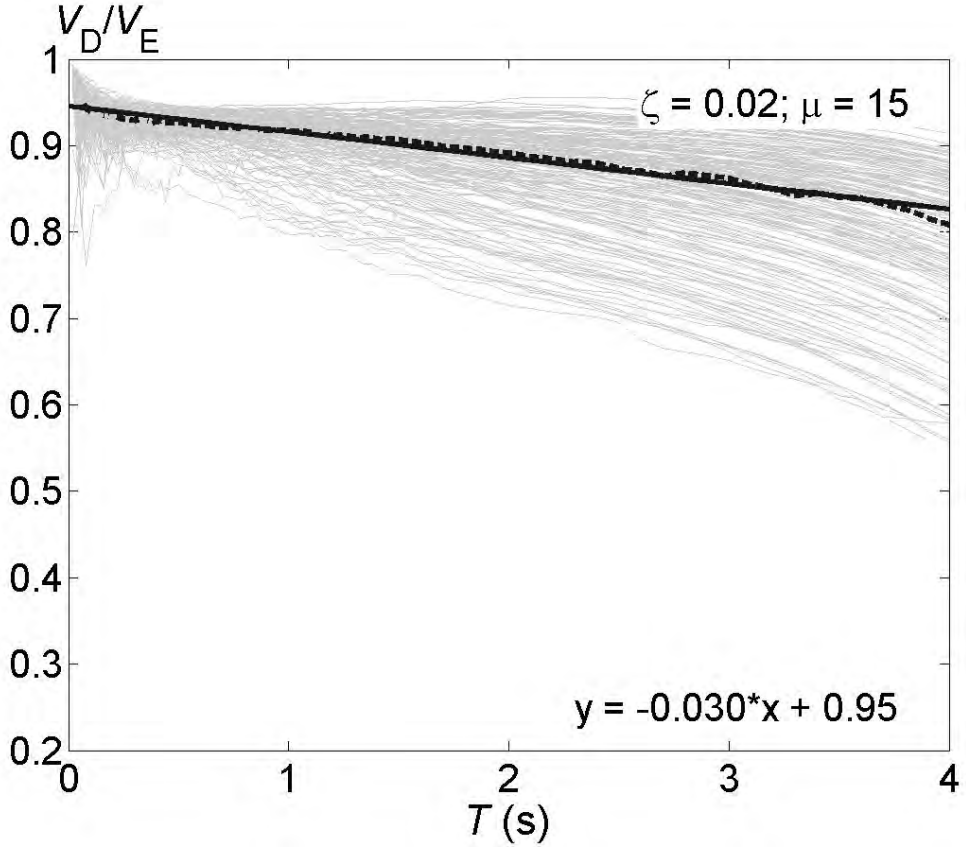

Figure 5-53 Spectra of the ratio V_D / V_E. ζ = 0.02; μ = 15

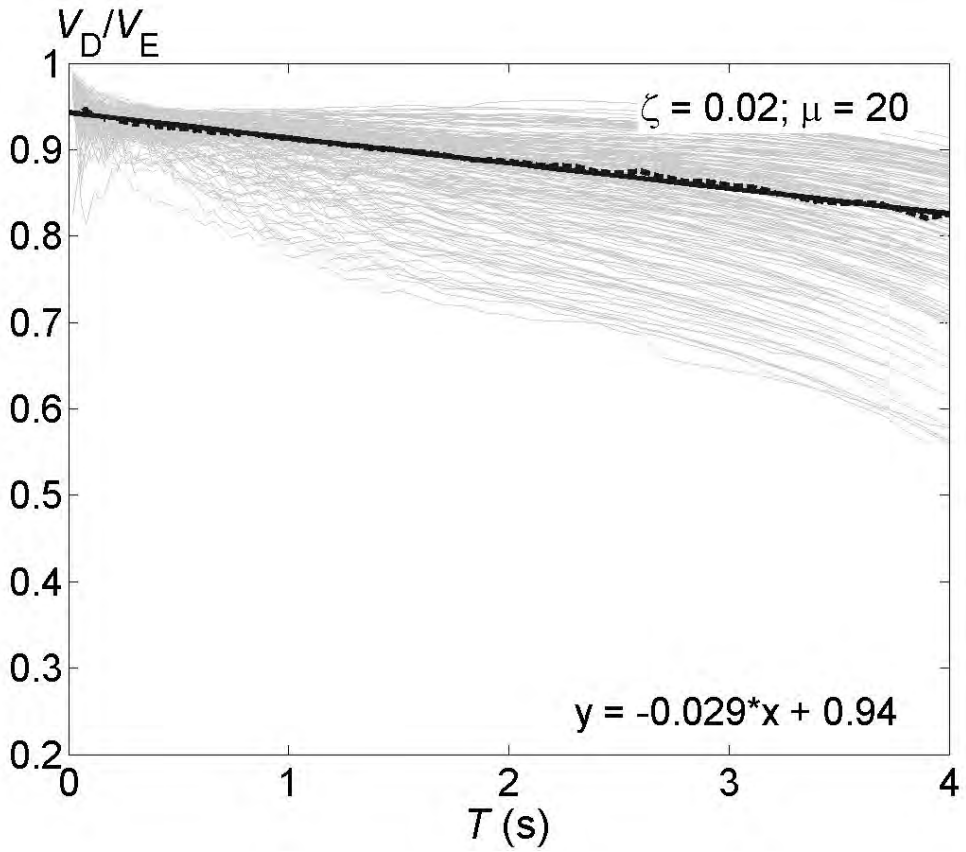

Figure 5-54 Spectra of the ratio V_D / V_E. ζ = 0.02; μ = 20

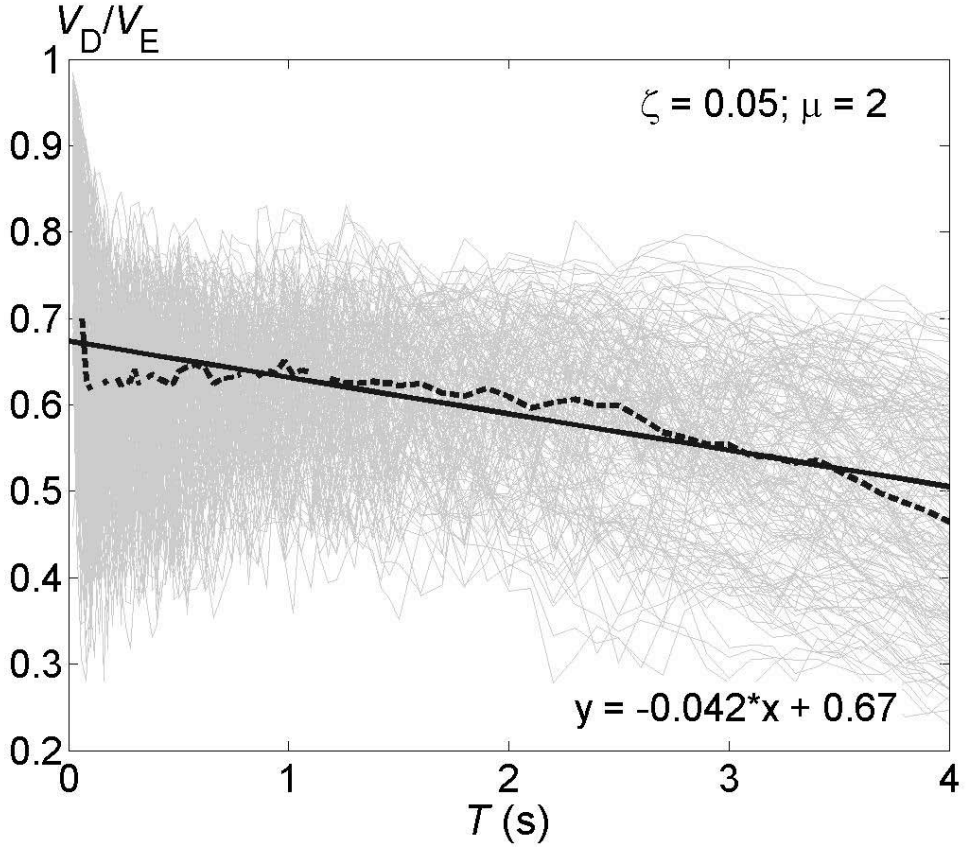

Figure 5-55 Spectra of the ratio V_D / V_E. ζ = 0.05; μ = 2

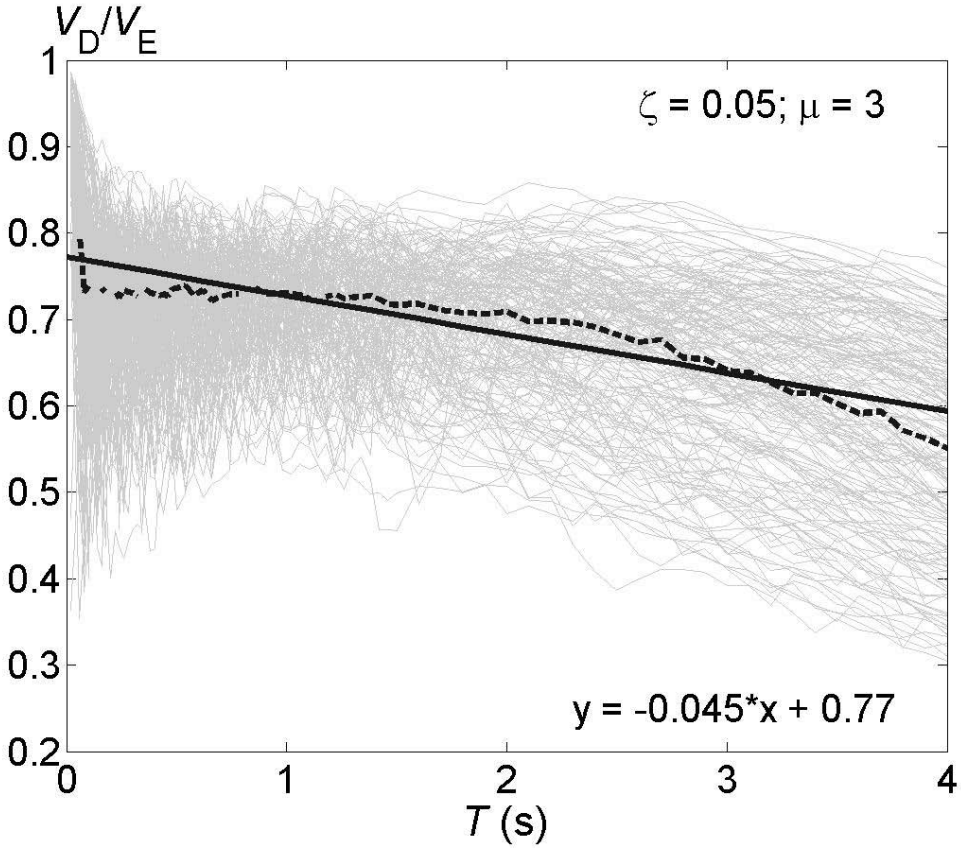

Figure 5-56 Spectra of the ratio V_D / V_E. ζ = 0.05; μ = 3

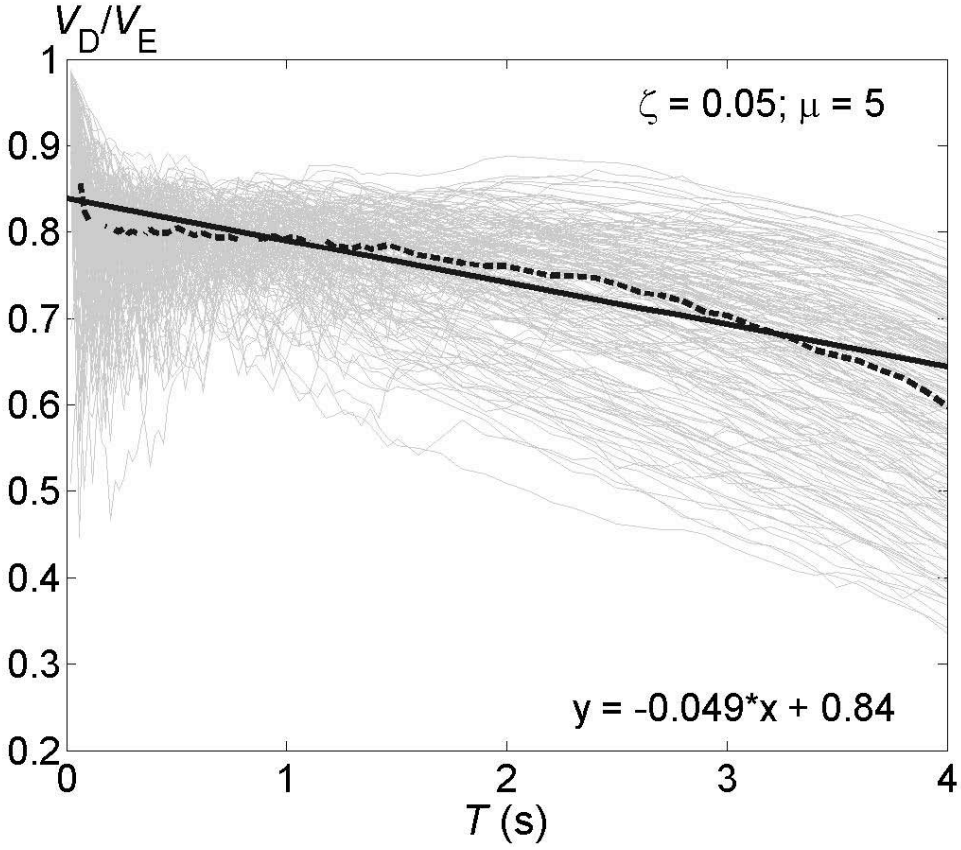

Figure 5-57 Spectra of the ratio V_D / V_E. ζ = 0.05; μ = 5

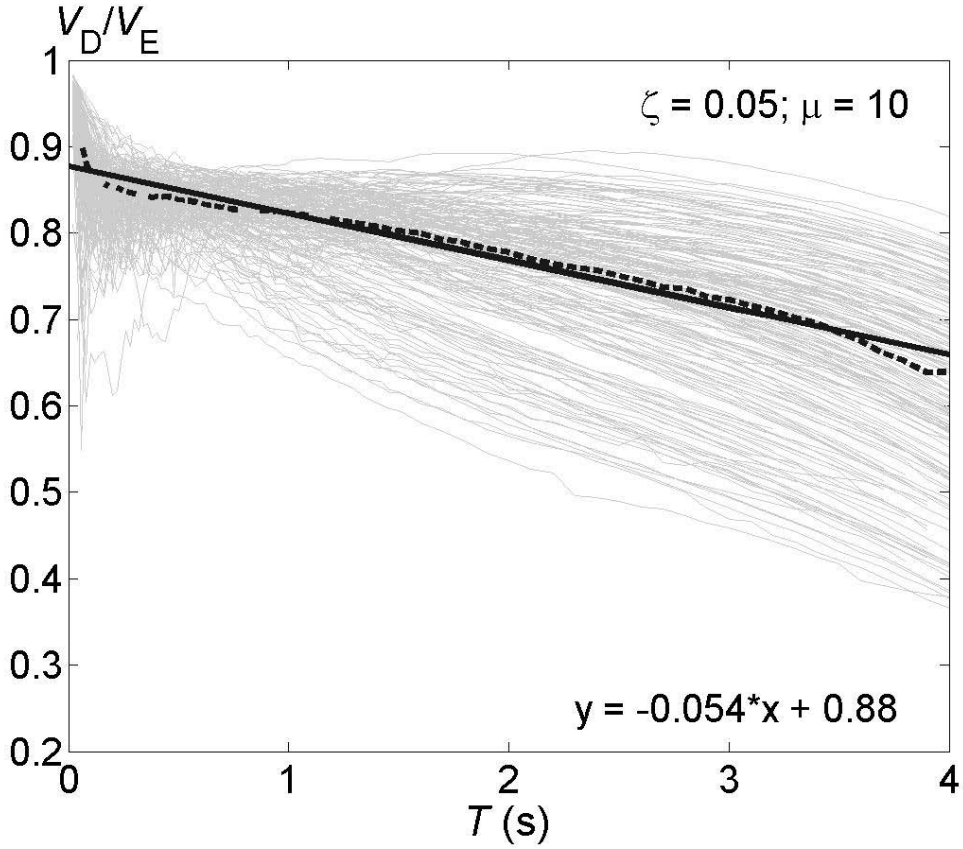

Figure 5-58 Spectra of the ratio V_D / V_E. ζ = 0.05; μ = 10

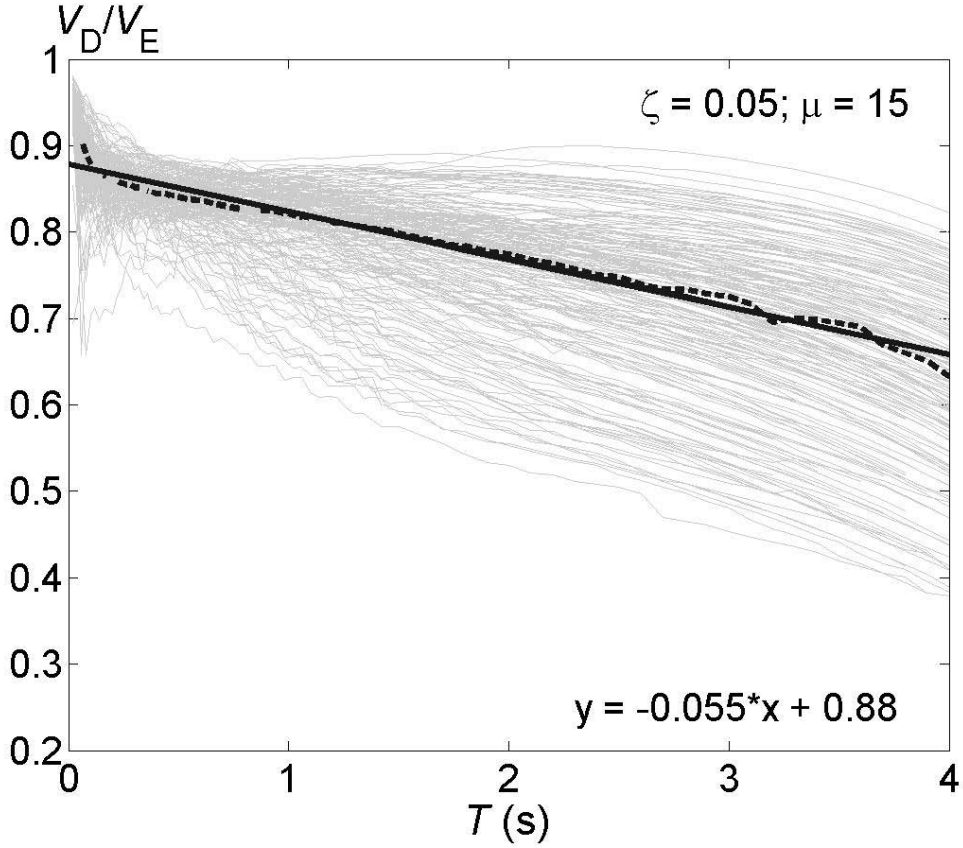

Figure 5-59 Spectra of the ratio V_D / V_E. ζ = 0.05; μ = 15

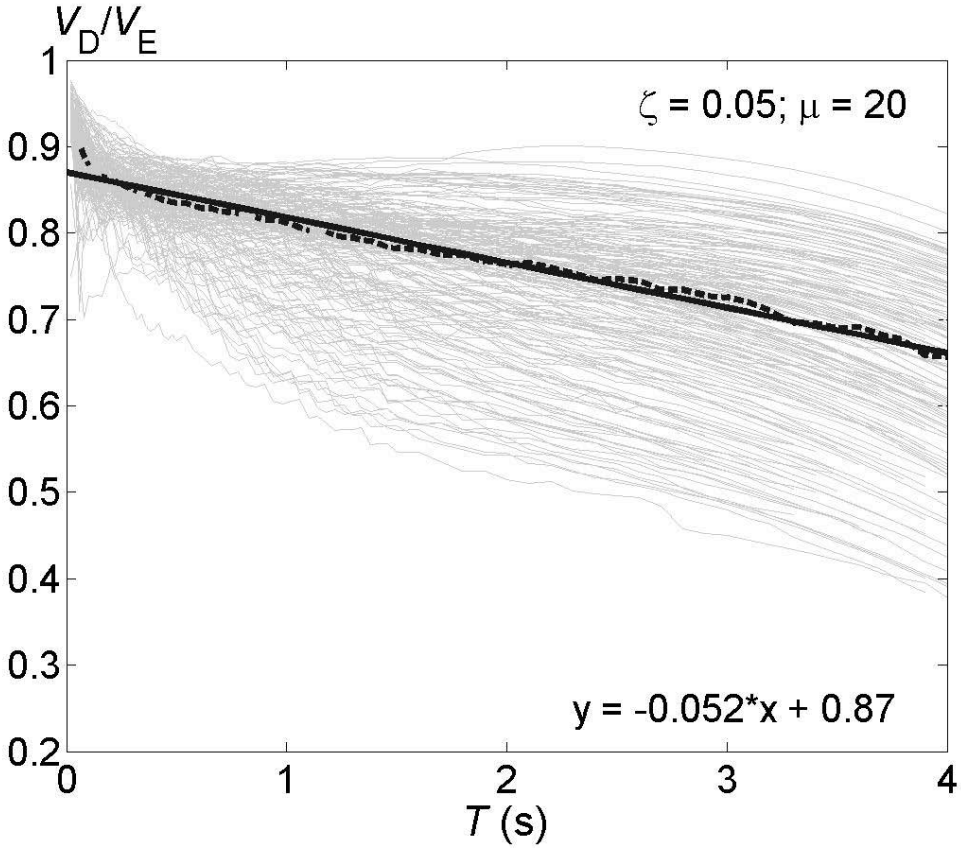

Figure 5-60 Spectra of the ratio V_D / V_E. ζ = 0.05; μ = 20

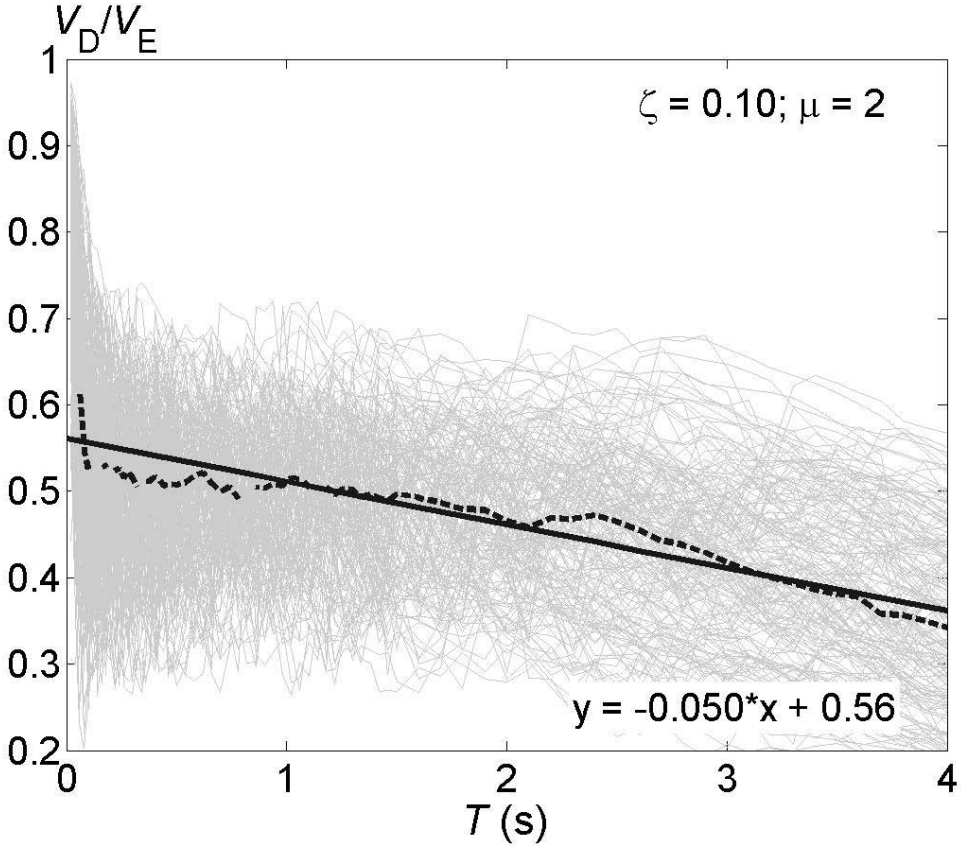

Figure 5-61 Spectra of the ratio V_D / V_E. ζ = 0.10; μ = 2

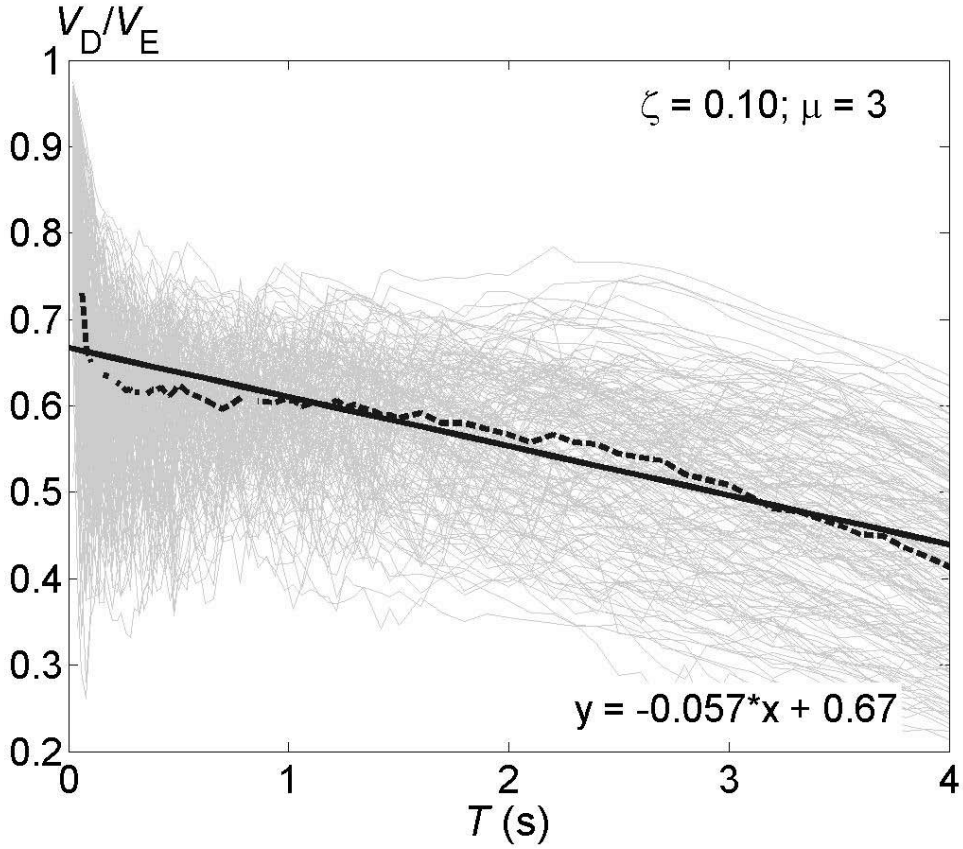

Figure 5-62 Spectra of the ratio V_D / V_E. ζ = 0.10; μ = 3

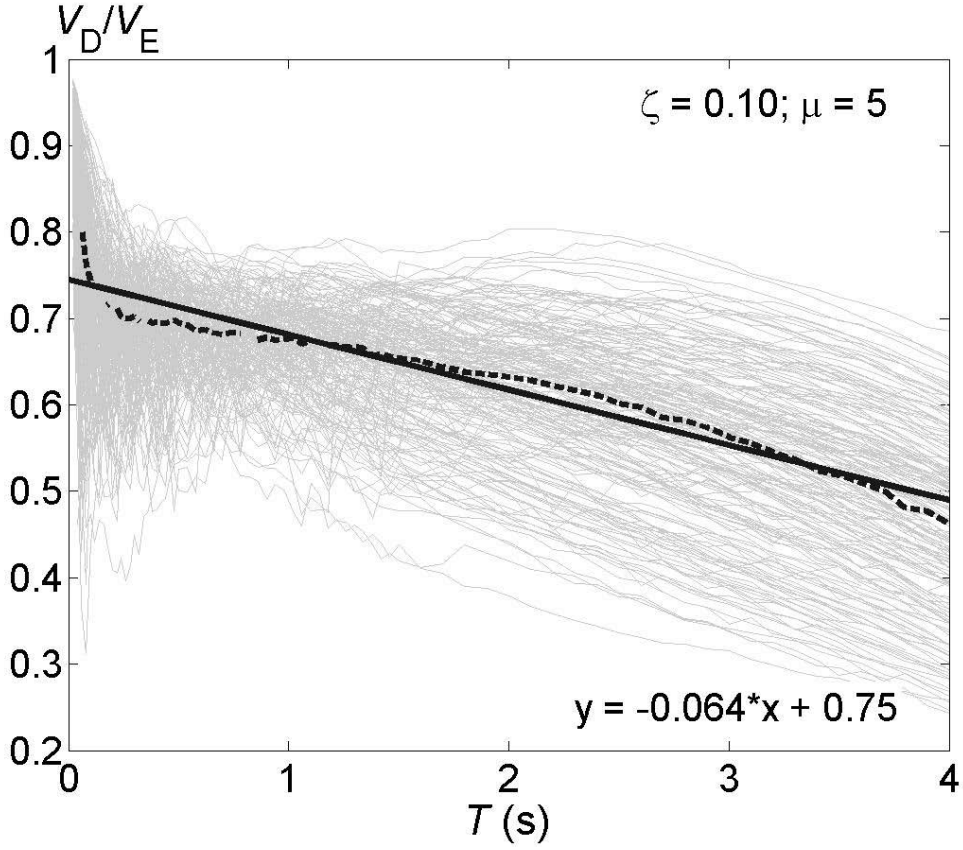

Figure 5-63 Spectra of the ratio V_D / V_E. ζ = 0.10; μ = 5

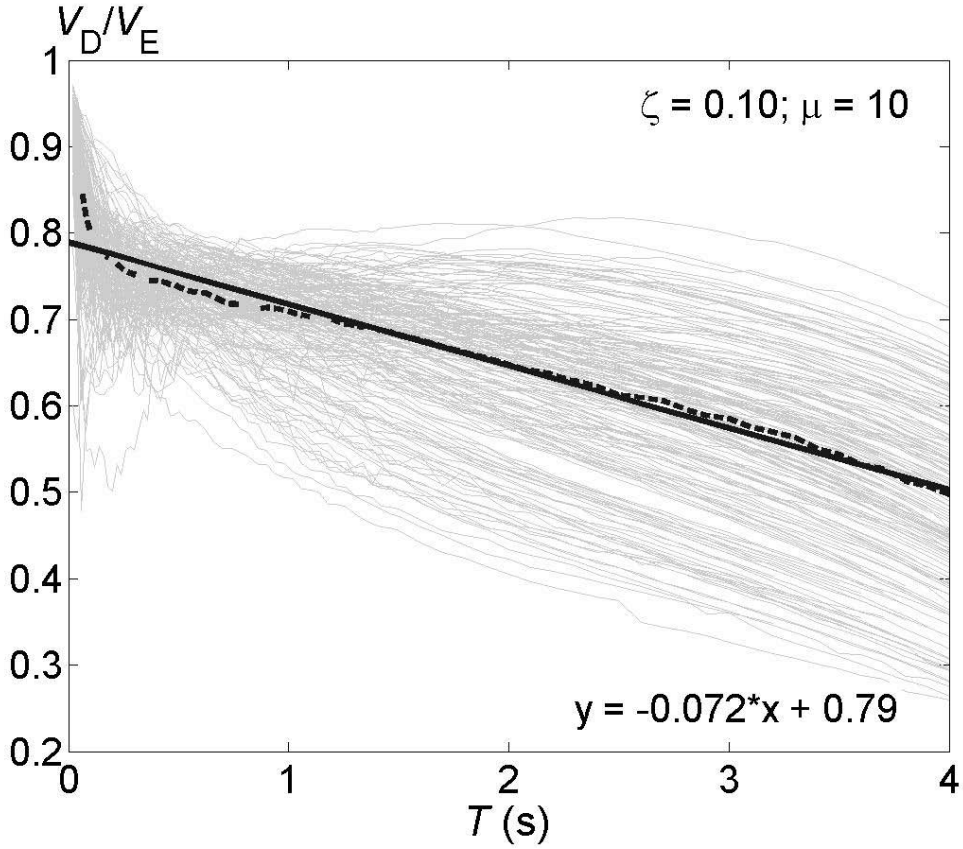

Figure 5-64 Spectra of the ratio V_D / V_E. ζ = 0.10; μ = 10

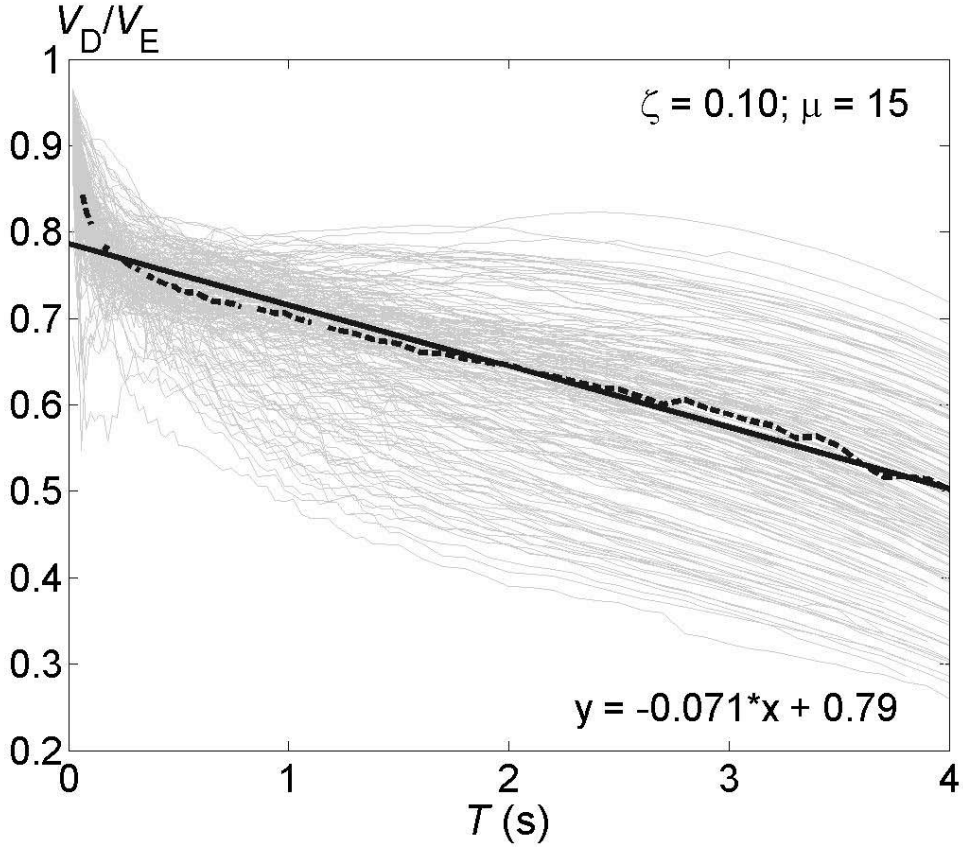

Figure 5-65 Spectra of the ratio V_D / V_E. ζ = 0.10; μ = 15

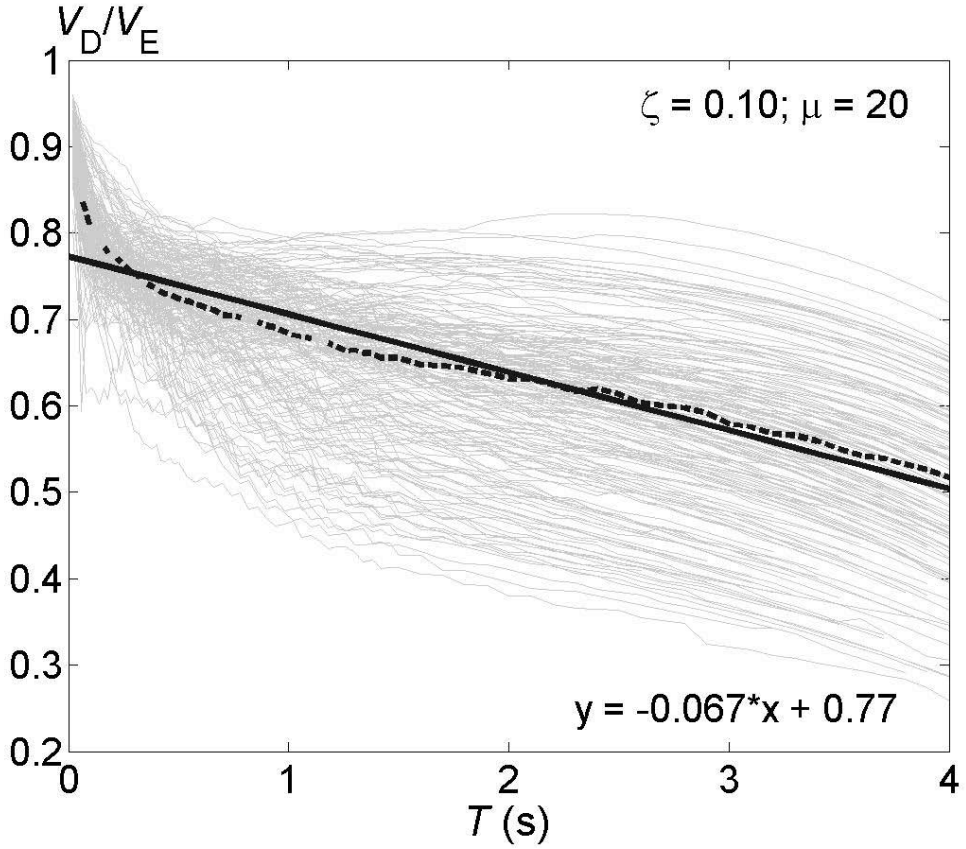

Figure 5-66 Spectra of the ratio V_D / V_E. ζ = 0.10; μ = 20

Table 5-3 Parameters for the linear fit of the V_D / V_E spectra

ζ	μ	p_1 (s^{-1})	p_2	SSE	R-Square	Spectral ordinate (T = 4 s)	Average spectral ordinate (T = 2 s)
0.02	2	-0.02713	0.7973	0.06843	0.506	0.692	0.746
	3	-0.02628	0.8726	0.03347	0.662	0.766	0.818
	5	-0.02721	0.9176	0.01788	0.797	0.812	0.866
	10	-0.03038	0.9436	0.00733	0.923	0.820	0.880
	15	-0.02986	0.9456	0.00340	0.960	0.830	0.890
	20	-0.02925	0.9429	0.00221	0.973	0.824	0.882
0.05	2	-0.04213	0.6737	0.59900	0.593	0.502	0.586
	3	-0.04468	0.7717	0.07249	0.724	0.590	0.680
	5	-0.04852	0.8383	0.04162	0.843	0.644	0.742
	10	-0.05449	0.8772	0.01815	0.939	0.664	0.772
	15	-0.05507	0.8785	0.01361	0.955	0.660	0.770
	20	-0.05227	0.8702	0.01393	0.959	0.662	0.766
0.10	2	-0.04996	0.5608	0.13750	0.633	0.360	0.460
	3	-0.0569	0.6671	0.11270	0.732	0.442	0.556
	5	-0.06388	0.745	0.07096	0.845	0.494	0.622
	10	-0.07167	0.7895	0.04307	0.919	0.502	0.646
	15	-0.07084	0.7865	0.04396	0.915	0.506	0.648
	20	-0.06719	0.7731	0.05378	0.888	0.502	0.636

Plots from Figure 5-49 to Figure 5-66 and data from Table 5-3 show that the overall trends about the influence of damping and of ductility that have been previously concluded (the ratio V_D / V_E decreases with increasing damping and increases with increasing ductility) are also

apparent from these results. Results for Table 5-3 show that the slope increases with damping. As well, the dependency of the slope on ductility increases with damping; roughly, it grows as ductility does. Table 5-3 also shows that the spectral ordinates that correspond to periods 2 and 4 s increase with ductility while decrease with damping.

As shown next, the comparison among the fits in Figure 5-49 to Figure 5-66 and the study by Decanini and Mollaioli [2001] show a reasonable agreement, except in the short period range; this difference is mainly due to the consideration of the absolute energy by such authors. As discussed in section 4.2, among the three considered soil categories, S1 and S2 correspond to "stiff soil" and "soft soil", respectively. Parameters *e* and *f* (see Fig. 16 and Table 11 in [Decanini, Mollaioli 2001]) can be compared, for $\zeta = 0.05$, to the squares of the spectral ordinates corresponding to T_3 (ranging in between 0.225 and 0.55 s) and to 4 s, respectively (Figure 5-49 to Figure 5-66 and Table 5-3); Table 5-4 shows a comparison among the values of the square roots of *e* and *f* and those of the aforementioned spectral ordinates. Period T_3 corresponds to period T_C in this study. Comparison among the second and fourth columns of Table 5-4 ($\sqrt{e}$ and spectral ordinate for period T_3) shows a satisfactory agreement; as well, comparison among the third and fifth columns of Table 5-4 ($\sqrt{f}$ and spectral ordinate for 4 s) shows a poorer agreement, where the proposed fit is more conservative.

Table 5-4 Comparison among the parameters for the proposed linear fit of the V_D / V_E spectra (for ζ = 0.05) and the one by Decanini and Mollaioli [2001]

μ	$\sqrt{e}$ (stiff soil / soft soil)	$\sqrt{f}$ (stiff soil / soft soil)	Spectral ordinate (T_3) (stiff soil / soft soil)	Spectral ordinate (T = 4 s)
2	0.693 / 0.707	0.632 / 0.686	0.657 / 0.645	0.502
3	0.742 / 0.758	0.671 / 0.731	0.758 / 0.745	0.590
5	0.800 / 0.822	0.714 / 0.781	0.829 / 0.817	0.644

It is obvious from Figure 5-49 to Figure 5-66 and from Table 5-4 that the common assumption that V_D / V_E is roughly independent of period is no longer sustainable; conversely, the approximation given by equation (with the values of the coefficients *a*, *b*, *c* and *d* listed in Table 5-3) corresponds to the average ordinate of the fits shown in Figure 5-49 to Figure 5-66. Such average ordinates are also listed in Table 5-3.

5.5 Proposed criteria for estimating V_D / V_E

The previous two sections allow deriving criteria for estimating the ratio V_D / V_E in terms of period *T*, ductility μ or η and damping ζ; the study described in section 5.4 provides criteria that depend on *T*, μ and ζ while the study depicted in section 5.3 illustrates the influence of η and ζ but needs to be complemented with section 5.4 to incorporate the effect of *T*. Accordingly, the first proposed criterion consists of the linear decreasing spectra drawn in Figure 5-49 to Figure 5-66; the values of the parameters of the linear fit are listed in Table 5-3 in terms of μ and ζ. The second proposed criterion consists of the two-term exponential curves plotted in Figure 5-48 and described in Table 5-2 multiplied by the ratio among the ordinate corresponding to the considered period and the average spectral ordinate (Figure 5-49 to Figure 5-66 and Table 5-3). Since there is no direct relation in between μ and η, both proposed criteria are not equivalent.

The V_D spectra can be obtained by multiplying the V_D / V_E spectra proposed in this section by the three-branched V_E spectra (linear spectra depicted in Figure 4-10 to Figure 4-17 and nonlinear modification of the initial branches described in Figure 4-42 to Figure 4-65).

6 Comparison with other studies

6.1 Introduction

In this section, the design energy input spectra proposed in this study for high seismicity regions based on Turkish ground motions are compared with those proposed by Decanini and Mollaioli [1998, 2001] and with those proposed from registers from Colombia [Benavent et al. 2010], Iran [Amiri el al. 2008] and Greece [Tselentis et al. 2010]. As well, the proposed spectra are compared with those proposed for Japan by the current Japanese seismic code [BSL 2009] and by Akiyama [Akiyama 1985]. (Figure 6-1 to Figure 6-6) shows with solid lines the characteristic energy input spectra proposed in this study for impulsive and vibratory earthquakes with $M_s > 5.5$ and $\mu = 1$ (see Figure 4-10 to Figure 4-17, Table 4-1 and Table 4-2), and with thin lines these spectra proposed by the aforementioned authors and codes. Descriptions of these comparisons are included next.

6.1.1 Spectra from Colombian registers

Figure 6-1 shows the design energy input spectra proposed by [Benavent-Climent el al. 2010] based on 144 Colombian registers associated with design PGA equal to 0.4 g. These authors considered three soil types: rock (shear wave velocity $v_s > 750$ m/s), stiff soil ($375 \leq v_s \leq 750$ m/s) and intermediate soil ($175 \leq v_s \leq 375$ m/s). As seen in the figure, the levels of input energy proposed in this study are approximately bounded by the levels proposed from Colombian records for soils type I and II.

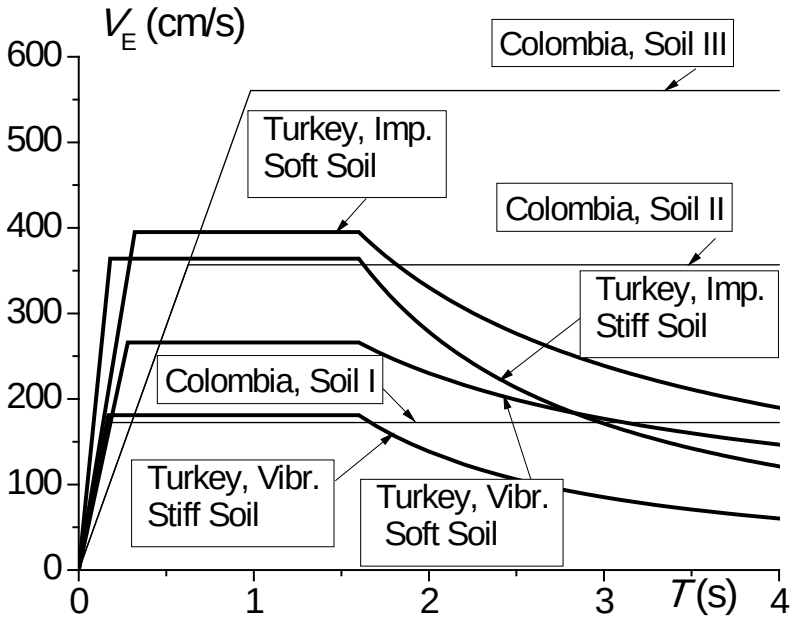

Figure 6-1 Comparison among the proposed spectra and the spectra proposed for Colombia

6.1.2 Spectra from the Japanese code.

Figure 6-2 shows with thin lines the design energy input spectra V_E prescribed by the current Japanese seismic code BSL [2009] to be used in conjunction with earthquake-resistant structural calculation based on energy balance. The BSL code classifies the surface geology in three types: (i) soil 1 is rock, stiff sand gravel and pre-Tertiary deposits; (ii) soil 3 includes alluvial layers mainly consisting of humus and mud whose depth is over 30 m or filled land more than 3 meters deep and worked within the past 30 years; (iii) soil 2 comprises layers other than types 1 and 3. The BSL code provides directly the V_D spectra. For comparison with the spectra proposed in this study, V_E has been estimated from V_D with the proposed equation (5-4) particularized for a vibratory earthquake with $M_s > 5.5$, and assuming $\zeta = 0.05$ and $\eta = 15$ (Table 5-1). The levels of V_E prescribed by BSL and those proposed in this study are similar in the medium period range (i.e. in the region where V_E is constant). However, in the short and large period ranges the levels prescribed by BSL are smaller and larger, respectively, than those proposed in this study. The levels proposed in this study for impulsive earthquakes are clearly larger than those proposed by BLS code.

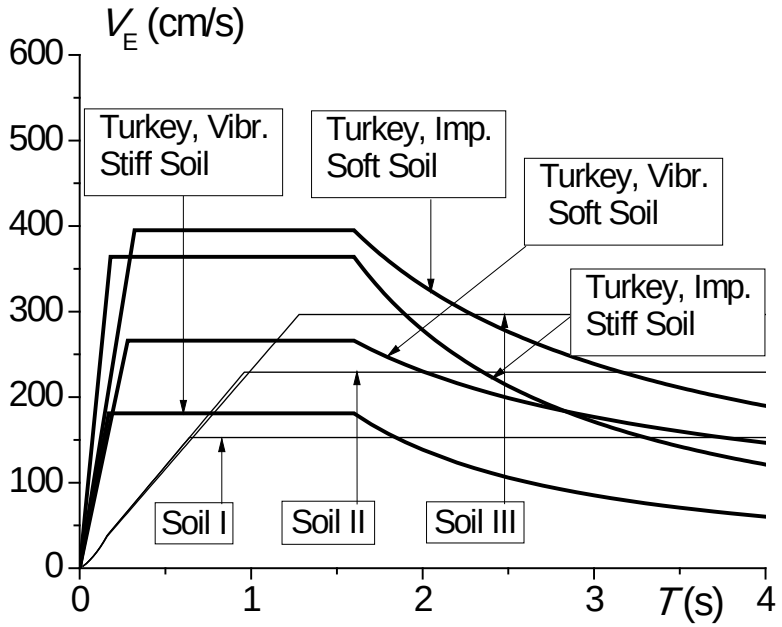

Figure 6-2 Comparison among the proposed spectra and the spectra proposed by BSL code

6.1.3 Spectra from [Akiyama 1999]

Figure 6-3 shows with thin lines the design energy input spectra proposed by Akiyama [1999] for Japan, considering four types of surface geology. Soil type I corresponds to hard rock or very hard conglomerates (shear wave velocity $v_s > 750$ m/s); type II corresponds to hard conglomerates, compact sand and gravel with $375 \le v_s \le 750$ m/s; type III corresponds to intermediate soils such as semi-compact sands and gravels with $175 \le v_s \le 375$ m/s; and type IV corresponds to soft soils with $v_s \le 175$ m/s. In the medium period range (i.e. the range where VE is constant) the spectra proposed in this study are close to those proposed by Akiyama.

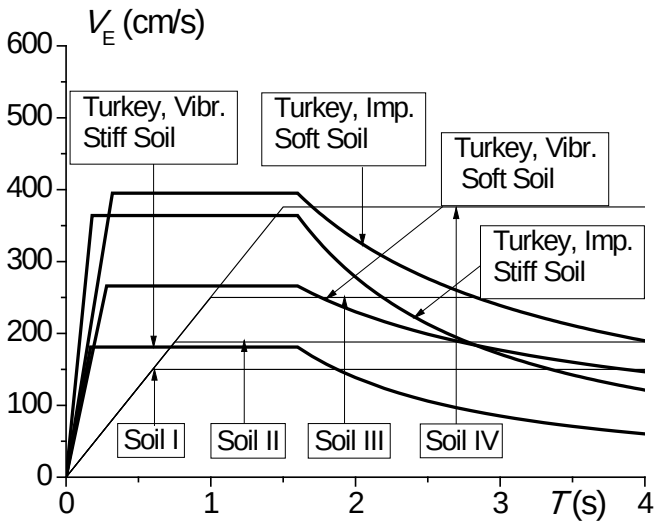

Figure 6-3 Comparison among the proposed spectra and the spectra proposed by Akiyama

6.1.4 Spectra from Iranian registers

Figure 6-4 shows the design energy input spectra proposed by Amiri el al. [2008] based on 110 Iranian earthquakes. These authors consider four types of soil (I, II, III and IV), corresponding to rock, stiff, medium and soft soil, respectively. It can be seen that the spectra proposed in this study for vibratory registers are approximately 30% larger in stiff soil and about 45% larger in soft soil, than those suggested by Amiri et al. For impulsive earthquakes the levels proposed in this study are about two times larger than those proposed by Amiri et al. It is worth noting that both regions (Iran and Turkey) have similar seismicity and the maximum design PGA in the Turkish seismic code (0.4 g) is similar to that of the Iranian code (0.35 g).

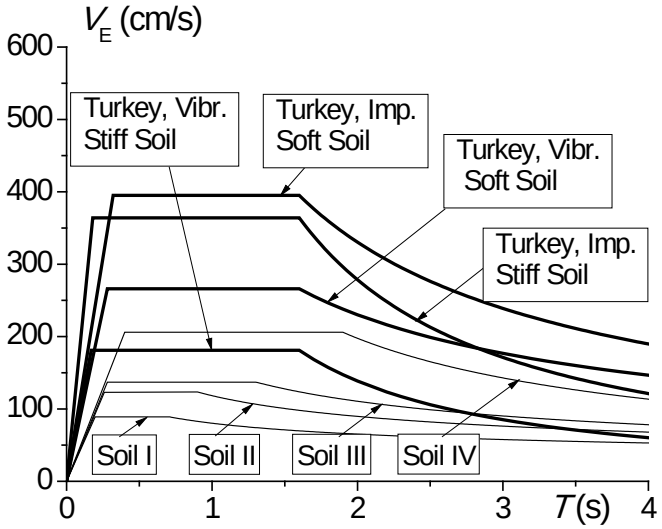

Figure 6-4 Comparison among the proposed spectra and the spectra proposed for Iran

6.1.5 Spectra from Greek registers

Figure 6-5 shows the VE spectra proposed by Tselentis et al. [2010] for six cities in Greece by applying a methodology different from that used in this study. These authors adopt the probabilistic approach originally developed by Cornell [1968] and extended later by Esteva [1970]. Each city has a different design PGA (0.16 g for Athens and Thessaloniki; 0.24 g for Patras, Korinthos and Chania; and 0.36 g for Argostolion), which varies in approximately the same range as the Turkish seismic code (i.e. from 0.15 g to 0.4 g). As observed in the figure, the spectra proposed by Tselentis et al. [2010] for these cities match quite well within the spectra developed in this study for vibratory records and for stiff and soft soil.

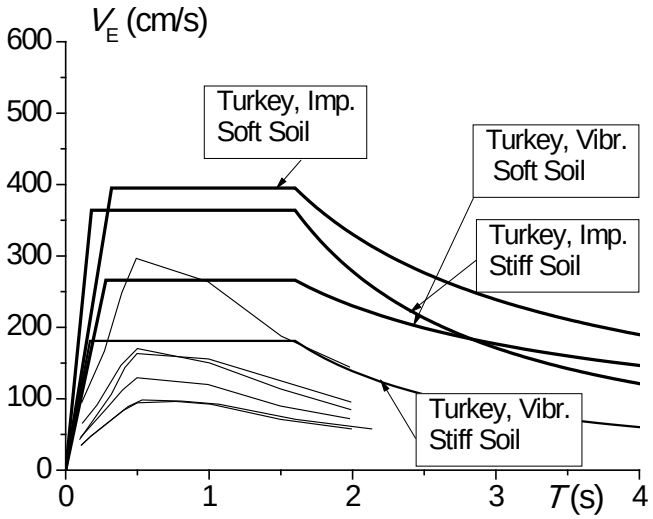

Figure 6-5 Comparison among the proposed spectra and the spectra proposed for Greece

6.1.6 Decanini, Mollaioli 1998 and 2001

Decanini and Mollaioli [1998] proposed general shapes for design energy input spectra (Figure 6-6), which are normalized by the Seismic Hazard Factor AE_I. These authors proposed different values for AE_I depending on the surface geology conditions, the interval of surface-wave magnitude M_S and the epicentral distance R_{epi}. For 12 km < R_{epi} < 30 km and 6.5 ≤ M_S ≤ 7.1, Decanini and Mollaioli proposed AE_I = 16000 cm^2/s for soil type S1 and AE_I = 50000 cm^2/s for soil type S2; this is identified as vibratory registers. For R_{epi} < 5 km and 6.5 ≤ M_S ≤ 7.1, Decanini and Mollaioli proposed AE_I = 65000 cm^2/s for soil type S1 and AE_I = 110000 cm^2/s for soil type S2; this is identified as impulsive registers. The design energy input spectra obtained by substituting these values of AE_I in the normalized spectra considered by Decanini and Mollaioli [1998] for μ = 1 are drawn in Figure 6-6 It can be seen that in the medium period range (i.e. constant input energy range) the levels of V_E proposed in this study are similar than those proposed by Decanini and Mollaioli; the descending branches begin earlier in the study by Decanini and Mollaioli but the rate of stabilization of the slope is higher.

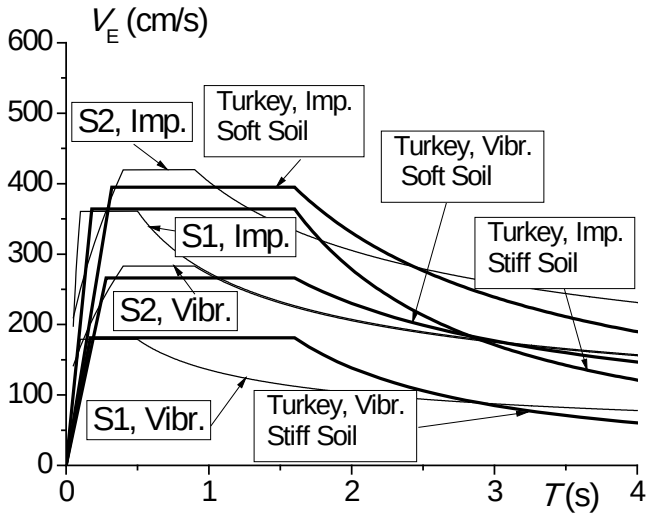

Figure 6-6 Comparison among the proposed spectra and the spectra proposed by Decanini and Mollaioli

7 Summary, Conclusions and Future Investigations

7.1 Summary

The main goal of this research is to propose design input energy spectra formulated in terms of equivalent velocity (V_E) and to propose empirical criteria for estimating the ratio between the hysteretic energy in terms of equivalent velocity (V_D) from the input energy (V_E). These spectra are intended for regions with design peak ground acceleration equal or higher than 0.3 g since they have been obtained from a number of Turkish inputs that were recorded in zones with such design PGAs, and many of the records used reached peak ground PGAs close or larger than 0.3 g.

The proposed spectra are derived through linear and nonlinear dynamic analyses for the selected Turkish registers. In the long and mid period ranges the analyses are linear, taking profit of the rather insensitivity of the spectra to the structural parameters other than the fundamental period; conversely, in the short period range, the spectra are more sensitive to the structural parameters and, hence, nonlinear analyses are required. The selected Turkish records are classified in eight groups with respect to the soil type (stiff soil and soft soil), the magnitude of the earthquake ($M_s \leq 5.5$ and $M_s > 5.5$) and the relevance of the near-source effects (impulsive and vibratory registers). For each of these groups, median and characteristic spectra are proposed; such levels are intended to correspond to the 50% and 95% percentiles, respectively. The proposed spectra have an initial linear growing branch (starting from the origin) in the short period range, a horizontal branch in the mid period range and a descending branch in the long period range. For nonlinear design, in each of the aforementioned eight groups empirical criteria are proposed to modify the slope of the initial branch according to the displacement ductility; the same criteria are considered for the median and characteristic spectra.

7.2 Conclusions

The linear and nonlinear V_E design spectra and the criteria for estimating the V_D / V_E ratio constitute the main output of this work.

The observation of the linear V_E spectra provides the following conclusions:

- As expectable, the higher magnitude earthquakes provide higher spectral amplitudes.
- The spectra for impulsive registers are larger than those for vibratory ones.
- The spectra for impulsive registers from high magnitude earthquakes show long-period peaks; they influence the rate of decreasing of the descending branch.
- For stiff soil the T_C corner periods (separating the initial and the flat branches) are smaller than for soft soil, mostly for high magnitude earthquakes. For impulsive registers the T_C periods are higher than for vibratory ones. For high magnitude earthquakes T_C periods are higher than for smaller magnitudes.
- For high magnitude earthquakes the T_D corner periods (separating the flat and the descending branches) are larger than for smaller magnitudes.

The observation of the nonlinear V_E spectra provides the following conclusions:

- The m_μ / m_1 ratios that correct the slopes of the initial branches are larger for higher values of μ.
- For medium and large values of μ, the ratios m_μ / m_1 tend to be higher for impulsive registers than for vibratory ones.
- Comparison among the constant value 1.2 suggested by Akiyama and the obtained ratios m_μ / m_1 shows that for displacement ductility bigger than about 5, the value proposed by Akiyama might be clearly unconservative.

The proposed criteria for estimating the ratio of V_E / V_D depend on period, on damping and on ductility; both displacement and accumulated ductility are considered. Noticeably, the influence of period is considered relevant; conversely, the influence of the parameters that characterize each group (soil type, earthquake magnitude and impulsivity) is negligible.

The proposed design spectra are compared with those obtained from other studies. The comparison shows that in some cases the proposed spectra are higher while in other cases they are smaller. Globally speaking, no huge differences are observed.

7.3 Future Investigations

From the obtained results, the following further researches are envisaged:

- To carry out similar studies for other seismic regions.

- The obtained spectra will be used to propose retrofit strategies for a number of vulnerable buildings in Turkey, focusing mainly in vulnerable concrete buildings. A significant part of this research will be oriented to obtain the damage concentration factors.

- The incorporation of the obtained spectra to the Turkish design code will be promoted.

- The influence of hysteretic behaviors other than the considered one (e.g. elastic-perfectly plastic) will be investigated.

- The influence of the impulsive character of the input (i.e. presence of velocity pulses) in the accumulated component of damage will be further investigated. The final objective is to assess the usefulness of energy spectra for impulsive registers.

References

1. ACI Committee 318 (2008). Building code requirements for structural concrete (ACI 318-08) and commentary. American Concrete Institute (ACI), Farmington Hills, Michigan.
2. Adang S. Earthquake-resistant structural design through energy demand and capacity. Earthquake Engineering & Structural Dynamics 36:2099–2117 (2007). DOI: 10.1002/eqe.718
3. Akiyama H. Earthquake-Resistant Design Method for Buildings Based on Energy Balance, Gihodo Shuppan, Tokyo (1999) 25-26.
4. Akiyama H. Earthquake-Resistant Limit-State Design for Buildings, University of Tokyo Press, Tokyo (1985).
5. Allen C. R. Active faulting in northern Turkey. Division of geological Science, California Institute of Technology Contribution (1969) No. 1577.
6. Ambraseys, N.N. and C. Finkel. The Seismicity of Turkey and Adjacent Areas, Eren Publications, Istanbul (1995) 37-43.
7. Amiri G.G. Darzi G.A. Amiri J.V. Design elastic input energy spectra based on Iranian earthquakes, Canadian Journal of Civil Engineering, 35 (2008) 635-646.
8. Arias A. A measure of earthquake intensity. Seismic Design for Nuclear Power Plants, edited by R. Hansen, MIT Press, Cambridge, MA (1970) 438–483.
9. ASCE 7-05. Minimum design loads for buildings and other structures. ASCE/SEI 7-05, American Society of Civil Engineers. Reston, VA. (2005).
10. Aschheim M., Gülkan P., Sezen H. Performance of buildings, 1999 Kocaeli, Turkey, Earthquake Reconnaissance Report, supplement to vol. 16 Earthquake Spectra (2000).
11. ATC-40, Seismic evaluation and retrofit of concrete buildings, volume 1, Report, SSC 96-01, Seismic Safety Commission, Redwood City, California, Applied Technology Council (1996).
12. ATC-58, Development of Performance-based Earthquake Design Guidelines, Applied Technology Council, Redwood City (2002).
13. Banon H. Veneciano D. Seismic safety of reinforced concrete members and structures, Earthquake Engineering and Structural Dynamics, 10 (1982) 179-193.
14. Barka, A.A. Kadinsky-Cade, K. Strike–slip fault geometry in Turkey and its influence on earthquake activity. Tectonics 7 (1998) 663–684.
15. Bayülke, N. Reedition history of seismic design code of Turkey, Bulletin of the İnternational İnstitute of Seismology and Earthquake Engineering (1992) 26:413-29.
16. Benavent-Climent A. Pujades L.G. López-Almansa F. Espectros de Input de Energía de Aplicación en el Proyecto Sismorresistente de Estructuras en Regiones de Sismicidad Moderada, CIMNE Monografía IS-43 (2001).
17. Benavent-Climent A. Pujades L.G. López-Almansa F. Design energy input spectra for moderate-seismicity regions, Earthquake Engineering and Structural Dynamics, 31 (2002) 1151–1172.
18. Benavent-Climent A. Akiyama H. López-Almansa F. Pujades L.G. Prediction of ultimate earthquake resistance of gravity-load designed RC buildings, Engineering Structures, 26, 8, (2004) 1103-1113. doi:10.1016/j.engstruct.2004.03.011.
19. Benavent-Climent A. An energy-based damage model for seismic response of steel structures, Earthquake Engineering and Structural Dynamics, 36 (2007) 1049–1064.
20. Benavent-Climent A. Zahran R. Seismic evaluation of existing RC frames with wide beams using an energy-based approach, Earthquakes and Structures, 1(1) (2010) 93-108.
21. Berg G.V. Thomaides S.S. Energy consumption by structures in strong-motion earthquakes, Proceedings of the Second World Conference on Earthquake Engineering, 2 (1960) 681-697.
22. Bertero R.D. Bertero V.V. Teran-Gilmore A. Performance-based earthquake-resistant design based on comprehensive design philosophy and energy concepts, Proceedings of the Eleventh World Conference on Earthquake Engineering, Disc 2 (1996) 611.
23. Boore D.M. On Pads and Filters, Processing Strong-Motion Data, Bulletin of the Seismological Society of America, 95 April (2005) 2, 745–750. doi: 10.1785/0120040160.
24. Bracci J.M. Kunnath S.K. Reinhorn A.M. Seismic performance and retrofit evaluation for reinforced concrete structures, Journal of Structural Engineering (ASCE), 123(1) (1997), 3–10.
25. Bruneau M. Wang N. Normalized energy-based methods to predict the seismic ductile response of SDOF structures, Engineering Structures (1996) 13-28.
26. BSL, The Building Standard Law of Japan, The Building Center of Japan, Tokyo (2009) (English version on CD available in http://118.82.115.195/en/services/publication.html).

27. Büyüköztürk, O. Güneş, O. Earthquake Risk Assessment and Hazard Reduction for Structures: Methodologies and Collaborative Research Needs. *Proceedings of NSF/TUBITAK Turkey/Taiwan Grantee Workshop* (2002) March 24-26, Antalya, Turkey.
28. Chai Y.H. Energy-based linear damage model for high-intensity seismic loading, Journal of Structural Engineering ASCE, 121(5) (1995) 857-863.
29. Chai Y.H. Incorporating low-cycle fatigue model into duration-dependent inelastic design spectra, Earthquake Engineering and Structural Dynamics, 34 (2004) 83–96.
30. Chapman M.C. On the use of elastic input energy for seismic hazard analysis, Earthquake Spectra, 15(4) (1999) 607-635.
31. Chintanapakdee C. Chopra A.K. Evaluation of modal pushover analysis using generic frames, Earthquake Engineering and Structural Dynamics, 32 (2003) 417–442.
32. Chopra A.K. Goel R.K. A modal pushover analysis procedure to estimating seismic demands for buildings: theory and preliminary evaluation, PEER Report 2001/03, Pacific Earthquake Engineering Research Center, University of California, Berkeley.
33. Chopra A.K. Goel R.K. A modal pushover analysis procedure for estimating seismic demands for buildings, Earthquake Engineering and Structural Dynamics, 31 (2002) 561–582.
34. Chou C.C. Uang C.M. Establishing absorbed energy spectra -an attenuation approach, Earthquake Engineering and Structural Dynamics, 29 (2000) 1441-1455.
35. Chou C.C. Uang C.M. A procedure for evaluating seismic energy demand of framed structures. Earthquake Engineering and Structural Dynamics 32 (2003) 229–44.
36. Clough R.W. Penzien J. Dynamics of Structures, McGraw Hill, New York (1993).
37. Cornell C.A. Engineering seismic risk analysis, Bulletin of the Seismological Society of America, 58 (1968) 1583-1606.
38. Cosenza E. Manfredi G. Ramasco K. An evaluation of the use of damage functional in earthquake-resistant design, Proc. 9th European Conference on Earthquake Engineering, The Kucherenko Tsniik of the USSR, Gosstroy, Moscow, 9 (1990) 303-312.
39. Decanini L. Mollaioli F. Formulation of Elastic Earthquake Input Energy Spectra, Earthquake Engineering and Structural Dynamics, 27 (1998) 1503-1522.
40. Decanini L.D. Mollaioli F. An energy-based methodology for the seismic assessment of seismic demand, Soil Dynamics and Earthquake Engineering, 21 (2001) 113-137.
41. De Leon D. Ang A.H.S. Determination of optimal target reliabilities for design and upgrading of structures, Structural Safety, 19(1) (1997) 19-103.
42. Dewey, J.F. Pitman, W.C. Ryan, W.B.F. and Bonnin, J. Plate tectonics and the evolution of the Alpine system, Geol. Soc. Am. B. 84, 3137–3180 (1973).
43. Douglas J. Earthquake ground motion estimation using strong-motion records: A review of equations for the estimation of peak ground acceleration and response spectral ordinates. Earth-Science Reviews, 61, 43-104 2003.
44. Duyguluer, M. F. The history of seismic design code of Turkey, Bulletin of the international Institute of Seismology and Earthquake Engineering 31: 177-92 (1997).
45. EERC 1995, Performance-based Seismic Design of Buildings: An Action Plan, The Earthquake Engineering Research Center Library, The Earthquake Image Information System (EqIIS), University of California, Berkeley (1995). http://nisee.ce.berkeley.edu/~eqiis/eqiis.html.
46. EN-1998 (EC-8), Provisions for the design of earthquake-resistant structures, European Committee of Normalization (2004).
47. Erberik A. Sucuoğlu H. Seismic energy dissipation in deteriorating systems through low cycle fatigue, Earthquake Engineering and Structural Dynamics, 33 (2004) 49–67.
48. Erdik, M. Alpay, B. Y. Onur, T. Sesetyan, K. and Birgoren, G.: Assessment of earthquake hazard in Turkey and neighboring regions, Annali di Geofisica, 42, 1125–1138 (1999).
49. Erdogan Ö. Main Seismological features of recently compiled Turkish strong motion database. Msc. Thesis. Middle East Technical University, Ankara, Turkey (2008).
50. Esteva L. Seismic risk and seismic design decision, Seismic Design for Nuclear Power Plants, Massachussetts Inst. of Tech. Press, (1970) 142-182.
51. Fajfar P. Fischinger M. N2. A method for nonlinear seismic analysis of regular structures, Proceedings of the 9th World Conference on Earthquake Engineering, Tokyo-Kyoto, Japan, 5 (1988) 111–116.
52. Fajfar P. Vidic T. Fischinger M. On energy demand and supply in SDOF systems, In: Nonlinear Seismic Analysis and Design of Reinforced Concrete Buildings, Elsevier, Amsterdam (1992) 41-61.
53. Fajfar P. Equivalent ductility factors taking into account low-cycle fatigue, Earthquake Engineering & Structural Dynamics, 21 (1992) 837-848.

54. Fajfar P. Vidic T. Consistent inelastic design spectra: hysteretic and input energy, Earthquake Engineering and Structural Dynamics, 23 (1994) 523-537.
55. FEMA 349, Action Plan for Performance-Based Seismic Design, FEMA/EERI, Washington DC, (2000).
56. FEMA 350, Recommended Seismic Design Criteria for New Steel Moment-Frame Buildings, FEMA/SEAOC/ATC/CUREe (2000).
57. FEMA 356, Guidelines for Seismic Rehabilitation of Buildings, Vol. 1: Guidelines, (formerly FEMA 273) FEMA, Washington DC (2000).
58. García Reyes L.E. Dinámica estructural aplicada al diseño sísmico, Universidad de Los Andes, Bogotá, Colombia (1998).
59. Gülkan P. Building code enforcement prospects: failure of public policy. Chapter 15 of 1999 Kocaeli, Turkey, earthquake reconnaissance report, supplement A Vol. 16, Earthquake Spectra, (2000) 351-367.
60. Gunturi S.K. Building specific earthquake damage estimation, Ph.D. Thesis, Stanford University, Stanford, California (1992).
61. Gupta B, Kunnath S.K. Adaptive spectra-based pushover procedure for seismic evaluation of structures, Earthquake Spectra, 16(2) (2000) 367–392.
62. Guyader A.C., Iwan, W.D. Determining Equivalent Linear Parameters for Use in a Capacity Spectrum Method. Journal of Structural Engineering, 132(1): 59-67 (2006).
63. Hall W.L. Nau J.M. Zahrah T.F. Scaling of response spectra and energy dissipation in SDOF systems, Proceedings of the Eighth World Conference on Earthquake Engineering, IV (1984) 7-14.
64. Hamburger R.O. Performance-Based Analysis and Design Procedure for Moment Resisting Steel Frames, Background Document, SAC Steel Project (1998).
65. Hempton, M. R. Structure and deformation history of Bitlis suture near lake Hazar, southeastern Turkey, B. Geol. Soc. Am. 96, 233–243 (1985).
66. Housner G.W. Limit design of structures to resist earthquakes, Proceedings of First World Conference on Earthquake Engineering, 5 1-12 (1956).
67. Housner G.W. Jennings P.C. The capacity of extreme earthquake motions to damage structures, Structural and Geotechnical Mechanics, A volume honoring Nathan M. Newmark (1977) 102-116.
68. Housner G.W. Historical Review of Earthquake Engineering, In: Selected Earthquake Engineering Papers of George W. Housner, American Society of Civil Engineers, New York (1990) 764–777.
69. IBC (International Building Code), International Code Council (2000).
70. Jiao Y. Yamada S. Kishiki S. Shimada Y. Evaluation of plastic energy dissipation capacity of steel beams suffering ductile fracture under various loading histories. Earthquake Engineering and Structural Dynamics 40:1553–1570 DOI: 10.1002/eqe.1103, (2011).
71. Kato B. Akiyama H. Energy input and damages in structures subjected to severe earthquakes, Journal of Structural and Construction Engineering Trans. AIJ, 235 (1975) 9-18 (in Japanese).
72. Kempton J.J. Stewart J.P. Prediction Equations for Significant Duration of Earthquake Ground Motions Considering Site and Near-Source Effects. Earthquake Spectra (2006) 22:4 985–1013.
73. Kircher, C. Nassar, A. Kustu, O. y Holmes, W. Development of building damage functions for earthquake loss estimation, Earthquake Spectra, 13(4) (1997) 663-682.
74. Krawinkler H. Pros and cons of a pushover analysis of seismic performance evaluation, Engineering Structures 20 (1998) 452-464.
75. Kunnath S.K. Gupta B. Validity of deformation demand estimates using nonlinear static procedures, Proceedings of U.S.–Japan Workshop on Performance-Based Earthquake Engineering Methodology for Reinforced Concrete Building Structures, Sapporo, Hokkaido, Japan (2000) 117–128.
76. Kuwamura H. Galambos T.V. Earthquake load for structural reliability, Journal of Structural Engineering ASCE, 115(6) (1989) 1446-1462.
77. Kuwamura H. Kirino Y. Akiyama H. Prediction of earthquake energy input from smoothed Fourier amplitude spectrum, Earthquake Engineering and Structural Dynamics, 23 (1994) 1125-1137.
78. Lawson R.S. Krawinkler H. Cumulative damage potential of seismic ground motion, Proceedings of the 10th European Conference on Earthquake Engineering, 10 (1995) 79-86.
79. Leelataviwat S., Saewon W., Goel S.C. Application of Energy Balance Concept in Seismic Evaluation of Structures. Journal of Structural Engineering (2009) 135(2) .
80. Leon D. and Ang A.H.S. A damage model for reinforced concrete buildings, further study with the 1985 Mexico City earthquake, Proc. 6th International Conference on Structural Safety and Reliability, Barkema A.A. Rotterdam, The Netherlands, 3, (1994) 2081-2087.
81. Lybas J. Sozen M. Effect of beam strength and stiffness on dynamic behavior of reinforced concrete coupled walls, Civil Engineering Studies, Structural Research Series, N.444, University of Illinois, Urbana (1977).

82. Malhotra P.K. Return Period of Recorded Ground Motions, Journal of Structural Engineering, 132(6) (2006) 833-839.
83. Manfredi G. Evaluation of seismic energy demand, Earthquake Engineering and Structural Dynamics, 30 (2001) 485-499.
84. Matsumori T. Otani S. Shiohara H. Kabeyasawa T. Earthquake member deformation demands in reinforced concrete frame structures, Proceedings of U.S.–Japan Workshop on Performance-Based Earthquake Engineering Methodology for Reinforced Concrete Building Structures, Maui, Hawaii, (2000) 79–94.
85. McCabe S.L. Hall W. J. Assessment of Seismic Structural Damage, J. Struct. Engrg. 115(9) (1989) 2166-2183.
86. McKenzie, D. P. Active tectonics of the Mediterranean region, Geophys. J. R. Astron. Soc. 30, 109–185 (1972).
87. McKenzie, D.P. Active tectonics of the Alpine-Himalayan belt: the Aegean Sea and surrounding regions, Geophys. J. Royal Astron. Soc. 55, 217–254 (1978).
88. Miranda E., Bertero V.V. Evaluation of strength reduction factors for earthquake-resistant design. Earthquake Spectra, 10:2, 357-379 (1994).
89. NBCC. National Building Code of Canada. Institute for Research in Construction, National Research Council of Canada, Ottawa Ont. (2005).
90. NCSE-02. Norma de Construcción Sismorresistente: Parte General y Edificación. Ministerio de Fomento (2002).
91. Newmark N.M., Hall W.J. Seismic design criteria for nuclear reactor facilities. Buildings practices for disaster mitigation. Rep. Nº 45. National Bureau of Standards. U. S. Dept. of commerce, 209-236 (1973).
92. NSR-98, Normas Colombianas de Diseño y Construcción Sismo Resistente, Asociación Colombiana de Ingeniería Sísmica (1998).
93. NSR-10, Normas Colombianas de Diseño y Construcción Sismo Resistente, Asociación Colombiana de Ingeniería Sísmica (2010).
94. Ohashi U. History of Structural Standards for Buildings in Japan, Japan Building Center (1993) (in japanese).
95. Ordaz M., Pérez-Rocha L.E. Estimation of strength-reduction factors for elastoplastic systems: a new approach, Earthquake Engineering and Structural Dynamics, Vol. 27, 889-901 (1998).
96. Papazachos, B. C. and Comninakis, P. E.: Geophysical and tectonic features of the Aegean arc, J. Geophys. Res. 76, 8517–8533 (1971).
97. Paret T.F. Sasaki K.K. Eilbeck D.H. Freeman S.A. Approximate inelastic procedures to identify failure mechanisms from higher mode effects, Proceedings of the 11th World Conference on Earthquake Engineering, Acapulco, Mexico, 966 (1996).
98. Park Y.J. Ang A. Mechanistic seismic damage model for reinforced concrete, Journal of Structural Engineering, ASCE 111 (1985) 722-739.
99. Park Y.J. Reinhorn A.M. Kunnath S.K. IDARC: Inelastic Damage Analysis of Reinforced Concrete Frame-Shear Wall Structures, Technical Report NCEER-87-0008, National Center for Earthquake Engineering Research, State University of New York at Buffalo (1987).
100. Powell, G. Performance based design using nonlinear analysis, Computers and Structures, Inc., (CSI). Berkeley (2007).
101. Priestley M.J.N. Calvi G.M. Kowalsky M.J. Displacement-Based Seismic Design of Structures, IUSS Press (2007).
102. Şaroğu, F. Emre, O. and Kuşcu, I.: Active fault map of Turkey, General Directorate of Mineral Research and Exploration, Ankara, Turkey (1992).
103. Sasaki K.K. Freeman S.A. Parent T.F. Multimode pushover procedure (MMP)—a method to identify the effects of higher modes in a pushover analysis, Proceedings of the 6th U.S. National Conference on Earthquake Engineering, Seattle, Washington (1998).
104. SEAOC, Vision 2000: Performance Based Seismic Engineering of Buildings, San Francisco (1995).
105. Şengör, A. M. C.: The North Anatolian Transform Fault: its age, offset and tectonic significance, J. Geol. Soc. London, 136, 269–282 (1979).
106. Şengör, A. M. C. Görür, N. and Şaroğu, F.: Strike-slip faulting and related basin formation in zones of tectonic escape: Turkey as a case study, in: Strike-slip Faulting and Basin Formation, edited by: Biddle K. T. Christie-Blick, N. Soc. Econ. Paleontol. Mineral. Sp. Pub. 37, 227–264 (1985).
107. Sezen H., Kenneth J.E., Whittaker A.S., Mosalam K.M., Wallace J.W., Stanton J.F. Structural Engineering Reconnaissance of the Kocaeli (Izmit) Turkey Earthquake of August 17 1999. Pacific Earthquake Engineering Research Center (2000) (PEER Report 2000-09).

108. Soo Y. Meyer C. Shizuoka M. Modeling of concrete damage, ACI Structural Journal, 86 (1989) 259-271.
109. Stone W.C. and Taylor A.W. ISDP: Integrated approach to seismic design of reinforced concrete structures, Journal of Structural Engineering, ASCE, 120(12) (1994) 3548-3566.
110. Sucuoğlu H. Erberik A. Energy-based hysteresis and damage for deteriorating systems, Earthquake Engineering and Structural Dynamics, 33 (2004) 69–88.
111. Tanahashi R. Studies on the non-linear vibrations of structures subjected to destructive earthquakes, Proceedings of first World Conference on Earthquake Engineering (1956).
112. Teran-Gilmore A. Jirsa J.O. A simple damage model for practical seismic design that accounts for low cycle fatigue, Earthquake Spectra, 21(3) (2005) 803-832.
113. Teran-Gilmore A. Jirsa J.O. Energy demands for seismic design against low-cycle fatigue, Earthquake Engineering and Structural Dynamics, 36 (2007) 383-404.
114. Triffunac M.D. Brady A.G. A study on the duration of strong earthquake ground motion. Bulletin of the Seismlological Society of America 65:3 (1975) 581-626.
115. TSC 2007. Turkish Seismic Code. Specification for Buildings to be constructed in Seismic Zones. Ministry of Public Works and Settlement Turkey (2007).
116. Tselentis G.A. Danciu L. and Sokos E. Probabilistic Seismic Hazard Assessment in Greece, Part II: Acceleration Response Spectra and Elastic Input Energy Spectra, Natural Hazards & Earth Science Systems (2010) 10, 41-49. doi:10.5194/nhess-10-41-2010
117. TS-500. Turkısh Standards Institute, Building code requirements for reinforced concrete, Ankara, TURKEY (1985).
118. Uang C.M. Bertero V.V. Use of energy as a design criterion in earthquake–resistant design, Report No. UBC/EERC-88/18, Earthquake Engineering Research Center, University of California (1988).
119. Uang C.M. Bertero V.V. Evaluation of seismic energy in structures, Earthquake Engineering and Structural Dynamics (1990) 77-90.
120. UBC, Uniform Building Code. International Council of Building Officials (1997).
121. Vamvatsikos D. Cornell C.A. Tracing and post-processing of IDA curves: Theory and software implementation, Report No. RMS-44, RMS Program, Stanford University, Stanford (2001).
122. Vamvatsikos D. Cornell C.A. Incremental dynamic analysis, Earthquake Engineering & Structural Dynamics, 31 (2002) 491–514.
123. Vamvatsikos D. Seismic performance, capacity and reliability of structures as seen through incremental dynamic analysis, Doctoral dissertation, Stanford University (2002).
124. Vega J. del Rey I. Alarcón E. Pounding force assessment in performance-based design of bridges, Earthquake Engineering & Structural Dynamics, 38 (2009) 1525-1544.
125. Veletsos A. Newmark N.M. Effect of inelastic behavior on response of simply systems to earthquake motions, Proceedings of the Second World Conference on Earthquake Engineering (1960) 895-912.
126. Yei L. Otani S. Maximum seismic displacement of inelastic systems based on energy concept. Earthquake Engineering and Structural Dynamics 28 (1999) 1483-1499.
127. Zahrah T.F. Hall W.J. Earthquake energy absorption in SDOF systems, Journal of Structural Engineering, 110 (1984) 1757-1772.
128. Zhu T.J. Tso W.K. Design of torsionally unbalanced structural systems based on code provisions II: strength distribution, Earthquake Engineering & Structural Dynamics, 21 (1992) 629-644.

Appendix A Construction Typologies in Turkey

In Turkey there are thousands of apartment buildings vulnerable to severe damage in a moderate or larger earthquake [Aschheim, Gulkan 2000]. Many different kinds of structural framing are being used in these buildings; where in new buildings frame-shear wall interactive systems are also used and industrial buildings are constructed usually either reinforced concrete (cast in-place or pre-cast) or steel frame structures (Figure A-1). In urban areas, the mainly used structural system consists of reinforced concrete frames with unreinforced masonry infills [Sezen et al. 2000]. This typical structural system is utilized for all building heights and occupancy, from single-story commercial to multistory residential and office buildings. These buildings are typically three to seven storeys and consist of relatively poorly detailed and constructed reinforced concrete frame members in filled to various extents by unreinforced masonry walls [Aschheim et al. 2000] (Figure A-2).

In Turkey both individuals and registered contractors undertake building construction work, so that the quality of the construction of residential and commercial buildings in Turkey varies widely. Commercial construction is typically built by registered contractors and was generally of better quality than residential construction. The damages to the reinforced concrete buildings in Turkey after the earthquakes can be attributed to several factors such as construction practices and design failures. The performance of these buildings mainly depends on their construction details [Gülkan 2000].

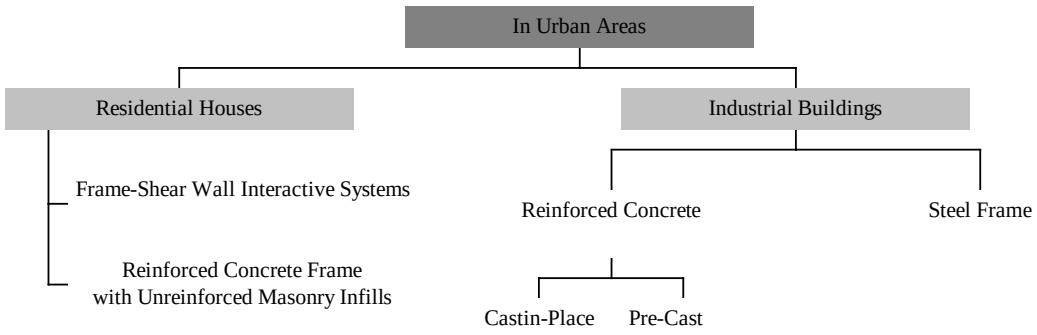

Figure A-1 Predominant structural system in urban areas in Turkey

.

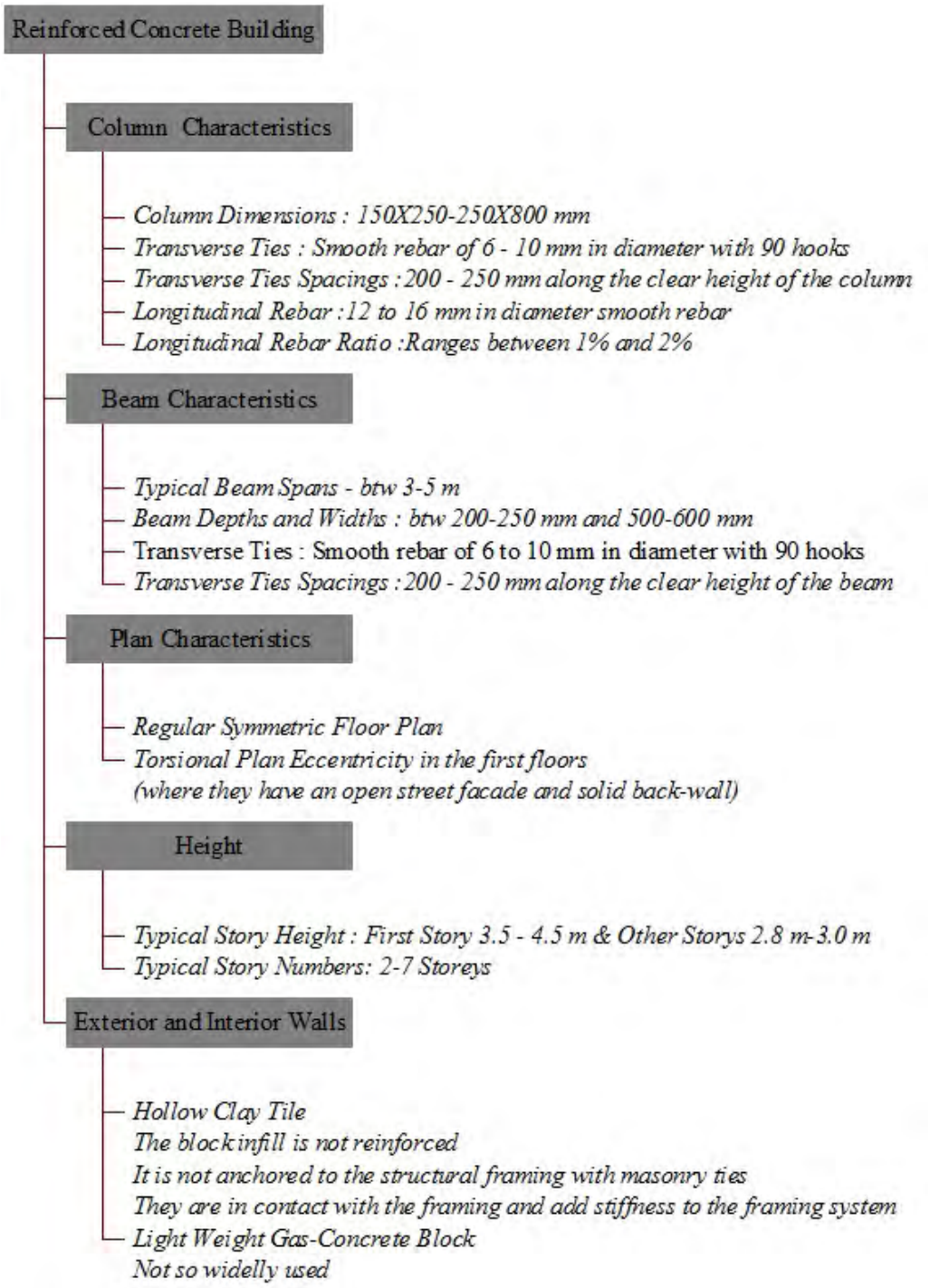

Figure A-2 Details of a typical reinforced concrete building in Turkey that experiences damages in earthquakes

Appendix B Calculation of the slope of the initial branch of input energy spectra

In this appendix it is described how to obtain the slope of the initial branch for the linear and nonlinear input energy spectra. This procedure is repeated for NS and EW component of each register.

For each nonlinear analysis the slope of the initial smoothed branch is obtained as the best linear fit in the range $0 - T_C$; such slope is termed m_μ. Figure B-2 to Figure B-19 display the values of m_μ corresponding to $\zeta = 0.02$, $\zeta = 0.05$ and $\zeta = 0.10$, respectively. The ratio m_μ / m_1 is shown in Figure B-20 to Figure B-22; m_1 (Figure B-1) is the linear slope, i.e. corresponding to $\mu = 1$.

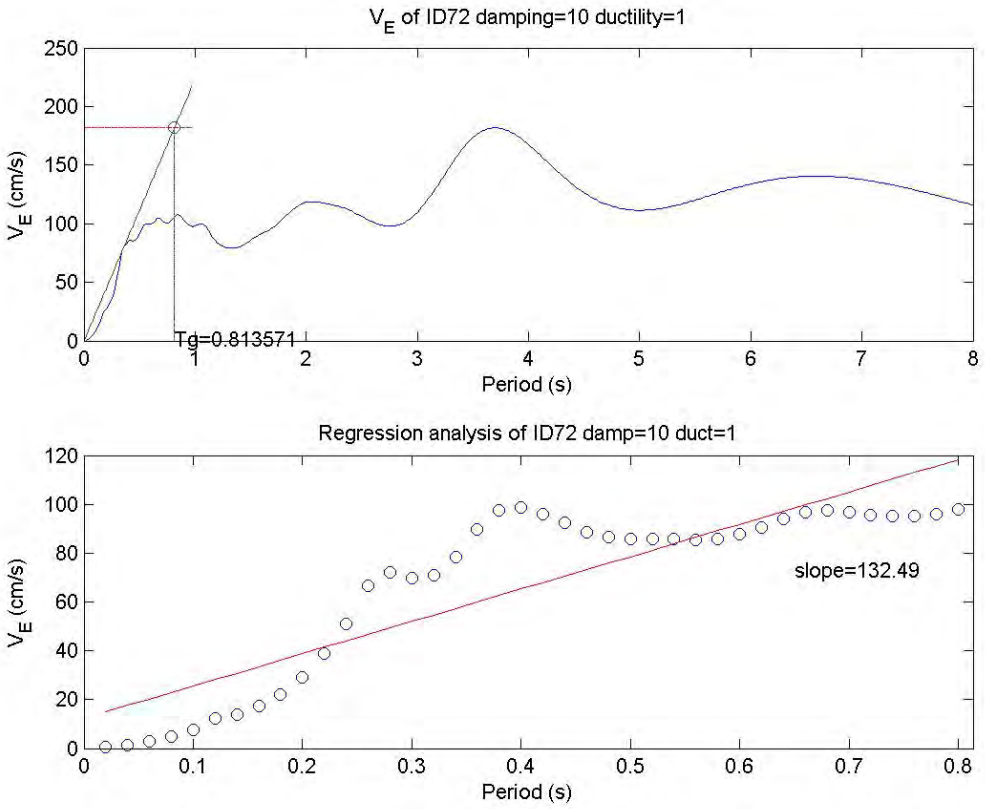

Figure B-1 Slope of the initial branch for the linear input energy spectra. $\zeta = 0.10$. $\mu = 1$

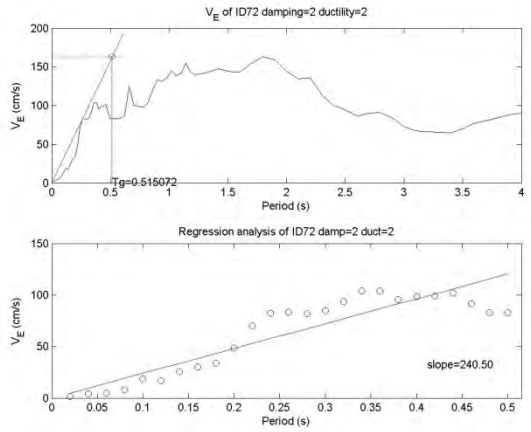

Figure B-2 Slope of the initial branch for the nonlinear input energy spectra. ζ = 0.02. μ= 2

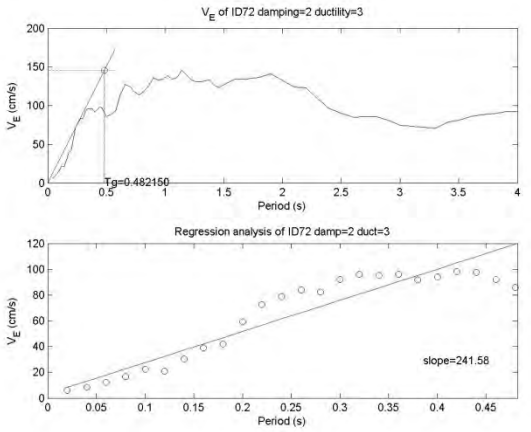

Figure B-3 Slope of the initial branch for the nonlinear input energy spectra. ζ = 0.02. μ= 3

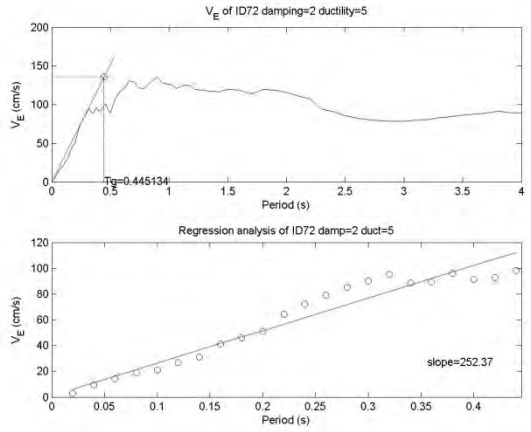

Figure B-4 Slope of the initial branch for the nonlinear input energy spectra. ζ = 0.02. μ= 5

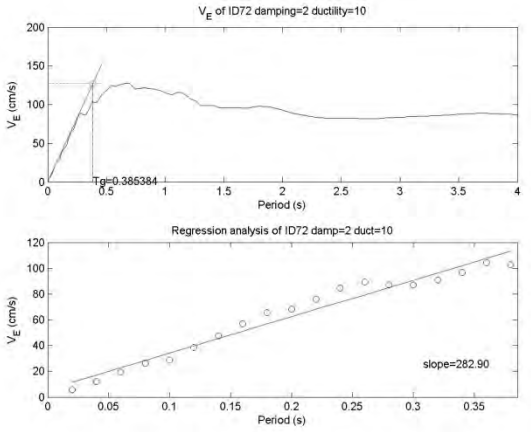

Figure B-5 Slope of the initial branch for the nonlinear input energy spectra. ζ = 0.02. μ= 10

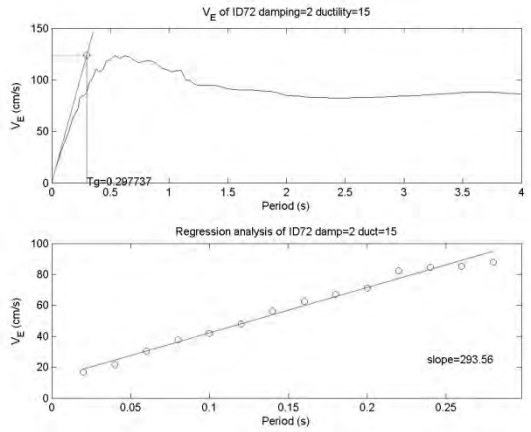

Figure B-6 Slope of the initial branch for the nonlinear input energy spectra. ζ = 0.02. μ= 15

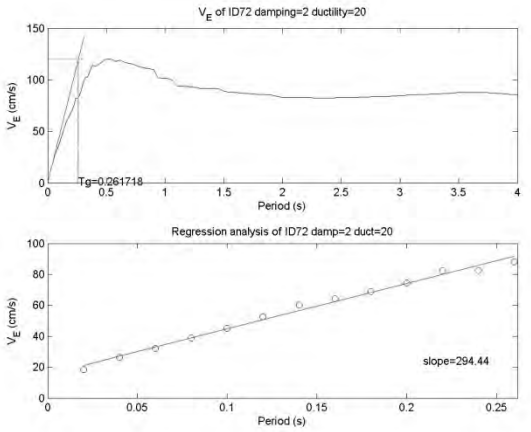

Figure B-7 Slope of the initial branch for the nonlinear input energy spectra. ζ = 0.02. μ= 20

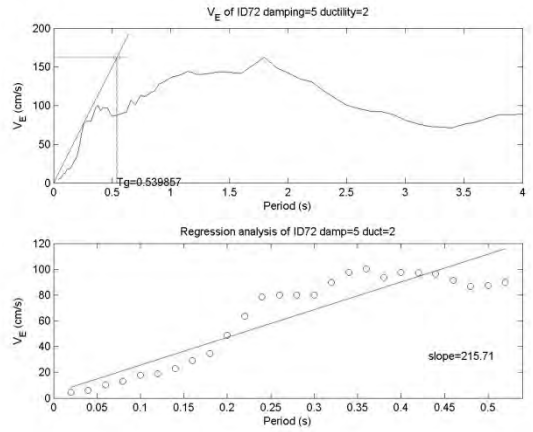

Figure B-8 Slope of the initial branch for the nonlinear input energy spectra. ζ = 0.05. μ= 2

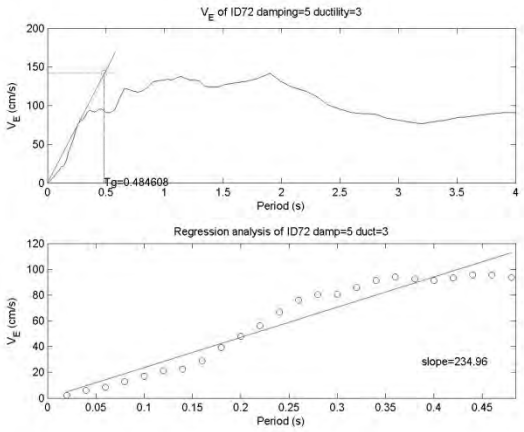

Figure B-9 Slope of the initial branch for the nonlinear input energy spectra. ζ = 0.05. μ= 3

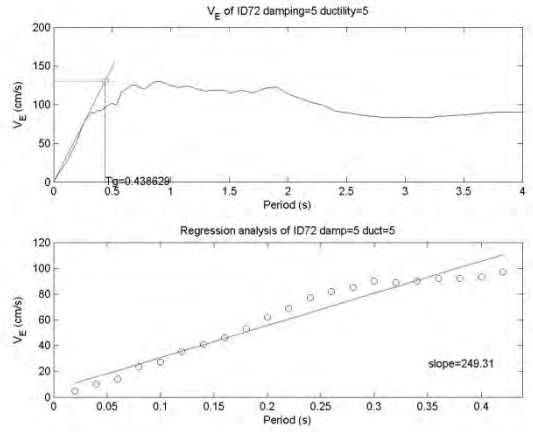

Figure B-10 Slope of the initial branch for the nonlinear input energy spectra. ζ = 0.05. μ= 5

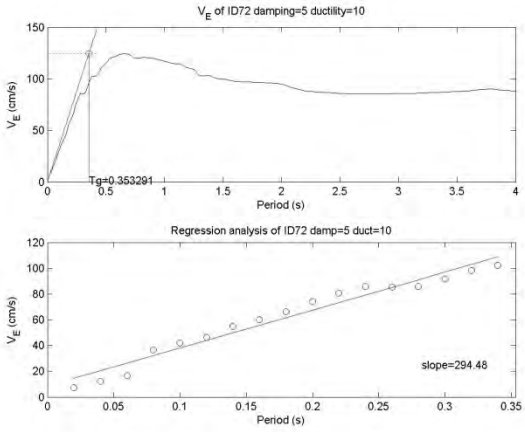

Figure B-11 Slope of the initial branch for the nonlinear input energy spectra. ζ = 0.05. μ= 10

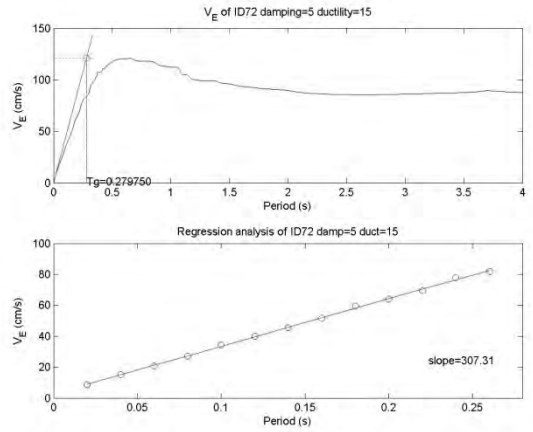

Figure B-12 Slope of the initial branch for the nonlinear input energy spectra. ζ = 0.05. μ= 15

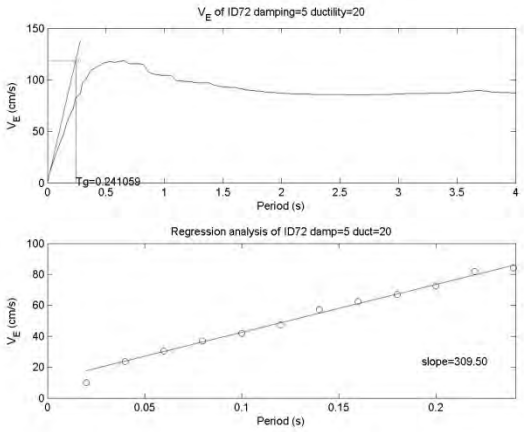

Figure B-13 Slope of the initial branch for the nonlinear input energy spectra. ζ = 0.05. μ= 20

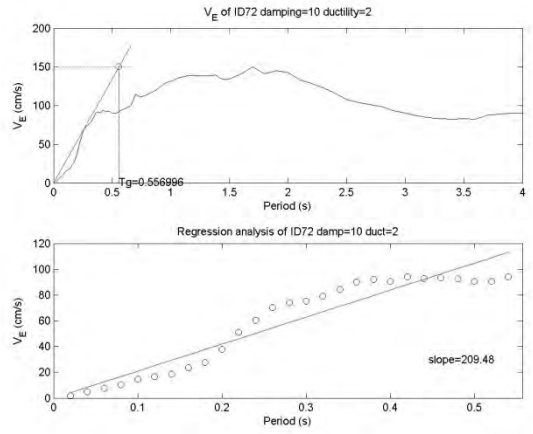

Figure B-14 Slope of the initial branch for the nonlinear input energy spectra. ζ = 0.10. μ= 2

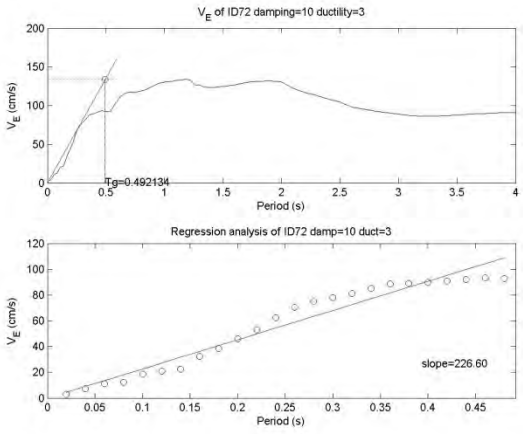

Figure B-15 Slope of the initial branch for the nonlinear input energy spectra. ζ = 0.10. μ= 3

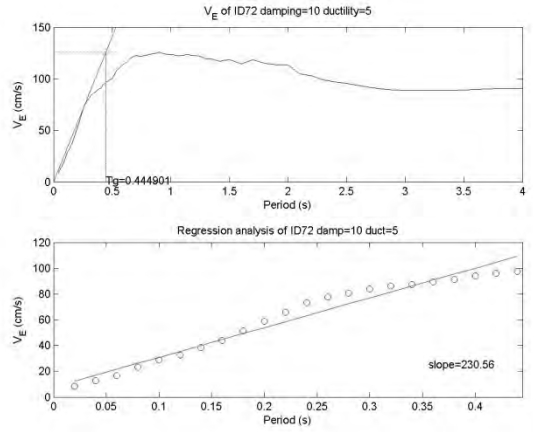

Figure B-16 Slope of the initial branch for the nonlinear input energy spectra. ζ = 0.10. μ= 5

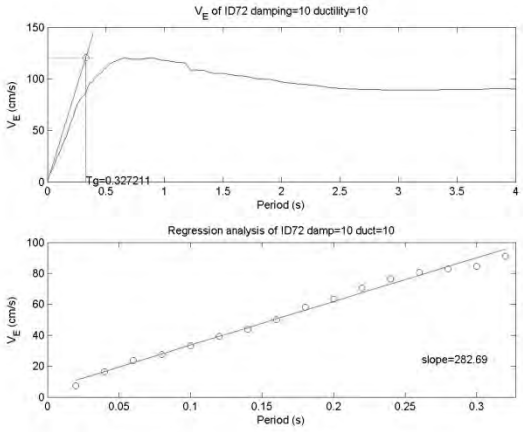

Figure B-17 Slope of the initial branch for the nonlinear input energy spectra. ζ = 0.10. μ= 10

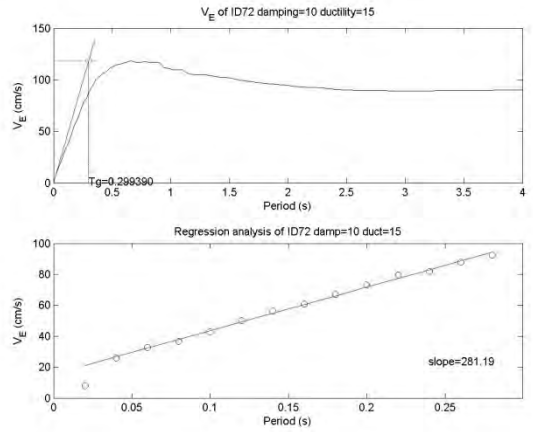

Figure B-18 Slope of the initial branch for the nonlinear input energy spectra. ζ = 0.10. μ= 15

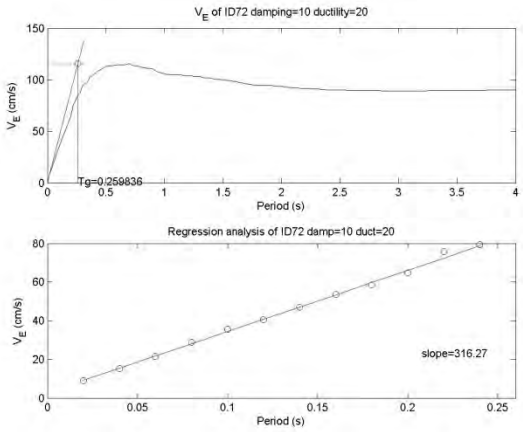

Figure B-19 Slope of the initial branch for the nonlinear input energy spectra. ζ = 0.10. μ= 20

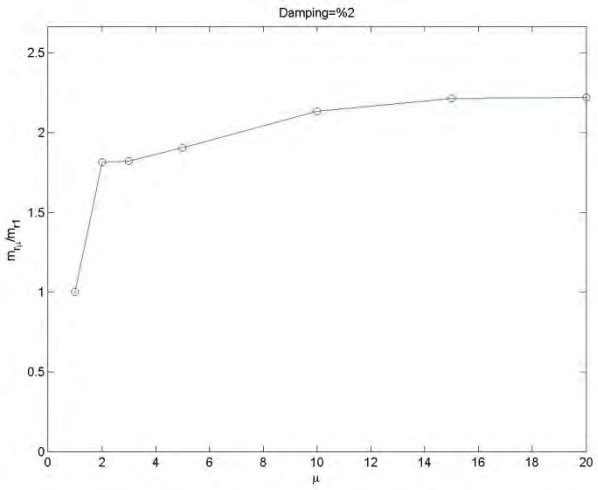

Figure B-20 Factor modifying the slope of the initial branch of the linear V_E spectra. $\zeta = 0.02$.

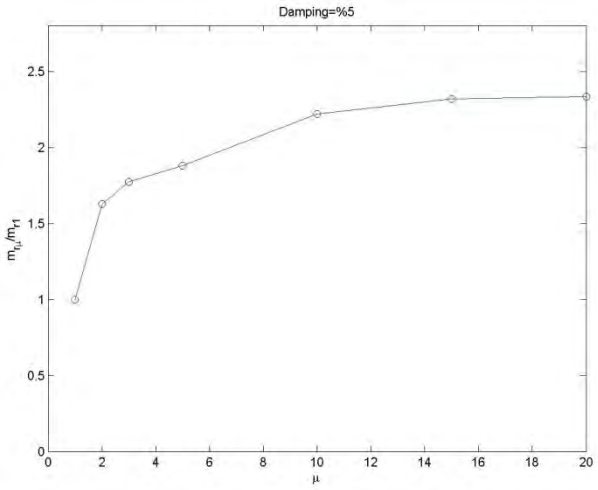

Figure B-21 Factor modifying the slope of the initial branch of the linear V_E spectra. $\zeta = 0.05$.

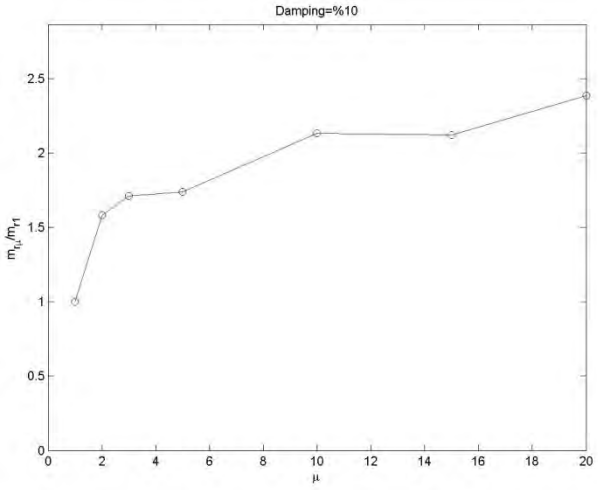

Figure B-22 Factor modifying the slope of the initial branch of the linear V_E spectra. $\zeta = 0.10$.

Appendix C Publications generated during this research

This appendix list the main publications generated during this research.

- H. Araníbar, G. Palazzo, U. Yazgan, J.M. Franco, F. López Almansa, F. Crisafulli. Mass use of energy dissipators for seismic protection and retrofit of buildings in earthquake-prone regions. Applications to Bolivia, Argentina and Turkey. 9th World Seminar on seismic isolation, energy dissipation and active vibration control of structures. Kobe (Japan). Japan Association for Vibration Technologies (JAVIT). Vol. II. Art. 28. 465-487 (2006).
- F. López Almansa, A. Benavent, D.A. Bravo, A.U. Yazgan. Design Energy Spectra for Colombia and Turkey. 14th European Conference on Earthquake Engineering (14ECEE). Ohrid (Macedonia) (2010).
- A.U. Yazgan, F. López Almansa, A. Benavent Climent. Proposal of design energy spectra based on Turkish registers. 4ª Conferencia Nacional de Ingeniería Sísmica. Granada (Spain) (2011).
- F. López Almansa, A.U. Yazgan, A. Benavent-Climent. Design energy spectra for Turkey. 15th World Conference on Earthquake Engineering (15WCEE). Lisbon, Portugal. Art. 531 (publication in CD) (2012).
- F. López Almansa, U. Yazgan, A. Benavent Climent. Design energy input spectra for moderate-to-high seismicity regions based on Turkish earthquakes. Bulletin of Earthquake Engineering. Submitted for possible publication.